ISSN 0031 - 9465

PHYTOPATHOLOGIA MEDITERRANEA

Plant health and food safety

Volume 63 • No. 1 • April 2024

The international journal of the
Mediterranean Phytopathological Union

FIRENZE UNIVERSITY PRESS

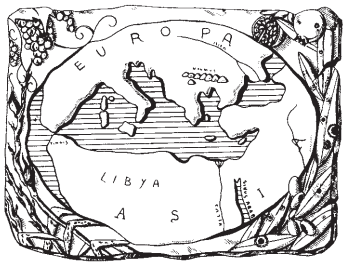

PHYTOPATHOLOGIA MEDITERRANEA

Plant health and food safety

The international journal edited by the Mediterranean Phytopathological Union
founded by A. Ciccarone and G. Goidànich

Phytopathologia Mediterranea is an international journal edited by the Mediterranean Phytopathological Union The journal's mission is the promotion of plant health for Mediterranean crops, climate and regions, safe food production, and the transfer of knowledge on diseases and their sustainable management.
The journal deals with all areas of plant pathology, including epidemiology, disease control, biochemical and physiological aspects, and utilization of molecular technologies. All types of plant pathogens are covered, including fungi, nematodes, protozoa, bacteria, phytoplasmas, viruses, and viroids. Papers on mycotoxins, biological and integrated management of plant diseases, and the use of natural substances in disease and weed control are also strongly encouraged. The journal focuses on pathology of Mediterranean crops grown throughout the world.
The journal includes three issues each year, publishing Reviews, Original research papers, Short notes, New or unusual disease reports, News and opinion, Current topics, Commentaries, and Letters to the Editor.

PHYTOPATHOLOGIA MEDITERRANEA

The international journal of the Mediterranean Phytopathological Union

Volume 63, April, 2024

Firenze University Press

***Phytopathologia Mediterranea*. The international journal of the Mediterranean Phytopathological Union**
Published by
Firenze University Press – University of Florence, Italy
Via Cittadella, 7–50144 Florence–Italy
http://www.fupress.com/pm
Direttore Responsabile: **Giuseppe Surico**, University of Florence, Italy

Phytopathologia Mediterranea
The international journal of the
Mediterranean Phytopathological Union

Firenze University Press
www.fupress.com/pm

Short Notes

Metagenomic analysis reveals the presence of prunus virus I in diseased *Clematis vitalba*: first record of this virus in Italy

Giuseppe PARRELLA*, Elisa TROIANO, Anna MIGNANO

Institute for Sustainable Plant Protection of the National Research Council (IPSP-CNR), Piazzale Enrico Fermi 1 – 80055 Portici (NA), Italy
*Corresponding author. giuseppe.parrella@ipsp.cnr.it

Summary. Prunus virus I (PrVI) was detected for the first time in *Clematis vitalba* in Italy using high-throughput sequencing and the complete genome of this isolate, named Clv-1, was assembled and characterized. The results of the bioinformatic analyses were further validated with RT-PCR assays using PrVI-specific primers and Sanger dideoxy sequencing. The Clv-1 genome included three RNA segments of nucleotide lengths of 3468 (RNA1), 2892 (RNA2) and 2225 (RNA3), with five predicted open reading frames. Phylogenetic analyses showed close relationships with other PrVI isolates from different geographical origins, including European and non-European countries. This new pathogen record extends the information on the geographical distribution of PrVI, and possibly reflects the international movement of infected clematis germplasm due to global trade. Further surveys on the presence and distribution of PrVI in weeds and crops, such as the two PrVI hosts sweet cherry and peach, are required in the countries where PrVI has been detected.

Keywords. PrVI, *Bromoviridae*, *Clematis* spp., high-throughput sequencing, emerging viruses.

OPEN ACCESS

Citation: G. Parrella, E. Troiano, A. Mignano (2024) Metagenomic analysis reveals the presence of prunus virus I in diseased *Clematis vitalba*: first record of this virus in Italy. *Phytopathologia Mediterranea* 63(1): 3-7. doi: 10.36253/phyto-14925

Accepted: December 22, 2023

Published: February 17, 2024

Data Availability Statement: All relevant data are within the paper and its Supporting Information files.

Competing Interests: The Author(s) declare(s) no conflict of interest.

Editor: Arnaud G Blouin, Institut des sciences en production végétale IPV, DEFR, Agroscope, Nyon, Switzerland.

ORCID:
GP: 0000-0002-0412-4014
ET: 0000-0001-7755-4915
AM: 0000-0001-5365-7186

INTRODUCTION

Clematis is a genus of perennial, chiefly climbing shrubs of *Ranunculaceae*, with 386 accepted species that are widely distributed, mainly in Asia and North America (POWO, 2023). Most *Clematis* spp. are cultivated for their attractive flowers, and more than 3000 cultivars have been obtained through breeding programmes (Mitrofanova *et al.*, 2021). The native European species, *Clematis vitalba* L., is a fast-growing climbing shrub which is often found in the vicinity of vineyards and orchards. It is considered a weed, and it can harbour many phytopathogens, including "flavescence dorée" phytoplasmas, which are often non-pathogenic for this plant (Angelini *et al.*, 2004). Approximately 11 different viruses have been reported to infect clematis plants. These viruses belong to: (i) *Bromoviridae*, including cucumber mosaic virus (CMV), tobacco streak virus (TSV), apple mosaic virus (ApMV) and prunus virus I (PrVI); (ii) *Virgaviridae*, including tobacco rattle virus (TRV); (iii) *Secoviridae*,

including tomato black ring virus (TBRV) and tomato ringspot virus (ToRSV); (iv) *Tombusviridae*, including tomato bushy stunt virus (TBSV), clematis chlorotic mottle virus (ClCMV) and Moroccan pepper virus (MPV); and (v) *Tospoviridae*, tomato spotted wilt virus (TSWV) (Mitrofanova *et al.*, 2018; Salamom *et al.*, 2023).

In the winter of 2023, *C. vitalba* plants showing previously undescribed symptomatology (Figure 1), were observed in a public garden in Assisi (PG), Umbria province, Central Italy (N 43.068927; E 12.61576). The presence of PrVI was detected in virome analyses of *C. vitalba* plants, using high-throughput sequencing (HTS) and Sanger sequencing. The whole genome sequence of PrVI was obtained and compared with PrVI isolates previously reported from other countries.

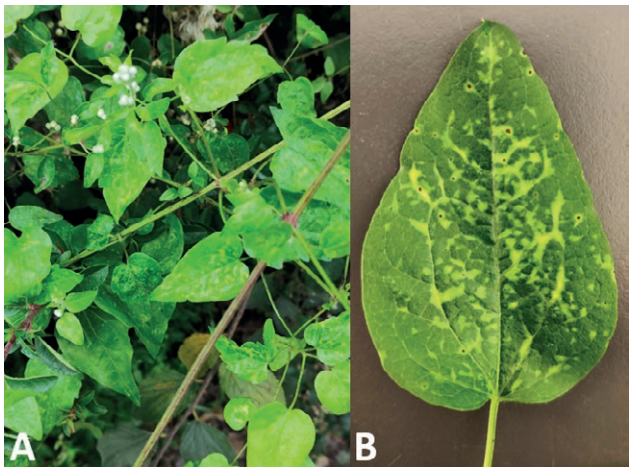

Figure 1. Symptoms in natural *Clematis vitalba* (A), and vein banding and pinpoint necrotic spot symptoms on a *C. vitalba* leaflet (B).

MATERIALS AND METHODS

Plant material, HTS and bioinformatic analysis

Total RNAs were isolated from leaf tissues of the sample Clv-1 (Figure 1) using the Viral Gene-spin™ Viral DNA/RNA Extraction Kit (iNtRON Biotechnology, Inc., Seongnam, South Korea), following the manufacturer's instructions. The RNA purity, concentration and integrity were determined by NanoDrop™ 2000 (NanoDrop). Ribosomal RNAs were depleted using a TruSeq RNA Sample Prep Kit, and the remaining RNAs were used for construction of RNA-seq libraries, which were sequenced on an Illumina Novaseq 6000 platform with paired-end reads length of 150 bp. Quality control on the sequencing data was performed with the software FastQC (v. 0.11.5; https://www.bioinformatics.babraham.ac.uk/projects/fastqc), then low quality bases and adapters were removed with the software BBDuk in the BBTools (v. 36; http://jgi.doe.gov/data-and-tools/software-tools/bbtools) package setting a minimum read quality of 25 and minimum read length of 35 bp. Taxonomic profiling of the reads were made with the software GAIA (v. 2.02; Paytuví *et al.*, 2019), which compare the reads against the databases Sila 132 (to identify ribosomal sequences) and NCBInr (to identify viral sequences). The resulting filtered reads were used to assemble the viral genome by using the algorithms Metaspades and RNAViral implemented in SPAdes (v. 3.15.3; Bankevich *et al.*, 2012). BLASTn/BLASTx analysis of the contigs were carried out against local and online databases.

Validation of HTS data

Total RNAs extracted from the sample Clv-1 was used in RT-PCR, using virus-specific primers and subsequent Sanger sequencing of the amplicons to confirm the presence of the virus identified by HTS. Virus-specific primers were designed according to the contig sequences of the target virus obtained in this study (Supplementary Table 1).

The complete viral genomic sequence was obtained from sequence assemblies of the amplicons generated from, respectively, RT-PCR and 5'-3'-RACE reactions (2nd generation 5'/3' RACE kit; Roche). RT-PCR was conducted according to the manufacturer's protocol (ImProm-II™ Reverse Transcription System, Promega). The 25 µL RT-PCR reaction contained 2 µL of total RNAs, 0.5 µL of each primer (50 pmol μL^{-1}), 12.5 µL of 2× Master Mix, 0.5 µL of Enzyme Mix and 9 µL of distilled water. The thermal cycling conditions were: one cycle of reverse transcription at 42°C for 90 min, one cycle of denaturation at 94°C for 2 min, followed by 35 cycles of amplification at 94°C for 45 s, 52°C for 1 min and 72°C for 2 min, and a final cycle of 72°C for 10 min.

Based on the nucleotide sequences that were obtained, specific primers (Supplementary Table 1) were redesigned to amplify fragments of the 5'-upstream and 3'-downstream regions, corresponding to each segmented genome by 5' and 3'-RACE (rapid amplification of cDNA ends), as described by Parrella and Troiano (2022). Amplicons of the expected sizes were directly sequenced in both directions at Microsynth Seqlab GmbH (Göttingen, Germany).

In addition, total RNAs extracted from five other symptomatic *C. vitalba* plants and one asymptomatic *C. vitalba* plant, from the vicinity of Clv-1, were assessed in RT-PCR assays for the presence of the virus identified in Clv-1, using PrV-CP1/PrV-CP2 primers (Supplementary Table 1) following the protocol described above.

Phylogenetic analyses

Multiple sequence alignments were conducted using MUSCLE (Edgar, 2004) implemented in MEGA11. Phylogenetic trees were constructed using the best fit model for each alignment, using the maximum likelihood (ML) method in the MEGA11 (Tamura *et al.*, 2021) with 500 bootstrap replicates. The trees were drawn to scale, with branch lengths measured in the number of substitutions per site.

RESULTS AND DISCUSSION

HTS of the Clv-1 sample yielded 25,409,477 raw reads. Using the results of the taxonomic classification, the trimmed reads were parsed to keep only those classified as "viral" or which were completely unclassified (i.e., 9,246,969 reads). Of the total trimmed reads, 0.068% were mapped on ilarvirus RNA1, 0.055% on ilavirus RNA2 and 0.095% on ilarvirus RNA3. These reads were used to perform viral genome assembly with the two algorithms implemented in the Spades program. Two sets of filtered contigs were obtained: 4,661 contigs with the algorithms implemented in Metaspades, and 4,920 contigs with algorithms implemented in viral RNA.

BLASTx search showed presence of contigs with the greatest amino acid (aa) sequence identities (99-81%) to PrVI (*Ilarvirus*, *Bromoviridae*). Three contigs showing the greatest nucleotide identities with the PrVI genome were identified by BLASTn. These contigs represented almost full-length genomic sequences of the corresponding viruses. No other viral contigs belonging to other viruses were generated by HTS library. Based on the PrVI mapped contig sequences, primers were designed for each of the three RNAs (Supplementary Table 1). RT-PCR using these primers targeting the three different putative viral RNAs amplified products of the expected sizes (Figure 2). Sequences obtained from these amplicons were identical to the corresponding genome regions sequenced by HTS, confirming presence of PrVI in the *C. vitalba* plant. After verifying the sequences at the 5' and 3' ends, the sequences of the three genomic ssRNA segments of the Clv-1 isolate consisted of 3468 nucleotides (nt) for RNA1, 2892 nt for RNA2, and 2225 nt for RNA3. These sequences were deposited in GenBank with the accession numbers OR502867 (RNA1), OR602868 (RNA2) and OR602869 (RNA3).

RNA1 contains a single ORF (1a) with the ATG codon at position 29 and ending with a TAG codon at position 3301. It encodes the 121 kDa viral replicase protein (p1), consisting of 1090 amino acids (aa). The protein shares 98.9–99.6% aa identity and 99.0% similarity with other PrVI isolates in GenBank.

RNA2 is bicistronic with the two ORFs overlapping by 272 nt. The first ORF at the 5' end of RNA2 encodes the viral polymerase protein of 807 aa (p2a) with a predicted molecular mass of 92 kDa. The second ORF encodes a 205 aa protein (p2b) involved in cell-to-cell movement and posttranscriptional gene silencing, with a predicted molecular mass of 22 kDa. The p2a protein shares 98.2–98.6% aa identity and 98–99% similarity, while the p2b protein shares 95.6-99.5% identity and 98–99% similarity with other PrVI isolates in GenBank.

RNA3 contains two ORFs. The ORF 3a encodes the movement protein (MP) of 300 aa (p3a), and has an estimated molecular mass of 32 kDa. The p3a protein has 96.0–99.0% identity and 97–100% similarity with the movement proteins of other PVrI isolates. The ORF 3b encodes the coat protein (CP) of 217 aa long protein (p3b) and has a predicted molecular mass of 24 kDa. The p3b protein shares 98.6–99.5% identity and 99–100% similarity with the coat protein of other PrVI isolates.

The expected amplicons were obtained by RT-PCR with the primers Prv-CP1/PrV-CP2, using the RNAs extracted from five other *C. vitalba* plants showing similar symptoms of Clv-1, while no reaction product was obtained with RNA extracted from asymptomatic plants. Sanger sequencing on these amplicons revealed 100% identity among these sequences and with Clv-1 sequence obtained by HTS. These results may indicate a common origin of the infection among the different clematis plants tested, and a possible role in the spread of the virus by vegetatively propagated infected host material.

Maximum likelihood-based phylogenetic analyses of the three RNAs, performed with MEGA 11 under the best fit substitution models, always placed Clv-1 in the

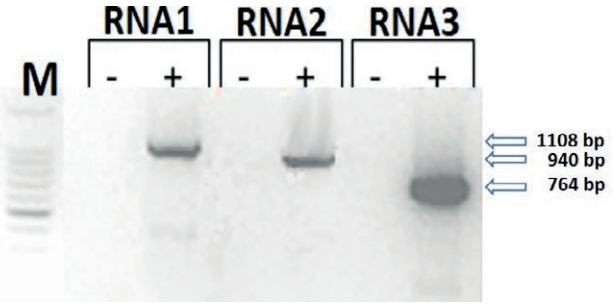

Figure 2. Agarose gel electrophoresis of the RT-PCR products obtained with the primers designed on the PrVI RNA1 (PrV-R1F/PrV-R1R), RNA2 (PrV-R2F/PrV-F2R), and RNA3 (PrV-R3F/PrV-R3R) (Supplementary Table 1). M = 100 bp ladder, - = negative control (healthy plant), + = RNA extracted from the infected *Clematis vitalba* plant.

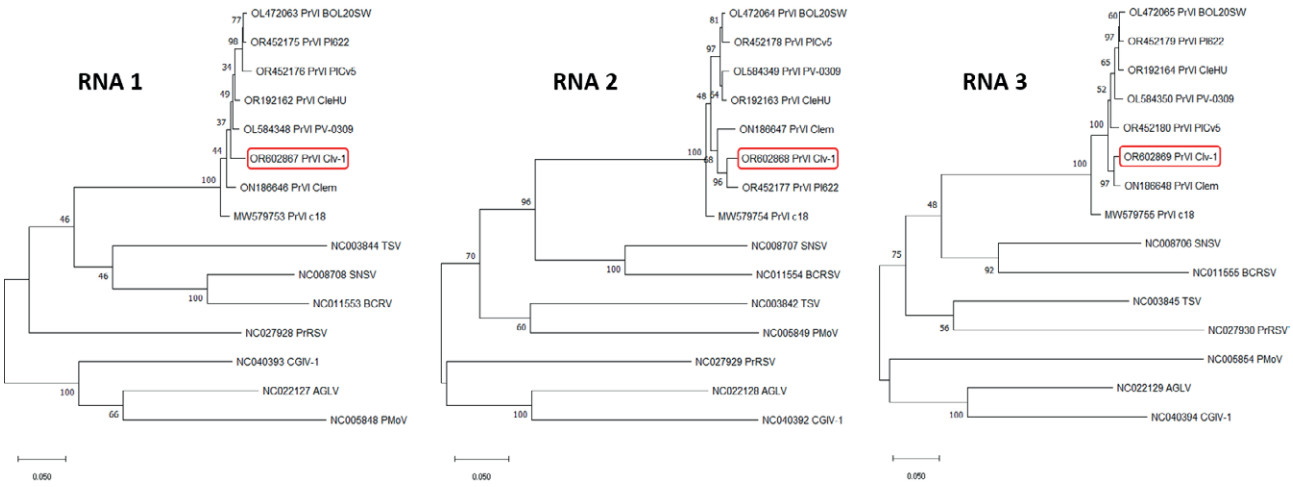

Figure 3. Phylogenetic relationships of the nucleic acid sequences of RNA1, RNA2, and RNA3 of PrVI isolates and ilarviruses belonging to subgroup I. Each label reports the GenBank accession number and the acronym of the virus: prunus virus I (PrVI), tobacco streak virus (TSV), strawberry necrotic shock virus (SNSV), blackberry chlorotic ringspot virus (BCRV), privet ring spot virus (PrRSV), cape gooseberry ilarvirus 1, ageratum latent virus (AGLV), and parietaria mottle virus (PMoV). Isolate names were also reported for PrVI. The position of the Italian isolate of PrVI (Clv-1) is highlighted with red boxes. Phylogenetic analyses were carried out using the maximum likelihood method in MEGA 11, with 500 bootstrap replicates based on the best substitution model found in MEGA 11. Bootstrap values at each node are shown.

same comparable well-supported clade for each RNA, comprising the recognized PrVI isolates within subgroup I in *Ilarvirus*. These results were confirmed by a high bootstrap value in all instances (Figure 3). In particular, for phylogenetic reconstruction based on RNA2, two well supported sub-clades were generated, with the Clv-1 isolate grouping with the two PrVI isolates from *C. vitalba*: isolate Clem identified in Russia and isolate Pl622, identified in Slovakia. The isolate c18 from *Picris echioides* (identified in Slovenia) was the most divergent, and was placed outside the clades of the PrVI isolates in all the three phylogenetic reconstructions, supported by 100% bootstrap values on each corresponding node (Figure 3).

The advances in sequencing metagenomic analysis have led to the discovery of new viruses, allowing the detection and prevention of emerging viruses. Using HTS analysis, PrVI was first described on asymptomatic sweet cherry (*Prunus avium*) in Greece (Orfanidou *et al.*, 2021), but was subsequently identified in the weed plant *P. echioides* (Rivarez *et al.*, 2022) and repeatedly in *Clematis* spp. plants, mainly in Eastern Europe, including Hungary, Slovenia, Slovakia, Croatia and Russia (Chirkov *et al.*, 2022; Rivarez *et al.*, 2022; Salamon *et al.*, 2023).

The recent discovery of PrVI in Italy described in the present study, although associated with different symptoms in *C. vitalba* plants from those described on the same host by previous authors (Chirkov *et al.*, 2022; Salamon *et al.*, 2023), confirms that this plant is an important natural host for this virus. Since PrVI was only recently described, it is not clear what is its diffusion in nature or its impacts on cultivated plants. In addition, accidental dispersion of infected propagative material of *Clematis* cannot be excluded. This could explain the recent findings of PrVI on *Clematis* in different European countries in a short period. For these reasons, the development of an effective, sensitive and specific PrVI diagnostic method is required, which can be used in extensive monitoring in the areas where PrVI was recently described. Wild and cultivated plants, particularly stone fruit crops, should be assessed for PrVI infections.

ACKNOWLEDGEMENTS

This research was supported by a MISE CRESO grant (Viabio No. F/200095/01-03/X45). The Authors thank Dr Ettore Magaldi and Dr Rosaria Fusco (IPSP-CNR) for their administrative support.

LITERATURE CITED

Angelini E., Squizzato F., Lucchetta G., Borgo M., 2004. Detection of a phytoplasma associated with Grapevine Flavescence dorée in *Clematis vitalba*. *European Journal of Plant Pathology* 110: 193–201.

Bankevich A., Nurk S., Antipov D., Gurevich A.A., Dvorkin M., … Pevzner P.A., 2012. SPAdes: a new genome

assembly algorithm and its applications to single-cell sequencing. *Journal of Computational Biology* 19(5): 455–477. https://doi.org/10.1089/cmb.2012.0021.

Chirkov S., Zakubanskiy A., Sheveleva A., Zubkova N., Mitrofanova I., 2022. Detection and molecular characterization of viruses infecting clematis in Russia. *Journal of Plant Pathology* 105: 173–183. https://doi.org/10.1007/s42161-022-01242-8

Edgar R. C., 2004. MUSCLE: multiple sequence alignment with high accuracy and high throughput, *Nucleic Acids Research* 32(5): 1792–1797.

Mitrofanova I.V., Zakubanskty A.V., Mitrofanova O.V., 2018. Viruses infecting main ornamental plants: an overview. *Ornamental Horticolturae* 24: 95–102.

Mitrofanova I., Ivanova N., Kuzmina T., Mitrofanova O., Zubkova N., 2021. In vitro regeneration of *Clematis* plants in the Nikita Botanical Garden via somatic embryogenesis and organogenesis. *Frontiers in Plant Science* 12: 541171. https://doi.org/10.3389/fpls.2021.541171

Orfanidou C.G., Xing F., Zhou J., Li S., Katis N., Maliogka V.I., 2021. Identification and sequence analysis of a novel ilarvirus infecting sweet cherry. *Plants* 10: 514. https://doi.org/10. 3390/plants1003 0514

Parrella G., Troiano E., 2022. A New Ilarvirus Found in French Hydrangea. *Plants* 11(7): 944. https://doi.org/10.3390/plants11070944

Paytuví A., Battista E., Scippacercola F., Aiese Cigliano R., Sanseverino W., 2019. GAIA: an integrated metagenomics suite. *bioRxiv* 804690. https://doi.org/10.1101/804690

POWO (2023). Plants of the World Online. Facilitated by the Royal Botanic Gardens, Kew. Published on the Internet; http://www.plantsoftheworldonline.org/ Retrieved 27 November 2023.

Rivarez M. P. S., Pecman A., Bačnik K., Ferreira O. M. C., Vučurović A., … Kutnjak D., 2022. In-depth study of tomato and weed viromes reveals undiscovered plant virus diversity in an agroecosystem. *bioRxiv* 2022.06.30.498278. https://doi.org/10.1101/2022.06.30.498278

Salamon P., Nagyne-Galbacs Z., Demian E., Achs A., Alaxin P., … Varallyay E., 2023. *Clematis vitalba* Is a Natural Host of the Novel Ilarvirus, Prunus Virus I. *Viruses*, 15: 1964. https://doi.org/10.3390/v15091964

Tamura K., Stecher G., Kumar S., 2021. MEGA11: Molecular Evolutionary Genetics Analysis version 11. *Molecular Biology and Evolution* 38: 3022–3027.

Phytopathologia Mediterranea
The international journal of the
Mediterranean Phytopathological Union

Firenze University Press
www.fupress.com/pm

New or Unusual Disease Reports

First report of virus detection in *Ficus carica* in Austria

Eduviges Glenda BORROTO FERNÁNDEZ[1,3,*], Toufic ELBEAINO[2], Florian FÜRNSINN[1], Anna KEUTGEN[3], Norbert KEUTGEN[3], Margit LAIMER[1]

[1] *Plant Biotechnology Unit, Department of Biotechnology, University of Natural Resources and Life Sciences, 1180 Vienna, Austria*
[2] *Department of Integrated Pest Management, Istituto Agronomico Mediterraneo di Bari, 70010 Valenzano Bari, Italy*
[3] *Department of Crop Sciences, Institute of Vegetables and Ornamentals, University of Natural Resources and Life Sciences, 1180 Vienna, Austria*
*Corresponding author: eduviges.borroto-fernandez@boku.ac.at

Summary. *Ficus carica* is one of the most ancient cultivated crops, and is grown mainly in the Mediterranean region. In Austria, due to milder winters and longer warm periods than normal, figs are becoming more productive and popular among private growers. For future propagation of some fig varieties, the phytosanitary status of eight fig accessions, representing four Austrian genotypes maintained in a varietal collection plot, was investigated using PCR assays for presence of eight fig-infecting viruses. The four fig trees were infected with fig mosaic virus (FMV), fig badnavirus 1 (FBV-1), fig leaf mottle-associated virus 1 (FLMaV-1), fig mild mottle-associated virus (FMMaV) and fig fleck-associated virus (FFkaV); whereas fig leaf mottle-associated virus 2 (FLMaV-2), fig latent virus 1 (FLV-1) and fig cryptic virus 1 (FCV-1) were not detected. The sequences of PCR amplicons obtained from different viruses and samples showed greatest nucleotide variability of 0.5% for FBV-1, 12% for FLMaV-1, 16.3% for FMV, 14% for FMMaV, and 15% for FFkaV, when compared to their homologues in GenBank. A phylogenetic tree for FMV constructed based on partial RNA1 sequences showed that the Austrian isolates were most closely related to previously described Spanish and Greek isolates. The different symptoms observed in the tested trees were mainly in similar to with those reported for FMV, the agent of fig mosaic disease. This is the first report on the presence of fig mosaic-associated viruses in Austria.

Keywords. Fig, mosaic disease, viruses, detection, phylogenetic analyses.

Citation: E.G. Borroto Fernández, T. Elbeaino, F. Fürnsinn, A. Keutgen, N. Keutgen, M. Laimer (2024) First report of virus detection in *Ficus carica* in Austria. *Phytopathologia Mediterranea* 63(1): 9-14. doi: 10.36253/phyto-14952

Accepted: December 17, 2023

Published: February 17, 2024

Data Availability Statement: All relevant data are within the paper and its Supporting Information files.

Competing Interests: The Author(s) declare(s) no conflict of interest.

Editor: Assunta Bertaccini, Alma Mater Studiorum, University of Bologna, Italy.

ORCID:
EGBF: 0000-0001-5560-394X
TE: 0000-0003-2211-7907
AK: 0000-0001-7825-9782
NK: 0000-0002-6625-5458
ML: 0000-0002-6796-8126

INTRODUCTION

Fig (*Ficus carica* L.) is an ancient domesticated crop, grown since *ca*. 11000 years BP in the lower Jordan Valley (Kislev *et al*., 2006). Fig orchards are mainly cultivated in the Mediterranean basin, in Algeria, Egypt, Tunisia, Turkey, Iran, and Morocco (FAO, 2019). In southern Europe, fig trees are widespread due to the favourable climate, while in northern and central

Europe a few varieties withstand the low winter temperatures. In Austria, due to changing climatic conditions (milder winters and longer warm periods), figs are becoming popular and more productive among private growers.

Fig plants are normally resistant to many diseases, but they are propagated from cuttings and this facilitates the spread of virus and phytoplasma infections. Mosaic disease (MD) is a major disorder affecting figs in the wild environments, and this disease was first described in California by Condit (1933). Trees affected by MD show leaf symptoms including chlorotic spots, mottling, mosaic patterns, necroses, and deformation (Elbeaino, 2022). To date, 13 viruses associated with MD have been identified, of which only fig mosaic virus (FMV) has been was confirmed as an etiologic agent by fulfilment of Koch postulates (Elbeaino, 2022). Phytoplasma and viroid infections have also been reported from fig hosts (Alsaheli *et al*., 2020; Elbeaino, 2022).

The present study investigated the presence of viruses in eight fig accessions of four cultivars deposited in a fig genotype collection plot, where the plants had symptoms of MD. These plants included two of the cultivar 'Negronne', three of 'Pastilière', two of 'Rivers Brown Turkey', and one plant designated as 'Laimer'. 'Negronne', also known as mulberry fig, is a summer and autumn twice-bearing variety that is native to France, which has shiny and glossy leaves of variable shape on each tree, varying from completely unlobed to deeply incised with five lobes. This give the plants an attractive appearance, and winter hardiness down to -16°C. 'Pastilière' is the best fig variety for fresh consumption, and is also native to France with comparable winter hardiness. 'Rivers Brown Turkey' is a summer and autumn fig native to England, and is a winter hardy variety able to tolerate temperatures as low as -19°C (Seiler, 2022). 'Laimer' is a garden fig of unknown origin.

MATERIALS AND METHODS

Source of plant material and extraction of total nucleic acids

Eight fig accessions representing four genotypes (Table 1) were surveyed in spring and autumn 2022. Leaf samples were collected from symptomatic plants in both seasons (Figure 1). In addition, leaves from two Italian fig cultivars ('Marangiana Bianca' and 'Figazzano Incognita') infected with five viruses (FLMaV-1, FMMaV, FMV, FBV-1 and FFkaV) were provided by the University of Bari (Dr A. Minafra), and these were used as positive controls in the molecular assays. Total nucleic acids (DNA and RNA) were extracted from 100 mg samples of leaf vein tissues excised from symptomatic and asymptomatic leaves, using DNeasy Plant Pro Kit and RNeasy Plant Mini Kit (Qiagen).

RT-PCR and PCR assays

Reverse-Transcription Polymerase Chain Reaction assays (RT-PCR) were each carried out on 100 ng of TNA, using the Qiagen One-Step RT-PCR kit (Qiagen) according to the manufacturers' instructions, and

Table 1. List of fig viruses and their corresponding specific primers used in PCR\RT-PCR assays.

Virus	Primer	Primer sequences (5'–3')	Amplicon (bp)	Reference
FLMaV-1	N17-s N17-a	CGTGGCTGATGCAAAGTTTA GTTAACGCATGCTTCCATGA	350	Elbeaino *et al.* (2006)
FLMaV-2	F3-s F3-a	GAACAGTGCCTATCAGTTTGATTTG TCCCACCTCCTGCGAAGCTAGAGAA	360	Elbeaino *et al.* (2007)
FMMaV	LM3-s LM3-a	AAGGGGAATCTACAAGGGTCG TATTACGCGCTTGAGGATTGC	311	Elbeaino *et al.* (2010)
FLV-1	CPtr-s CPtr-a	CCATCTTCACCACACAAATGTC CAATCTTCTTGGCCTCCATAAG	389	Gattoni *et al.* (2009)
FMV	E5-s E5-a	CGGTAGCAAATGGAATGAAA AACACTGTTTTTGCGATTGG	302	Elbeaino *et al.* (2009)
FFkaV	D8-s D8-a	TCAATCCCAAGGAGGTGAAG ACACGGTCAATGAGGGAGTC	270	Elbeaino *et al.* (2011b)
FCV-1	R1-s R1-a	TCGGATTGTCTTTGGAGAGG CGCATCCACAGTATCCCATT	353	Elbeaino *et al.* (2011a)
FBV-1	1094F 1567R	ACCAGACGGAGGGAAGAAAT TCCTTGCCATCGGTTATCTC	474	Laney *et al.* (2012)

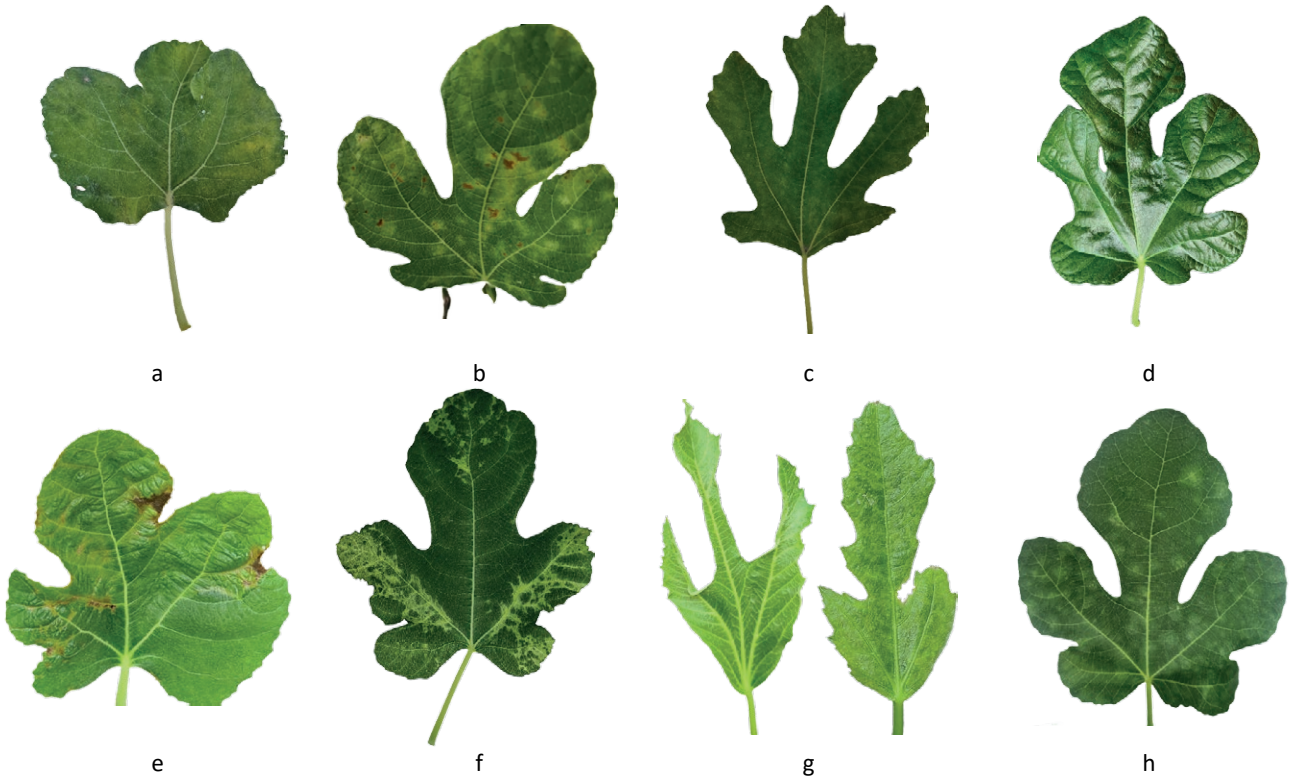

Figure 1. Leaves of Austrian fig plants of the cultivars 'Pastilière' (a and e), 'Rivers Brown Turkey' (b and f), 'Negronne' (c and g), and 'Laimer' (d, h), displaying typical MD leaf symptoms during Autumn 2022 (a to d) and Spring 2023 (e to h). The symptoms consisted of lobe deformations (a and e); vein clearing and mosaic (b and f), and leaf deformations (c and g); and leaf puckering and ringspots (d and h).

the specific primer pairs for each of eight fig-infecting viruses (Table 1). The one-step RT-PCR reaction was performed at 50°C for 30 min, 95°C for 15 min, followed by 40 cycles each at 94°C for 30 sec, 55°C for 30 sec, and 72°C for 1 min, and a final extension step at 72°C for 10 min. PCR products were analyzed by agarose gel electrophoresis. FBV-1 detection was carried out with PCR, using HotStarTaq Master Mix (Qiagen), and the reactions were carried out at 94°C for 2 min, followed by 35 cycles of 94°C for 30 sec, 55°C for 20 sec, and 72°C for 30 sec, and 10 min extension.

Sequence and phylogenetic analyses

PCR amplicons were sequenced bi-directionally using the sense and antisense primers specific to each virus (Eurofins Genomics and Microsynth AG). Multiple alignments of nucleotide sequences were made using Geneious Prime v.2023.1.1. Searches for homologies with nucleotides were conducted with the Blastn program (Altschul *et al.*, 1990). A phylogenetic tree for Austrian FMV isolates (Figure 2) was constructed using the NJPLOT package in Geneious Prime v.2023.1.1. The Neighbor-Joining algorithm, with p-distance method and bootstrap of 1000 replicates were used. European mountain ash ringspot-associated emaravirus (EMARaV, acc.no: NC 013105) was used as the outgroup species to root the tree.

RESULTS AND DISCUSSION

Detection of fig viruses

Based on the PCR and RT-PCR results, the viruses FLMaV-1, FMMaV, FMV, FBV-1 and FFkaV, were detected in the analyzed fig samples. All four fig genotypes were infected with at least three of these viruses. Of the viruses analyzed, FBV-1 and FLMaV-1 were the most prevalent, followed by FMV (Table 2). FLMaV-2, FLV-1 and FCV-1 were not detected in any of the samples. The analyses carried out in the two seasons were gave the same results, and these are summarized in Table 2.

At sequence levels, PCR amplicons generated from three fig genotypes infected with FBV-1 were

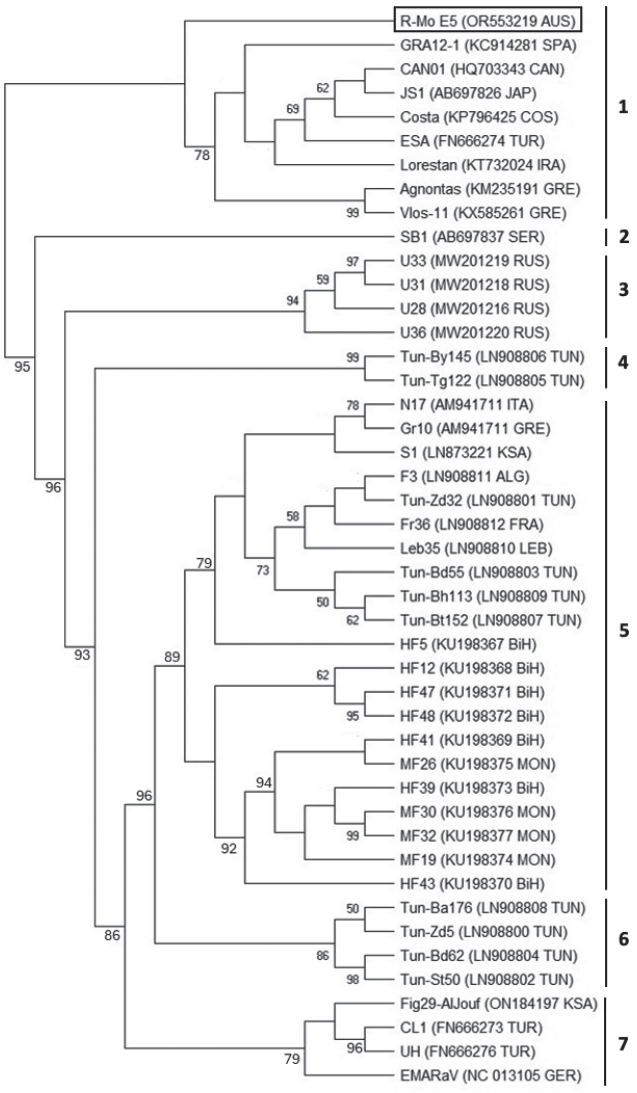

Figure 2. Phylogenetic tree generated from the nucleotide sequence alignment of partial RNA-dependent RNA polymerase genes (RNA1) of FMV isolates from Austria (boxed), and from virus sequences reported in GenBank, using the NJPLOT method implemented in 'Geneious Prime' program. GenBank accession numbers of the sequences used are reported in parentheses. European mountain ash ringspot-associated emaravirus (EMARaV) was used as the outgroup species. Bootstrap values >50% are shown at branch points (1000 replicates). Branch lengths represent bootstrap values. Bar represents 0.01 changes per site. Bootstrap values less than 50% were dropped. The numerals 1 to 7 are number of clades.

sequenced. This yielded three different sequences in the cultivars 'Negronne' (Acc. no. OR553220), 'Pastilière' (Acc. no. OR553221), 'Rivers Brown Turkey' (Acc. no. OR553222) that shared 99.2 to 99.7% identity. In the Blastn analysis they showed 99.7 to 100% identity with isolate Podg2015 (Acc. no. MG584625) from Montenegro, and isolate HF19 (Acc. no. KY473907) from Bosnia and Herzegovina.

The four fig genotypes were infected with FLMaV-1, and sequencing of PCR amplicons of the genotypes 'Pastilière' and 'Rivers Brown Turkey' yielded two sequences (Acc. nos. OR553223 and OR553224) that shared 91.4% nucleotides identity. Blastn analysis showed the greatest identity (respectively, 95.1 and 95.4%) with isolates MF39 (Acc. no. KU198387) and HF43 (Acc. no. KU198382) from Bosnia and Herzegovina.

FMV was detected in the four fig genotypes, and the isolates shared 100% nucleotide identity with each other (Acc. no. OR553219). Blastn analysis showed the greatest nucleotide identity (respectively, 91 and 92%) with isolates Agnontas (Acc. no. KM235191) from Greece and GRA12-1 (Acc. no. KC914281) from Spain.

PCR results showed that FMMaV was present in the fig genotypes 'River Brown Turkey' and 'Laimer'. Pairwise sequence comparisons of PCR amplicons showed 90.6% of identity, whereas with those of from GenBank they showed greatest identities (respectively, 95.7 and 92.5%) with isolate MAZ-1 (Acc. no. MG242131) from Iran, and isolate Cas-12.2 (Acc. no. KC914283) from Spain.

FFkaV was found in two fig genotypes, and Blast analysis of the two sequences (Acc. nos. OR553225 and OR553226) showed 90.5 and 89.7% nucleotide identities with isolate N17 (Acc. no. NC_015229) from Italy; and there was 91.2% identity between them.

Mosaic-disease on figs

All the fig accessions examined in two different seasons over 2 years showed consistent MD leaf symptoms induced by FMV. These mainly consisted of vein clearing and mottling, ringspots, leaf deformation and mosaic (Figure 1). The symptoms observed and the infections found in the three commercial fig accessions tested confirmed the etiology of FMV with MD. Repeated testing did not detect FMV in the fourth assessed fig accession.

Phylogenetic analysis of FMV

Due to the importance of FMV as a fig pathogen, a phylogenetic tree was constructed based on the FMV sequences obtained and those retrieved from the GenBank from different origins. FMV isolates have been designated in seven clades based on their geographical origins, with some exceptions. The Austrian isolate was allocated to clade 1, together with homologues from Spain, Greece and Turkey, whereas clade 2 groups virus isolates from Serbia and clade 3 groups those from Rus-

Table 2. Results of PCR and RT-PCR assays, indicating presence (+) or absence (-) of eight fig viruses in four fig genotypes.

Fig genotype	FMV	FLMaV-1	FLMaV-2	FMMaV	FLV-1	FCV-1	FFkaV	FBV
'Pastilière' (plants 1, 2 and 3)	+	+	-	-	-	-	+	+
'River Brown Turkey' (plants 1 and 2)	+	+	-	+	-	-	-	+
'Negronne' (plants 1 and 2)	+	+	-	-	-	-	-	+
'Laimer' (plant 1)	-	+	-	+	-	-	+	+

sia. Clade 4 includes isolates from the Mediterranean basin (Algeria, France, Greece, Italy, Lebanon, Tunisia), and clade 5 includes isolates from the Balkan area (Montenegro and Bosnia & Herzegovina). Clades 6 and 7, similarly grouped with Mediterranean isolates, with some exceptions.

CONCLUSIONS

The present study is the first to record the presence of five viruses (FLMaV-1, FMMaV, FMV, FBV-1 and FFkaV) in different FMD-associated fig accessions in Austria. FLMaV-2, FLV-1 and FCV-1 were not not be detected in the host plants assessed. The presence of FMV in three of four genotypes is not surprising given the cosmopolitan nature of this virus. The phylogenetic analysis conducted on the set of FMV isolates reported in GenBank showed distinct distribution of FMV isolates according to their geographical origins, with some exceptions. These exceptions are probably due to infections by FMV isolates different from those naturally indigenous to a specific area, thus breaking the rule of geographic origin of FMV. The presence of FBV-1 in all the assessed fig accessions represent a major challenge in attempts to produce virus-free fig planting material. The results obtained in this study could be useful for further monitoring and diagnosis of fig viruses in Austrian plantations. Further investigations of these viruses, in different plots, varieties, and locations, are ongoing in Austria, to support a future certification programme for fig in this country.

AUTHOR CONTRIBUTIONS

ML and EB designed the experiment, carried out the analyses and wrote the paper. TE analyzed the virus sequences and assisted drafting of the manuscript. AK and NK assisted with cultivars descriptions, and reviewed the text. FF assisted with the sampling and the analyses of the experiments.

LITERATURE CITED

Alsaheli Z., Contaldo N., Mehle N., Dermastia M., Elbeaino T., Bertaccini A., 2020. First detection of "*Candidatus* Phytoplasma asteris"-and "*Candidatus* Phytoplasma solani"-related strains in fig trees. *Journal of Phytopathology* 168(1): 63-71.

Altschul S.F., Stephen F., Gish W., Miller W., Myers E.W., Lipman D.J., 1990. Basic local alignment search tool. *Journal of Molecular Biology* 215: 403–410.

Condit I.J. 1933. A mosaic of the fig in California. *Phytopathology* 23: 887–896.

Elbeaino T., 2022. Fig Pathogens: Viruses, Viroids, and Phytoplasmas. In: *Advances in Fig Research and Sustainable Production* (pp. 279–292). GB: CABI.

Elbeaino T., Digiaro M., de Stradis A., Martelli G.P., 2006. Partial characterization of a Closterovirus associated with a chlorotic mottling of fig. *Journal of Plant Pathology* 88: 187–192.

Elbeaino T., Digiaro M., De Stradis A., Martelli G.P., 2007. Identification of a second member of the family Closteroviridae in mosaic-diseased figs. *Journal of Plant Pathology* 89: 199–124.

Elbeaino T., Digiaro M., Alabdullah A., De Stradis A., Minafra A., … Martelli G.P., 2009. A multipartite single-stranded negative-sense RNA virus is the putative agent of fig mosaic disease. *Journal of General Virology* 90: 1–8.

Elbeaino T., Digiaro M., Heinoun K., De Stradis A., Martelli G.P., 2010. Fig mild mottle-associated virus, a novel closterovirus infecting fig. *Journal of Plant Pathology* 92: 165–172.

Elbeaino, T., Kubaa R.A., Digiaro M., Minafra A., Martelli G.P., 2011a. The complete nucleotide sequence and genome organization of Fig cryptic virus, a novel bipartite dsRNA virus infecting fig, widely distributed in the Mediterranean basin. *Virus Genes* 42: 415–421.

Elbeaino T., Digiaro M., Martelli G.P., 2011b. Complete nucleotide sequence of Fig fleck-associated virus, a novel member of the family *Tymoviridae*. *Virus Research* 16: 198–202.

FAO, 2019. http://www.fao.org/faostat/en/#rankings/countries_by_commodity. Accessed 23 July 2020. Food and Agriculture Organization of the United Nations, Rome, Italy

Gattoni G., Minafra A., Castellano M.A., De Stradis A., Boscia D., … Martelli G.P., 2009. Some properties of Fig latent virus 1, a new member of the family Flexiviridae. *Journal of Plant Pathology* 91: 555–564.

Kislev M.E., Hartmann A., Bar-Yosef O., 2006. Early domesticated fig in the Jordan Valley. *Science* 312(5778): 1372–1374.

Laney A.G., Mohamed H., Ioannis E.T., 2012. An integrated badnavirus is prevalent in fig germplasm. *Phytopathology* 102: 1182–1189. https://doi.org/10.1094/phyto-12-11-0351

Seiler C., 2022. *Feigen aus dem eigenen Garten: Über 30 leckere Sorten, die sich selbst befruchten*. Ulmer, Stuttgart, Germany, 128 pp.

Phytopathologia Mediterranea
The international journal of the
Mediterranean Phytopathological Union

Firenze University Press
www.fupress.com/pm

Research Papers

Complete genome assemblies of several *Xylella fastidiosa* subspecies *multiplex* strains reveals high phage content and novel plasmids

María Pilar VELASCO-AMO[1,2], Luis F. ARIAS-GIRALDO[1], Blanca B. LANDA[1,*]

[1] *Institute for Sustainable Agriculture, Consejo Superior de Investigaciones Científicas (CSIC), Córdoba, Spain*
[2] *Programa de Doctorado ingeniería agraria, alimentaria, forestal y de desarrollo rural sostenible. Universidad de Córdoba, Córdoba, Spain*
*Corresponding author. E-mail: blanca.landa@ias.csic.es

Summary. The Gram-negative bacterium *Xylella fastidiosa* (*Xf*) was originally found in the Americas, but has now been identified in more than 20 countries across America, Asia, and Europe. This plant pathogen is currently listed as a priority pest in Europe due to its socio-economic and ecological impacts. Within the three *Xf* subspecies *fastidiosa*, *multiplex* and *pauca*, subsp. *multiplex* displays a notably wider range of host plants than the other two subspecies. Comparative genomics may allow determination of how *Xf* subsp. *multiplex* adapts to new and diverse hosts and environments, so it is important that more genomes of this subspecies are defined. Twelve complete closed genomes sequences of *Xf* subsp. *multiplex* were obtained using a hybrid assembly approach combining Illumina and Oxford Nanopore technologies. The combined use of Canu and Unicycler assemblers enabled identification and closure of several plasmid sequences with high similarity to other plasmids described in strains of *Xf* subsp. *fastidiosa* and subsp. *pauca*. The analysis also revealed prophage sequences and contigs outside the chromosomes, annotated as phages. These new genomes, in conjunction with those existing in GenBank, will facilitate exploration of the evolutionary dynamics of *Xf* subsp. *multiplex,* its host adaptation mechanisms, and the potential emergence of novel strains of this important plant pathogen.

Keywords. Hybrid assembly, prophages, quarantine phytopathogen.

OPEN ACCESS

Citation: M.P. Velasco-Amo, L.F. Arias-Giraldo, B.B. Landa (2024) Complete genome assemblies of several *Xylella fastidiosa* subspecies *multiplex* strains reveals high phage content and novel plasmids. *Phytopathologia Mediterranea* 63(1): 15-23. doi: 10.36253/phyto-14931

Accepted: January 31, 2024

Published: February 17, 2024

Data Availability Statement: All relevant data are within the paper and its Supporting Information files.

Competing Interests: The Author(s) declare(s) no conflict of interest.

Editor: Anna Maria D'Onghia, CIHEAM/Mediterranean Agronomic Institute of Bari, Italy.

ORCID:
MPV-A: 0000-0001-7176-0435
LFA-G: 0000-0003-4861-8064
BBL: 0000-0002-9511-3731

INTRODUCTION

Xylella fastidiosa is a fastidious, Gram-negative, xylem-limited bacterium in the *Xanthomonadaceae*, which is a major transcontinental plant health threat, with serious socioeconomic impacts. The bacterium causes diseases on a wide range of agricultural crops, ornamental and landscape plants, and plants with cultural and heritage values (EFSA *et al.*, 2023). This Gram-negative bacterium affects many plant species, leading to symptoms such as leaf scorching, wilting, decline, and complete canopy death. Some important

diseases caused by *X. fastidiosa* include Pierce's Disease (PD) of grapevine, Citrus Variegated Chlorosis (CVC), Almond Leaf Scorch (ALS), and Olive Quick Decline Syndrome (OQDS) (EFSA *et al.*, 2023). This bacterium can also severely impact urban trees (Sherald *et al.*, 1987; Harris *et al.*, 2014; Desprez-Loustau *et al.*, 2021), and plants within natural environments (Denancé *et al.*, 2017). The range of hosts susceptible to *X. fastidiosa* continues to expand, with over 690 plant species across 306 genera and 88 families as hosts (EFSA *et al.*, 2023).

Although *X. fastidiosa* has allopatric origins in the Americas (Almeida and Nunney, 2015; Vanhove *et al.*, 2019), its current distribution is now in more than 20 countries in the Americas, Asia, and Europe (EFSA *et al.*, 2023; EPPO, 2023). In Europe, *X. fastidiosa* emerged as an important pathogen in 2013, associated with a severe epidemic in olive trees in Italy. This epidemic, associated to OQDS, is ongoing, causing the loss of hundreds of olive trees annually. European territories have witnessed other *X. fastidiosa* outbreaks impacting mainly native plant species in natural environments and ornamentals in France and Portugal, while Spain has faced epidemics mainly affecting almonds and grapes (Velasco-Amo *et al.*, 2022; EFSA *et al.*, 2023). Sánchez *et al.* (2019) ranked *X. fastidiosa* amongst first priority pests for the European Union (EU) when considering economic, social, and environmental domains. These authors estimated, in a scenario where *X. fastidiosa* would spread extensively across Europe, that potential annual costs would exceed €5.5 billion. This accounted for potential losses in the olive, almond, citrus, and grape sectors, reflecting the substantial economic impacts that this pathogen could cause (Sanchez *et al.*, 2019).

Xylella fastidiosa is a genetically diverse bacterium that includes three main subspecies: subspp. *fastidiosa, multiplex* and *pauca;* although other subspecies have been proposed (Schaad *et al.*, 2004; Schuenzel *et al.*, 2005; Denancé *et al.*, 2019). These subspecies can be further grouped below subspecies level into Sequence Types (ST), based on Multilocus Sequence Typing (MLST) analyses (Yuan *et al.*, 2010). The subspecies *multiplex* has gained particular attention due to its ability to infect a diverse range of hosts, as a damaging and adaptable pathogen. Considering the EFSA list of confirmed *X. fastidiosa* hosts for which molecular-characterization typing approaches have been carried out to characterize subspecies, approx. 62% of the records were for plants infected by subsp. *multiplex*, while 17.1% subsp. *fastidiosa* and 16.6% by subsp. *pauca* (EFSA *et al.*, 2023).

Complete genome sequences are important for describing the biology of plant pathogens, identifying virulence factors, and understanding genetic diversity, potential origins, and introductory pathways (Landa *et al.*, 2019). Comparative genomics, facilitated by multiple genomes of different strains and subspecies, offers a powerful means to explore the evolutionary dynamics of *X. fastidiosa*, its adaptation to new hosts, and the emergence of novel strains (Potnis *et al.*, 2019; Vanhove *et al.*, 2019; Castillo and Almeida, 2023).

Despite the advances made in *X. fastidiosa* genomics, understanding of *X. fastidiosa* subsp. *multiplex* at the genomic level remains limited. Several genomes from other *X. fastidiosa* subspecies are available, but scarcity of complete genomes from *multiplex* restricts ability to comprehensively study the genetics, biology, and evolution of this pathogen. This underscores the urgent need for an expanded dataset of *X. fastidiosa* subsp. *multiplex* genomes.

The present study has provided the genome sequences of 12 strains of *X. fastidiosa* subsp. *multiplex*, from different host plants in different countries, and shows the significance of acquiring additional genomes of this subspecies as a critical step in advancing understanding of this versatile and destructive plant pathogen.

MATERIALS AND METHODS

Table 1 shows the 12 strains of *X. fastidiosa* subsp. *multiplex* sequenced in this study. These strains are deposited at the *X. fastidiosa* collection of the Institute for Sustainable Agriculture (IAS-CSIC), Córdoba, Spain. Strains XYL466/19, XYL468 and Santa29b belonging to the ST81 were isolated from leaf petioles of *Olea europaea* var. *sylvestris* and *Santolina chamaecyparissus* on periwinkle wilt-modified (PW) (for XYL466/19 and XYL468) and PD2 (for Santa29b) solid media, following the EPPO isolation procedures (EPPO, 2023). The remaining strains were provided by researchers from different laboratories, or were acquired at the CIRM-CFBP collection of plant-pathogenic bacteria, INRAE, France (Table 1).

The strains were grown in PD2 solid medium at 28˚C in the dark during 7 to 12 days (depending on the strain). Genomic DNA was extracted using the Quick DNA Fungal/Bacteria Miniprep kit (Zymo Research Group). The integrity of DNA was measured by gel electrophoresis and concentrations were estimated using a spectrofluorometer (Qubit; Thermo Fisher Scientific).

Illumina sequencing libraries were prepared following manufacturer recommendations, and were sequenced using the platforms Hiseq 4000 at the StabVida sequencing facility, Caparica, Portugal (for strains XYL466/18 and XYL468), or iSeq 100 at the

Table 1. Information related to the strains belonging to *Xylella fastidiosa* subspecies *multiplex* used in this study.

Strain	Other names	ST[a]	Host	Geographical origin	Isolation Year
CFBP8417	LSV 46.78	6	*Spartium junceum*	France: Alata, Corsica	2015
CFBP8418	LSV 46.79	6	*Spartium junceum*	France: Alata, Corsica	2015
CFBP8070	GA Plum LSV 40.38	10	*Prunus* sp.	USA: Georgia	2004
CFBP8075	LSV 42.30	27	*Prunus* sp.	USA: California	unknown
CFBP8068	ATCC35873, 2687 ELM-1, LSV 00.54	41	*Ulmus americana*	USA: Washington	unknown
CFBP8173	LSV40.39, ICPB50039, Hopkins PL788, Wells2679, ATCC228771, ATCC35871, ICMP15199, ICMP8735, ICMP8746, LMG9063, Labo13350, Labo13352, Labo13355, NCPPB4431	41	*Prunus salicina*	USA: Georgia	unknown
Santa29b		81	*Santolina chamaecyparissus*	Spain: Alcafar, Menorca	2022
XF3348		81	*Prunus dulcis*	Spain: Binissalem, Mallorca	2018
XYL1752		81	*Prunus dulcis*	Spain: Ciudatella, Menorca	2017
XYL1966/18		81	*Olea europaea*	Spain: Ciudatella, Menorca	2018
XYL466/19		81	*Olea europaea* var. *sylvestris*	Spain: Sant Llorenç, Mallorca	2019
XYL468		81	*Olea europaea* var. *sylvestris*	Spain: Manacor, Mallorca	2019

[a] Sequence Type (ST) was determined by MLST analysis or by BLAST search of whole genome against the *Xylella fastidiosa* MLST database (https://pubmlst.org/xfastidiosa/; accessed on 02 November 2022).

IAS-CSIC facility (for strains CFBP8068, CFBP8070, CFBP8075, CFBP8173, and Santa29b). For the remaining strains, Illumina data were retrieved from the Sequence Read Archive (SRA) database: Strains CFBP8417 (SRR8454254), CFBP8418 (SRR8454358), and XYL1966/18 (SRR11931336). Illumina reads were trimmed and filtered with the fastp tool v0.23.2 (Chen *et al.*, 2018). Before the assembly process, resulting fastq files were analyzed with Krakren2 v2.1.2 (Wood *et al.*, 2019) using the PlusPFP v.6-5-2023 database (https://benlangmead.github.io/aws-indexes/k2) to identify and remove any contamination from the reads that may have been introduced during the library preparation, and to only retain reads assigned to the *X. fastidiosa* taxon.

Oxford Nanopore Technologies (ONT) sequencing libraries were prepared by multiplexing, using the ligation sequencing gDNA and Native barcoding kit SQK-NBD114.24 or the VolTRAX Multiplex Kit VMK004 in the VolTRAX v0.21.0 system. These libraries were loaded in, respectively, R9.4.1 or R10.4.1 flow cells, in a MK1C v6.0.7 sequencing device. ONT sequencing reads were basecalled with Guppy v6.4.2, and were trimmed with Porechop v0.2.4 (Wick *et al.*, 2017).

Long-read *de novo* genome assemblies were carried out using Canu v2.2. The draft genomes obtained were subsequently polished using the Illumina high-quality short-reads (Q > 25), first using Polypolish v0.5.0 (Wick and Holt, 2022), and then two rounds with POLCA v4.0.9 (Zimin and Salzberg, 2020). Two of the *X. fastidiosa* genomes required an additional step, which involved scaffolding and direction of contigs with a reference genome (strain IVIA5901 from *X. fastidiosa* subsp. *multiplex*). This was carried out using RagTag v2.1.0 (Alonge *et al.*, 2022), and gap filling was then carried out using TGS-GapCloser 1.0.3 (Xu *et al.*, 2020) with Racon v1.4.20. Final assemblies were annotated using the NCBI Prokaryotic Genome Annotation Pipeline (Tatusova *et al.*, 2016) before submission to GenBank.

A phylogenetic analysis using a total of 111 *X. fastidiosa* whole genomes belonging to subsp. *multiplex* was carried out including all the genomes available at the GenBank database (https://www.ncbi.nlm.nih.gov/genome/browse/#!/prokaryotes/173/), in combination with the 12 complete genomes obtained in this study. The genomes were annotated with prokka v1.14.6 (Seemann, 2014) with default parameters, and coding sequences (CDSs) were used to estimate the core genome with CoreCruncher using the MAFFT (Katoh and Standley, 2013) algorithm to build the core genome alignment. Following this, ambiguous sequences or poorly aligned regions were eliminated from the multiple sequence alignment using ClipKIT v 1.3. A maximum likelihood (ML) tree was then constructed with IQtree v2.2.0 using the GTR+I+G4 substitution model determined by ModelTest-NG c0.1.6 (Nguyen *et al.*, 2015; Darriba *et al.*, 2020), and was plotted with ggtree v3.6.2 (Yu *et al.*, 2017). Strain IVIA5235 of subsp. *fastidiosa* was used as an outgroup. Tree topology was midpoint rooted, and branch support was assessed using 1,000 bootstrap replicates.

RESULTS AND DISCUSSION

The hybrid sequencing and assembly approach allowed reconstruction and circularization of the complete genomes of ten of the strains (Table 2). The genome of strains XYL466/18 and XYL468 resulted in scaffolds due to conflicting regions.

Three complete plasmids were identified and assembled in strain CFBP8070, designated as pXF-P1. CFBP8070 (43,491 bp), pXF-P2.CFBP8070 (26,328 bp), and pXF-P3.CFBP8070 (1,286 bp) (Table 2). Johnson *et al.* (2023) highlighted the challenges that long-read assemblers like Canu faced for detecting bacterial plasmids. To reconstruct and close the plasmids in the CFBP8070 strain, a combination of Canu and Unicycler assemblers was necessary. Results of BLASTN revealed similarities with previously-described plasmids. Plasmid pXF-P1.CFBP8070 exhibited a 96% similarity, covering less than 80% of the query, with plasmid pXF51ud from strain U24D, a member of subsp. *pauca* isolated from a citrus plant in Brazil (Pierry *et al*., 2020). Plasmid pXF-P2.CFBP8070 displayed 99% similarity, covering the entire query, with plasmid pXF26-Oak35874 from strain Oak35874, belonging to subsp. *multiplex* and isolated from *Quercus* in Washington DC, United States of America (USA: O'Leary and Burbank, 2023). Plasmid pXF-P3.CFBP8070 showed 90% similarity with 99% coverage to plasmid pUCLAb from strain UCLA, of subsp. *fastidiosa* isolated from grapevine in California, USA (Guilhabert *et al*., 2006).

The discovery of identical plasmids in distinct *X. fastidiosa* subspecies further supports the possibility of horizontal gene transfer (HGT) among bacterial strains (Rogers and Stenger, 2012). HGT and recombination are key factors in the emergence of new strains capable of colonizing new hosts (Burbank and Van Horn, 2017). This phenomenon could elucidate the high ability of subsp. *multiplex* to infect a wide range of host plants.

A Maximum-likelihood phylogenetic tree was constructed showing the different STs, hosts, and geographical origins of the strains included, which agreed with those of described in previous studies (Denancé *et al*., 2017; Landa *et al*., 2019; Dupas *et al*., 2023) (Figure 1). As previously reported, strains identified as belonging to ST6 from France and Spain were polyphyletic (Landa *et al*., 2019; Dupas *et al*., 2023), with strains belonging to ST7 from France clustering together with those from the USA from the same ST, and closer to Spanish ST6 strains. In contrast, French ST6 strains clustered with Dixon strain from ST6, isolated from almonds in California, and closer to a subgroup formed by ST81 strains from Spain. These ST81 strains clustered with Fillmore and Riv5 strains from California, USA, from the same ST, which suggests a potential introduction of ST81 strains from the USA into the Balearic Islands (Moralejo *et al*., 2020).

The remaining *X. fastidiosa* strains, including strains from Italy belonging to ST87 and four of the strains sequenced in this study, were grouped according to their ST in more ancestral clades. These clades include ten strains isolated in Italy from the host plants *Polygala myrtifolia, Prunus dulcis, Rhamnus alaternus* and *Spartium junceum*, one strain isolated in Brazil from *Prunus domestica,* and 20 strains isolated in the USA from *Lupinus, Platanus*, *Prunus*, *Quercus*, *Ulmus*, *Vaccinium* and *Vinca* sp. All the strains within these ancestral clades were primarily isolated from the southeastern USA, with two exceptions: two strains isolated from *Prunus* in California, CFBP8075 assigned to ST27 and ICMP8739 assigned to ST41 (Kant *et al*., 2023), and the strain RAAR14 plum327 from Brazil from ST26. This further supports the hypothesis that subsp. *multiplex* likely originated in the southeastern USA (Landa *et al*., 2019).

The presence of *X. fastidiosa* strains in California, deviating from typical geographical distribution, prompts consideration. Those strains were sourced from different bacterial collections and could signify introductions from the southeastern USA. However, data inaccuracies could have occurred during strain documentation in the collection database, or errors may have occurred during handling, as these have occurred in the past (Nunney *et al*., 2012), and at least one of the strains was isolated in 1985. This underscores the necessity of providing precise metadata when depositing microorganisms into culture collections. It also emphasizes the significance of open sharing and preserving genome data associated with respective correct metadata to ensure accuracy and reliability (Nunney *et al*., 2012; Sabot, 2022).

Annotation of *X. fastidiosa* subsp. *multiplex* genomes with the RAST server (Aziz *et al*., 2008) revealed the presence of prophage sequences and phage contigs within most of the bacterial chromosomes assessed in the present study (Table 2). Strains isolated from Menorca Island exhibited three phage sequences, in contrast to the strains isolated from Mallorca Island. Both of these islands are in the Balearic Archipelago in Spain, where no phage sequences were annotated. Despite belonging to the same subspecies and ST81, strains from Menorca Island were proposed to have been introduced from Mallorca Island (Moralejo *et al*., 2020). Among the strains analyzed, strain CFBP8418 displayed two contigs annotated as phages, while strains CFBP8070 and CFBP8417 each presented one contig annotated as phages.

Table 2. General genome features and assembly statistics for strains of *Xylella fastidiosa* subspecies *multiplex* used in the study.

Strain	Number of contigs	Contigs type	Size (bp)	Assembly	Total Cove-rage (X)	Contami-nation (%) [a]	Complete-ness (%) [a]	GC content (%)	Number of CDS [b]	Number of tRNA	Number of rRNA	Number of ncRNA	Accession number	Additional contigs [c]	Size of additional contigs (bp) [c]
CFBP8417	1	Chr	2,672,285	Canu	180	0.19	99.08	51.9	2,423	49	6	4	CP136980	1	44,569
CFBP8418	1	Chr	2,692,457	Canu	128	0.19	99.08	51.9	2,460	49	6	4	CP136979	2	22,299 32,325
CFBP8070	4	Chr pXF-P1.CFBP8070 pXF-P2.CFBP8070 pXF-P3.CFBP8070	2,796,854 43,491 26,328 1,286	Canu Unicycler Unicycler Unicycler	360	0.31	98.98	52.1	2,686	49	6	4	CP136975 CP136976 CP136977 CP136978	1	42,466
CFBP8075	1	Chr	2,439,524	Canu	115	0.19	99.03	51.9	2,085	49	6	4	CP136974	-	-
CFBP8068	1	Chr	2,548,602	Canu	904	0.19	99.06	51.9	2,233	49	6	4	CP136973	-	-
CFBP8173	1	Chr	2,548,622	Canu	105	0.19	99.06	51.9	2,243	49	6	4	CP136972	-	-
Santa29b	1	Chr	2,593,199	Canu	213	0.19	99.08	52.7	2,313	49	6	4	CP136971	3	35,805 35,815 35,805
XF3348	1	Chr	2,682,254	Canu	1,110	0.19	99.08	52.1	2,426	49	6	4	CP136970	-	-
XYL1752	1	Chr	2,769,601	Canu	847	1.88	99.08	52.3	2,541	50	6	4	CP136969	3	40,489 42,412 42,428
XYL1966/18	1	Chr	2,708,059	Canu	511	0.19	99.08	52.2	2,453	49	6	4	CP136968	-	-
XYL466/19	2	Chr-Scaffold	2,790,648	Canu	1,026	0.19	99.09	52.3	2,552	49	6	4	CP136967	-	-
XYL468	2	Chr-Scaffold	2,809,670	Canu	787	0.19	99.08	52.2	2,610	49	6	4	CP136966	-	-

[a] Genome Contamination (Redundancy) and Completeness were checked with checkM (Parks *et al.*, 2014).
[b] Coding sequence (CDS) were annotated with NCBI Prokaryotic Genome Annotation Pipeline.
[c] Contigs annotated as candidate phage with RAST server (Aziz *et al.*, 2008).

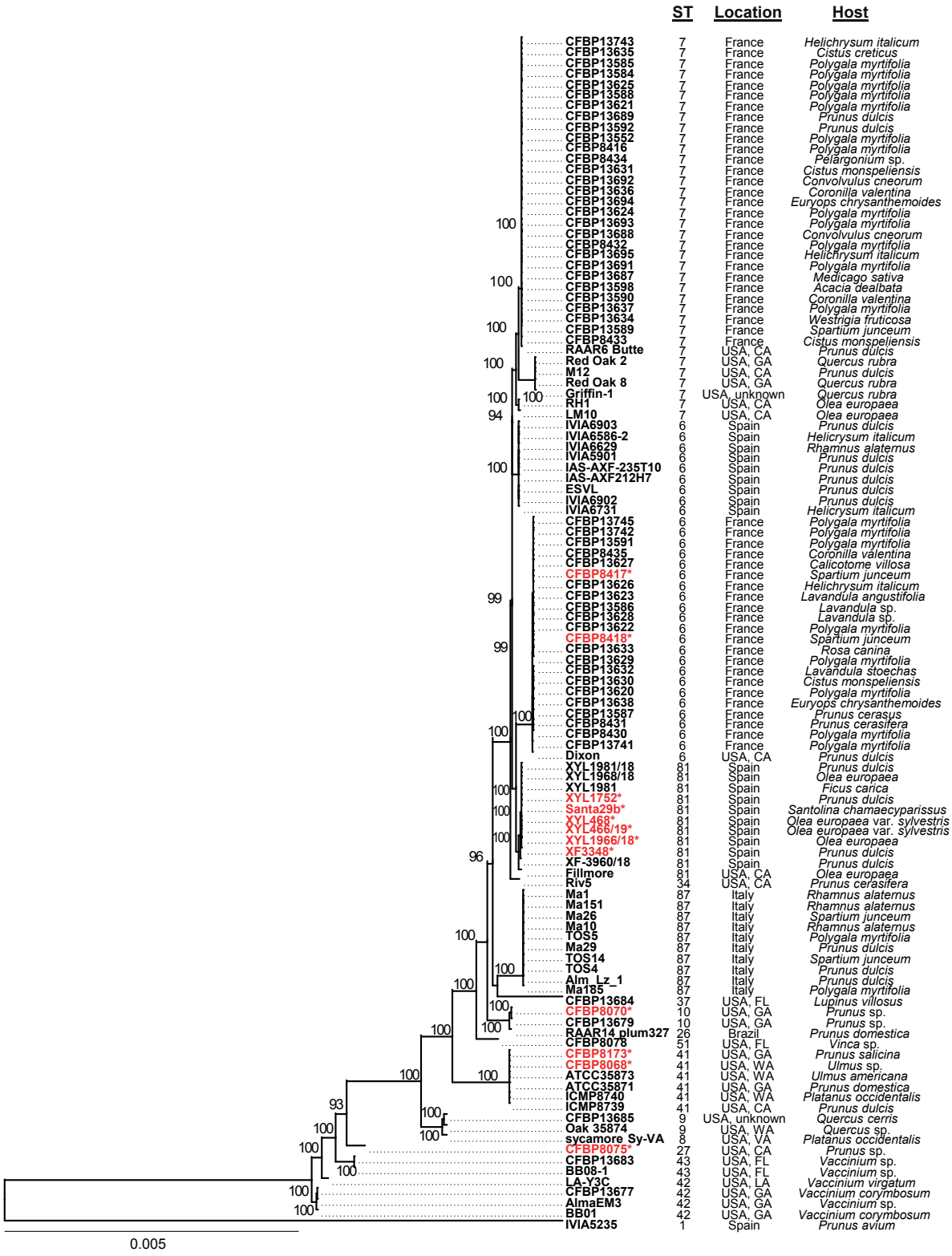

Figure 1. Maximum-likelihood phylogenetic reconstruction of the core genome for 111 *Xylella fastidiosa* subsp. *multiplex* strains. The strain IVIA5235 belonging to *X. fastidiosa* subsp. *fastidiosa* ST1 was used as the outgroup. Sequence type was known and/or confirmed by genome query at the *Xylella fastidiosa* pubMLST database (Jolley *et al.*, 2018), and location and host of isolation are provided. Strains sequenced in this study are shown in red accompanied with an asterisk. Numbers indicate bootstrap values.

Previous studies have documented the existence of prophages and phages in strains of *X. fastidiosa* across different subspecies, associating the presence of prophages with genomic rearrangements and strain divergence (Varani *et al*., 2008, 2013; O'Leary *et al*., 2022). Absence of observable plaques (calvus) on the culture media where these strains grow suggests that the assembled contigs may correspond to phages in lysogenic states (Chen and Civerolo, 2008). The high prevalence of these sequences in strains from subsp. *multiplex* is particularly notable. This prompts the need for further investigation to comprehensively elucidate their significance, the underlying reasons for their abundance, and to provide insights into the mechanisms and potential implications of these sequences for *X. fastidiosa* biology and evolution.

DATA AVAILABILITY STATEMENT

The complete genome sequences of *X. fastidiosa* subsp. *pauca* were deposited at NCBI under BioSample accession numbers: SAMN37751223 (CFBP8417), SAMN37751224 (CFBP8418), SAMN37751225 (CFBP8070), SAMN37751226 (CFBP8075), SAMN37751227 (CFBP8068), SAMN37751228 (CFBP8173), SAMN37751229 (Santa29b), SAMN37751230 (XF3348), SAMN3775131 (XYL1751/17), SAMN37751232 (XYL1966/18), SAMN37751233 (XYL466/19), and SAMN37751234 (XYL468). All these accession numbers are associated with BioProject PRJNA 1026562.

ACKNOWLEDGMENTS

This research was funded by Project BeXyl (Beyond *Xylella*, Integrated Management Strategies for Mitigating *Xylella fastidiosa* impact in Europe; Grant ID No. 101060593) from the European Union Horizon Action 'Food, Bioeconomy Natural Resources, Agriculture and Environment' Programme; Project E-RTA2017-00004-C06-02 (Desarrollo de estrategias de erradicación, contención y control de *X. fastidiosa* en España) from 'Programa Estatal de I+D+I Orientada a los Retos de la Sociedad of the Spanish Government AEI-INIA Spain', Qualifica Project QUAL21-023 IAS from Junta de Andalucía, Spain, and the Interdisciplinary Thematic Platform PTI-SolXyl from CSIC. The authors thank the Spanish Ministry of Agriculture, Fisheries and Food for support to the Reference Laboratory of the Institute for Sustainable Agriculture. M. P. Velasco Amo was recipient of a contract financed by the Intramural Project 201840E111 from CSIC. M. Román-Écija gave assistance with *Xylella fastidiosa* strain collection maintenance. Members of the Institut de Recerca I Formació Agroalimentària i Pesquera (IRFAP, Palma de Mallorca, Spain) and E. Moralejo (Tragsa, Palma de Mallorca, Spain), Mallorca, Balearic Island, Spain gave support during isolation of some of the strains used in this study.

LITERATURE CITED

Almeida R.P.P., Nunney L., 2015. How do plant diseases caused by *Xylella fastidiosa* emerge? *Plant Disease* 99: 1457–1467. https://doi.org/10.1094/PDIS-02-15-0159-FE

Alonge M., Lebeigle L., Kirsche M., Jenike K., Ou S., … Soyk S., 2022. Automated assembly scaffolding using RagTag elevates a new tomato system for high-throughput genome editing. *Genome Biology* 23: 258. https://doi.org/10.1186/s13059-022-02823-7

Aziz R.K., Bartels D., Best A.A., DeJongh M., Disz T., … Zagnitko O., 2008. The RAST Server: Rapid Annotations using Subsystems Technology. *BMC Genomics* 9: 75. https://doi.org/10.1186/1471-2164-9-75

Burbank L.P., Van Horn C.R., 2017. Conjugative plasmid transfer in *Xylella fastidiosa* is dependent on *tra* and *trb* Operon Functions. *Journal of Bacteriology* 199: e00388-17. https://doi.org/10.1128/JB.00388-17

Castillo A.I., Almeida R.P.P., 2023. The multifaceted role of homologous recombination in a fastidious bacterial plant pathogen. *Applied and Environmental Microbiology* 89: e00439-23. https://doi.org/10.1128/aem.00439-23

Chen J., Civerolo E.L., 2008. Morphological evidence for phages in *Xylella fastidiosa*. *Virology Journal* 5: 75. https://doi.org/10.1186/1743-422X-5-75

Chen, Zhou Y., Chen Y., Gu J., 2018. fastp: an ultra-fast all-in-one FASTQ preprocessor. *Bioinformatics* 34: i884–i890. https://doi.org/10.1093/bioinformatics/bty560

Darriba D., Posada D., Kozlov A.M., Stamatakis A., Morel B., Flouri T., 2020. ModelTest-NG: A new and scalable tool for the selection of DNA and protein evolutionary models. *Molecular Biology and Evolution* 37: 291–294. https://doi.org/10.1093/molbev/msz189

Denancé N., Legendre B., Briand M., Olivier V., Boisseson C. de, … Jacques M.-A., 2017. Several subspecies and sequence types are associated with the emergence of *Xylella fastidiosa* in natural settings in France. *Plant Pathology* 66: 1054–1064. https://doi.org/10.1111/ppa.12695

Denancé N., Briand M., Gaborieau R., Gaillard S., Jacques M.-A., 2019. Identification of genetic rela-

tionships and subspecies signatures in *Xylella fastidiosa*. *BMC Genomics* 20: 239. https://doi.org/10.1186/s12864-019-5565-9

Desprez-Loustau M.-L., Balci Y., Cornara D., Gonthier P., Robin C., Jacques M.-A., 2021. Is *Xylella fastidiosa* a serious threat to European forests? *Forestry: An International Journal of Forest Research* 94: 1–17. https://doi.org/10.1093/forestry/cpaa029

Dupas E., Durand K., Rieux A., Briand M., Pruvost O., … Jacques M.-A., 2023. Suspicions of two bridgehead invasions of *Xylella fastidiosa* subsp. *multiplex* in France. *Communications Biology* 6: 1–13. https://doi.org/10.1038/s42003-023-04499-6

EFSA E.F.S., Gibin D., Pasinato L., Delbianco A., 2023. Update of the *Xylella* spp. host plant database – systematic literature search up to 31 December 2022. *EFSA Journal* 21: e08061. https://doi.org/10.2903/j.efsa.2023.8061

EPPO, 2023. PM 7/24 (5) *Xylella fastidiosa*. *EPPO Bulletin* 53: 205–276. https://doi.org/10.1111/epp.12923.

Guilhabert M.R., Stewart V.J., Kirkpatrick B.C., 2006. Characterization of putative rolling-circle plasmids from the Gram-negative bacterium *Xylella fastidiosa* and their use as shuttle vectors. *Plasmid* 55: 70–80. https://doi.org/10.1016/j.plasmid.2005.06.004

Harris J.L., Di Bello P.L., Lear M., Balci Y., 2014. Bacterial Leaf Scorch in the district of Columbia: Distribution, host range, and presence of *Xylella fastidiosa* among urban trees. *Plant Disease* 98: 1611–1618. https://doi.org/10.1094/PDIS-02-14-0158-SR

Johnson J., Soehnlen M., Blankenship H.M., 2023. Long read genome assemblers struggle with small plasmids. *Microbial Genomics* 9. https://doi.org/10.1099/mgen.0.001024

Jolley K.A., Bray J.E., Maiden M.C.J., 2018. Open-access bacterial population genomics: BIGSdb software, the PubMLST.org website and their applications. *Wellcome Open Research* 3: 124. https://doi.org/10.12688/wellcomeopenres.14826.1

Kant P., Brohier N., Mann R., Rigano L., Taylor R., … Constable F., 2023. High-quality full genome assembly of historic *Xylella fastidiosa* strains from ICMP collection using a hybrid sequencing approach. *Microbiology Resource Announcements* 12: e00536-23. https://doi.org/10.1128/MRA.00536-23

Katoh K., Standley D.M., 2013. MAFFT Multiple Sequence Alignment Software Version 7: Improvements in performance and usability. *Molecular Biology and Evolution* 30: 772–780. https://doi.org/10.1093/molbev/mst010

Landa B.B., Castillo A.I., Giampetruzzi A., Kahn A., Román-Écija M., … Almeida R.P.P., 2019. Emergence of a plant pathogen in Europe associated with multiple intercontinental introductions. *Applied and Environmental Microbiology* 86: e01521-19, /aem/86/3/AEM.01521-19.atom. https://doi.org/10.1128/AEM.01521-19

Moralejo E., Gomila M., Montesinos M., Borràs D., Pascual A., … Olmo D., 2020. Phylogenetic inference enables reconstruction of a long-overlooked outbreak of almond leaf scorch disease (*Xylella fastidiosa*) in Europe. *Communications Biology* 3: 1–13. https://doi.org/10.1038/s42003-020-01284-7

Nguyen L.-T., Schmidt H.A., von Haeseler A., Minh B.Q., 2015. IQ-TREE: A fast and effective stochastic algorithm for estimating maximum-likelihood phylogenies. *Molecular Biology and Evolution* 32: 268–274. https://doi.org/10.1093/molbev/msu300

Nunney L., Elfekih S., Stouthamer R., 2012. The importance of multilocus sequence typing: cautionary tales from the bacterium *Xylella fastidiosa*. *Phytopathology* 102: 456–460. https://doi.org/10.1094/PHYTO-10-11-0298

O'Leary M.L., Arias-Giraldo L.F., Burbank L.P., De La Fuente L., Landa B.B., 2022. Complete genome resources for *Xylella fastidiosa* strains AlmaEM3 and BB08-1 reveal prophage-associated structural variation among blueberry-infecting strains. *Phytopathology®*, Scientific Societies 112: 732–736. https://doi.org/10.1094/PHYTO-08-21-0317-A

O'Leary M.L., Burbank L.P., 2023. Natural recombination among type I restriction-modification systems creates diverse genomic methylation patterns among *Xylella fastidiosa* strains. *Applied and Environmental Microbiology* 89: e01873-22. https://doi.org/10.1128/aem.01873-22.

Parks D.H., Imelfort M., Skennerton C.T., Hugenholtz P., Tyson G.W., 2015. CheckM: Assessing the quality of microbial genomes recovered from isolates, single cells, and metagenomes. *Genome Research* 25: 1043–1055. https://doi.org/10.1101/gr.186072.114

Pierry P.M., Uceda-Campos G., Feitosa-Junior O.R., Martins-Junior J., de Santana W.O., … da-Silva A.M., 2020. Genetic Diversity of *Xylella fastidiosa* plasmids assessed by comparative genomics. *Tropical Plant Pathology* 45: 342–360. https://doi.org/10.1007/s40858-020-00359-4

Potnis N., Kandel P.P., Merfa M.V., Retchless A.C., Parker J.K., … De La Fuente L., 2019. Patterns of inter- and intrasubspecific homologous recombination inform eco-evolutionary dynamics of *Xylella fastidiosa*. *The ISME Journal* 13: 2319–2333. https://doi.org/10.1038/s41396-019-0423-y.

Rogers E.E., Stenger D.C., 2012. A conjugative 38 kb plasmid is present in multiple subspecies of *Xylella fas-*

tidiosa. *PLoS ONE* 7. https://doi.org/10.1371/journal.pone.0052131

Sabot F., 2022. On the importance of metadata when sharing and opening data. *BMC Genomic Data* 23: 79. https://doi.org/10.1186/s12863-022-01095-1

Sánchez B., Barreiro-Hurle J., Soto Embodas I., Rodriguez-Cerezo E., 2019. The impact Indicator for Priority Pests (I2P2) – A tool for ranking pests according to Regulation (EU) 2016/2031. Publications Office of the European Union.

Schaad N.W., Postnikova E., Lacy G., Fatmi M., Chang C.-J., 2004. *Xylella fastidiosa* subspecies: *X. fastidiosa* subsp. *fastidiosa* subsp. nov., *X. fastidiosa* subsp. *multiplex* subsp. nov., and *X. fastidiosa* subsp. *pauca* subsp. nov. *Systematic and Applied Microbiology* 27: 290–300. https://doi.org/10.1078/0723-2020-00263

Schuenzel E.L., Scally M., Stouthamer R., Nunney L., 2005. A multigene phylogenetic study of clonal diversity and divergence in north American strains of the plant pathogen *Xylella fastidiosa*. *Applied and Environmental Microbiology* 71: 3832–3839. https://doi.org/10.1128/AEM.71.7.3832-3839.2005

Seemann T., 2014. Prokka: rapid prokaryotic genome annotation. *Bioinformatics* (Oxford, England) 30: 2068–2069. https://doi.org/10.1093/bioinformatics/btu153

Sherald J.L., Wells J.M., Hurtt S.S., Kostka S.J., 1987. Association of fastidious, xylem-inhabiting bacteria with leaf scorch in red maple. *Plant Disease* 71: 930–933.

Tatusova T., DiCuccio M., Badretdin A., Chetvernin V., Nawrocki E.P., … Ostell J., 2016. NCBI prokaryotic genome annotation pipeline. *Nucleic Acids Research* 44: 6614–6624. https://doi.org/10.1093/nar/gkw569

Vanhove M., Retchless A.C., Sicard A., Rieux A., Coletta-Filho H.D., … Almeida R.P., 2019. Genomic Diversity and Recombination among *Xylella fastidiosa* Subspecies. *Applied and Environmental Microbiology* 85: e02972-18. https://doi.org/10.1128/AEM.02972-18

Varani A., Souza R.C., Nakaya H.I., Lima W.C. de, Almeida L.G.P. de, … Sluys M.-A.V., 2008. Origins of the *Xylella fastidiosa* prophage-like regions and their impact in genome differentiation. *PLOS ONE* 3: e4059. https://doi.org/10.1371/journal.pone.0004059

Varani A., Monteiro-Vitorello C.B., Nakaya H.I., Van Sluys M.-A., 2013. The role of prophage in plant-pathogenic bacteria. *Annual Review of Phytopathology* 51: 429–451. https://doi.org/10.1146/annurev-phyto-081211-173010

Velasco-Amo M.P., Vicent A., Zarco-Tejada P.J., Navas-Cortés J.A., Landa B.B., 2022. Recent research accomplishments on early detection of *Xylella fastidiosa* outbreaks in the Mediterranean Basin. *Phytopathologia Mediterranea* 61: 549–561. https://doi.org/10.36253/phyto-14171

Wick R.R., Holt K.E., 2022. Polypolish: Short-read polishing of long-read bacterial genome assemblies. *PLOS Computational Biology* 18: e1009802. https://doi.org/10.1371/journal.pcbi.1009802

Wick R.R., Judd L.M., Gorrie C.L., Holt K.E., 2017. Unicycler: Resolving bacterial genome assemblies from short and long sequencing reads. *PLOS Computational Biology* 13: e1005595. https://doi.org/10.1371/journal.pcbi.1005595

Wood D.E., Lu J., Langmead B., 2019. Improved metagenomic analysis with Kraken 2. *Genome Biology* 20: 257. https://doi.org/10.1186/s13059-019-1891-0

Xu M., Guo L., Gu S., Wang O., Zhang R., … Zhang Y., 2020. TGS-GapCloser: A fast and accurate gap closer for large genomes with low coverage of error-prone long reads. *GigaScience* 9: giaa094. https://doi.org/10.1093/gigascience/giaa094

Yu G., Smith D.K., Zhu H., Guan Y., Lam T.T.-Y., 2017. ggtree: an r package for visualization and annotation of phylogenetic trees with their covariates and other associated data. *Methods in Ecology and Evolution* 8: 28–36. https://doi.org/10.1111/2041-210X.12628

Yuan X., Morano L., Bromley R., Spring-Pearson S., Stouthamer R., Nunney L., 2010. Multilocus Sequence Typing of *Xylella fastidiosa* causing Pierce's Disease and Oleander Leaf Scorch in the United States. *Phytopathology* 100: 601–611. https://doi.org/10.1094/PHYTO-100-6-0601

Zimin A.V., Salzberg S.L., 2020. The genome polishing tool POLCA makes fast and accurate corrections in genome assemblies. *PLOS Computational Biology* 16: e1007981. https://doi.org/10.1371/journal.pcbi.1007981

Phytopathologia Mediterranea
The international journal of the
Mediterranean Phytopathological Union

Firenze University Press
www.fupress.com/pm

Research Papers

Combined interaction between the diazotrophic *Niallia circulans* strain YRNF1 and arbuscular mycorrhizal fungi in promoting growth of eggplant and mitigating root rot stress caused by *Rhizoctonia solani*

Younes M. RASHAD[1], Nahla Alsayd BOUQELLAH[2,*], Mohamed HAFEZ[3], Sara A. ABDALLA[1], Mohamed M. SLEEM[1], Adel K. MADBOULY[4]

[1] *Plant Protection and Biomolecular Diagnosis Department, Arid Lands Cultivation Research Institute (ALCRI), City of Scientific Research and Technological Applications (SRTA-City), New Borg El-Arab, Alexandria, 21934, Egypt*
[2] *Biology Department, College of Science, Taibah University, 42317-8599, Al Madinah Al Munawwarah, Saudi Arabia*
[3] *Land and Water Technologies Department, Arid Lands Cultivation Research Institute (ALCRI), City of Scientific Research and Technological Applications (SRTA-City), New Borg El-Arab, 21934, Egypt*
[4] *Microbiology Department, Faculty of Science, University of Ain Shams, Abbassia, Cairo, Egypt*
*Corresponding author. E-mail: nahlaalsaydbouqellah1992@gmail.com

Summary. Rhizoctonia root rot of eggplant, caused by *Rhizoctonia solani*, is an economically important disease. *Niallia circulans* YRNF1 and arbuscular mycorrhizal fungi (AMF) were assessed for their biocontrol and biofertilizing effects against *R. solani*, as potential replacements for synthetic fungicides and fertilizers. The diazotrophic *N. circulans* YRNF1, isolated from soil, reduced *in vitro* growth of *R. solani* by 42%. GC-MS analysis of culture filtrate of *N. circulans* YRNF1 detected bioactive compounds, including butyric acid (85%) and ethylene glycol (8%). In greenhouse experiments, combined application of *N. circulans* YRNF1 and AMF reduced the severity of eggplant root rot by 26%. This combined treatment triggered the transcriptional expression of five resistance genes (*JERF3, PAL1, C3H*, *CHI2*, and *HQT*) in the treated eggplants. Biochemical analyses of the infected eggplant roots treated with the combined bio-inoculants showed enhancement of the phenol content (+188%), and increased antioxidant enzyme activity, mainly of POD (+104%) and PPO (+72%). Combined application of *N. circulans* YRNF1 and AMF also promoted eggplant growth and improved the total NPK concentrations in treated plant leaves. Inoculation of eggplant with *N. circulans* YRNF1 in the presence of AMR increased the mycorrhization level. This is the first report of *N. circulans* and AMF as potential agents for biological control of Rhizoctonia root rot and growth promotion of eggplant.

Keywords. Biocontrol, mycorrhization, antifungal activity, biofertilizer, biofungicide.

OPEN ACCESS

Citation: Y.M. Rashad, N.A. Bouqellah, M. Hafez, S.A. Abdalla, M.M. Sleem, A.K. Madbouly (2024) Combined interaction between the diazotrophic *Niallia circulans* strain YRNF1 and arbuscular mycorrhizal fungi in promoting growth of eggplant and mitigating root rot stress caused by *Rhizoctonia solani*. *Phytopathologia Mediterranea* 63(1): 25-43. doi: 10.36253/phyto-14896

Accepted: February 19, 2024

Published: April 9, 2024

Data Availability Statement: All relevant data are within the paper and its Supporting Information files.

Competing Interests: The Author(s) declare(s) no conflict of interest.

Editor: Maurizio Vurro, National Research Council, (CNR), Bari, Italy.

ORCID:
YMR: 0000-0002-7702-8023
NAB: 0000-0002-2379-3475
MH: 0000-0001-9269-2128
SAA: 0000-0002-1050-2894
MMS: 0000-0002-2748-2615
AKM: 0000-0002-6261-9779

INTRODUCTION

Solanum melongena L. (eggplant) is the most important member of *Solanaceae* (Kaniyassery *et al*., 2022). China is the greatest eggplant producer and Egypt is the 3rd largest producer, recording annual production of 1,396,725 tons (FAOSTAT, 2024). Rhizoctonia root rot of eggplant is caused by *Rhizoctonia solani* Kühn (Almammory and Matloob, 2019). The soil-borne pathogen causes diseases of several hosts, including root rots, damping-off, leaf spots, and leaf blights, which result in a significant reductions in crop yields (Rashad *et al*., 2018).

Effective control of *R. solani* is difficult, due to its wide host range (Cook *et al*., 2002). The most widely used control method is application of synthetic fungicides, but these can have deleterious effects on human and animal health, may induce fungicide resistance in pathogens (Hollomon, 2015), and lead to environmental pollution (Baite *et al*., 2021). Biological control of plant diseases has received increasing attention as a possible effective, eco-friendly and safe control strategy against various plant diseases (Al-Askar *et al*., 2014).

Arbuscular mycorrhizal fungi (AMF: *Glomeromycotina*) live in symbiotic associations with more than 85% of the terrestrial plants (Spatafora *et al*., 2016; Mathur *et al*., 2018). AMF have been extensively studied as potential bio-protectants against several fungal pathogens, including *R. solani, Colletotrichum* spp., *Alternaria* spp., *Phytophthora* spp., *Fusarium* spp., and *Puccinia* spp. (Devi *et al*., 2022). AMF can also promote plant growth (de Oliveiraa *et al*., 2022). For example, mycorrhization of pea roots gave effective biocontrol of Rhizoctonia root rot (Rashad *et al*., 2022a). However, improvement of AMF biocontrol efficiency by application with other compatible antifungal microorganisms may also be worthwhile.

Nitrogen-fixing bacteria convert atmospheric nitrogen to ammonia, which can be absorbed by plants. These bacteria can promote plant growth, facilitate nutrient uptake and phosphorous solubilization, and produce siderophores and phytohormones (Shameem *et al*., 2023). In addition, *Bacillus circulans* CB7 Jordan, 1890 (now known as *Niallia circulans*), a non-symbiotic nitrogen-fixing bacterium, with plant growth-promoting properties due to auxin production, P-solubilization and siderophore production, has also shown antagonistic effects against *Dematophora necatrix* (Mehta *et al*., 2015).

Triggering immunity-related genes in plants is an important mode of action of biocontrol agents. Jasmonic acid and ethylene-response factor 3 gene (*JERF3*), the responsive gene that manages several defence-response genes through the jasmonate/ethylene signalling pathway, is elicited by abiotic and biotic plant stresses (Rashad *et al*., 2022b).

Polyphenols have potential as natural antioxidants, which can protect the living organisms from deleterious effects of the reactive oxygen species (ROS) (Elshafie *et al*., 2023). These compounds have antioxidant activity, as well as antihypertensive, antimicrobial, and antiviral activity (Losada-Barreiro *et al*., 2022). Excessive production of ROS causes oxidative stress in humans, leading to the development of several ailments (Forman, and Zhang, 2021). Antioxidant polyphenols have several modes of action, including reductive ability to neutralize ROS, chelation of metal ions that elicit the oxidative stress, inhibition of enzymes involved in the formation of ROS, and activation of the antioxidant enzymes (Dias *et al*., 2021). Upon infection of plants by the microbial pathogens, their cell walls accumulate large amounts of lignin (Rashad *et al*., 2020a). Increased lignification is a main barrier against the pathogen spread, and reduces the infiltration of toxins and fungal enzymes into plant cell walls. Lignin compounds also cause fungal pathogens to lose abilities to infect host plants, and prevent pathogen movement and multiplication (Ma *et al*., 2017). Flavonoids are plant responsive metabolites that contribute to host resistance in response to various abiotic and biotic stresses. These compounds act as physical or chemical barriers to prevent the microbial invasion, and are toxic defences against the microbial pathogens and/or insects. They interfere with pathogen cellular processes and structures (Ramaroson *et al*., 2022). The phenylalanine ammonia lyase 1 gene (*PAL1*) encodes phenylalanine ammonia lyase, which is involved in biosynthesis of polyphenolic compounds that have roles in host plant systemic resistance (Rashad *et al*., 2020a). During the early stages of lignin biosynthesis, the 4-coumarate 3-hydroxylase gene (*C3H*) catalyzes conversion of 4-coumarate to caffeate (Shrestha *et al*., 2022). The Chalcone isomerase 2 gene (*CHI2*) encodes for chalcone flavonone isomerase that catalyses the first two steps of flavonoid biosynthesis (Chao *et al*., 2021). Niggeweg *et al*. (2004) reported that the Hydroxycinnamoyl-CoA quinate hydroxycinnamoyl transferase gene (*HQT*) catalyzes biosynthesis of chlorogenic acid from caffeoyl-CoA and quinic acid.

The present study had the following objectives: 1) to investigate *in vitro* suppressive potential of the diazotrophic bacterium *N. circulans* YRNF1 against *R. solani*; 2) to assess biocontrol effects of a combined treatment with *N. circulans* YRNF1 and AMF on Rhizoctonia root rot of eggplant, 3) elucidate the host defensive mechanisms elicited by these combined bioagents, based on the transcription of some responsive genes, phenolic com-

pound content, and antioxidant activity; and 4) assess effects of combined bioagents on eggplant development.

MATERIALS AND METHODS

Fungi and eggplant cultivar

The pathogenic fungus *R. solani* (AG-2-2 IIIB) was provided from Mansoura University, Egypt. To prepare the inoculum, a 500 ml glass flask containing 100 g of sterilized oat grains mixed with sand (1:2 v:v) was aseptically inoculated with five discs (6 mm diam.) cut from a 5-d-old culture of *R. solani*, incubated at 28±2°C, and was shaken daily for two weeks to ensure uniform growth of the fungus (Youssef *et al.*, 2016). AMF inoculum (73% colonization index) was provided by the Agricultural Research Center (ARC), Giza, Egypt. The mixed inoculum of potential biocontrol AMF contained spores of *Claroideoglomus etunicatum* (W.N. Becker & Gerd.) C. Walker & A. Schüsler and *Rhizoglomus intraradices* (N.C. Schenck & G.S. Sm.) Sieverd, G.A. Silva & Oehl (in an equal ratio). AMF were propagated by inoculation of sterilized sandy-clay soil with 10 g of grain of the AMF inoculum (approx. 50 AM spores and root pieces g^{-1} soil). The inoculum was applied as a grain bed before planting grains of maize (potential host) in a sterilized plastic pot under the greenhouse conditions (27/22°C, 75% relative humidity, and 16 h daily light period). No fertilizers were added and irrigation was regularly applied to 50% field capacity. After 3 months, the AMF colonized roots were cut using a sterile scalpel into small segments, and were mixed with the AMF spores in the maize rhizosphere soil to be used as AMF inoculum (approx. 45 AM spores and mycorrhizal root pieces g^{-1} soil) (Nafady *et al.*, 2019). Seeds of the eggplant cultivar 'Rondona' were used, which were provided by the ARC, Giza, Egypt.

Collection of soil samples

Twenty-one soil samples were collected from several cultivated fields in Alexandria and El- Beheira governorates, Egypt, and were immediately transported to the laboratory. These samples were stored for subsequent studies at 4°C.

Isolation of the diazotrophic bacteria

Approximately 10 g of each soil sample were added aseptically to 90 mL of sterilized water in an Erlenmeyer flask, vigorously mixed for 45 min at 150 rpm, and then serial dilutions were prepared (10^{-1} to 10^{-4}). Diazotrophic bacteria were isolated from the soil according to Döbereiner (1988) with slight modifications. Plates of nitrogen free (NF) agar medium, containing glucose (20 g L^{-1}); K_2HPO_4 (0.2 g L^{-1}), NaCl (0.2 g L^{-1}), $MgSO_4.7H_2O$ (0.2 g L^{-1}), K_2SO_4 (0.1 g L^{-1}), $CaCO_3$ (5 g L^{-1}), and agar (20 g L^{-1}), were individually inoculated with 0.1 mL of each serial dilution of soil suspension; Three replicated plates were used for each dilution. The plates were then incubated for 5 d at 28±2°C. Growing bacterial colonies were then singly transferred onto fresh NF plates and incubated at the same conditions. The resulting cultures were stored in 15% glycerol at -80°C until used (Kifle and Laing, 2016).

Screening of the diazotrophic bacteria for antifungal potential against R. solani

The ability of the isolated diazotrophic bacteria to antagonize *R. solani* was evaluated using the *in vitro* dual plate method (Jasim *et al.*, 2016) on potato dextrose agar plates (PDA, Difco). In each plate, 10 µL of each bacterial isolate (10^6 cells mL^{-1}) were streaked aseptically as a longitudinal line 2 cm away from the border of the plate. A disc (6 mm diam.) cut from a freshly grown *R. solani* culture was placed 20 mm from the opposite side of the plate. Plates inoculated only with pathogen discs served as experimental controls. Each treatment was applied in six replicates, and the assay was repeated twice. After incubating the plates for 4 d at 25°C, and upon complete coverage of control plates with fungal growth, inhibition of fungal growth in the dual plates was measured using a calibrated ruler, and compared with the fungal diameter in the corresponding control plate. Suppression of the fungal growth (S %) was determined using the equation of Ferreira *et al.* (1991):

$$S\,\% = \frac{C - T}{C} \times 100$$

where C = radial growth in the control plate, and T = radial growth in the treated plate.

Biochemical analyses of bacterial culture filtrate using gas chromatography-mass spectrometry (GC-MS)

Secondary metabolites in cell free culture filtrate of *N. circulans* YRNF1 were identified qualitatively using GC-MS. The culture filtrate of *N. circulans* YRNF1 was obtained by inoculating 200 µL of the bacterial suspension in sterile distilled water (6×10^6 cfu mL^{-1}) into a 500 mL capacity Erlenmeyer flask containing 250 mL of

nutrient broth (NB) [1% (w/v) each of beef extract and peptone, and 5% (w/v) NaCl]. The culture was incubated under shaking at 120 rpm at 28°C (Nisa *et al.*, 2019). After 3 d, the NB was centrifuged for 10 min. at 4°C at 11,200 g (Thermo Fisher Scientific). The collected cell-free supernatant was filter sterilized using 0.22 µm filters (Millex-GS, Millipore). The cell-free culture filtrate was lyophilized to complete dryness, re-suspended in methoxyamine hydrochloride (50 µL) dissolved in pyridine, followed by incubation for 90 min. For derivatization of the sample, 50 µL of silylation reagent [bis(trimethylsilyl) trifluoroacetamide + trimethylchloro-silane, 99:1 v:v] were added to the sample. The GC-MS system (GCMS-QP2010 Plus, Shimadzu), equipped with a gas chromatograph (7890B) and a mass spectrometer detector (5977A), was used to analyze the sample, at the Central Laboratories Network, NRC, Giza, Egypt. This system involved an HP-5MS column (30 m × 0.25 mm × 0.25 µm). Hydrogen was used as the carrier gas at the flow rate of 2.0 mL min^{-1}. In this assay, 1 µL was used as an injection volume according to several processing conditions, including 50°C for 5 min, which rose at 10°C min^{-1} to 100°C, and then at 20°C min^{-1} to 320°C. Mass spectra were obtained by electron ionization (EI) at 70 eV, involving a spectral range of m/z 50–700, and a solvent delay of 4 min, where 230°C was the mass temperature used and the Quad was at 150°C. Biochemical characterization of the different bacterial filtrate constituents was obtained by comparing the spectrum fragmentation pattern with that stored in the data of Wiley and the National Institute of Standards and Technology (NIST) Mass Spectral Library.

*Detection of the nitrogenase gene (*nifH*)*

Presence of the nitrogenase (*nifH*) gene was detected in the isolated diazotrophic bacteria according to Tan *et al.* (2009), as follows:

DNA extraction. A 2-d culture of each bacterial isolate grown on NF medium was centrifuged for 2 min at 1792 g. The resulting pellet was re-suspended in sterilized water (100 mL) and re-centrifuged for an additional 2 min at 1792 g, followed by heating in a water bath (90°C) for 10 min. After re-centrifugation, the supernatant was added to a sterile tube (0.5 mL capacity) and used as a DNA template. The resulting crude DNA concentration was estimated at using a UV spectrophotometer at OD_{260} and OD_{280} (PERSEE).

Polymerase chain reaction (PCR). The reaction mixture (25 mL) of PCR reaction involved a template DNA (≈ 100 ng); primer (1 mM of each primer), DNA polymerase (25 μL^{-1}), 5 × buffer, $MgCl_2$ (1 mM), dNTPs (0.2 mM), and sterile H_2O. Sequences of the *nifH* primers used were as follows: *nifH*-F (5'AAAGGYGGWATCG-GYAARTCCACCAC3') and *nif*H-R (5'TTGTTSGCS-GCRTACATSGCCATCAT3') (Turk-Kubo *et al.*, 2012). The processing reaction was conducted on a thermocycler (Eppendorf) under processing conditions of one cycle (95°C for 3 min), then 30 cycles (each of 95°C for 1 min, 52°C for 1 min, 72°C for 1 min, and 72°C for 5 min).

Molecular identification of the selected bacterium using 16S rRNA gene

DNA of the promising nitrogen-fixing bacterial isolate was subjected to amplification of the 16S-rRNA region, using the primer 16S-27F: 5'-AGAGTTTGATC-MTGGCTCAG-3' and 16S-1492R: 5'-CGGTTACCTT-GTTACGACTT-3' (dos Santos *et al.*, 2019). The PCR mixture was subjected to the Exosap-IT (GE Healthcare) PCR clean up protocol. The 16S rRNA gene nucleotide sequence was determined through Sanger sequencing using the DNA Analyzer of Applied Biosystems 3730 × l. Using the Big Dye Terminator from ABI; the two primers 27b F and 1492uR were used for setting up the PCR reactions (dos Santos *et al.*, 2019). The Vector NTI software (Invitrogen) was used to align the sequences from the forward and reverse primers, while the contigs were subjected to BLAST to search for nucleotide similarity (Zhang *et al.*, 2000). The maximum likelihood method through MEGA X software (10.2.4) was used to generate a phylogenetic tree of the selected isolate.

Greenhouse experiment

Eggplant seeds were surface sterilized (using 0.05% sodium hypochlorite) and planted (one per pot) into 20 cm diam. plastic pots containing sterilized clay soil. The soil physical composition was: silt (35 ± 0.13 g kg^{-1}), sand (110.2 ± 0.21 g kg^{-1}), and clay (453 ± 0.18 g kg^{-1}). The soil chemical properties were: pH = 7.58, EC, 1.32 dS m^{-1}, available P (26 mg kg^{-1}), total N (2.84 g kg^{-1}), available K (310 mg kg^{-1}), organic matter (1.72 g kg^{-1}), total organic carbon (0.99 g kg^{-1}), and total $CaCO_3$ (5.9%). For AMF colonization, an AMF inoculum was added to each pot under the seeds (10 g $seed^{-1}$ of the AMF inoculum). Infestation of the soil was carried out by mixing the upper layer with the *R. solani* inoculum (3% w/w), and the pots were watered daily for 10 d before planting. For preparation of bacterial inoculum, the diazotrophic bacterium *N. circulans* strain YRNF1 was grown in NF broth on a rotary shaker for 3 d. The resulting bacterial suspension (adjusted at 10^8 cell mL^{-1}) was mixed with 1% Arabic gum. For application of *N. circulans* YRNF1,

eggplant seeds were soaked for 30 min before planting in freshly prepared bacterial inoculum. Three hours before planting, the seeds in control pots were treated with the fludioxonil (50.0%) fungicide at 3.5 mL kg^{-1} as a positive fungicide control. The negative control involved a set of pots that was untreated. Nine treatments were applied in this experiment. These were:

- non-mycorrhizal, untreated, uninfected plants (designated C);
- non-mycorrhizal, untreated and infected plants (P);
- non-mycorrhizal, treated with *N. circulans* YRNF1 and uninfected plants (B);
- mycorrhizal, untreated and uninfected plants (M);
- mycorrhizal, treated with *N. circulans* YRNF1 and uninfected plants (B+M);
- non-mycorrhizal, treated with *N. circulans* YRNF1 and infected plants (B+P);
- mycorrhizal, untreated and infected plants (M+P);
- non-mycorrhizal, treated with the fungicide and infected plants (F+P); and
- mycorrhizal, treated with *N. circulans* YRNF1 and infected plants (B+M+P).

No fertilization was applied in this experiment. Five replicates were used, and the pots were arranged in a randomized complete block design. They were maintained at 70% relative humidity, in a 27°C day 17°C night temperature regime in a greenhouse, and were irrigated with tap water when necessary. This experiment was repeated twice

Assessment of the disease severity

Five plants from each treatment were carefully uprooted, and the adhering soil was removed with tap water. The disease severity was evaluated according to Wen *et al.* (2005). This scale included six severity categories: 0 = no necrosis; 1 = small root necroses (2.5 mm length); 2 = necrosis (2.5–5 mm); 3 = necrosis ≥ 5 mm; 4 = crown and shoots covered with necrotic lesions; or 5 = seedlings damped-off. The disease severity (DS%) was estimated according to Taheri and Tarighi (2010):

$$\mathrm{DS}\ (\%) = \frac{1n1 + 2n2 + 3n3 + 4n4 + 5n5}{5N} \times 100$$

where n1 was the number of plants that had severity category 1; n2 was number of plants that had level 2; *etc*., and N was the total number of evaluated plants.

Quantifying the expression of the defense-related genes using qPCR

Transcription of some responsive genes in eggplant roots was quantified at 14 d post planting (dpp). The studied genes included *JERF3*, *PAL1*, *C3H*, *CHI2*, and *HQT*. *α*-Tubulin and *β*-actin were used as reference genes, based on their stability in the mycorrhizal plants (Fuentes *et al*., 2016). The primer sequences used are shown in Table 1. The RNeasy Kit (Qiagen) was used for extraction of total RNA, in accordance with the manufacturer's instructions. A SureCycler 8800 (Agilent, USA) was used to synthesize the cDNA. The total volume (20 µL) of the reaction mixture was composed of 3.5 µL RNase-free H_2O; 3 µL 5×-buffer; 3 µL RNA (30 ng), 3 µL of dNTPs (10 mM), 7 µL of dT primer (5 pmol μL^{-1}), and 0.5 µL of the RT enzyme.

The reaction was carried out using the RotorGen 6000 (Qiagen) real-time system The qPCR was run for 1 h at 43°C, then 10 min at 71°C. The qPCR mixture consisted of 3 µL cDNA, 1.6 µL sterile water, 1.5 µL of each

Table 1. Primer sequences of the defense-related genes used in this study (Rashad *et al*., 2020b).

Primer name	Abbreviation		(5'-3')
Jasmonate and ethylene-responsive factor 3	*JERF3*	F	GCCATTTGCCTTCTCTGCTTC
		R	GCAGCAGCATCCTTGTCTGA
Phenylalanine ammonia lyase 1	*PAL1*	F	ACGGGTTGCCATCTAATCTGACA
		R	CGAGCAATAAGAAGCCATCGCAAT
4-coumarate 3-hydroxylase	*C3H*	F	TTGGTGGCTACGACATTCCTAAGG
		R	GGTCTGAACTCCAATGGGTTATTCC
Chalcone isomerase 2	*CHI2*	F	GGCAGGCCATTGAAAAGTTCC
		R	CTAATCGTCAATGATCCAAGCGG
Hydroxycinnamoyl-CoA quinate hydroxycinnamoyl transferase	*HQT*	F	CCCAATGGCTGGAAGATTAGCTA
		R	CATGAATCACTTTCAGCCTCAACAA
α-tubulin	*α*-tubulin	F	TATCTGCTACCAGGCTCCCGAGAA
		R	TGGTGTTGGACAGCATGCAGACAG
β-actin	*β*-actin	F	GTGGGCCGCTCTAGGCACCAA
		R	CTCTTTGATGTCACGCACGATTTC

primer, and 12.4 µL 2× SYBR® Green Mix. The qPCR reaction was run with one cycle at 95°C (for 3 min), 45 cycles each of 95°C for 15 s and 56°C for 35 s, then 75°C for 250 s. The comparative CT method ($2^{-\Delta\Delta CT}$) was used to estimate the transcriptional expression of the tested genes, in accordance with Schmittgen and Livak (2008). Triplicates of each treatment (biological and technical) were used, and the assay was conducted twice.

Determination of the biochemical plant defense responses

At 30 dpp, samples from the eggplant roots were collected from each treatment. Estimation of the total phenolics, and activities of peroxidase (POD) and polyphenol oxidase (PPO) were assessed (five replicates). The Folin-Ciocalteu test was used to determine the total phenolic content (Singleton *et al.*, 1999). Approximately 1 g of roots was ground in 5 mL of 80% methanol, at 5°C overnight. This homogenate was then centrifuged at 1344 g for 10 min. The supernatant (100 µL) was then mixed with 20% Na_2CO_3 (50 µL), 1750 µL of dH_2O, and 250 µL of Folin-Ciocalteu reagent (Sigma-Aldrich), and the resulting mixture was left at 40°C for 35 min. Caffeic acid was used as a reference. Phenolic contents were estimated using spectrophotometry at 760 nm. For POD activity determination, approx. 1 g of the root was ground in 3 mL of 0.1 M Na_2HPO_4 buffer, and the homogenate was centrifuged for 10 min at 1792 g. POD enzyme activity was estimated spectrophotometrically at 470 nm, which was represented as ΔA_{470} min^{-1} g^{-1} f wt (Gong *et al.*, 2001). Estimation of the PPO activity was carried out according to Singh and Ravindranath (1994). Five g of root tissue were homogenized and kept for 35 min in acetone at 4°C. PPO enzyme potential was evaluated spectrophotometrically at 420 nm using catechin as the substrate, and was recorded as ΔA_{420} min^{-1} g^{-1} f wt.

Estimation of levels of plant mycorrhization

Mycorrhizal colonization in eggplant roots was estimated 45 dpp according to Trouvelot *et al.* (1986). Plant roots were fragmented (10 mm diam.) using a scalpel and were boiled in 10% potassium hydroxide solution. The treated segments were stained using 0.05% trypan-blue, as described by Phillips and Hayman (1970). For each root treatment, approx. 50 stained fragments were checked under a light microscope. Three mycorrhization parameters were assessed, including frequency of mycorrhizal colonization, colonization intensity, and frequency of formation of arbuscules (Trouvelot *et al.*, 1986). Estimation of mycorrhization was repeated twice, each time on 50 stained fragments.

Evaluation of the eggplant growth parameters

At 45 dpp, approx. five replicate eggplant were carefully uprooted. Adhering soil particles were removed and plant growth was estimated using the following parameters: shoot height, root length, shoot and root dry weights, and leaf area. For the evaluation of the dry weights, the plants were dried at 80°C in an oven (3 d). This assay was conducted twice.

Influence of bioagents on macronutrient contents of eggplant leaves

For quantitative analysis of the nutrients content in eggplant leaves, approx. ten leaves from each treatment were collected, and then air dried. The leaves were fragmented using a grinding machine, and then used for estimation of the total contents of nitrogen (N), phosphorus (P), and potassium (K). Using Kjeldhal assays, N was estimated by titration following distillation (Goyal *et al.*, 2022). Total P was evaluated as per Singh *et al.* (2022). Total K was determined based on Goyal *et al.* (2022). Determinations were each carried out twice.

Statistical analyses

The results were statistically analyzed using CoStat software 6.4. Data were checked for normality before applying the analyses of variance. Treatment means were compared using Tukey's HSD test ($P \leq 0.05$).

RESULTS

Antagonistic potential of the isolated diazotrophic bacteria against R. solani

Eight isolates of diazotrophic bacteria were recovered from the collected soil samples. Results of the *in vitro* antifungal assays against *R. solani* showed that inhibition of *R. solani* mycelial growth varied among the eight isolates ranging from no inhibition to medium inhibition. The greatest level of growth inhibition (42% growth, compared to control plates) was observed with the isolate designated as YRNF (Figure 1, a and b). Growth of the *R. solani* colony was suppressed and the colony had an arc-shaped border with the diazotrophic bacterium YRNF1, with a clear no-growth zone in

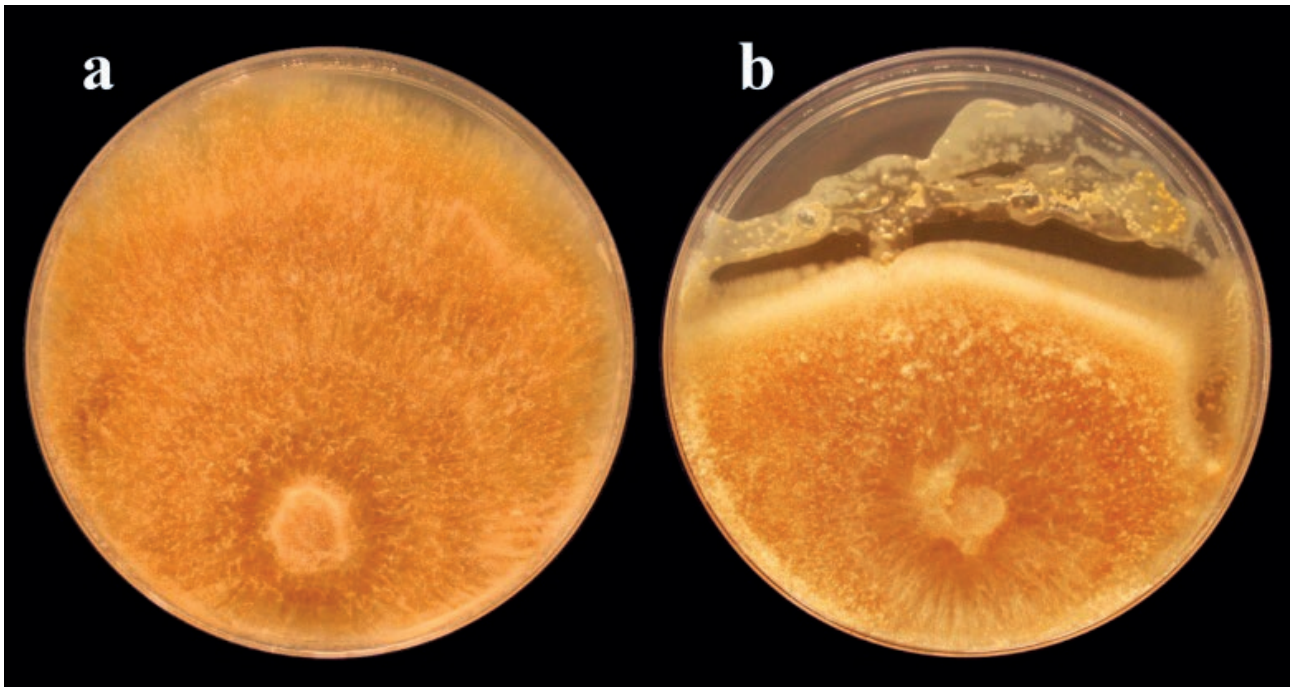

Figure 1. *In vitro* antagonism of the diazotrophic bacterium *Niallia circulans* strain YRNF1 against *Rhizoctonia solani*. Confrontation test in dual culture; a) Unchallenged *R. solani* (control); b) *R. solani* challenged by *N. circulans* strain YRNF1.

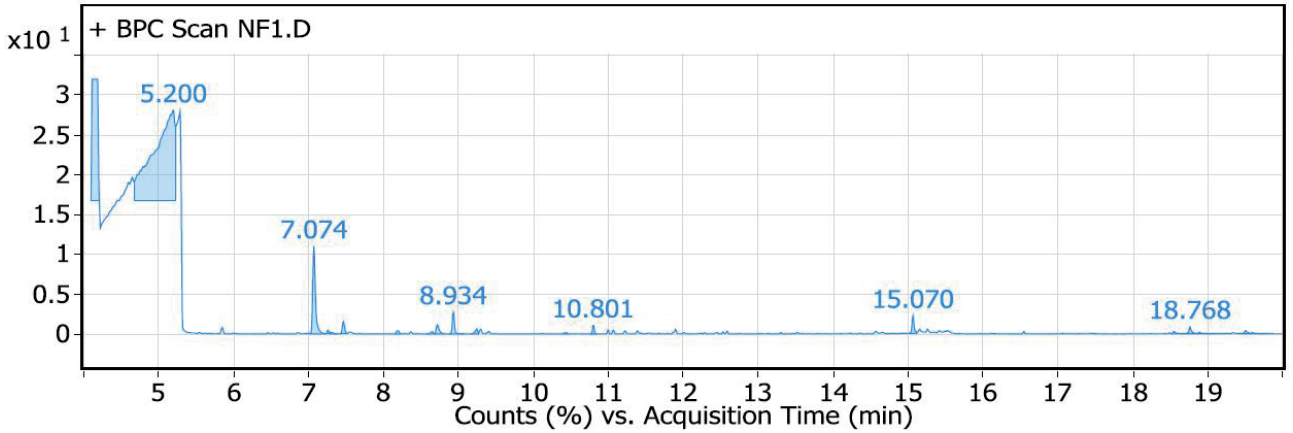

Figure 2. GC-MS chromatogram of the secondary metabolites detected in culture filtrates of *Niallia circulans* YRNF1.

between the fungus and bacterium, indicating release of antifungal metabolites by the bacterium, and an antibiosis-based mechanism of antifungal activity (Figure 1).

GC-MS analysis of the bacterial culture filtrate

Nineteen chemical constituents were detected in the culture filtrate of *N. circulans* YRNF1, which were identified by the GC-MS analysis (Figure 2). As presented in Table 2, the major biochemical constituents were butyric acid (85%) and ethylene glycol (8%). Some metabolites were recorded at intermediate proportions, including lactic acid, propanoic acid, 2-[(trimethylsilyl)oxy]-, trimethylsilyl ester (2TMS) derivative (1.5%) and α-D-mannopyranoside, methyl, cyclic 2,3:4,6-bis (butylboronate) (1.2%). The least detected components were β-hydroxyquebrachamine; 1,3-Dipalmitin trimethylsilyl ester (TMS) derivative; octadecanoic acid, 2,3-bis[(trimethylsilyl) oxylpropyl ester (Glycerol mon-

Table 2. Secondary metabolites identified in culture filtrates of *Niallia circulans* YRNF1.

Peak no.	Retention time (min)	Peak area (%)	Compound name	Chemical formula
1	4.153	23.11	Butyric Acid, TMS derivative	$C_7H_{16}O_2Si$
2	5.2	61.53	Butyric acid	$C_4H_8O_2$
3	7.074	7.75	Ethylene glycol, 2TMS derivative	$C_8H_{22}O_2Si_2$
4	7.265	0.22	Cyclobarbital	$C_{12}H_{16}N_2O_3$
5	7.309	0.16	2,4,6(1H,3H,5H)-Pyrimidinetrione, 5-(1-cyclohexen-1-yl)-5-ethyl-	$C_{12}H_{16}N_2O_3$
6	7.47	0.91	Propylene glycol, 2TMS derivative	$C_9H_{24}O_2Si_2$
7	8.195	0.28	2-Ethoxyethanol, TMS derivative	$C_7H_{18}O_2Si$
8	8.649	0.17	Cedran-diol, 8S,13-	$C_{15}H_{26}O_2$
9	8.722	0.85	1-Ethyl-1-(2-phenylethoxy)-1-silacyclohexane	$C_{15}H_{24}OSi$
10	8.934	1.48	Lactic Acid, 2TMS derivative	$C_9H_{22}O_3Si_2$
11	9.249	0.4	β-D-Galactopyranoside, methyl 2,3-bis-O-(trimethylsilyl)-, cyclic butylboronate	$C_{17}H_{37}BO_6Si_2$
12	10.443	0.11	β-Hydroxyquebrachamine	$C_{19}H_{26}N_2O$
13	10.801	0.46	Acetin, bis-1,3-trimethylsilyl ether	$C_{11}H_{26}O_4Si_2$
14	15.07	1.19	α-D-Mannopyranoside, methyl, cyclic 2,3:4,6-bis (butylboronate)	$C_{15}H_{28}B_2O_6$
15	18.555	0.23	1-Heptatriacotanol	$C_{37}H_{76}O$
16	18.768	0.57	1-Monopalmitin, 2TMS derivative	$C_{25}H_{54}O_4Si_2$
17	18.892	0.13	1,3-Dipalmitin trimethylsilyl ester (TMS) derivative	$C_{38}H_{76}O_5Si$
18	19.507	0.31	2-Oleoylglycerol, 2TMS derivative	$C_{27}H_{56}O_4Si_2$
19	19.603	0.14	Glycerol monostearate, 2TMS derivative	$C_{27}H_{58}O_4Si_2$

ostearate, 2TMS derivative); 2,4,6(1H,3H,5H)-pyrimidine-trione, 5-(1-cyclohexen-1-yl)-5-ethyl- (cyclobarbital), and cedrane-8,13-diol (cedran-diol, 8S,13-).

Detection of the nitrogenase gene (nifH) in the diazotrophic bacteria

Results obtained from PCR analyses showed that the selected isolate YRNF1 possessed the *nifH* nitrogenase gene, which was observed as a single band at 450 bp (Figure 3). This indicated that the isolate was a nitrogen fixing bacterium.

Molecular identification of the diazotrophic bacterium YRNF1

Results of BLAST analysis of the 16S rRNA sequence showed that the diazotrophic bacterial strain YRNF1 had 99.71% similarity with *N. circulans* (reference strain MH130347). The nucleotide sequence of *N. circulans* YRNF1 was deposited in the GenBank under accession number OP703372. The phylogenetic analysis of *N. circulans* YRNF1 in comparison to ten species of the genus *Bacillus* (Figure 4) showed that the strain grouped with *B. circulans* (MW547978) in a single distinct clade, with 66% bootstrap support. The *Bacillus* spp. strains clustered in two major groups. The first contained *B. altitudenis* (MK424248), *B. velezensis* (MG651075), and *B. subtilis* (HE610894), with 70% bootstrap support. *Bacillus mycoides* (ON464184) clustered with 64% bootstrap support in the other clade, while *B. toyonensis* (MZ773910) represented an outgroup. The second major group also included *B. licheniformis* (MK280728) and *B. amyloliquefaciens* (MF423459), with 64% bootstrap support, and clustered in a separate clade. The other clade involved *B. cereus* (OQ152624) and *B. thuringiensis* (MY912020), with 62% bootstrap support.

Disease severity

Mean severity of Rhizoctonia root rot in the infected, non-treated eggplant plants was 69%, which was the greatest of the nine treatments. Control plants with either one of the two bio-inoculants had no disease. Moderate disease severity was observed for the infected plants inoculated with *N. circulans* YRNF1 (45%), and 32% for that inoculated with AMF. Application of both bio-inoculants reduced disease severity by 26% compared to the non-treated infected plants. This indicated additive activity of these two bio-inoculants. Treatment with fludioxonil decreased the disease severity by 25% (Figure 5).

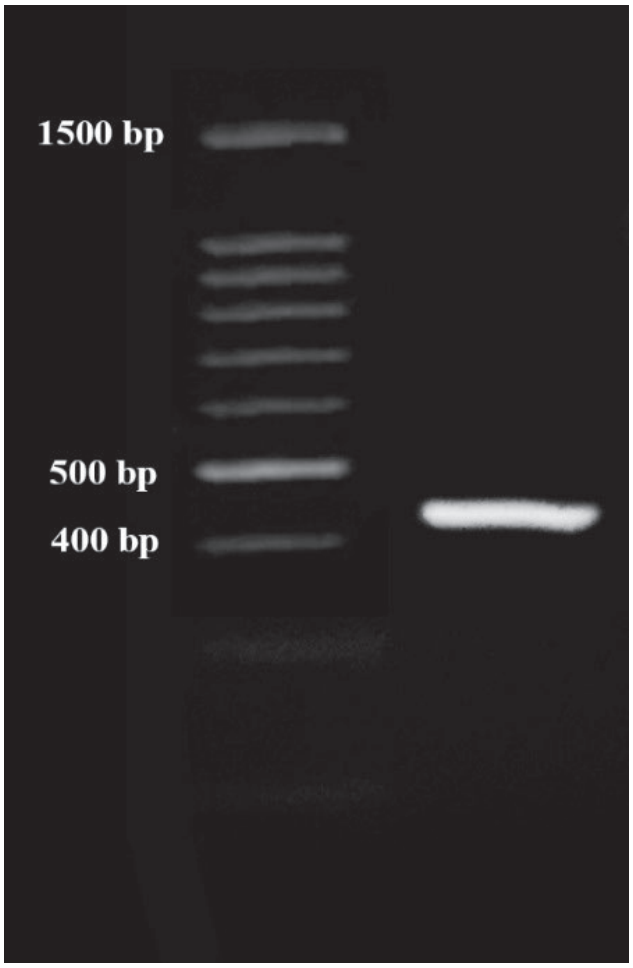

Figure 3. Agarose gel showing the amplified DNA product of the nitrogenase gene (*nifH*) of the diazotrophic bacterium YRNF1 as a single band (450 bp).

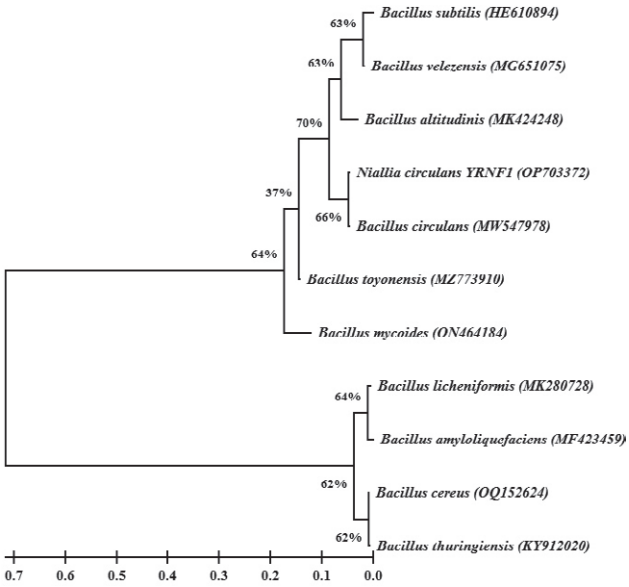

Figure 4. Phylogenetic tree of the diazotrophic bacterium *Niallia circulans* YRNF1.

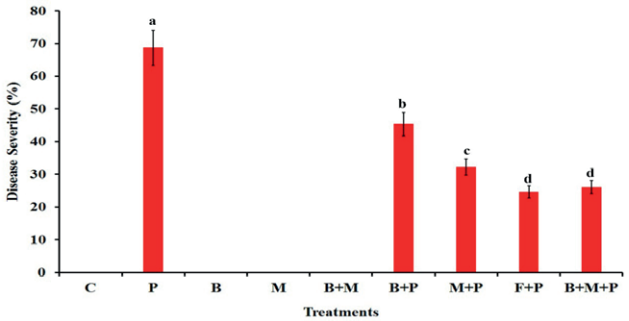

Figure 5. Mean root rot disease severities of eggplant plants treated with the diazotrophic bacterium *Niallia circulans* YRNF1 and/or AMF. Columns accompanied by the same superscript letters are not significantly different (Tukey's HSD test, $P \leq 0.05$). Error bars are Standard deviations (± SD). Treatments were: C, non-mycorrhizal, untreated and uninfected; P, non-mycorrhizal, untreated and infected; B, non-mycorrhizal, treated with *N. circulans* YRNF1 and uninfected; M, mycorrhizal, untreated and uninfected; B+M, mycorrhizal, treated with *N. circulans* YRNF1 and uninfected; B+P, non-mycorrhizal, treated with *N. circulans* YRNF1 and infected; M+P, mycorrhizal, untreated and infected; F+P, non-mycorrhizal, treated with the fungicide and infected; and B+M+P, mycorrhizal, treated with *N. circulans* YRNF1 and infected.

Triggering of the resistance-related genes in eggplant roots

Transcriptional expression of the resistance genes *JERF3, PAL1, C3H, CHI2,* and *HQT* in eggplant roots inoculated with *N. circulans* YRNF1 and colonized with AMF is shown in Figure 6. Compared to the control treatment, all of the experimental treatments elicited expression of *JERF3*. Combined application of *N. circulans* YRNF1 and AMF up-regulated the *JERF3* gene more than the single treatments. The greatest gene expression (29.4-fold) was for infected eggplant roots after inoculation with *N. circulans* YRNF1 and colonization by the AMF. Both applied bioagents increased the expression of *PAL1,* compared to the control plants. Greatest gene expression (17-fold) was for infected eggplant roots inoculated with *N. circulans* YRNF1 and colonized with the AMF. This was the same for *C3H,* where all the treatments induced expression of this gene, compared to the control treatment. Overexpression (8.6-fold) was detected for infected eggplant roots inoculated with *N. circulans* YRNF1 and colonized with the AMF. The applied treatments up-regulated expression of *CHI2*

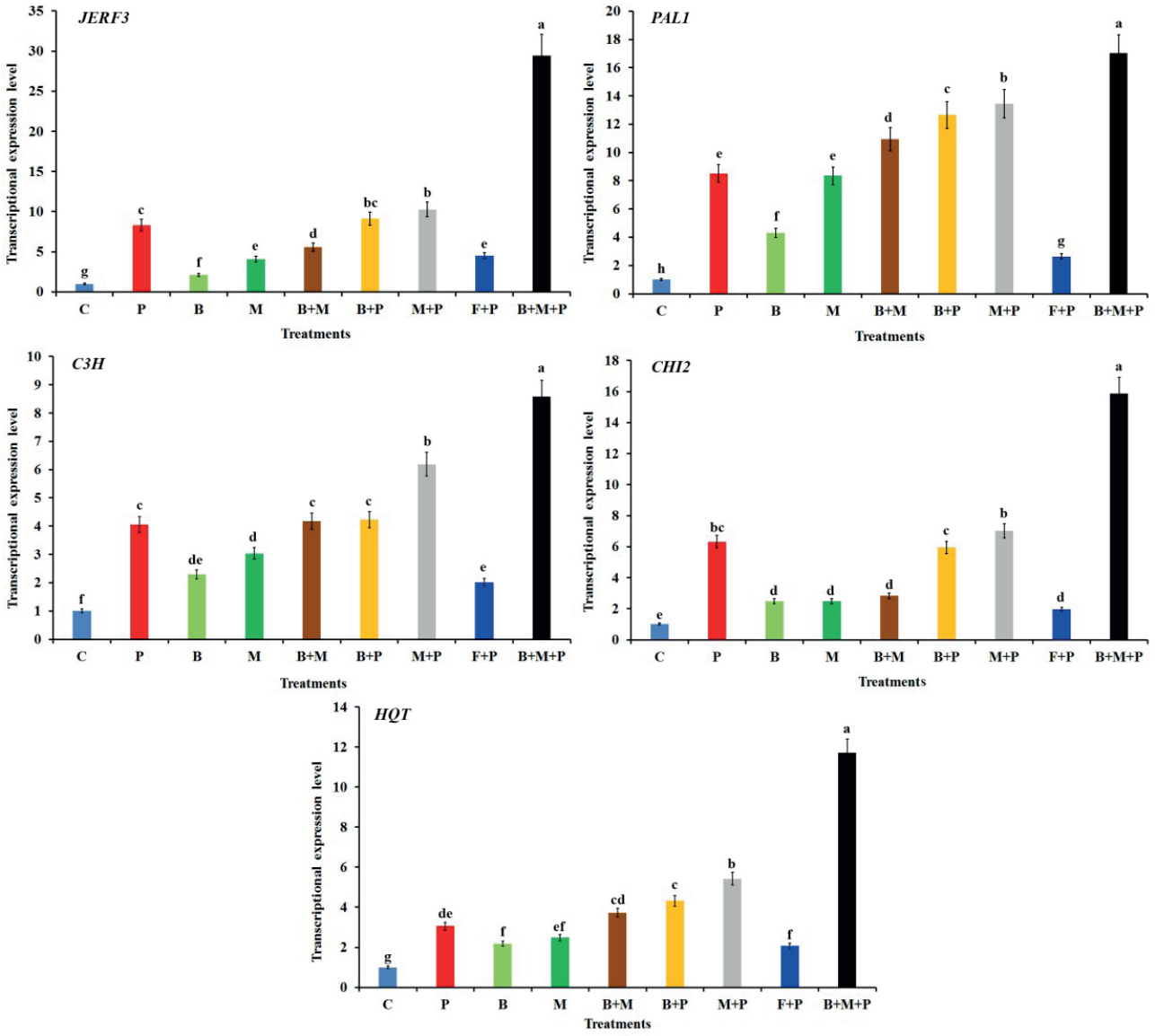

Figure 6. Mean transcriptional expression of resistance genes (*JERF3*, *PAL1*, *C3H*, *CHI2*, and *HQT*) in eggplant roots treated with *Niallia circulans* YRNF1 and colonized with AMF and inoculated with *Rhizoctonia solani*. For each gene, columns accompanied by the same superscript letter are not different ($P \leq 0.05$), according to Tukey's HSD test. The error bars are the standard deviations of the means. The experimental treatments were: C, non-mycorrhizal, untreated and uninfected; P, non-mycorrhizal, untreated and infected; B, non-mycorrhizal, treated with *N. circulans* YRNF1 and uninfected; M, mycorrhizal, untreated and uninfected; B+M, mycorrhizal, treated with *N. circulans* YRNF1 and uninfected; B+P, non-mycorrhizal, treated with *N. circulans* YRNF1 and infected; M+P, mycorrhizal, untreated and infected; F+P, non-mycorrhizal, treated with the fungicide and infected; and B+M+P, mycorrhizal, treated with *N. circulans* YRNF1 and infected.

at varying levels compared to the untreated non-infected eggplants, with greatest expression of this gene recorded value showing a 15.9-fold increase. Application of all the treatments led to overexpression of *HQT*, compared to the control plants. The infected eggplant roots inoculated with *N. circulans* YRNF1 and colonized with the AMF had maximum expression of 11.7-fold.

Effects of bioagents on phenol levels and antioxidant enzyme activities in treated eggplant roots

Eggplants challenged with *N. circulans* YRNF1 and AMF and inoculated with *R. solani* had increased level in total phenol contents, and increased POD and PPO enzyme potential (Table 3). At 30 dpp, mean phenolic content increased in the infected, non-treated eggplant

Table 3. Mean phenolic contents and antioxidant enzyme (POD or PPO) activities in eggplant roots 30 d after inoculation with *Rhizoctonia solani* and treatments with *Niallia circulans* YRNF1 and/or mycorrhizae.

Treatment	Phenolic content ($mg^{-1}g^{-1}$ f wt)*	POD (ΔA_{470} min^{-1} g^{-1} f wt)*	PPO (ΔA_{420} min^{-1} g^{-1} f wt)*
C	415.7 ± 8.19^{f}	1.14 ± 0.07^{h}	1.08 ± 0.05^{g}
P	673.2 ± 11.20^{d}	1.53 ± 0.05^{e}	1.34 ± 0.04^{e}
B	579.0 ± 7.32^{e}	1.38 ± 0.05^{f}	1.24 ± 0.05^{f}
M	594.4 ± 8.17^{e}	1.76 ± 0.09^{d}	1.56 ± 0.07^{c}
B+M	763.3 ± 8.41^{c}	1.90 ± 0.07^{c}	1.47 ± 0.09^{d}
B+P	772.5 ± 10.50^{c}	1.68 ± 0.05^{d}	1.57 ± 0.07^{c}
M+P	832.4 ± 9.13^{b}	2.12 ± 0.08^{b}	1.69 ± 0.05^{b}
F+P	668.2 ± 4.88^{d}	1.25 ± 0.04^{g}	1.29 ± 0.07^{ef}
B+M+P	1197.4 ± 12.02^{a}	2.32 ± 0.08^{a}	1.86 ± 0.09^{a}

*Means followed by different superscript letters are significantly different ($P \leq 0.05$), according to Tukey's HSD tests. The data are means of five replicates ± SD. Treatments applied were: C, non-mycorrhizal, untreated and uninfected; P, non-mycorrhizal, untreated and infected; B, non-mycorrhizal, treated with *N. circulans* YRNF1 and uninfected; M, mycorrhizal, untreated and uninfected; B+M, mycorrhizal, treated with *N. circulans* YRNF1 and uninfected; B+P, non-mycorrhizal, treated with *N. circulans* YRNF1 and infected; M+P, mycorrhizal, untreated and infected; F+P, non-mycorrhizal, treated with the fungicide and infected; B+M+P, mycorrhizal, treated with *N. circulans* YRNF1 and infected, and peroxidase (POD) and polyphenol oxidase (PPO).

roots, to 673.2 mg g^{-1} f wt compared to the control plants (415.7 mg g^{-1} f wt). Phenolic content of the non-infected eggplant roots treated with *N. circulans* YRNF1 was 579.0 mg g^{-1} f wt, and for roots treated with AMF was 594.4 mg g^{-1} f wt. Combination of both bio-inoculants increased phenolic content of the non-infected eggplant roots to 763.3 mg g^{-1} f wt. Treatment of the infected eggplant roots with a combination of both bioagents resulted in increased phenolic content up to 1197.4 mg g^{-1} f wt. Application of fludioxonil increased phenolic content to 668.2 mg g^{-1} f wt.

Compared to the control plants, POD enzyme activity increased in the infected non-treated eggplant roots to 1.53 ΔA_{470} min^{-1} g^{-1} f wt, and for PPO activity increased to 1.34 ΔA_{420} min^{-1} g^{-1} f wt. Enhancements in POD and PPO potential were recorded after treatments of plants with the two bio-agents, either singly or in combination. Greatest activity of both enzymes was recorded in the infected eggplant roots treated with *N. circulans* YRNF1 (2.32 ΔA_{470} min^{-1} g^{-1} f wt) and AMF (1.86 ΔA_{420} min^{-1} g^{-1} f wt). Compared to *R. solani*-inoculated non-treated plants, activity of both enzymes increased after treatment of infected roots with both bio-inoculants. However, the increases in enzyme activity attributable to the combined treatment (B+M+P) was higher than each single treatment. Application of the fungicide resulted in a recognizable increase in the POD and PPO activity, compared to the control plants.

Mycorrhization of eggplants after treatment with Niallia circulans *YRNF1*

Effects of *N. circulans* YRNF1 on mycorrhizal colonization of eggplant roots infected with *R. solani* are summarized in Table 4. Eggplant roots un-treated with AMF did not develop mycorrhizal colonization. In contrast, all eggplant roots treated with AMF showed varying levels of mycorrhization. Greatest colonization parameters were recorded for roots treated with *N. circulans* YRNF1 and AMF, which gave means of 88.7% colonization frequency, 56.1% colonization intensity, and 39.7% arbuscule formation frequency, while the eggplants colonized by AMF only had 76.3% colonization frequency, 45.3% colonization intensity, and 27.4% arbuscule formation frequency. These results indicated the compatibility between the two potential bio-agents. However, *R. solani* inoculation of the mycorrhizal eggplants reduced the mycorrhization levels, compared to

Table 4. Mean proportions (%) of mycorrhizal colonization frequency, intensity and arbuscule frequency 45 d after treatments of eggplants with *Niallia circulans* YRNF1.

Treatment	Colonization frequency (%)*	Colonization intensity (%)*	Frequency of arbuscules (%)*
C	0	0	0
P	0	0	0
B	0	0	0
M	76.3 ± 4.12^{b}	45.3 ± 6.13^{b}	27.4 ± 3.17^{b}
B+M	88.7 ± 6.23^{a}	56.1 ± 5.41^{a}	39.7 ± 5.11^{a}
B+P	0	0	0
M+P	63.9 ± 4.55^{d}	35.4 ± 6.04^{c}	20.5 ± 4.03^{c}
F+P	0	0	0
B+M+P	70.33.4 ± 4.81^{c}	43.4 ± 5.22^{b}	24.5 ± 5.15^{bc}

*Means accompanied by the same superscript letter are not significantly different ($P \leq 0.05$), according to Tukey's HSD test. The values are means of five replicates ± SD. Treatments applied were: C, non-mycorrhizal, untreated and uninfected; P, non-mycorrhizal, untreated and infected; B, non-mycorrhizal, treated with *N. circulans* YRNF1 and uninfected; M, mycorrhizal, untreated and uninfected; B+M, mycorrhizal, treated with *N. circulans* YRNF1 and uninfected; B+P, non-mycorrhizal, treated with *N. circulans* YRNF1 and infected; M+P, mycorrhizal, untreated and infected; F+P, non-mycorrhizal, treated with the fungicide and infected; and B+M+P, mycorrhizal, treated with *N. circulans* YRNF1 and infected.

the mycorrhizal eggplants not inoculated by the pathogen. This was also the case for the mycorrhizal-infected roots treated with *N. circulans* YRNF1.

Eggplants growth in response to application of N. circulans *YRNF1 and AMF*

Results from treatments of *R. solani* inoculated eggplants with *N. circulans* YRNF1 and AMF showed increases in most of the measured plant growth parameters (Table 5). Compared to experimental controls, the *R. solani*-inoculated had 20.5% reduction in mean shoot height and 26.3% reduction in mean root length. Eggplant roots colonized by AMF had 54.6% greater shoot height and 54.7% greater root length. Treating the non-*R. solan*i inoculated plants with *N. circulans* YRNF1 and AMF increased shoot height by 71.4% and root length by 41.8%. Treatment of the *R. solan*i inoculated eggplants with both bio-inoculants, increased shoot height by 53.7% and root length 66.5%. Treatment with fludioxonil also increased shoot height and root length of the *R. solani*-inoculated eggplants. Compared to controls, inoculation of the plants reduced shoot dry weight by 41.0% and root dry weight by 60.0%. Treatment of the non-infected eggplants with *N. circulans* YRNF1 and AMF increased shoot dry weight 79.5 and root dry weight by 130%. Application of both bio-agents to infected plants increased shoot dry weight by 51.3% and root dry weight by 90%. Treatment of infected plants with fludioxonil also increased shoot and root dry weights. Inoculation of plants with *R. solani* also reduced mean leaf area by 34.3%. Application of both bio-inoculants increased the leaf area by 115.7%. Combined treatment of the infected eggplants with both bio-agents increased mean leaf area by 85.8%. Treatment of the infected eggplants with fludioxonil increased leaf area, compared to the untreated infected plants.

Influence of Niallia circulans *YRNF1 and AMF on the macronutrient contents in the eggplant leaves*

Total nitrogen (TN) contents in eggplant leaves varied across the different treatments (Table 6). Compared to experimental controls, all the treatments caused increased TN. Greatest mean TN increases resulted for *R. solani*-inoculated plants colonized by AMF (3.9%), inoculated with *N. circulans* YRNF1 (3.6%) or treated with fludioxonil (3.6%). Greatest total phosphorus (TP: 2.55%) was measured in non-inoculated plants colonized with AMF, and in *R. solani*-inoculated plants colonized with AMF (TP = 2.26%). Most of the applied treatments also increased total potassium (TK) contents in the eggplant leaves, compared to control. Measured N/P ratios were increased in the *R. solani* inoculated plants either treated with the fludioxonil (mean N/P ratio = 4.29), inoculated with *N. circulans* YRNF1 (N/P = 3.86), or colonized with AMF (N/P = 3.85).

DISCUSSION

Rhizoctonia solani is a damaging pathogen that infects several economically important host plants. In

Table 5. Mean eggplant shoot heights, root lengths, shoot and root dry weights, and leaf areas 45 d after inoculation with *Rhizoctonia solani* and treatments of *Niallia circulans* YRNF1 and/or mycorrhizal colonization.

Treatment	Shoot height (cm)*	Root length (cm)*	Shoot dry weight (g)*	Root dry weight (g)*	Leaf area (cm^2)*
C	12.50 ± 1.12^{d}	5.17 ± 0.80^{e}	0.39 ± 0.03^{c}	0.10 ± 0.02^{c}	17.99 ± 1.23^{f}
P	10.00 ± 0.99^{e}	3.81 ± 0.73^{f}	0.23 ± 0.05^{d}	0.04 ± 0.01^{d}	11.82 ± 1.01^{g}
B	13.50 ± 1.37^{cd}	7.16 ± 0.95^{bcd}	0.62 ± 0.04^{ab}	0.22 ± 0.02^{a}	24.71 ± 2.33^{d}
M	19.33 ± 1.40^{b}	8.00 ± 1.00^{ab}	0.68 ± 0.06^{a}	0.21 ± 0.04^{ab}	33.54 ± 2.15^{b}
B+M	21.42 ± 1.22^{a}	7.33 ± 0.87^{bc}	0.70 ± 0.09^{a}	0.23 ± 0.05^{a}	38.82 ± 2.56^{a}
B+P	13.17 ± 0.87^{cd}	7.33 ± 0.74^{bc}	0.39 ± 0.08^{c}	0.10 ± 0.03^{c}	21.76 ± 1.81^{e}
M+P	18.14 ± 1.13^{b}	7.30 ± 0.81^{bc}	0.58 ± 0.07^{b}	0.21 ± 0.05^{ab}	28.48 ± 1.64^{c}
F+P	15.83 ± 1.41^{c}	6.33 ± 0.89^{cd}	0.36 ± 0.06^{c}	0.11 ± 0.06^{c}	$17.43 \pm .98^{f}$
B+M+P	19.21 ± 1.42^{b}	8.61 ± 0.78^{a}	0.59 ± 0.08^{b}	0.19 ± 0.07^{b}	33.42 ± 1.11^{b}

*Means accompanied by the same superscript letter are not significantly different ($P \leq 0.05$), according to Tukey's HSD test. The values are means of five replicates ± SD. Treatments applied were: C, non-mycorrhizal, untreated and uninfected; P, non-mycorrhizal, untreated and infected; B, non-mycorrhizal, treated with *N. circulans* YRNF1 and uninfected; M, mycorrhizal, untreated and uninfected; B+M, mycorrhizal, treated with *N. circulans* YRNF1 and uninfected; B+P, non-mycorrhizal, treated with *N. circulans* YRNF1 and infected; M+P, mycorrhizal, untreated and infected; F+P, non-mycorrhizal, treated with the fungicide and infected; and B+M+P, mycorrhizal, treated with *N. circulans* YRNF1 and infected.

Table 6. Mean contents of nitrogen, phosphorus, and potassium, and N/P ratios 45 d after treatments of eggplants with *Niallia circulans* YRNF1 and/or AMF.

Treatment	Total nitrogen (%)*	Total phosphorus (%)*	Total potassium (%)*	N/P ratio*
C	2.66 ± 0.08^{e}	1.59 ± 0.04^{d}	2.15 ± 0.08^{c}	3.72 ± 0.21^{ab}
P	3.15 ± 0.04^{cd}	2.17 ± 0.03^{bc}	2.70 ± 0.15^{ab}	3.20 ± 0.02^{b}
B	3.22 ± 0.08^{cd}	2.01 ± 0.06^{bc}	2.9 ± 0.06^{a}	3.57 ± 0.20^{ab}
M	3.50 ± 0.08^{bc}	2.55 ± 0.09^{a}	2.77 ± 0.06^{ab}	3.06 ± 0.17^{b}
B+M	3.23 ± 0.02^{cd}	2.04 ± 0.02^{bc}	2.89 ± 0.07^{a}	3.52 ± 0.05^{ab}
B+P	3.64 ± 0.16^{ab}	2.15 ± 0.15^{bc}	2.81 ± 0.02^{ab}	3.86 ± 0.06^{ab}
M+P	3.92 ± 0.09^{a}	2.26 ± 0.04^{ab}	3.04 ± 0.09^{a}	3.85 ± 0.45^{ab}
F+P	3.64 ± 0.04^{ab}	1.88 ± 0.02^{cd}	3.09 ± 0.11^{a}	4.29 ± 0.08^{a}
B+M+P	3.10 ± 0.08^{d}	2.12 ± 0.06^{bc}	2.45 ± 0.03^{bc}	3.24 ± 0.08^{b}

*Means accompanied by the same superscript letter are not significantly different ($P \leq 0.05$), according to Tukey's HSD test. The values are means of five replicates ± SD. Treatments applied were: C, non-mycorrhizal, untreated and uninfected; P, non-mycorrhizal, untreated and infected; B, non-mycorrhizal, treated with *N. circulans* YRNF1 and uninfected; M, mycorrhizal, untreated and uninfected; B+M, mycorrhizal, treated with *N. circulans* YRNF1 and uninfected; B+P, non-mycorrhizal, treated with *N. circulans* YRNF1 and infected; M+P, mycorrhizal, untreated and infected; F+P, non-mycorrhizal, treated with the fungicide and infected; and B+M+P, mycorrhizal, treated with *N. circulans* YRNF1 and infected.

this study, isolation of diazotrophic bacteria from the soil samples resulted in the recovery of eight bacterial isolates. Results of *in vitro* antagonism assays of these isolates against *R. solani* showed that one strain YRNF1, molecularly identified as *N. circulans*, considerably inhibited *R. solani* growth in culture. This was probably because of antifungal compounds production (antibiosis) by *N. circulans*. Analysis of *N. circulans* YRNF1 culture filtrate using GC-MS indicated occurrence of 19 metabolites. Butyric acid and ethylene glycol were the major components of the culture filtrate. Previous studies have reported antifungal activity of butyric acid, which is a short chain fatty acid produced by bacteria (e.g. *Lactobacilli* spp.), and this compound is widely used as a bio-preservative in dairy products due to its high antifungal activity (Garnier *et al.*, 2020). Ethylene glycol is widely used as an effective antifungal component in the hand sanitizers (Vuai *et al.*, 2022). The *in vitro* antifungal potential of *N. circulans* YRNF1 may be due to additive actions of butyric acid and ethylene glycol. It is possible that ethylene glycol, thanks to its amphiphilic nature, facilitates contact between butyric acid, which is a hydrophobic and antifungal compound, and *R. solani* cells, whose contents are hydrophilic (Abouloifa *et al.*, 2022).

Nitrogen fixation is an important biological process as nitrogen (N) is a limiting nutrient for crop growth. The nitrogen fixing ability of *N. circulans* YRNF1 was confirmed by the presence of *nifH* gene in its DNA, which provides marker for N fixation ability (Young, 1992). Nitrogen fixation by *N. circulans* YRNF1 is probably the main mechanism of the observed promotion of the eggplant growth, as shown by the increases of NPK contents in leaves of the treated plants. Nitrogen is the most important element in plant nutrition, and nitrogen nutrition *via* nitrogen fixation increases plant vegetative vigor. Phosphorus and potassium are also vital for plant biochemical processes, such as photosynthesis and for the nitrogen fixation process itself (Abdelraouf *et al.*, 2020). Potassium has an important function in activating enzymes including nitrogenase (Rashad *et al.*, 2023). Coskun *et al.* (2017) highlighted that the form of available N, particularly NH_4^+ and NO_3^-, and the transformation of N in soil, also affect K uptake by plants. These authors reported that administration of NH_4^+ to barley plants enhanced K^+ uptake. Phosphorus nutrition is also important for N fixation processes, where conversion of N_2 to NH_4^+ catalyzed by nitrogenase depends on ATP (Bello *et al.* 2023). Nitrogen fertilization also positively affects P uptake by plant roots (Krouk and Kiba, 2020).

The results obtained in the present study from the greenhouse assays showed that application of *N. circulans* YRNF1 suppressed disease severity caused by *R. solani* in the treated eggplants. The bio-control efficacy of *N. circulans* YRNF1 was probably due to its ability to produce metabolites (particularly butyric acid and ethylene glycol) with antifungal potential. Other possible mechanisms of action include the ability to inhibit the growth of *R. solani* and limit severity of root rot through colonization of root infection sites, competitive exclusion of the fungal pathogen, and secretion of antifungal and/or cell wall hydrolyzing enzymes (Lugtenberg *et al.*, 2009; Berendsen *et al.*, 2012). Systemic immunity may also be triggered by *N. circulans* in treated eggplants. All the above mentioned results are promising for the potential use of *N. circulans* YRNF1 as an effective biocontrol agent. Disease severity may also be reduced by AMF colonization of eggplants infected by *R. solani*, which triggers host defense responses in plants under stress caused by plant pathogens (Rashad *et al.* 2020b). AMF can also enhance plant resistance, by promoting plant growth and vigor *via* improvement of plant nutrition (El-Sharkawy *et al.*, 2023) and production of plant hormones (Song *et al.*, 2020). In the present study, co-inoculation of infected plants with the two biocontrol agents decreased disease severity by 26%, indicating an additive action of the *N. circulans* YRNF1 and AMF.

Both potential biocontrol agents affected expression of the defense genes *JERF3, PAL1, C3H, CHI2*, and *HQT*. The *JERF3* gene was particularly expressed in response to treatment of eggplants with *N. circulans* YRNF1 and AMF. The gene *JERF3* controls several plant defense genes (Rashad *et al*., 2022b). *PAL1* regulates the main step in the polyphenolic biosynthetic pathway, through conversation of phenylalanine to *t*-cinnamic acid (Mouradov and Spangenberg, 2014). *C3H* has an important role in biosynthesis of monolignols that constitute lignin (Tao *et al*., 2015), where lignification of the infected cell walls is a pivotal physical mechanism preventing pathogen penetration of hosts and cell to cell proliferation. *CHI2* catalyzes the bioconversion of coumaroyl CoA to naringenin involved in the biosynthesis of several fungitoxic compounds, including flavonoids and phytoalexins (Zhou *et al*., 2018). *HQT* regulates biosynthesis of chlorogenic acid from caffeoyl CoA (André *et al*., 2009). Triggering expression of these defense genes indicates induction of effects of the combined application of *N. circulans* YRNF1 and AMF for eggplant resistance.

Increases in phenolics and in activities of POD and PPO were detected in response to applying *N. circulans* YRNF1 and AMF. This is similar to the results of Singh *et al.* (2016). Increments of phenolic compounds content is a plant defense response associated with induced resistance (IR) in plants infected by pathogens (Chin *et al*., 2022). POD and PPO are important antioxidant enzymes, which catalyze formation of lignin, thus contributing to structural reinforcement of plant cells and formation of physical barriers against invading pathogens (Nasr-Esfahani *et al*., 2020). In addition, POD and PPO scavenge the oxidative ROS generated within infection processes.

Results from the present study have demonstrated that the frequency of colonization of eggplant roots by AMF, the level of colonization, and the frequency of arbuscule formation were greater after treating eggplants with a combination of *N. circulans* YRNF1 and AMF. This revealed the inducing effect of *N. circulans* YRNF1 on mycorrhizal colonization, which indicates compatibility of the two potential biocontrol agents.

In the present study, the two applied potential biocontrol agents promoted eggplant growth. Colonization of plant roots by two or more AMF species has previously been reported to provide a spectrum of advantages, and has more benefits to host plants than colonization by one species (Sharma and Kapoor, 2023). The strain *N. circulans* E9 has been found to promote plant growth (Sarmiento-López *et al*., 2022), which is associated with production of IAA and promotion of growth through stimulation of cell division and increased nutrient and water uptake, resulting in increased crop yield and quality (Sarmiento-López *et al*., 2022). In the present study, increases in the growth parameters of *R. solani*-infected eggplants were detected after individual treatments with each of the two bio-inoculants. This may be due to the biocontrol potential of *N. circulans* YRNF1 and growth promotion from each of the bio-inoculants. The recorded enhancement of eggplant growth after colonization with AMF was also similar to effects reported by Han *et al.* (2023), where treating lettuce by AMF increased the plant height by 30% and root length by 64%. Colonization by AMF is known to improve the host plants through multiple modes of action, including increases in active and passive nutrient and water uptake, and increased hyphal networks on root radicles, which magnify the hydraulic conductivity of water from the soil (Rashad *et al*., 2020c). In addition, AMF can produce hydrolyzing phosphatases, pectinases, and cellulases, as well as organic acids, which assist in nutrient utilization and improve their plant availability (Liu *et al*., 2021). AMF also produce phytohormones (e.g. abscisic acid and strigolactones) that enhance plant growth (Pozo *et al*., 2015).

Niallia circulans YRNF1 also enhanced eggplant nitrogen nutrition *via* the N-fixation, which probably promoted eggplant growth, whether or not colonized by AMF. The enhancements of eggplant growth parameters were increased after applying the two bio-gents, suggesting their additive action. This observation is consistent with that of El-Sharkawy *et al.* (2022), who showed that co-treating of pea plants by *Streptomyces viridosporus* HH1 and the mycorrhizal fungus *Rhizophagus irregularis* increased pea growth, compared to individual treatments with these two microorganisms. The AMF supply host plants with mineral nutrients, mainly phosphorus, which play prominent roles in plant growth (Adolfsson *et al*., 2015). The present results also demonstrated that combined application of *N. circulans* YRNF1 and mycorrhizal colonization improved the NPK contents in eggplant leaves, which was probably due to a cumulative effect of *N. circulans* YRNF1 and AMF. These data were similar to those of Hafez *et al.* (2022), who reported that combined application of growth-promoting rhizobacteria with organic fertilizers increased total N, P, and K in treated plant tissues, compared to untreated plants, and to individual applications of the mineral fertilizers.

The present study is the first to report effective use and the additive effects of the diazotrophic bacterium *N. circulans* and AMF, as biofungicides and biofertilizers, for potential management of Rhizoctonia root rot and growth-promotion in eggplant.

ACKNOWLEDGMENTS

This research did not receive specific grants from public, commercial or not-for-profit funding agencies.

LITERATURE CITED

Abdelraouf R.E, Abdou S.M.M., Mahmoud Abbas M.M., Hafez M., Popov A.I., Hamed L.M.M., 2020. Influence of N-fertigation stress and agro-organic wastes (biochar) to improve yield and water productivity of sweet pepper under sandy soils conditions. *Plant Archives* 20(1): 3208–3217.

AbouloifaH., Hasnaoui I., Rokni Y, Bellaouchi R., Ghabbour N., … Asehraou A., 2022. Chapter Two - Antifungal activity of lactic acid bacteria and their application in food biopreservation. *Advances in Applied Microbiology* 120: 33–77. https://doi.org/10.1016/bs.aambs.2022.07.001

Adolfsson L., Solymosi K., Andersson M.X., Keresztes Á., Uddling J., … Spetea C., 2015. Mycorrhiza Symbiosis Increases the Surface for Sunlight Capture in *Medicago truncatula* for Better Photosynthetic Production. *PLoS One* 10(1): e0115314. https://doi.org/10.1371/journal.pone.0115314

Al-Askar A.A., Abdulkhair W.M., Rashad Y.M., Hafez E.E., Ghoneem K.M., Baka Z.A., 2014. *Streptomyces griseorubens* E44G: A potent antagonist isolated from soil in Saudi Arabia. *Journal of Pure and Applied Microbiology* 8: 221–230.

Almammory M.K.N., Matloob A.A.H., 2019. Efficiency of *Trichoderma harzianum* and bio-fertilizer Bokashi and salicylic acid in the control of fungi causing Eggplant damping off disease. *Plant Archives* 19(1): 73–82.

André C.M., Schafleitner R., Legay S., Lefèvre I., Aliaga C.A.A., … Evers D., 2009. Gene expression changes related to the production of phenolic compounds in potato tubers grown under drought stress. *Phytochemistry* 70(9): 1107–1116. https://doi.org/10.1016/j.phytochem.2009.07.008

Baite M.S., Khokhar M.K., Meena R.P., 2021. Management of False Smut Disease of Rice: A Review, In: *Cereal Grains* (A.K. Goyal, ed.), IntechOpen 1. https://doi.org/10.5772/intechopen.97329

Bello S.K., Muraina T.O., Jimoh S.O., Olasupo I.O., Usman S., 2023. Phosphorus Nutrition Enhancement of Biological Nitrogen Fixation in Pastures. In: *Sustainable Agriculture Reviews* (Iqbal A., *et al.,* ed), Springer, Cham., 58. https://doi.org/10.1007/978-3-031-16155-1_10

Berendsen R.L., Pieterse C.M.J., Bakker P.A.H.M., 2012. The rhizosphere microbiome and plant health. *Trends in Plant Science* 17: 478–486. https://doi.org/10.1016/j.tplants.2012.04.001

Chao N., Wang R.F., Hou C., Yu T., Miao K., … Liu L., 2021. Functional characterization of two chalcone isomerase (CHI) revealing their responsibility for anthocyanins accumulation in mulberry. *Plant Physiology and Biochemistry* 161: 65–73. https://doi.org/10.1016/j.plaphy.2021.01.044

Chin J.M., Lim Y.Y., Ting A.S.Y., 2022. Biopriming chilli seeds with *Trichoderma asperellum*: A study on biopolymer compatibility with seed and biocontrol agent for disease suppression. *Biological Control* 165: 104819. https://doi.org/10.1016/j.biocontrol.2021.104819

Cook R.J., Schillinger W.F., Christensen N.W., 2002. *Rhizoctonia* root rot and take-all of wheat in diverse direct-seed spring cropping systems. *Canadian Journal of Plant Pathology* 24: 349–358. https://doi.org/10.1080/07060660209507020

Coskun D., Britto D.T., Kronzucker H.J., 2010. Regulation and mechanism of potassium release from barley roots: an *in planta* $^{42}K^{+}$ analysis. *New Phytologist* 188(4): 1028–1038. https://doi.org/10.1111/j.1469-8137.2010.03436.x

Coskun D., Britto D.T., Kronzucker H.J., 2017. The nitrogen–potassium intersection: membranes, metabolism, and mechanism. *Plant, Cell & Environment* 40: 2029–2041. https://doi.org/10.1111/pce.12671

de Oliveira E.P., de Souza Soares P.P., Santos G.L., Coutrim R.L., do Val de Assis F.G., … Leal, P.L., 2022. Single inoculation with arbuscular mycorrhizal fungi promotes superior or similar effects on cowpea growth compared to co-inoculation with *Bradyrhizobium*. *South African Journal of Botany* 151: 941–948. https://doi.org/10.1016/j.sajb.2022.11.011

Devi N.O., Devi R.K.T., Debbarma M., Hajong M., Thokchom S., 2022. Effect of endophytic *Bacillus* and arbuscular mycorrhiza fungi (AMF) against *Fusarium* wilt of tomato caused by *Fusarium oxysporum* f. sp. *lycopersici*. *Egyptian Journal of Biological Pest Control* 32: 1. https://doi.org/10.1186/s41938-021-00499-y

Dias M.C., Pinto D., Silva A.M.S., 2021. Plant flavonoids: Chemical characteristics and biological activity. *Molecules* 26(17): 5377. https://doi.org/10.3390/molecules26175377

Döbereiner J., 1988. Isolation and identification of root associated diazotrophs. *Plant Soil* 110: 207–212. https://doi.org/10.1007/BF02226800

dos Santos H.R.M., Argolo C.S., Argôlo-Filho R.C., Loguercio L.L., 2019. A 16S rDNA PCR-based theo-

retical to actual delta approach on culturable mock communities revealed severe losses of diversity information. *BMC Microbiology* 19: 74. https://doi.org/10.1186/s12866-019-1446-2

Elshafie H.S., Camele I., Mohamed A.A.A., 2023. A comprehensive review on the biological, agricultural and pharmaceutical properties of secondary metabolites based-plant origin. *International Journal of Molecular Sciences* 24(4): 3266. https://doi.org/10.3390/ijms24043266

El-Sharkawy H.H.A., Rashad Y.M., Elazab N.T., 2022. Synergism between *Streptomyces viridosporus* HH1 and *Rhizophagus irregularis* Effectively Induces Defense Responses to *Fusarium* Wilt of Pea and Improves Plant Growth and Yield. *Journal of Fungi* 8: 683. https://doi.org/10.3390/jof8070683

El-Sharkawy H.H.A., Rashad Y.M., Elazab N.T., 2023. Induction of multiple defense responses in wheat plants against stripe rust using mycorrhizal fungi and *Streptomyces viridosporus* HH1. *BioControl* 68: 525–535. https://doi.org/10.1007/s10526-023-10207-4

FAOSTAT, 2024. Food and Agriculture Organization of the United Nations. 10 World's biggest producers of eggplants. Available at: https://en.wikipedia.org/wiki/List_of_countries_by_eggplant_production

Ferreira J.H., Mathee F.N., Thomas A.C., 1991. Biological control of Eutypalota on grapevine by an antagonistic strain of *Bacillus subtilis*. *Phytopathology* 81: 283–287.

Forman H.J., Zhang H., 2021. Targeting oxidative stress in disease: Promise and limitations of antioxidant therapy. *Nature Reviews Drug Discovery* 20(9): 689–709. https://doi.org/10.1038/s41573-021-00233-1

Fuentes A., Ortiz J., Saavedra N., Salazar L.A., Meneses C., Arriagada, C., 2016. Reference gene selection for quantitative real-time PCR in *Solanum lycopersicum* L. inoculated with the mycorrhizal fungus *Rhizophagus irregularis*. *Plant Physiology and Biochemistry* 101: 124–131. http://dx.doi.org/10.1016/j.plaphy.2016.01.022

Garnier L., Penland M., Thierry A., Maillard M-B., Jardin J., … Mounier, J., 2020. Antifungal activity of fermented dairy ingredients: Identification of antifungal compounds. *International Journal of Food Microbiology* 322: 108574. https://doi.org/10.1016/j.ijfoodmicro.2020.108574

Gong Y., Toivonen P., Lau O.L., Wiersma P.A., 2001. Antioxidant system level in 'Braeburn' apple is related to its browning disorder. *Botanical Bulletin of Academia Sinica* 42: 259–264.

Goyal K., Singh N., Jindal S., Kaur R., Goyal A., Awasthi R., 2022. Kjeldahl Method. In: *Advanced Techniques of Analytical Chemistry* (Goyal A., Kumar H., ed.), 11: 105–112. https://doi.org/10.2174/9789815050233122010011

Hafez M., Abdallah A.M., Mohamed A.E., Rashad M., 2022. Influence of environmental-friendly bio-organic ameliorants on abiotic stress to sustainable agriculture in arid regions: A long term greenhouse study in northwestern Egypt. *Journal of King Saud University-Science* 34(6): 102212. https://doi.org/10.1016/j.jksus.2022.102212

Han Z., Zhang Z., Li Y., Wang B., Xiao Q., … Chen, J., 2023. Effect of Arbuscular mycorrhizal fungi (AMF) inoculation on endophytic bacteria of lettuce. *Physiological and Molecular Plant Pathology* 126: 102036. https://doi.org/10.1016/j.pmpp.2023.102036

Hollomon D.W., 2015. Fungicide Resistance: Facing the Challenge-a Review. *Plant Protection Science* 51(4): 170–176. https://doi.org/10.17221/42/2015-PPS

Jasim B., Benny R., Sabu R., Mathew J., Radhakrishnan E.K., 2016. Metabolite and mechanistic basis of antifungal property exhibited by endophytic *Bacillus amyloliquefaciens* BmB1. *Applied Biochemistry and Biotechnology* 179: 830–845. https://doi.org/10.1007/s12010-016-2034-7

Kaniyassery A., Thorat S.A., Kiran K.R., Murali T.S., Muthusamy A., 2022. Fungal diseases of eggplant (*Solanum melongena* L.) and components of the disease triangle: A review. *Journal of Crop Improvement* 37(4): 543–594. https://doi.org/10.1080/15427528.2022.2120145

Kifle M.H., Laing M.D., 2016. Isolation and Screening of Bacteria for Their Diazotrophic Potential and Their Influence on Growth Promotion of Maize Seedlings in Greenhouses. *Frontiers in Plant Science* 6: 1225. https://doi.org/10.3389/fpls.2015.01225

Krouk G., Kiba T., 2020. Nitrogen and phosphorus interactions in plants: from agronomic to physiological and molecular insights. *Current Opinion in Plant Biology* 57: 104–109. https://doi.org/10.1016/j.pbi.2020.07.002

Liu Y., Zhang G., Luo X., Hou E., Zheng M., Zhang L., He X., Shen W., Wen D., 2021. Mycorrhizal fungi and phosphatase involvement in rhizosphere phosphorus transformations improves plant nutrition during subtropical forest succession. *Soil Biology and Biochemistry* 153: 108099. https://doi.org/10.1016/j.soilbio.2020.108099

Losada-Barreiro S., Sezgin-Bayindir Z., Paiva-Martins F., Bravo-Díaz C., 2022. Biochemistry of antioxidants: Mechanisms and pharmaceutical applications. *Biomedicines* 10(12): 3051. https://doi.org/10.3390/biomedicines10123051

Lugtenberg B., Kamilova F., 2009. Plant-growth-promoting rhizobacteria. *Annual Review of Microbiol-*

ogy 63: 541–556. https://doi.org/10.1146/annurev.micro.62.081307.162918

Ma Q.H., Zhu H.H., Han J.Q., 2017. Wheat ROP proteins modulate defense response through lignin metabolism. *Plant Science* 262: 32–38. https://doi.org/10.1016/j.plantsci.2017.04.017

Mathur S., Sharma M.P., Jajoo A., 2018. Improved photosynthetic efficacy of maize (*Zea mays*) plants with arbuscular mycorrhizal fungi (AMF) under high temperature stress. *Journal of Photochemistry and Photobiology B: Biology* 180: 149–154. https://doi.org/10.1016/j.jphotobiol.2018.02.002

Mehta P., Walia A., Kulshrestha S., Chauhan A., Shirkot C.K., 2015. Efficiency of plant growth-promoting P-solubilizing *Bacillus circulans* CB7 for enhancement of tomato growth under net house conditions. *Journal of Basic Microbiology* 55: 33–44. https://doi.org/10.1002/jobm.201300562

Mouradov A., Spangenberg G., 2014. Flavonoids: a metabolic network mediating plants adaptation to their real estate. *Frontiers in Plant Science* 5: 1–16. https://doi.org/10.3389/fpls.2014.00620

Nafady N.A., Hashem M., Hassan E.A., Ahmed H.A.M., Alamri S.A., 2019. The combined effect of arbuscular mycorrhizae and plant-growth-promoting yeast improves sunflower defense against *Macrophomina phaseolina* diseases. *Biological Control* 138: 104049. https://doi.org/10.1016/j.biocontrol.2019.104049

Nasr-Esfahani M., Hashemi L., Nasehi A., Nasr-Esfahani A., Nasr Esfahani A., 2020. Novel *Cucumis* enzymes associated with host-specific disease resistance to *Phytophthora melonis* Katsura. *Biotechnology & Biotechnological Equipment* 34(1): 873–884. https://doi.org/10.1080/13102818.2020.1810123

Niggeweg R., Michael A.J., Martin C., 2004. Engineering plants with increased levels of the antioxidant chlorogenic acid. *Nature Biotechnology* 22: 746–754. https://doi.org/10.1038/nbt966

Nisa K., Rosyida V.T., Nurhayati S., Indrianingsih A.W., Darsih C., Apriyana W., 2019. Total phenolic contents and antioxidant activity of rice bran fermented with lactic acid bacteria. *IOP Conference Series: Earth and Environmental Science* 251: 012020. https://doi.org/10.1088/1755-1315/251/1/012020

Phillips J.M., Hayman D.S., 1970. Improved procedures for clearing roots and staining parasitic and vesicular-arbuscular mycorrhizal fungi for rapid assessment of infection. *Transactions of the British Mycological Society* 55: 158–IN18. https://doi.org/10.1016/S0007-1536(70)80110-3

Pozo M.J., López-Ráez J.A., Azcón-Aguilar C., García-Garrido J.M., 2015. Phytohormones as integrators of environmental signals in the regulation of mycorrhizal symbioses. *New Phytologist* 205: 1431–1436. https://doi.org/10.1111/nph.13252

Ramaroson M.L., Koutouan C., Helesbeux J.J., Le Clerc V., Hamama L., Geoffriau E., Briard M., 2022. Role of Phenylpropanoids and Flavonoids in Plant Resistance to Pests and Diseases. *Molecules* 27: 8371. https://doi.org/10.3390/molecules27238371

Rashad Y.M., Aseel D.G., Hafez E.E., 2018. Antifungal potential and defense gene induction in maize against Rhizoctonia root rot by seed extract of *Ammi visnaga* (L.) Lam. *Phytopathologia Mediterranea* 57(1): 73–88. https://doi.org/10.14601/Phytopathol_Mediterr-21366

Rashad Y.M., Aseel D.G., Hammad S.M., 2020a. Phenolic Compounds against Fungal and Viral Plant Diseases. In: *Plant Phenolics in Sustainable Agriculture* (Lone R., Shuab R., Kamili A., ed.), Springer Nature, Singapore, Pte Ltd, 201–219. https://doi.org/10.1007/978-981-15-4890-1_9

Rashad Y.M., Aseel D.G., Hammad S.M., ElKelish A.A., 2020b. *Rhizophagus irregularis* and *Rhizoctonia solani* differentially elicit systemic transcriptional expression of polyphenol biosynthetic pathways genes in sunflower. *Biomolecules* 10(3): 379. https://doi.org/10.3390/biom10030379

Rashad Y.M., Abbas M.A., Soliman H.M., Abdel-Fattah G.G., Abdel-Fattah G.A., 2020c. Synergy between endophytic *Bacillus amyloliquefaciens* GGA and arbuscular mycorrhizal fungi induces plant defense responses against white rot of garlic and improves host plant growth. *Phytopathologia Mediterranea* 59(1): 169–186. https://doi.org/10.36253/phyto-11019

Rashad Y.M., El-Sharkawy H.H.A., Elazab N.T., 2022a. *Ascophyllum nodosum* Extract and Mycorrhizal Colonization Synergistically Trigger Immune Responses in Pea Plants against *Rhizoctonia* Root Rot, and Enhance Plant Growth and Productivity. *Journal of Fungi* 8: 268. https://doi.org/10.3390/jof8030268

Rashad Y.M., Abdalla S.A., Shehata A.S., 2022b. *Aspergillus flavus* YRB2 from *Thymelaea hirsuta* (L.) Endl., a non-aflatoxigenic endophyte with ability to overexpress defense-related genes against *Fusarium* root rot of maize. *BMC Microbiology* 22: 229. https://doi.org/10.1186/s12866-022-02651-6

Rashad M., Hafez M., Popov A., Gaber H., 2023. Toward sustainable agriculture using extracts of natural materials for transferring organic wastes to environmental-friendly ameliorants in Egypt, *International Journal of Environmental Science and Technology* 20(7): 7417–7432. https://link.springer.com/article/10.1007/s13762-022-04438-8

Sarmiento-López L.G., López-Meyer M., Maldonado-Mendoza I.E., Quiroz-Figueroa F.R., Sepúlveda-Jiménez G., Rodríguez-Monroy M., 2022. Production of indole-3-acetic acid by *Bacillus circulans* E9 in a low-cost medium in a bioreactor. *Journal of Bioscience and Bioengineering* 134(1): 21–28. https://doi.org/10.1016/j.jbiosc.2022.03.007

Schmittgen T.D., Livak K.J., 2008. Analyzing real-time PCR data by the comparative C_T method. *Nature Protocols* 3: 1101–1108. https://doi.org/10.1038/nprot.2008.73

Shameem M.R., Sonali J.M.I., Kumar P.S., Rangasamy G., Gayathri K.V., Parthasarathy V., 2023. *Rhizobium mayense* sp. Nov., an efficient plant growth-promoting nitrogen-fixing bacteria isolated from rhizosphere soil. *Environmental Research* 220: 115200. https://doi.org/10.1016/j.envres.2022.115200

Sharma K., Kapoor R., 2023. Arbuscular mycorrhiza differentially adjusts central carbon metabolism in two contrasting genotypes of *Vigna radiata* (L.) Wilczek in response to salt stress. *Plant Science* 332: 111706. https://doi.org/10.1016/j.plantsci.2023.111706

Shrestha H.K., Fichman Y., Engle N.L., Tschaplinski T.J., Mittler R., … Abraham P.E., 2022. Multi-omic characterization of bifunctional peroxidase 4-coumarate 3-hydroxylase knockdown in *Brachypodium distachyon* provides insights into lignin modification-associated pleiotropic effects. *Frontiers in Plant Science* 13: 908649. https://doi.org/10.3389/fpls.2022.908649

Singh H.P., Ravindranath S.D., 1994. Occurrence and distribution of polyphenol oxidase activity in floral organs of some standard and local cultivars of tea. *Journal of the Science of Food and Agriculture* 64: 117–120. https://doi.org/10.1002/jsfa.2740640117

Singh B., Kumar M., Cabral-Pinto M.M., Bhatt B.P., 2022. Seasonal and altitudinal variation in chemical composition of *Celtis australis* L. tree foliage. *Land* 11(12): 2271. https://doi.org/10.3390/land11122271

Singh U.B., Malviyaa D., Wasiullaha Singha S., Pradhana J.K., … Sharma A.K., 2016. Bio-protective microbial agents from rhizosphere eco-systems trigger plant defense responses provide protection against sheath blight disease in rice (*Oryza sativa* L.). *Microbiological Research* 192: 300–312. https://doi.org/10.1016/j.micres.2016.08.007

Singleton V.L., Orthofer R., Lamuela-Raventos R.M., 1999. Analysis of total phenols and other oxidation substrates and antioxidants by means of Folin-Ciocalteu reagent. *Methods in Enzymology* 299: 152–178. https://doi.org/10.1016/S0076-6879(99)99017-1

Song Z., Bi Y., Zhang J., Gong Y., Yang H., 2020. Arbuscular mycorrhizal fungi promote the growth of plants in the mining associated clay. *Scientific Reports* 10: 2663. https://doi.org/10.1038/s41598-020-59447-9

Spatafora J.W., Chang Y., Benny G.L., Lazarus K., Smith M.E., … Stajich J.E., 2016. A phylum-level phylogenetic classification of zygomycete fungi based on genome-scale data. *Mycologia* 108(5): 1028–1046. https://doi.org/10.3852/16-042

Taheri P., Tarighi S., 2010. Riboflavin induces resistance in rice against *Rhizoctonia solani via* jasmonate-mediated priming of phenylpropanoid pathway. *Journal of Plant Physiology* 167(3): 201–208. http://dx.doi.org/10.1016/j.jplph.2009.08.003

Tan J.W., Thong K.L., Arumugam N.D., Cheah W.L., Lai Y.W., … Vikineswary S., 2009. Development of a PCR assay for the detection of *nifH* and *nifD* genes in indigenous photosynthetic bacteria. *International Journal of Hydrogen Energy* 34(17): 7538–7541. https://doi.org/10.1016/j.ijhydene.2009.04.029

Tao S., Wang D., Jin C., Sun W., Liu X., … Khanizadeh, S., 2015. Cinnamate-4-Hydroxylase Gene Is Involved in the Step of Lignin Biosynthesis in Chinese White Pear. *Journal of the American Society for Horticultural Science* 140(6): 573–579. https://doi.org/10.21273/JASHS.140.6.573

Trouvelot A., Kough J.L., Gianinazzi-Pearson V., 1986. Estimation of VA mycorhizal infection levels. Research for method having a functional significance. In: *Proceedings of the 1st European Symposium on Mycorrhizae*. (Gianinazzi S., Gianinazzi-Pearson V., eds), INRA, Paris, 217–221.

Turk-Kubo K.A., Achilles K.M., Serros T.R.C., Ochiai M., Montoya J.P., Zehr J.P., 2012. Nitrogenase (*nifH*) gene expression in diazotrophic cyanobacteria in the Tropical North Atlantic in response to nutrient amendments. *Frontiers in Microbiology* 3: 386. https://doi.org/10.3389/fmicb.2012.00386

Vuai S.A.H., Sahini M.G., Sule K.S., Ripanda A.S., Mwanga H.M., 2022. A comparative *in-vitro* study on antimicrobial efficacy of on-market alcohol-based hand washing sanitizers towards combating microbes and its application in combating Covid-19 global outbreak. *Heliyon* 8(11): E11689. https://doi.org/10.1016/j.heliyon.2022.e11689

Wen K., Seguin P., Arnaud M.S., Jabaji-Hare S., 2005. Real-Time quantitative RT-PCR of defense associated gene transcripts of *Rhizoctonia solani* infected bean seedlings in response to inoculation with a nonpathogenic binucleate *Rhizoctonia* isolate. *Phytopathology* 95(4): 345–353. https://doi.org/10.1094/PHYTO-95-0345

Young J.P.W., 1992. Phylogenetic classification of nitrogen-fixing organisms. In: *Biological Nitrogen Fixation*

(Stacey G., Burris R.H., Evans H.J., eds), Chapman and Hall, New York, NY, 43–86.

Youssef S.A., Tartoura K.A., Abdelraouf G.A., 2016. Evaluation of *Trichoderma harzianum* and *Serratia proteamaculans* effect on disease suppression, stimulation of ROS-scavenging enzymes and improving tomato growth infected by *Rhizoctonia solani*. *Biological Control* 100: 79–86. https://doi.org/10.1016/j.biocontrol.2016.06.001

Zhang Z., Schwartz S., Wagner L., Miller W., 2000. A greedy algorithm for aligning DNA sequences. *Journal of Computational Biology* 7(1–2): 203–214. https://doi.org/10.1089/10665270050081478

Zhou W., Nielsen J.B., Fritsche L.G., Dey R., Gabrielsen M.E., … Lee, S., 2018. Efficiently controlling for case-control imbalance and sample relatedness in large-scale genetic association studies. Nature *Genetics* 50: 1335–1341. https://doi.org/10.1038/s41588-018-0184-y

Phytopathologia Mediterranea
The international journal of the
Mediterranean Phytopathological Union

Firenze University Press
www.fupress.com/pm

Research Papers

First report of root rot of goji (*Lycium barbarum*), caused by *Fusarium sambucinum*

Pingping SUN[1], Yuchen GUO[1], Lei ZHANG[1], Rong YANG[2], Zhengnan LI[1,*]

[1] *College of Horticulture and Plant Protection, Inner Mongolia Agricultural University, Hohhot, Inner Mongolia 010018, China*
[2] *Inner Mongolia Academy of Forestry Sciences, Hohhot, Inner Mongolia 010010, China*
*Corresponding author. E-mail: lizhengnan@imau.edu.cn

Summary. In July 2022, root rot was observed in several goji (*Lycium barbarum*) orchards located in Qinghai Province, China. Approximately 40% of the goji plants were affected in the orchards. Morphology of fungi isolated from affected plant, phylogenetic analyses, using internal transcribed spacer (ITS), translation elongation factor 1-alpha (TEF), and trichothecene (Tri5) sequences, as well as pathogenicity assays, were conducted to characterize and identify the causing agent of goji root rot. Isolate GQGF1-3 caused typical symptoms of *L. barbarum* root rot. Fungal colony characteristics and conidium morphology, combined with ITS, TEF, and Tri5 sequences showed that isolate GQGF1-3 was *Fusarium sambucinum*. This is the first report of *F. sambucinum* causing root rot of goji.

Keywords. Pathogen identification, *Lycium barbarum*.

Citation: P. Sun, Y. Guo, L. Zhang, R. Yang, Z. Li (2024). First report of root rot of goji (*Lycium barbarum*), caused by *Fusarium sambucinum*. *Phytopathologia Mediterranea* 63(1): 45-51. doi: 10.36253/phyto-15146

Accepted: February 19, 2024

Published: April 29, 2024

Data Availability Statement: All relevant data are within the paper and its Supporting Information files.

Competing Interests: The Author(s) declare(s) no conflict of interest.

Editor: Maurizio Vurro, National Research Council, (CNR), Bari, Italy.

ORCID:
PS: 0009-0005-6140-2307
YG: 0009-0007-1094-6317
LZ: 0000-0001-7479-952X
RY: 0009-0004-4828-8573
ZL: 0000-0003-3268-2096

INTRODUCTION

Goji (*Lycium barbarum* L.) is a perennial shrub in *Solanaceae*. Berries of this plant are rich in polysaccharides, carotenoids, and flavonoids, and are widely used as a traditional Chinese functional food (Potterat, 2010). Goji plants are tolerant to salinity, drought, and low temperatures, and are widely cultivated as medicinal or ornamental trees, or for soil amelioration in arid and semi-arid regions of China, Japan, South Korea, and southeast Europe (Zhang *et al.*, 2022).

Qinghai province is one of the most important areas in China for production of goji berries (Lu *et al.*, 2021). Continuous expansion of planting of *L. barbarum*, together with poor crop management, has caused goji root rot to become one of the most severe diseases during goji cultivation (Cariddi *et al.*, 2018). The affected roots show exposed xylem and visible dark brown vascular bundles, and these symptoms lead to reductions in fruit yields and death of whole plants. Incidence of goji root rot has been reported to be more than 30%, and the disease has caused approx. 35% reduction of goji yields (Cariddi *et al.*, 2018; Bai *et al.*, 2020).

In July 2022, root rot was observed in several goji orchards located in Qinghai Province, China (36°62'N, 101°78'E). Approximately 40% of the goji

plants in the orchards showed root rot symptoms. The affected plants had withered leaves, black rotten roots, and detached root bark, and the disease often caused death of the affected plants.

In this study potential goji root rot causal agents were isolated, characterized, and identified, using morphology, molecular identification and pathogenicity tests. This study was undertaken to provide the basic information for formulating effective management of goji root rot.

MATERIALS AND METHODS

Collection of Lycium barbarum *plants and isolation of potential pathogens*

Diseased *L. barbarum* plants were collected from several orchards in Qinghai Province, China, during July 2022, and were sent to the Laboratory of Pathogen Biology and Comprehensive Control of Horticultural Diseases at the Inner Mongolia Agricultural University. Boundaries between healthy and diseased plant tissues were cut, and then surface sterilized by immersing in 1% NaClO for 3 min, 75% ethanol for 30 s, followed by rinsing three times with sterile distilled water. The tissue pieces were then incubated on potato dextrose agar (PDA) at 28°C. Frontier mycelium of resulting fungal colonies was transferred onto fresh PDA, and incubated for 14 d. Serial dilutions of conidia from cultures were applied to PDA plates to obtain single conidium isolates. Single conidium cultures were then maintained on PDA for further tests.

Pathogenicity test

Pathogenicity of isolates was assessed by inoculating each isolate into healthy goji seedlings. To produce large quantities of conidia, the isolates were inoculated into potato dextrose broth, which was then incubated on a rotary shaker (180 rpm) at 28°C. After 7 d, mycelium with conidia and broth were filtered through three layers of sterilized gauze to remove the hyphae. Conidium concentration was adjusted to approx. 10^7 conidia mL^{-1}. Healthy goji seedlings were grown in plastic pots containing sterilized peat soil and sand (1:1 volume). For inoculations, four holes were made in the potting medium in each pot at approx. 3 cm from the seedlings. A scalpel was used to cut the roots of each plant. Ten mL of conidium suspension was poured into the holes. Six replicate pots were inoculated with each isolate, and sterilized water was similarly applied as the inoculation control. The treated plants were transferred to a greenhouse with temperature between 20 and 28°C, and were watered every second day. Disease symptoms were observed at 15 to 20 d post inoculation.

Identification of pathogenic isolates

Morphological and molecular methods were used to identify the isolates obtained from diseased plants. Isolates were transferred onto PDA, mung bean residue agar (MBRA: 20 g mung bean, 1 L water, autoclaved for 30 min, mixed by a blender, 20 g agar, autoclaved for 20 min at 121°C), carnation leaf agar (CLA), and synthetic low nutrient medium (SNA), and were cultured at 28°C in an incubator. Macroconidia were observed on PDA, MBRA, and CLA, and microconidia were observed on SNA medium.

Mycelia of one selected isolate were collected, and ground with liquid nitrogen. The fungal DNA extraction kit (Sangon Biotech) was used to extract DNA. With DNA as a template, universal primers ITS1/ITS4 were used to amplify the internal transcribed spacer (ITS) regions (White *et al.*, 1990). The PCR reaction system was as follows: 10 μL of 2× M5 HiPer plus Taq HiFi

Table 1. Details of amplification conditions, including sequence primers, annealing temperatures, and extension timse.

Target	Primers	Sequence 5'→3'	PCR conditions	Product size (bp)	References
ITS	ITS1/ITS4	TCCGTAGGTGAACCTGCGG TCCTCCGCTTATTGATATGC	55°C, 40 s	~550	White *et al.* (1990)
Fusarium sambucinum	FSF1/FSR1	ACATACCTTTATGTTGCCTCG GGAGTGTCAGACGACAGCT	58°C, 30 s	315	Mishra *et al.* (2003)
TEF	ef1'/ef2'	ATGGGTAAGGAAGACAAGAC GGAGGTACCAGTGATCATGTT	58°C, 55 s	700	Du *et al.* (2012)
Tri5	Tri5F/Tri5R	AGCGACTACAGGCTTCCCTC AAACCATCCAGTTCTCCATCTG	60°C, 30s	545	Nicholson *et al.* (2004)

PCR Mix, 7 µL of dd H_2O, 1 µL of DNA template, 1 µL of each upstream and downstream primers; The reaction conditions were: 95°C for 3 min; 35 cycles of 94°C for 25 s, 55°C for 30 s, and 72°C for 40 s, and then 72°C for 10 min.

Based on the resulting ITS sequence, *Fusarium sambucinum* species-specific primer pair FSF1/FSR1 (Mishra *et al*., 2003) was used. The ef1'/ef2' (Du *et al*., 2012) were used for amplification of the partial translation elongation factor 1-alpha (TEF).

Potential ability by cultures to produce trichothecenes was tested using primers specific for the gene Tri5 (Nicholson *et al*., 2004). Sequences of all primers, product sizes, annealing temperature and extension time for each assay are presented in Table 1. The PCR amplification products were detected by 1.2% agarogel electrophoresis, and were recovered and purified using an agarogel DNA recovery kit (Tiangen). The products were sent to Sangon Biotech (Shanghai, China) for sequencing. The homologous sequence was retrieved by NCBI using BLASTn to determine its taxonomic status.

RESULTS

A total of 18 fungal isolates were obtained from goji samples. Pathogenicity tests showed that *L. barbarum* plants inoculated with isolate GQGF1-3 showed typical symptoms of root rot 3 weeks after inoculation, while the control plants and the plants inoculated with other isolates were asymptomatic. The pathogenicity test was repeated three times, with similar results. Leaves of the infected plants were chlorotic and wilted, and the roots of inoculated plants were rotted, with brown vascular bundles (Figure 1).

Isolate GQGF1-3 had yellow to light grey, dense and floccose aerial mycelium, and yellow mycelium on the reverse sides of PDA culture plates. On MBRA, the isolate had white, fluffy aerial mycelium, and yellow to brown colouration on reverse sides (Figure 2, A to D). Macrospores of the isolate were sickle-shaped, with 3 to 4 septa, and measured 11 to 25 × 2.5 to 4.5 µm on PDA (Figure 2, E), 15 to 26 × 1.5 to 3.5 µm on MBRA (Figure 2, F), and 15 to 19 × 1.5 to 3 µm on CLA (G). Single-celled and ovoid microspores measured 4.0 to 7.5 × 0.8 to 1.2 µm on SNA (Figure 2, H).

Isolate GQGF1-3 was morphologically identified as a *Fusarium* sp. The internal transcribed spacer (ITS) region of the isolate was amplified, and the obtained sequence was submitted to GenBank, with accession number of OR342306. Blastn analysis of the isolate ITS sequence revealed 100% similarity to 17 isolates of *Fusarium sambucinum*, which had been isolated in China, India, Eygpt, or Canada. The phylogenetic tree based on the ITS sequence showed that GQGF1-3 clustered with *F. sambucinum* strains (Figure 3, A). *Fusarium sambucinum* species-specific primer pair FSF1/FSR1 amplified GQGF1-3, and gave a 350 bp sequence (Figure. 3, B). Phylogenetic trees based on TEF (Genbank accesion number: PP294739) and Tri5 (Genbank accesion number: PP294738) both showed that isolate GQGF1-3 clustered with *Fusarium sambucinum* (Figure 4).

Based on colony characteristics, conidium morphology, and ITS, TEF and Tri5 sequences, isolate GQGF1-3 was identified as *F. sambucinum*. In addition, re-isolation of this fungus from inoculated goji roots in the pathogenicity test confirmed Koch's postulates for the pathogen.

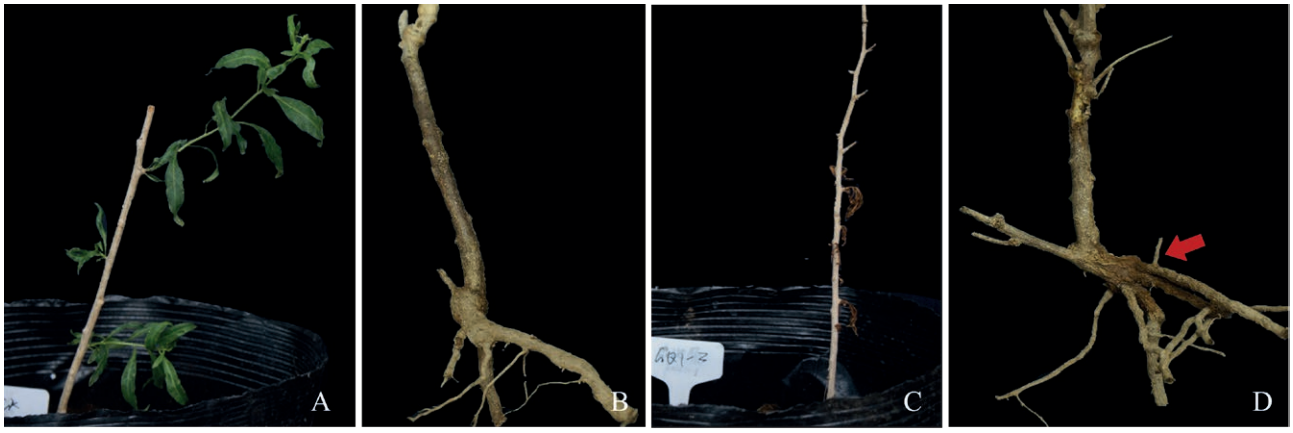

Figure 1. Symptoms on goji plants inoculated with isolate GQGF1-3. A and B show symptoms of control (non-inoculated) plants, C and D are plants that were inoculated with isolate GQGF1-3.

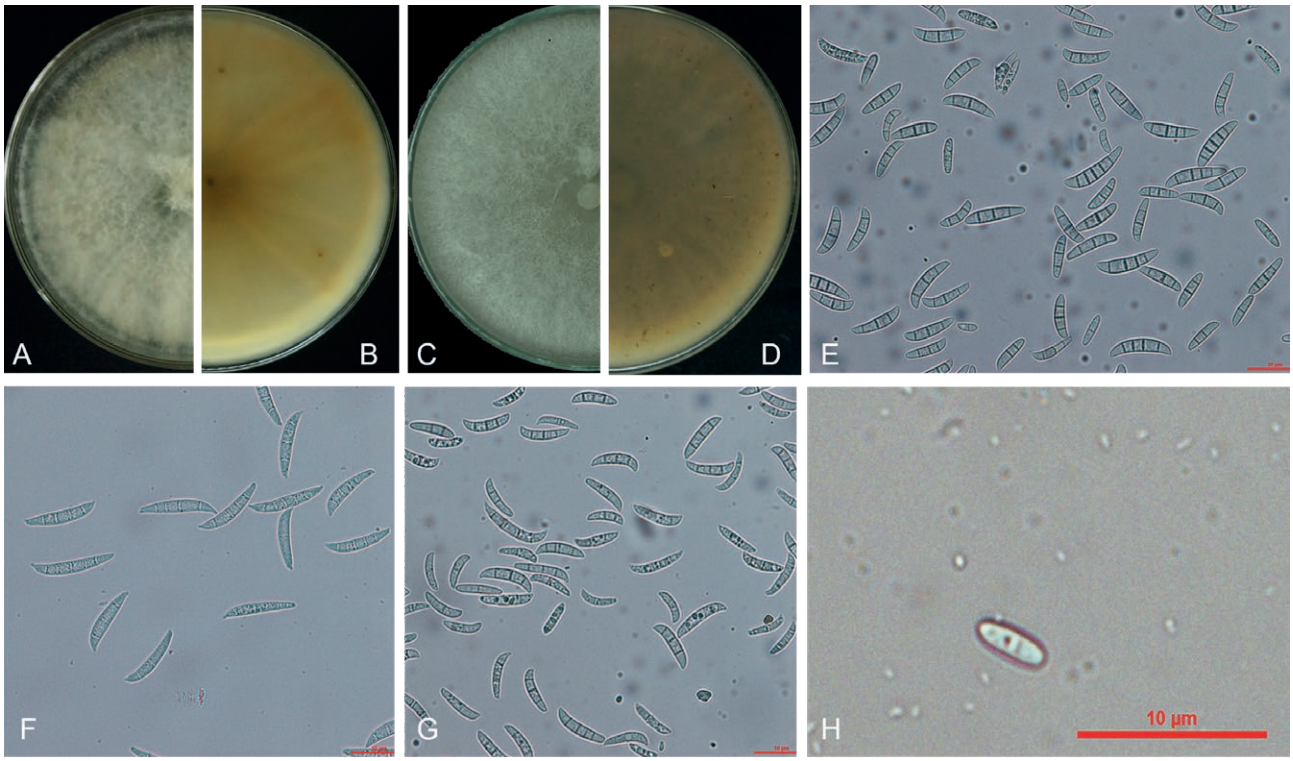

Figure 2. Colony and conidium morphology of isolate GQGF1-3. A, upper and B, reverse side of a GQGF1-3 colony on PDA, and C, upper and D, reverse side on MBRA. Macroconidia of GQGF-3 on PDA (E), MBRA(F), and CLA (G), and a microspore on SNA (H). Scale bars in E to H indicate 10 μm.

DISCUSSION

Isolate *Fusarium sambucinum* GQGF1-3 caused typical root rot symptoms on *L. barbarum* plants. Pathogens previously found on *L. barbarum* include: *Fusarium oxysporum*, *F. solani*, *F. concolor*, *F. moniliforme*, *F. equiseti*, *F. incarnatum, F. culmorum*, *F. tricinctum*, *Phytophthora nicotianae* var. *parasitica*, and *Rhizoctonia solani*, of which *F. oxysporum* is the prevalent species (Bai *et al.*, 2020; Cariddi *et al.*, 2018; Chen *et al.*, 2021; Zhu *et al.*, 2023; Jia *et al.*, 2023).

This is the first report of root rot caused by *F. sambucinum* on *L. barbarum*. *Fusarium sambucinum* is a common pathogen for agricultural plants, causing head blight of wheat, maize, and barley, and dry rot of potato tubers, soybean, squash, and chilli (Alejandra *et al.*, 2019; Iwase *et al.*, 2020; Yikilmazsoy and Tosun, 2021; Kitabayashi *et al.*, 2022).

Identifying the causal agent of root rot of *L. barbarum* will support efforts for the future control and management of this disease of goji, which is an economically important perennial Solanaceous shrub.

ACKNOWLEDGEMENT

This research was funded by the Start-up Program of Innovation and Entrepreneurship for Returned Overseas Chinese Scholars in the Inner Mongolia Autonomous Region (DC2100001765), the Higher Education Reform and Development Project—Young Science and Technology Talents Programme (NJYT23079), Natural Science Foundation of Inner Mongolia, China (2023LHMS03020), and the Research Start-up Funds for High-level Researchers in Inner Mongolia Agricultural University (NDYB2019–1).

LITERATURE CITED

Alejandra A.S., Victoria A., Ibar T.S., Daniel N.A., 2019. *Fusarium sambucinum* Fuckel causal agent of fruit rot of manzano chilli pepper (*Capsicum pubescens*) in Mexico. *Mexican Journal of Phytopathology* 37: 159–169. https://doi.org/10.18781/r.mex.fit.1810-2

Bai L., Li X., Cao Y., Song Z., Ma K., … Ma M., 2020. *Fusarium culmorum* and *Fusarium equiseti* causing root rot disease on *Lycium barbarum* (Goji ber-

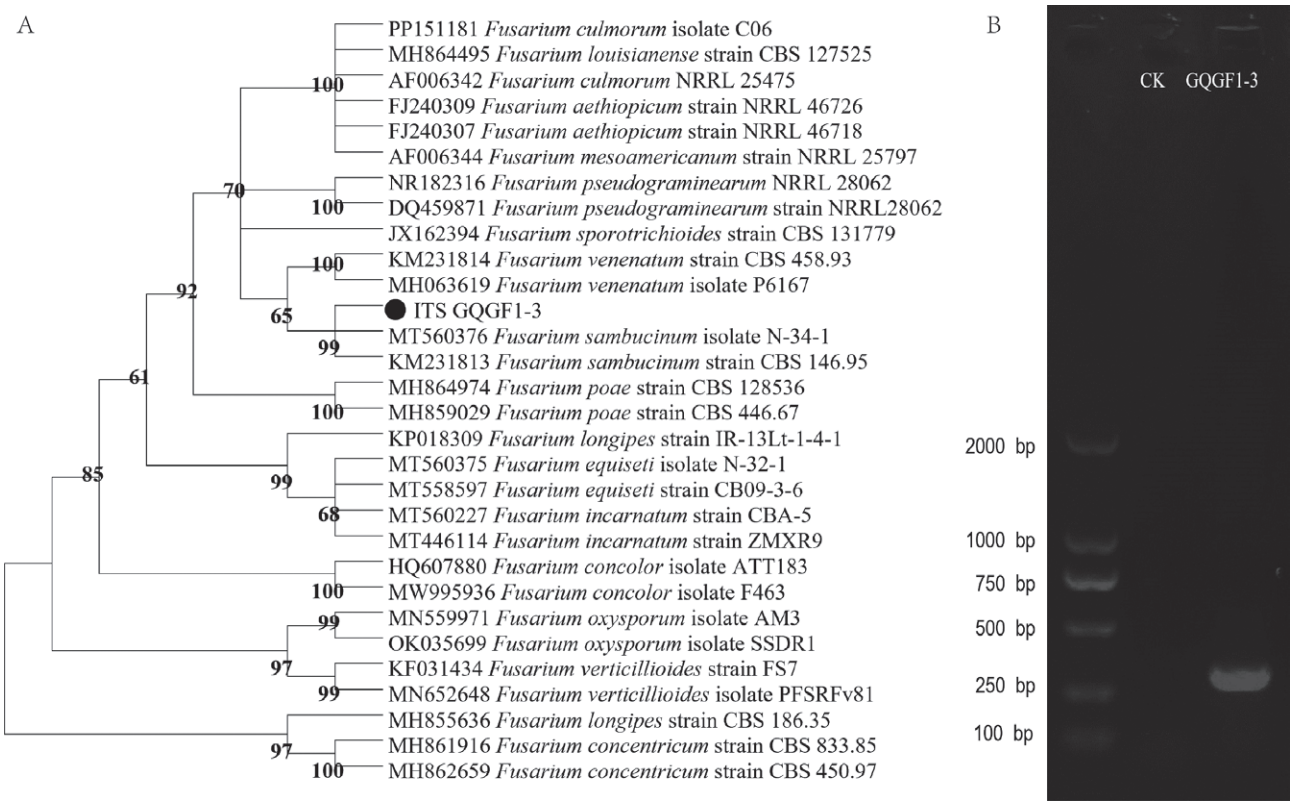

Figure 3. A, Phylogenetic tree for isolate GQGF1-3, based on ITS sequences, and B, amplification of GQGF1-3 with the species-specific primer pair FSF1/FSR1.

ry) in China. *Plant Disease* 104: 3066. https://doi.org/10.1094/PDIS-11-19-2313-PDN

Cariddi C., Mincuzzi A., Schena L., Ippolito A., Sanzani S. M., 2018. First report of collar and root rot caused by *Phytophthora nicotianae* on *Lycium barbarum*. *Journal of Plant Pathology* 100: 361–361. https://doi.org/10.1007/s42161-018-0076-0

Chen S., Du J., Zhang T., Gu P., 2021. Studies on the pathogen of root rot of *Lycium Barbarum* in Ningxia. *Journal of Agricultural Sciences* 42: 7–11. (in Chinese)

Du M., Ren X., Sun Q., Wang Y., Zhang R., 2012. Characterization of *Fusarium* spp. causing potato dry rot in China and susceptibility evaluation of Chinese potato germplasm to the pathogen. *Potato Research* 55: 175–184. https://doi.org/10.1007/s11540-012-9217-6

Iwase C.H., Piacentini K.C., Giomo P.P., Čumová M., Wawroszová S., … Rocha L., 2020. Characterization of the *Fusarium sambucinum* species complex and detection of multiple mycotoxins in Brazilian barley samples. *Food Research International* 136: 109336. https://doi.org/110.1016/j.foodres.2020.109336

Jia C., An Y., Du Z., Gao H., Su J., Xu C., 2023. Differences in soil microbial communities between healthy and diseased *Lycium barbarum* cv. Ningqi-5 Plants with Root Rot. *Microorganisms* 11: 694. https://doi.org/10.3390/microorganisms11030694

Kitabayashi S., Kawaguchi A., Yoshida M., Kami D., Sugiyama K., Kawakami A., 2022. First report of *Fusarium sambucinum* causing postharvest fruit rot of winter squash (*Cucurbita maxima*). *Journal of General Plant Pathology* 88: 207–211. https://doi.org/10.1007/s10327-022-01053-w

Lu Y., Guo S., Zhang F., Yan H., Qian D., … Duan J., 2021. Nutritional components characterization of Goji berries from different regions in China. *Journal of Pharmaceutical and Biomedical Analysis* 195: 113859. https://doi.org/10.1016/j.jpba.2020.113859

Mishra P.K., Fox R.T., Culham A., 2003. Development of a PCR based assay for rapid and reliable identification of pathogenic Fusaria. *Microbiology Letters* 218: 329–332. https://doi.org/10.1111/j.1574-6968.2003.tb11537.x

Nicholson P., Simpson D.R., Wilson A.H., Chandler E., Thomsett M., 2004. Detection and differentiation of trichothecene and enniatin-producing *Fusarium* species on small-grain cereals. *European Journal of Plant Pathology* 110: 503–514. https://doi.org/10.1023/B:EJPP.0000032390.65641.a7

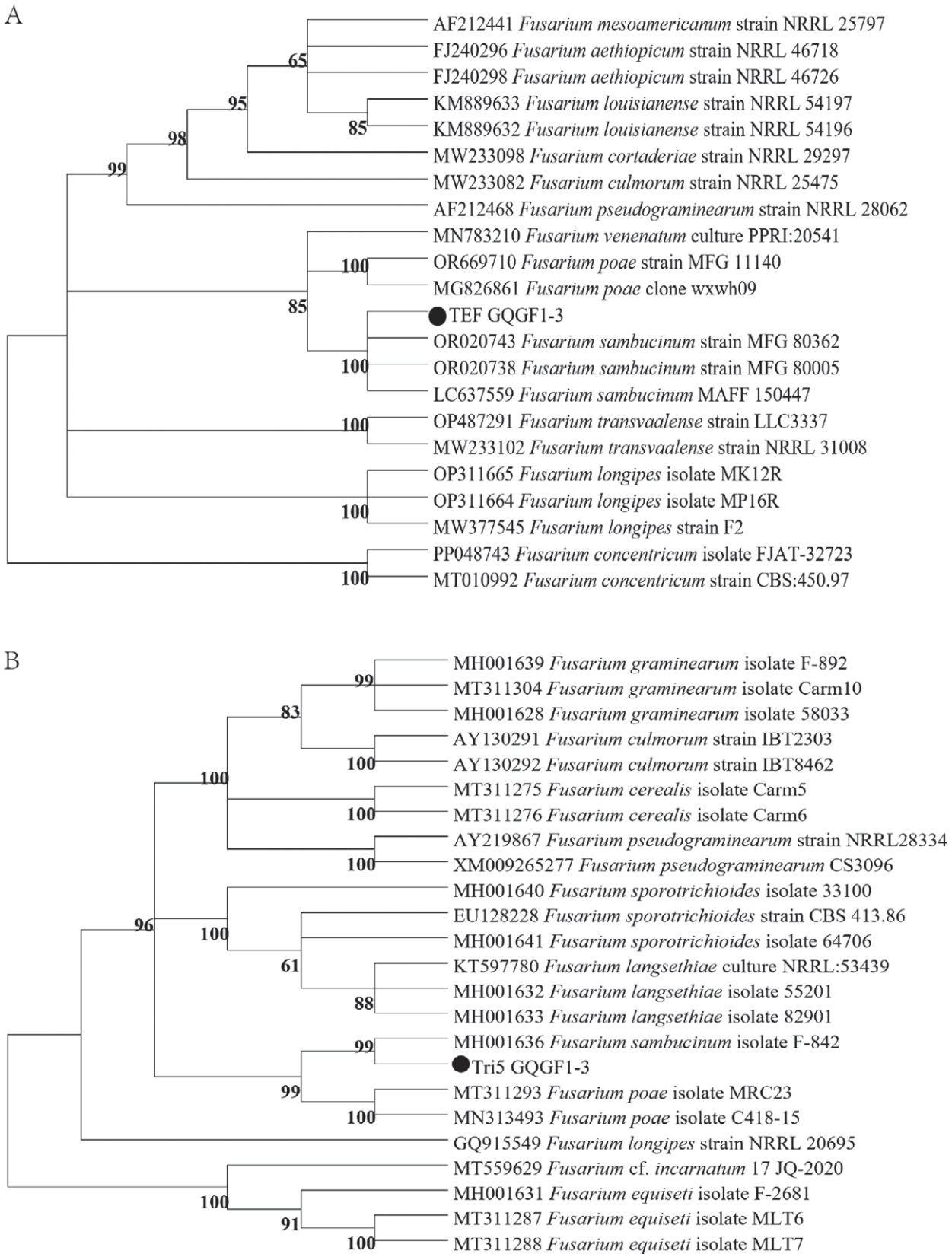

Figure 4. Phylogenetic trees for isolate GQGF1-3, based on TEF (A) and Tri5 (B) sequences.

Potterat O., 2010. Goji (*Lycium barbarum* and *L. chinense*): Phytochemistry, pharmacology and safety in the perspective of traditional uses and recent popularity. *Planta Medica* 76: 7–19. https://doi.org/10.1055/s-0029-1186218

White T.J., Bruns T.D., Lee S.B., Taylor J.W., 1990. PCR Protocols: A guide to methods and applications. in amplification and direct sequencing of fungal ribosomal RNA genes for phylogenetics, Academic Press, San Diego, California, United States of America, 315–322.

Yikilmazsoy G., Tosun N., 2021. Characterization of *Fusarium sambucinum* isolates associated with potato dry rot and evaluation of cultivar susceptibility and fungicides. *Turkish Journal of Agriculture and Forestry* 45: 222–233. https://doi.org/10.3906/tar-2006-100

Zhang Y., Qin J., Wang Y., Zhou T., Feng N., … Zhu M., 2022. Levels and health risk assessment of pesticides and metals in *Lycium barbarum* L. from different sources in Ningxia, China. *Scientific Reports* 12: 561. https://doi.org/10.1038/s41598-021-04599-5

Zhu J., Chen L., Yao Q., Li Q., Chen H., Guo Q., 2023. Isolation and identification of pathogenic fungi and antagonistic bacteria from *Lycium barbarum* root rot. *Acta Agriculturae Boreali-occidentalis Sinica* 32: 1120–1130. https://doi.org/10.1016/j.biocontrol.2022.105120

Phytopathologia Mediterranea
The international journal of the
Mediterranean Phytopathological Union

Firenze University Press
www.fupress.com/pm

Research Papers

Phytosanitary problems in elephant garlic (*Allium ampeloprasum* var. *holmense)* in the "Val di Chiana" area (Central Italy), and evaluation of potential control strategies

Francesco TINI[1], Giovanni BECCARI[1,*], Niccolò TERZAROLI[1], Enrica BERNA[2], Lorenzo COVARELLI[1], Mara QUAGLIA[1]

[1] *Department of Agricultural, Food and Environmental Sciences, University of Perugia, Borgo XX Giugno 74, 06121 Perugia, Italy*
[2] *BMP Agronomic Farm Counselling, Via Guidonami 18, 06060, Porto, Castiglione del Lago, Perugia, Italy*
*Corresponding author. E mail: giovanni.beccari@unipg.it

Summary. *Allium ampeloprasum* var. *holmense* (elephant garlic) is traditionally cultivated in "Val di Chiana", an area between Umbria and Tuscany regions of Central Italy, under the name "Aglione della Valdichiana". This product has recently increased in importance, becoming a key economic resource for local farmers. In 2019, phytosanitary problems of elephant garlic cloves ready for transplanting emerged in this cultivation area. Symptom/sign observations and fungal isolations were performed for cloves divided into four components (tunic, basal plate, reserve tissue and shoot) from six farms in the "Val di Chiana" area. Isolates obtained were identified, using partial *β-tubulin* (*BenA*) and *calmodulin* (*CaM*) or *translation elongation factor 1α* (*tef1α*) genes sequences, as belonging to *Penicillium* [*P. allii* (95%), *P. citrinum* (4%), *P. brevicompactum* (1%)] or *Fusarium* [*F. oxysporum* (81%), *F. proliferatum* (19%)]. *Fusarium* spp. were mainly associated with clove tunics and basal plates, while *Penicillium* spp. with basal plates, reserve tissues and shoots. Fungi often also developed from asymptomatic components, but a correlation was found between isolated pathogens and disease symptoms. Pathogenicity and virulence towards elephant garlic cloves were verified for a representative isolate of each identified species, and *Penicillium allii* was the most virulent. Strategies to control *Fusarium* and *Penicillium* spp. on cloves were assessed, including chemicals, a biocontrol agent, surface sterilization and heat treatment. Among these, treatments with Patriot Gold® (active ingredient [a.i.] *Trichoderma asperellum* TV1, approved in organic farming on crops similar to elephant garlic), or Signum® (a.i. boscalid + pyraclostrobin, approved for Integrated Pest Management systems on crops similar to elephant garlic), were effective in simultaneous reduction of *Penicillium* spp. and *Fusarium* spp. Transplanting of asymptomatic cloves combined with the use of the above treatments showed promising effects for pathogens control, and to assist elephant garlic crop establishment.

Keywords. Bulb diseases, *Fusarium*, *Penicillium*, *Trichoderma*, disease management.

OPEN ACCESS

Citation: F. Tini, G. Beccari, N. Terzaroli, E. Berna, L. Covarelli, M. Quaglia (2024) Phytosanitary problems in elephant garlic (*Allium ampeloprasum* var. *holmense*) in the "Val di Chiana" area (Central Italy), and evaluation of potential control strategies. *Phytopathologia Mediterranea* 63(1): 53-72. doi: 10.36253/phyto-14911

Accepted: February 14, 2024

Published: April 29, 2024

Data Availability Statement: All relevant data are within the paper and its Supporting Information files.

Competing Interests: The Author(s) declare(s) no conflict of interest.

Editor: Jean-Michel Savoie, INRA Villenave d'Ornon, France.

ORCID:
FT: 0000-0002-6427-8234
GB: 0000-0002-9227-9023
NT: 0000-0001-6411-1664
LC: 0000-0002-4568-6160
MQ: 0000-0002-1137-2585

INTRODUCTION

Allium (*Amaryllidaceae* J.St.-Hil., subfamily *Allioideae* Herb) is a broad genus including many bulbous species (Han *et al.*, 2020). Within *Allium*, the species complex *Allium ampeloprasum* L. has wide distribution in the Mediterranean area. The important species *Allium ampeloprasum* var. *porrum* (L.) J. Gay (leek) and *A. ampeloprasum* var. *holmense* (Mill) Asch. et Graebn (commonly referred as elephant garlic) (Guenaoui *et al.*, 2013; Ascrizzi and Flamini, 2020; Terzaroli and Caproni, 2020) are included in the *A. ampeloprasum* species complex.

Allium spp. are appreciated for their health benefits as they contain bioactive compounds with antifungal, antibacterial, antiviral, antitoxic and anticancer properties (Keusgen *et al.*, 2006; Kim *et al.*, 2018; Ceccanti *et al.*, 2021). Among these compounds, the sulfur-containing substances (i.e. alliin and its derivatives) have antimicrobial activities, and are also responsible for human smell, taste, poor digestion and bad breath (Borlinghaus *et al.*, 2014). The very low amounts of alliin and related derivatives present in elephant garlic make these bulbs potential cuisine substitutes for common garlic (*Allium sativum* L.), because their flavour is very close to that of common garlic, but with milder impacts on human breath and digestion (Block, 2011; Ascrizzi and Flamini, 2020; Ceccanti *et al.*, 2021).

Allium ampeloprasum var. *holmense*, native to the Mediterranean basins, is cultivated in many other regions (Fritsch and Friesen, 2002; Guenaoui *et al.*, 2013). It has oversized bulbs and large cloves (Guenaoui *et al.*, 2013). In Italy, elephant garlic is mainly cultivated in "Val di Chiana", a valley between Umbria and Tuscany Regions (Central Italy), as a local landrace named "Aglione della Valdichiana" (Terzaroli *et al.*, 2022). In this territory, elephant garlic was cultivated in family gardens by elderly farmers, and was very close to extinction (Terzaroli, 2015; Terzaroli and Caproni, 2020). However, recent expansion of demand for this product had led to cultivation in "Val di Chiana", and, at the same time, many imitations on the market. For this reason, "Aglione della Valdichiana" has been included in several regional and national traditional product lists (Ministry of Agriculture, Food and Forestry Policies, 2016; Tuscany Region, 2016; Umbria Region, 2020; Slow Food Foundation, 2023). The "Association of Manufacturers and Transformers of Aglione della Valdichiana" is also attempting to obtain the "Protected Designation of Origin" award (PDO) for elephant garlic.

Despite this increasing interest in elephant garlic cultivation, little is known about phytopathological problems of bulbs caused by fungal pathogens, and related disease control strategies. Since elephant garlic is vegetatively propagated due to inability to produce seeds (Terzaroli *et al.*, 2022), bulb phytosanitary status is important during propagation, as well as for commercialisation. As for other *Allium* spp., the health of cloves/bulbs can be compromised by fungal pathogens, including *Fusarium* and *Penicillium* (Dugan *et al.*, 2011; Le *et al.*, 2021). For example, in Chile, *P. hirsutum*, *P. aurantiogriseum*, *P. echinulatum*, *P. funiculosum* and *P. rugulosum*, and *F. oxysporum*, were isolated from stored elephant garlic bulbs showing lesions (Besoain *et al.*, 2002). In addition, *F. proliferatum* has been isolated from rotten elephant garlic cloves in Serbia (Ignjatov *et al.*, 2019). *Fusarium* and *Penicillium* are also well-known causal agents of bulb rot of common garlic (Crowe, 1995; Valdez *et al.*, 2006; Valdez *et al.*, 2009; Gálvez *et al.*, 2017a; Chrétien *et al.*, 2020; Gálvez and Palmero, 2021; Mondani *et al.*, 2021a).

To date, while reports are available on treatments to control *Fusarium* (Dugan *et al.*, 2007; Palmero Llamas *et al.*, 2013; Gálvez *et al.*, 2017b; Mondani *et al.*, 2021b; 2021c; 2022) and *Penicillium* (Greathead, 1978; Bogo, 1997; Johnson, 2013; Ciabanal *et al.*, 2021) in common garlic, no strategies have been tested or developed to control these pathogens on elephant garlic cloves.

Symptoms and signs of fungal infections on elephant garlic cloves ready for planting have been reported in 2019 from several farms of the "Val di Chiana" area in Tuscany and Umbria (Central Italy). For this reason, the present study aimed to: 1) observe the distribution and characteristics of the symptoms/signs in elephant garlic cloves; 2) determine the fungal community associated with components of elephant garlic cloves by isolation into culture; 3) confirm identification of the fungi with molecular methods; 4) assess their pathogenicity and virulence to elephant garlic cloves; 5) test different potential clove treatments for control of clove pathogens.

MATERIALS AND METHODS

Sampling and symptom/sign observations

This study was carried out on elephant garlic cloves collected from six farms located in the "Val di Chiana" area (Figure 1). After harvest (June 2019), the cloves were stored at each farm using the common farming practices. At the time of transplanting (September 2019), 50 cloves were randomly sampled from each farm, from cloves already selected by the farmer for transplanting, to give a total of six samples. These were

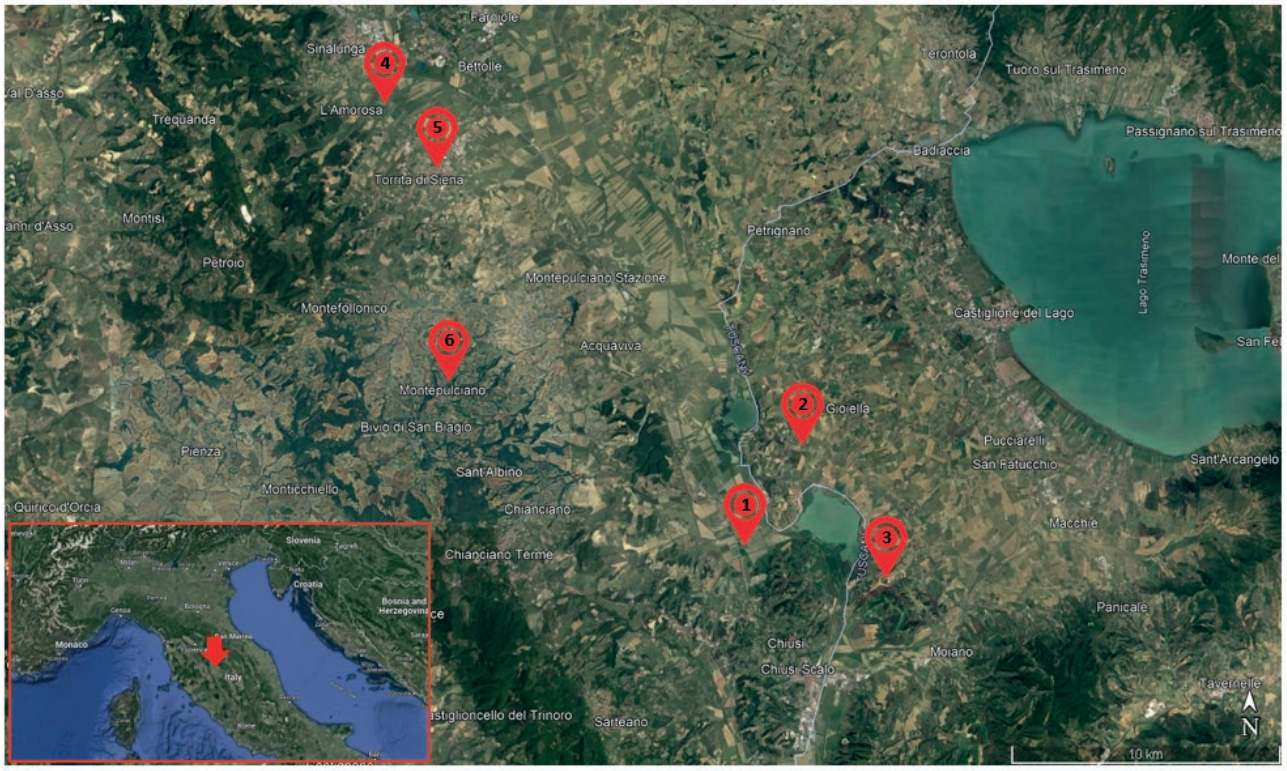

Sample	Location	Province	Region	Previous crop	Harvest season	Presence of other *Allium* spp. in the crop system
1	Montallese	Siena	Tuscany	Alfalfa	2019	No
2	Porto	Perugia	Umbria	Tomato	2019	No
3	Villastrada	Perugia	Umbria	Sunflower	2019	Yes (common garlic)
4	Sinalunga	Siena	Tuscany	Wheat	2019	No
5	Torrita di Siena	Siena	Tuscany	Barley	2019	No
6	Montepulciano	Siena	Tuscany	Grassland	2019	No

Figure 1. Map showing the six sampling locations in "Val di Chiana" area, a valley in the Umbria and Tuscany regions of Central Italy. The inset (bottom left) shows a map indicating (red arrow) "Val di Chiana" location. The table presents details relating to each sample location.

brought to the laboratory and 20 cloves per sample were randomly selected. Each clove was divided into four components: tunic (outer husk); basal plate (the attachment point of roots in the bulb); reserve tissue (fleshly part of the clove); and shoot (the shoot primordium within each clove). A sterilized blade was used for each clove dissection to avoid contamination. After defining the symptom/sign categories observed in the cloves, incidence (% of symptoms/signs for each clove component on each sample) was assessed and expressed as the average for 20 cloves. In addition, incidence (% of symptoms/signs per clove component) on all the cloves analysed in the survey was calculated and expressed as the average for 120 cloves.

Determination of the fungal community associated with elephant garlic cloves

The different components (tunic, basal plate, reserve tissue and shoot) of the cloves used for symptom/sign observation were used for isolations of fungi, using the method of Beccari *et al.* (2018). From symptomatic cloves, isolations were made by taking portions showing signs or symptoms, while, for the asymptomatic cloves, isolations were made from portions of the different clove components. Each clove component was disinfected for 1 min by immersion in a solution of 95% ethanol (Sigma Aldrich) + 7% sodium hypochlorite (Carlo Erba Reagents) solution (82:10:8 % vol.), and was then rinsed

three times in sterile deionized water. After disinfection, each component was cut into seven pieces (approx. 2 × 3 mm) that were placed into a Petri dish (90 mm diam., Nuova Aptaca) containing potato dextrose agar (PDA, Biolife Italiana) amended with streptomycin sulphate (0.16 g L^{-1}, Sigma Aldrich). From each clove, four Petri dishes (one per component) were used, giving a total of 80 Petri dishes per original component sample and 480 for the entire survey. The Petri dishes were incubated at 22 ± 2°C in the dark. After 5 d of incubation, a combination of a visual, stereomicroscope (SZX9, Olympus) and microscope (Axiophot, Zeiss) observations were carried out on each Petri dish, to examine development of fungal colonies and to ascribe these to fungus genera.

Incidence (%) of each fungal genus was calculated. Because fungi from cloves were mainly from *Fusarium* or *Penicillium*, the averages of isolates belonging to these genera in each clove component were compared. In addition, for each sample, the number of *Fusarium* and *Penicillium* colonies isolated from each clove component was compared to the numbers isolated from the other components. The average number of *Fusarium* and *Penicillium* isolates obtained from each clove component for each sample was also assessed.

Identification of Fusarium *and* Penicillium *isolates*

Based on the above observations, *Fusarium* and *Penicillium* were the most frequently isolated genera, so isolates potentially belonging to these genera were identified by molecular means, adapting the method described by Beccari *et al.* (2020). All *Fusarium* and *Penicillium* colonies were transferred from isolation PDA cultures into new Petri dishes (one dish per isolate), and these were incubated in the dark at 22 ± 2°C for 10 d. Resulting colonies were assigned to morphotypes according to their shapes and colours, detected visually, and morphology of conidiophores and conidia, detected by optical microscope (Axiophot, Zeiss). A subset of representative isolates was chosen, one from each morphotype. For each representative isolate, a monosporic culture was obtained on PDA and incubated in the dark at 22 ± 2°C. After 10 d, mycelium was scraped from PDA in each dish and placed into a 2 mL capacity sterile plastic tube (Eppendorf) at -80°C, lyophilized with a Heto Powder Dry LL3000 freeze-drier (Thermo Fisher Scientific), and reduced to a fine powder with a Mixer Mill MM400 (Retsch) set at frequency of 25 Hz for 6 min.

DNA extraction was carried out using the methods of Covarelli *et al.* (2015) and Beccari *et al.* (2018). Genomic DNA was quantified using a Qubit® 3.0 fluorometer (Thermo Fisher Scientific), using the dsDNA Broad Range Assay kit (Thermo Fisher Scientific), following the manufacturer's protocol. Each DNA sample was adjusted to a concentration of 30 ng μL^{-1} adding sterile water for molecular biology (5prime). DNA extracts were subjected to partial *translation elongation factor 1α* (*tef1α*) gene amplification and sequencing for *Fusarium* isolates (O'Donnel *et al.*, 1998; Geiser *et al.*, 2004), or partial *β-tubulin* (*BenA*) and *calmodulin* (*CaM*) gene amplification and sequencing for *Penicillium* isolates (Houbraken and Samson, 2011; Visagie *et al.*, 2014). The primers used in the PCR assays are shown in Table S1. Each PCR protocol used a total reaction volume of 50 µL. Each reaction contained 29 µL of sterile water for molecular biology, 5 µL of dNTPs mix 10 mM (Thermo Fisher Scientific), 2.5 µL 10× Dream Taq Buffer + magnesium chloride (Thermo Fisher Scientific), 3.75 µL of cresol red (Sigma Aldrich), 2.5 µL of 10 µM of primers, 0.25 µL of 5 U μL^{-1} Dream Taq Polymerase (Thermo Fisher Scientific), and 2 µL of template DNA (≈60 ng DNA). The PCR cycle consisted of an initial denaturation step (94°C for 5 min), followed by 30 cycles of denaturation (94°C for 1 min), annealing (1 min at the temperature shown in Table S1), extension (72°C for 1 min), and final extension (72°C for 10 min). PCR assays were carried out on a T-100 thermal cycler (Bio-Rad). PCR fragments were visualized on TAE 1X agarose gel (2%) containing 500 µL L^{-1} of RedSafe™ (4% v/v) (Chembio). DNA fragments were separated at 110 V for ≈40 min and observed with a gel documentation system (Essential V6, Uvitec). The sizes of the amplified fragments were obtained by comparison with HyperLadder 100-1000 bp (Bioline Meridian Bioscience).

PCR fragments were purified and sequenced by a commercial service (Genewiz Genomic Europe, Leipzig, Germany). The sequences obtained were verified and edited by Chromatogram Explorer Lite v4.0.0 (Heracle Biosoft srl 2011), and were compared with those deposited in the NCBI Basic Local Alignment Search Tool (BLAST) database (Altschul *et al.*, 1990).

Phylogenetic analyses were carried out for *Fusarium* and *Penicillium* isolates using *tef1α* (O'Donnel *et al.*, 1998; Geiser *et al.*, 2004; Southwood *et al.*, 2012; Taylor *et al.*, 2016; Crous *et al.*, 2021) for *Fusarium*, or *BenA* and *CaM* partial genes sequences (Houbraken and Samson, 2011; Visagie *et al.*, 2014) for *Penicillium*. The sequences of the *Fusarium* or *Penicillium* representative isolates obtained in the present study were analyzed together with those of validated phylogenetic species reported in GenBank (Tables S2 and S3), using MEGA software version 7.0 (Kumar *et al.*, 2016). *Fusarium redolens* NL_96 (Taylor *et al.*, 2016) was used as the outgroup for *Fusarium* phylogeny, and *Talaromyces flavus*

isolate CBS 310.38 (Houbraken and Samson, 2011) was used as the outgroup for *Penicillium* phylogeny. After sequence alignments, nucleotide gaps and missing data were deleted and phylogenetic trees were built using the neighbor-joining method (Saitou and Nei, 1987) with the bootstrap test for 1000 replicates (Felsenstein, 1985). The maximum composite likelihood method (Tamura *et al*., 2004) was used to compute the evolutionary distances.

Pathogenicity and virulence tests

Pathogenicity and virulence tests were carried out using one representative isolate each of *F. proliferatum* (isolate F 88), *F. oxysporum* subclade 1 (isolate F 129), *F. oxysporum* subclade 2 (isolate F 125), *F. oxysporum* subclade 3 (isolate F 42), *Penicillium allii* (isolate P 104), *Penicillium citrinum* (isolate P 41), and *Penicillium brevicompactum* (isolate P 150). Pathogenicity and virulence were evaluated using the methods of Dugan *et al.* (2007) and Ignjatov *et al*. (2019), with slight modifications. Asymptomatic elephant garlic cloves obtained shortly after harvest were disinfected by dipping for 30 sec in water-ethanol-sodium hypochlorite solution (see above), and rinsed three times with sterile water. Cloves were each wounded in two sites by a sterile cork-borer producing wounds of 4 mm depth and 5 mm width. Each wound was filled with a mycelium plug (5 mm diam.) taken from a 7-d-old colony grown on PDA in the dark at 22 ± 2°C. For each fungal isolate, four cloves (replicates) were inoculated, for a total of 32 cloves. In addition, four cloves were used as inoculation controls and were treated with sterile PDA. Inoculated and control cloves were placed in separate transparent plastic trays, which were sealed to maintain a 100% moisture, and were then incubated in a climatic chamber (F.lli Bertagnin) at 22°C, 16 h daily photoperiod. On each clove wound, symptoms were assessed at 30 d post-inoculation (dpi), as the average diameter of dry rot lesion (cm), calculated as the mean of two diameters perpendicular to each other. In addition, to obtain the virulence indices (VIs), average lesion diameter was multiplied by the average wound depth (cm), given by the mean of the depth of the two lesions for each clove, each measured with a ruler. For each isolate, the VI index expressed its aggressiveness (virulence), as the average of the four replicates (cloves).

Evaluation of control of Fusarium *and* Penicillium *spp. on elephant garlic cloves*

A pot trial evaluated different treatments applied to cloves at planting for efficacy against *Fusarium* and *Penicillium* infections. Treatments applied are listed in Table 1. These included: sodium hypochlorite disinfection (2% NaOCl), either alone or with heat treatment (50°C/30 min) in a water bath, also followed by the application of Patriot Gold®, a commercial preparation of *Trichoderma asperellum* strain TV1. Other treatments included: Patri-

Table 1. Treatments applied to elephant garlic cloves for the control of *Fusarium* spp. and *Penicillium* spp.

Treatment	Application	Company	Active ingredient	Dose	Notes
Untreated control	-	-	-	-	-
Sodium hypochlorite (2%)	Immersion	-	Sodium hypochlorite	-	Immersion for 3 min in a water-sodium hypochlorite (2%) solution
Sodium hypochlorite (2%) and heating	Immersion + heating	-	Sodium hypochlorite	-	Immersion for 3 min in a water-sodium hypochlorite (2%) solution, followed by immersion in water for 30 min at 50°C
Sodium hypochlorite (2%), heating and Patriot Gold®	Immersion + heating + dressing	Sumitomo Chemical	Sodium hypochlorite + *Trichoderma asperellum* (TV1 strain, 1×10^6 UFC g^{-1})	0.01 g 6 mL^{-1}	Immersion for 3 min in a water-sodium hypochlorite (2%) solution followed by immersion in water for 30 min at 50°C, and treated with Patriot Gold® (see below).
Patriot Gold®	Dressing	Sumitomo Chemical	*Trichoderma asperellum* (TV1 strain, 1×10^6 UFC g^{-1})	0.01 g 6 mL^{-1}	For each treatment, cloves were placed in a plastic bag containing the product. The plastic bags were gently shaken for 3 min to promote the maximum contact between the product and the cloves.
Signum®	Dressing	BASF	Pyraclostrobin (6.7 g) + boscalid (26 g)	0.09 g 6 mL^{-1}	
Celest Trio®	Dressing	Syngenta	Fludioxonil (25 g L^{-1}) + difenoconazole (25 g L^{-1}) + tebuconazole (10 g L^{-1})	4 mL 40 mL^{-1}	

ot Gold®, without previous hypochlorite and heat treatments, and the fungicides Signum® (pyraclostrobin + boscalid), or Celest Trio® (fludioxonil + difenoconazole + tebuconazole), applied at label rates by shaking cloves in solutions for 3 min, followed by 24 h at room temperature to dry (Table 1). Patriot Gold® and Signum® are currently registered in Italy for use on common garlic (*Allium sativum* L.), onion (*Allium cepa* L.) and leek (*Allium ampeloprasum* L.). Celest Trio® is registered in Italy for treatment of cereal seeds against *Fusarium*. Each treatment, including an untreated control, consisted of ten asymptomatic cloves (ten replicates). Each clove was planted in sterile peat in a plastic pot (8 × 8 × 9 cm) and maintained in a growth cabinet for 30 d at 22°C with a 15 h light 9 h dark daily cycle. At 30 d after the treatments, clove germination rate (%), shoot length (cm), shoot fresh weight (g) and shoot dry weight (g: obtained by placing the shoots in a drying oven at 50°C for 48 h) were measured. In addition, to evaluate effects of the different treatments on frequencies of *Fusarium* spp. and *Penicillium* spp. infections, fungal isolations were carried out for each clove from the four different components (tunic, basal plate, reserve tissue, and shoot) following the method described above, but because the cloves were sprouted, the first centimetre of each seedling was taken for the isolation procedure. Frequencies of isolations (n) of *Fusarium* spp. and *Penicillium* spp. were recorded.

Statistical analyses

All data were subject to one-way analysis of variance (ANOVA). In all cases, Tukey Honestly Significant Difference (HSD) ($P \leq 0.05$) was used to assess pairwise treatment contrasts. All statistical analyses was carried out using Microsoft Excel Macro "DSAASTAT" ver. 1.0192 (Onofri and Pannacci, 2014).

RESULTS

Symptoms and signs on elephant garlic cloves

Different symptoms and signs were observed on the clove components (tunic, basal plate, reserve tissue, or shoot) of the six samples analysed (Table 2, Figure 2). On tunics (Table 2, Figure 2, a, b, and c), pink-purple spotting was detected on average on 28% of the 120 cloves analysed, and browning was detected on 45% of these cloves. Asymptomatic tunics were also detected (27%). Considering the average of the whole survey, no statistically significant differences ($P > 0.05$) were detected between pink-purple spotting, browning and asymptomatic tunics. On basal plates (Table 2, Figure 2, d, e, and f), grey mould signs (35% of cloves) were the most commonly detected, followed by symptoms of sponge-like rot (23%) and pink mould signs (13%). Of total cloves analysed 29% had asymptomatic basal plates. Also on the basal plates, no differences ($P > 0.05$) were detected between the different symptom/sign categories recorded. On reserve tissues (Table 2, Figure 2, g, h and i), rot symptoms (soft watery, or dry) were very common (87% of the total number of cloves analysed and 100% of samples 2, 3 and 6). Black-purple streaks (7%) or asymptomatic tissues were less frequent (present only in sample 5). In this clove component, incidence (%) of rot symptoms was greater ($P \leq 0.05$) compared to black-purple streaks or no symptoms. On shoots (Table 2, Figure 2, j, k, and l), basal grey mould (15%) was the most detected sign followed by dry rot symptoms (3%) and white mould signs (2%). Asymptomatic shoots were very common, detected in 81% of the total cloves analysed, more ($P \leq 0.05$) than for samples with basal grey mould, dry rot or white mould.

Fungal communities associated with elephant garlic cloves

After 7 d of incubation on PDA, from all the clove components of the six clove samples (480), 66% of the total isolated fungi were morphologically identified as *Penicillium*, and 32% were identified as *Fusarium* (Figure 3 a). Fungi not included in these two genera ("other genera"), were isolated with incidence of 2% (Figure 3 a).

The average number of fungal isolates (n) belonging to *Fusarium* and *Penicillium* per analysed clove component are shown in Figure 3 b. The average number of *Fusarium* isolates was greater ($P \leq 0.05$) than *Penicillium* only on the clove tunics. For the other clove components (basal plates, reserve tissues, shoots) greater numbers ($P \leq 0.05$) of *Penicillium* isolates than *Fusarium* isolates were obtained (Figure 3 b). The distribution of *Fusarium* across the four clove components showed the following gradient: tunic > basal plate > shoot ≥ reserve tissue (Figure 3 b). In contrast, the *Penicillium* distribution gradient decreased as follows: shoot > basal plate ≥ reserve tissue > tunic (Figure 3 b).

For the four clove components (tunic, basal plate, reserve tissue, shoot) of each of the six field clove samples (20 cloves per sample), there was no sample or clove component from which the two fungal genera (*Fusarium* or *Penicillium*) were not co-isolated, with the exceptions of the reserve tissue of clove sample 6 and the shoots of samples 5 and 6, where only *Penicillium* was obtained (Figure S1). *Penicillium* was the prevalent genus isolated from the shoots and reserve tissues in each sample ($P \leq 0.05$), while *Fusarium* was the prevalent genus ($P \leq 0.05$)

Table 2. Symptoms and signs detected on elephant garlic clove components (tunic, basal plate, reserve tissue, shoot), and related incidence per sample. For each symptom type within each clove component, average incidence (± standard error [SE]) was calculated.

TUNIC: symptoms incidence %							BASAL PLATE: symptoms or signs incidence %							
Sample	Pink-purple spotting	MCP[a]	Browning	MCP	Asymptomatic	MCP	Sample	Pink mould	MCP	Grey mould	MCP	Sponge-like rot	MCP	Asymptomatic	MCP
1	35		40		25		1	5		90		0		5	
2	30		70		0		2	0		100		0		0	
3	0		85		15		3	0		20		80		0	
4	95		5		0		4	75		0		5		20	
5	0		10		90		5	0		0		10		90	
6	10		60		30		6	0		0		40		60	
Average	28.3	a	45.0	a	26.7	a	Average	13.3	a	35.0	a	22.5	a	29.2	a
SE	14.6		13.3		13.6		SE	12.4		19.3		13.0		15.3	
RESERVE TISSUE: symptoms incidence %							SHOOT: symptoms or signs incidence %							
Sample	Black-purple streaks	MCP	Rot	MCP	Asymptomatic	MCP	Sample	White mould	MCP	Basal grey mould	MCP	Dry rot	MCP	Asymptomatic	MCP
1	15		85		0		1	0		0		5		95	
2	0		100		0		2	0		60		0		40	
3	0		100		0		3	0		20		0		80	
4	5		95		0		4	10		0		0		90	
5	20		40		40		5	0		10		0		90	
6	0		100		0		6	0		0		10		90	
Average	6.7	a	86.7	b	6.7	a	Average	1.7	a	15.0	a	2.5	a	80.8	b
SE	3.6		9.6		6.7		SE	1.7		9.6		1.7		8.4	

[a]MCP = multiple comparison procedure. Values with different letters are significantly different based on Tukey Honestly Significant difference test ($P < 0.05$).

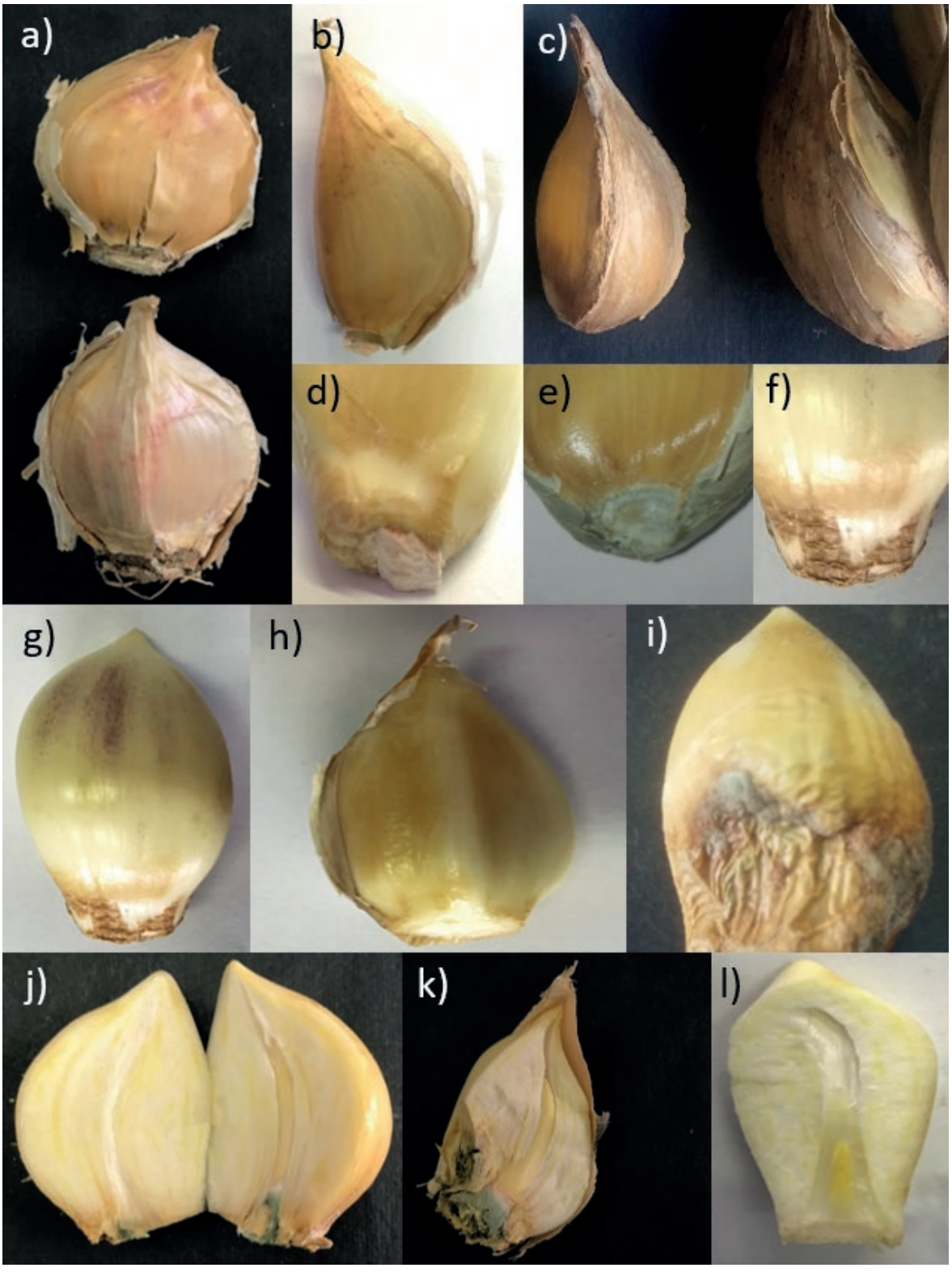

Figure 2. Different symptoms and signs detected on elephant garlic cloves collected in 2019 in "Val di Chiana" area (Central Italy). Pink-purple spotting (a, b) and browning (c) on bulb tunics; pink mould (d), grey mould (e) and sponge-like rot (f) on basal plates; black-purple streaks (g), soft watery rot (h), dry rot and grey mould (i) on reserve tissues; basal grey mould on shoots (j and k), and apparently healthy shoot (I; free of symptoms and signs).

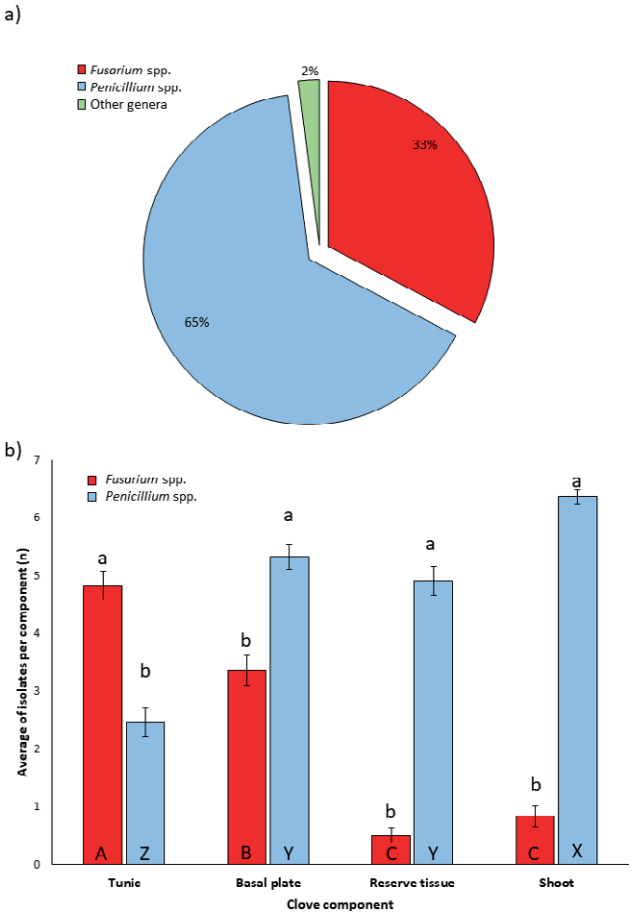

Figure 3. Incidence (%) of isolates of different fungal genera developed from sampled elephant garlic cloves (a), and distribution of the isolates of the two mainly obtained fungal genera (*Fusarium* or *Penicillium*) for each clove component (tunic, basal plate, reserve tissue, shoot) for all sampled cloves (n = 120) (b). Data were subjected to one way analyses of variance (ANOVA), considering fungal genera or clove component as the variables. Columns represent averages (± standard errors) of the number of isolates belonging to each fungal genus. Letters indicate differences ($P \leq 0.05$) between fungal genera within each clove component (letters above error bars) or between clove components within a fungal genus (letters within columns).

isolated from the tunics of three samples and from the basal plates of one sample (Figure S1). Generally, *Fusarium* was isolated less ($P \leq 0.05$) from shoots and reserve tissues of all the field samples compared to tunics and basal plates.

Identification of Fusarium *and* Penicillium *species isolated from elephant garlic cloves*

From the analysed elephant garlic cloves, a total of 47 fungal isolates were collected as representatives of all the observed morphotypes. Of these isolates, 31 were morphologically identified as *Fusarium* spp. and 16 as *Penicillium* spp. This identification was also confirmed by BLAST analysis of the amplified regions (*tef1α* for *Fusarium* spp., *BenA* and *CaM* for *Penicillium* spp.).

Considering the *Fusarium* isolates, according to Crous *et al.* (2021), in the phylogram constructed on the sequences of the *tef1α* gene, two major clades emerged (Figure 4): the first included species of the *Fusarium oxysporum* species complex (FOSC), while the second clade included species of the *Fusarium fujikuroj* species complex (FFSC). In the FOSC clade, three main subclades, here named as 1, 2 and 3, emerged (Figure 4). Subclade 1 included most of the *Fusarium* isolates obtained in this study (16 isolates), which clustered together with reference isolates of *Fusarium oxysporum* f. sp. *cepae* (Table S2). Subclade 2 included only one isolate, which clustered with reference isolates of *Fusarium oxysporum* f. sp. *lactucae*. Subclade 3 included five isolates, which clustered with reference isolates of *Fusarium oxysporum* f. sp. *dianthi*. The FFSC clade included nine isolates which clustered with the reference isolate of *F. proliferatum*.

According to Houbraken and Samson (2011) and Visagie *et al.* (2014), in the phylogram constructed on the concatenated sequences of *BenA* and *CaM* genes of *Penicillium* isolates, four major clades emerged (Figure 5). These were: clade A, which included species of the section *Fasciculata*; clade B, which included species of the section *Chrysogena*; clade C, of section *Brevicompacta*; and clade D, of sections *Exilicaulis* and *Citrina*. Most of the isolates (13) clustered in clade A together with a reference strain of *P. allii*. Of the four remaining isolates, two clustered in clade C with reference isolates of *P. brevicompactum*, and one clustered in clade D with reference isolates of *P. citrinum*.

Thus, as indicated by BLAST and phylogenetic analyses, the *Fusarium* and *Penicillium* communities isolated from elephant garlic cloves (tunics, basal plates, reserve tissues, or shoots) were composed of three *Penicillium* species and two different *Fusarium* species (Figures 4, 5 and 6).

The *Fusarium* community (Figures 4 and 6 a) was mainly composed of *F. oxysporum* subclade 1 (56%), followed by *F. oxysporum* subclade 3 (20%), *F. proliferatum* (19%) and *F. oxysporum* subclade 2 (5%). For the different clove components, *F. oxysporum* subclade 1 was the most isolated ($P \leq 0.05$) from bulb tunics and basal plates. *Fusarium oxysporum* subclade 1 was also mainly isolated (but with no statistically significant differences with respect to the other species) from shoots and reserve tissues (Figure 6 a).

Fusarium oxysporum subclade 1 incidence showed differences ($P \leq 0.05$) between the elephant garlic clove

components, as follows: tunics > basal plates > shoots = reserve tissues. A similar trend was also observed for *F. oxysporum* subclade 3 ($P \leq 0.05$: tunics ≥ basal plates ≥ shoots = reserve tissues), and for *F. oxysporum* subclade 2 ($P \leq 0.05$: tunics ≥ basal plates = shoots ≥ reserve tissues). The pattern for *F. proliferatum* was slightly different: tunics = basal plates ≥ shoots ≥ reserve tissues ($P \leq 0.05$).

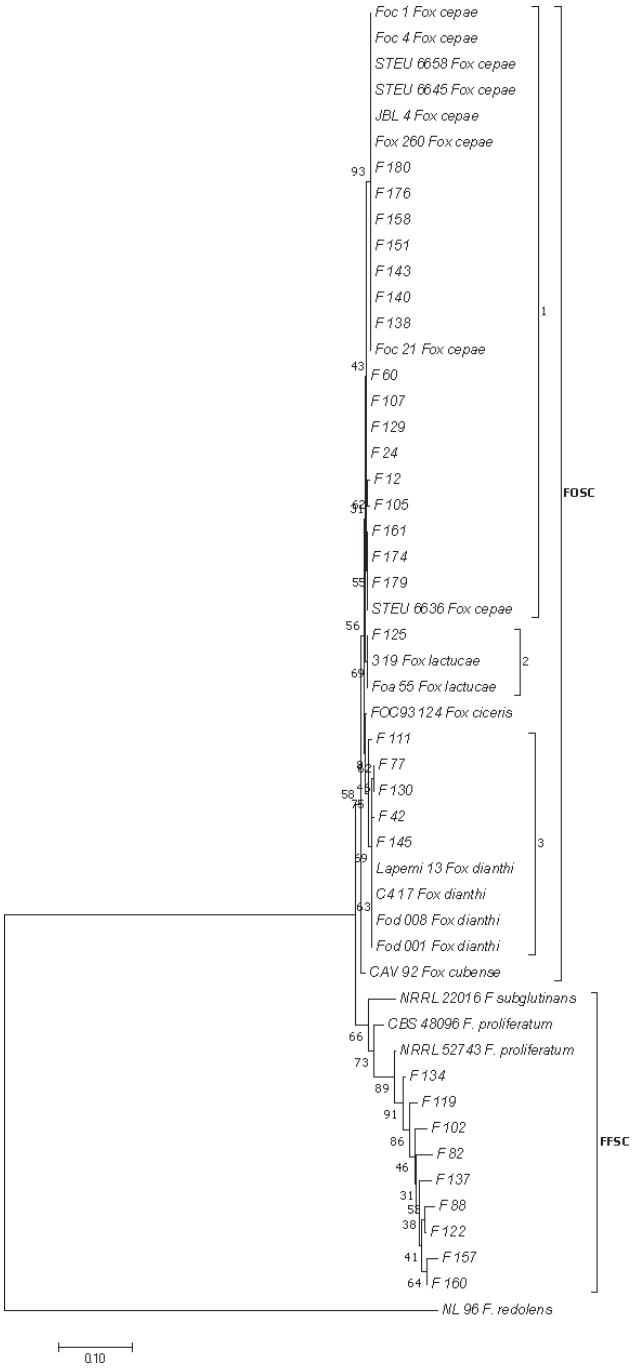

The *Penicillium* community almost entirely included *P. allii* (95%), which was the most ($P \leq 0.05$) isolated species from all the four clove components. The other two isolated species, *P. citrinum* and *P. brevicompactum*, were less common (4% and 1%, respectively) (Figure 6 b). *Penicillium allii* was the most commonly isolated from all the four clove components, but a pattern ($P \leq 0.05$) was recorded: shoots > basal plates = reserve tissues > tunics. The incidences of isolation from tunics, basal plates, reserve tissues and shoots of the other three species were not significantly different ($P > 0.05$). However, *P. allii, P. brevicompactum* and *P. citrinum* were not different ($P > 0.05$) for the numbers of colonies isolated from the four components of assessed elephant garlic cloves.

The number (n) of *Fusarium* isolates ascribable to the different species/subclades is shown in Figure S2 a. *Fusarium proliferatum*, and *F. oxysporum* subclades 1, 2 and 3 were simultaneously isolated only from the clove tunics of samples 1 and 2, and from the basal portions of sample 2, with no differences ($P > 0.05$) in average incidence. *Fusarium oxysporum* subclade 1 was the only isolated subclade from the basal plates of the six different field samples, but also from all the portions of sample 6. *Fusarium proliferatum* and *F. oxysporum* subclades 1, 2 and 3 did not show differences ($P > 0.05$) in incidence in the reserve tissues and shoots of the six field samples.

For *Penicillium* (Figure S2 b), *P. allii* was the only species isolated from all the examined clove components of the six field samples. In addition, *P. citrinum* was isolated from all the analysed portions of sample 4, and *P. brevicompactum* from the tunics of samples 5 and 6.

Pathogenicity and virulence of Fusarium *and* Penicillium *isolates on elephant garlic cloves*

All *Fusarium* and *Penicillium* isolates used in the pathogenicity tests showed abilities to cause rot symp-

Figure 4. Phylogeny of *Fusarium* isolates obtained in this study. The evolutionary history of *Fusarium* isolates was inferred using the Neighbor-Joining method (Saitou and Nei, 1987) and the dataset of partial *translation elongation factor 1α* (*tef1α*) gene sequences. The optimal tree with the sum of branch length = 1.36523273 is shown. The percentages of replicate trees in which the associated *taxa* clustered together in the bootstrap test (1000 replicates) are shown next to the branches (Felsenstein, 1985). The tree is drawn to scale, with branch lengths in the same units as those of the evolutionary distances used to infer the phylogenetic tree. The evolutionary distances were computed using the Maximum Composite Likelihood method (Tamura *et al.*, 2004), and are in the units of the number of base substitutions per site. The analysis involved 51 nucleotide sequences. All positions containing gaps and missing data were eliminated. There was a total of 490 positions in the final dataset. Evolutionary analyses were conducted in MEGA7 (Kumar *et al.*, 2016).

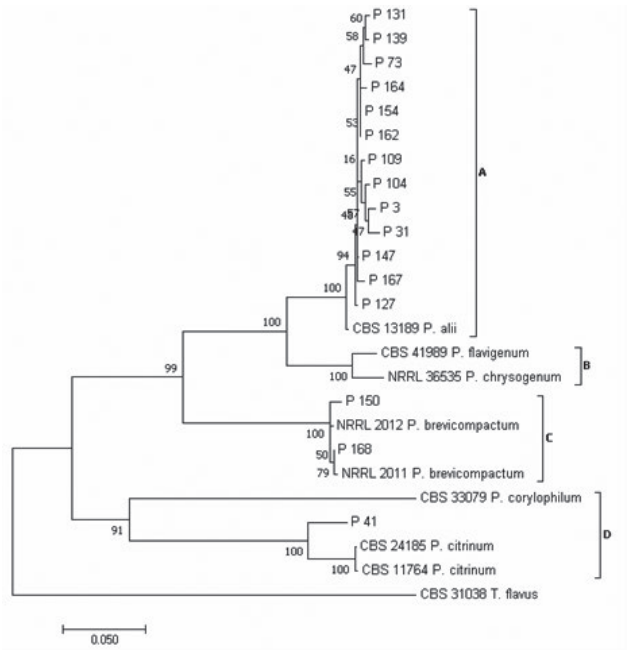

Figure 5. Phylogeny of *Penicillium* isolates obtained in this study. The evolutionary history of *Penicillium* isolates was inferred using the Neighbor-Joining method (Saitou and Nei, 1987) and the combined dataset of partial *β-tubulin* (*BenA*) and *calmodulin* (*CaM*) genes sequencing. The optimal tree with the sum of branch length = 1.04059653 is shown. The percentages of replicate trees in which the associated taxa clustered together in the bootstrap test (1000 replicates) are shown next to the branches (Felsenstein, 1985). The tree is drawn to scale, with branch lengths in the same units as those of the evolutionary distances used to infer the phylogenetic tree. The evolutionary distances were computed using the Maximum Composite Likelihood method (Tamura *et al.*, 2004) and are in the units of the number of base substitutions per site. The analysis involved 25 nucleotide sequences. All positions containing gaps and missing data were eliminated. There was a total of 547 positions in the final dataset. Evolutionary analyses were conducted in MEGA7 (Kumar *et al.*, 2016).

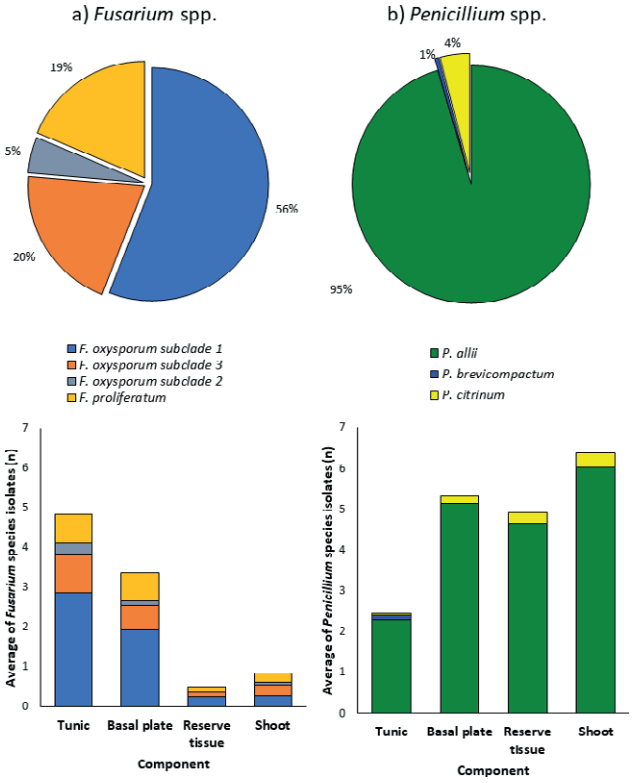

Figure 6. *Fusarium* species/subclades and *Penicillium* species isolated from different elephant garlic clove components from six analyzed field samples. Incidence (%) of the isolated species/subclades, as identified by partial *translation elongation factor 1α* sequencing of *Fusarium* (a), or by *β-tubulin* (*BenA*) and *calmodulin* (*CaM*) partial gene sequencing of *Penicillium* (b), are shown in the pie charts. Columns of the histograms represent the *Fusarium* (a) and *Penicillium* (b) community compositions, expressed as the average number of isolates (n) of different species/subclades that developed on PDA from each analysed elephant garlic clove component.

toms in elephant garlic cloves, so these fungi were shown to be pathogenic towards this crop (Figure 7). However, the tested isolates showed differences in ability to cause clove rots (Figure 7). A gradient in VI was evident for the pathogens (Figure 8), as *P. allii* > *P. brevicompactum* ≥ *F. proliferatum* ≥ *P. citrinum* = *F. oxysporum* subclade 1 ≥ *F. oxysporum* subclade 3 ≥ *F. oxysporum* subclade 2 = experimental control (nil inoculation). The *P. allii* isolate showed greatest virulence ($P \leq 0.05$) compared to the isolates of the other fungi (Figures 7 and 8). *Penicillium brevicompactum* (Figures 7 and 8) and *F. proliferatum* (Figures 7 and 8) were more virulent than *F. oxysporum* subclade 2 ($P \leq 0.05$).

Strategies for the control of Fusarium *and* Penicillium *on elephant garlic cloves*

At 30 days after application, the tested treatments (Table 1) did not affect ($P > 0.05$) garlic clove germination rates compared to the untreated controls (data not shown). No differences ($P > 0.05$) were observed between control or treated cloves for mean shoot length, fresh weight, or dry weight (data not shown). However, the treatments gave different effects on isolation frequency of *Fusarium* and *Penicillium* from the cloves. There were no differences ($P > 0.05$) in frequency of isolations of *Fusarium* spp. from all the clove components between the untreated control, and treatments of Celest Trio®, sodium hypochlorite, sodium hypochlorite + heat treatment, or sodium hypochlorite + heat treatment + Patriot

Figure 7. Symptoms of dry rot on elephant garlic cloves and related sections, at 30 d after fungal inoculations (two mycelial plugs on each clove, taken from 7-d-old cultures grown on potato dextrose agar). Each image is representative of four replicates (cloves). Control (a), *Fusarium proliferatum* (F 88) (b), *F. oxysporum* subclade 1 (F 129) (c), *F. oxysporum* subclade 2 (F 125) (d), *F. oxysporum* subclade 3 (F 42) (e), *Penicillium allii* (P 104) (f), *P. citrinum* (P 41) (g), and *P. brevicompactum* (P 150) (h).

Gold® (Figure 9 a). Only two treatments, Patriot Gold® and Signum®, gave reduced frequency of *Fusarium* spp. isolations ($P \leq 0.05$) compared with the untreated control (Figure 9 a). In comparison to the untreated control, frequency of isolations of *Penicillium* spp. was reduced ($P \leq 0.05$) by all the treatments except sodium hypochlorite (Figure 9 b), with no difference ($P > 0.05$) between the other treatments.

DISCUSSION

The elephant garlic cloves analyzed in this survey showed different symptoms or signs on their four clove components (tunics, basal plates, reserve tissues and shoots). Some of these symptoms or signs have previously been described in elephant garlic cloves (Besoain *et al.* 2002; Ignjatov *et al.* 2019). In addition, some of the symptoms or signs detected in the present study have been previously described on common garlic cloves (Schwartz and Mohan, 2006; Tonti *et al.*, 2012; Gálvez and Palmero, 2021; Horáková *et al.*, 2021; Le *et al.*, 2021; Gálvez and Palmero, 2022). Comparing the symptoms and signs detected in the analyzed cloves with those previously described for elephant and common garlic, there was high probability that the material assessed here was infected by *Fusarium* and *Penicillium* species (Gálvez and Palmero, 2021).

Fusarium and *Penicillium* have also been reported to be associated with asymptomatic cloves of common garlic (Mondani *et al.*, 2021b). Similarly, also in the present

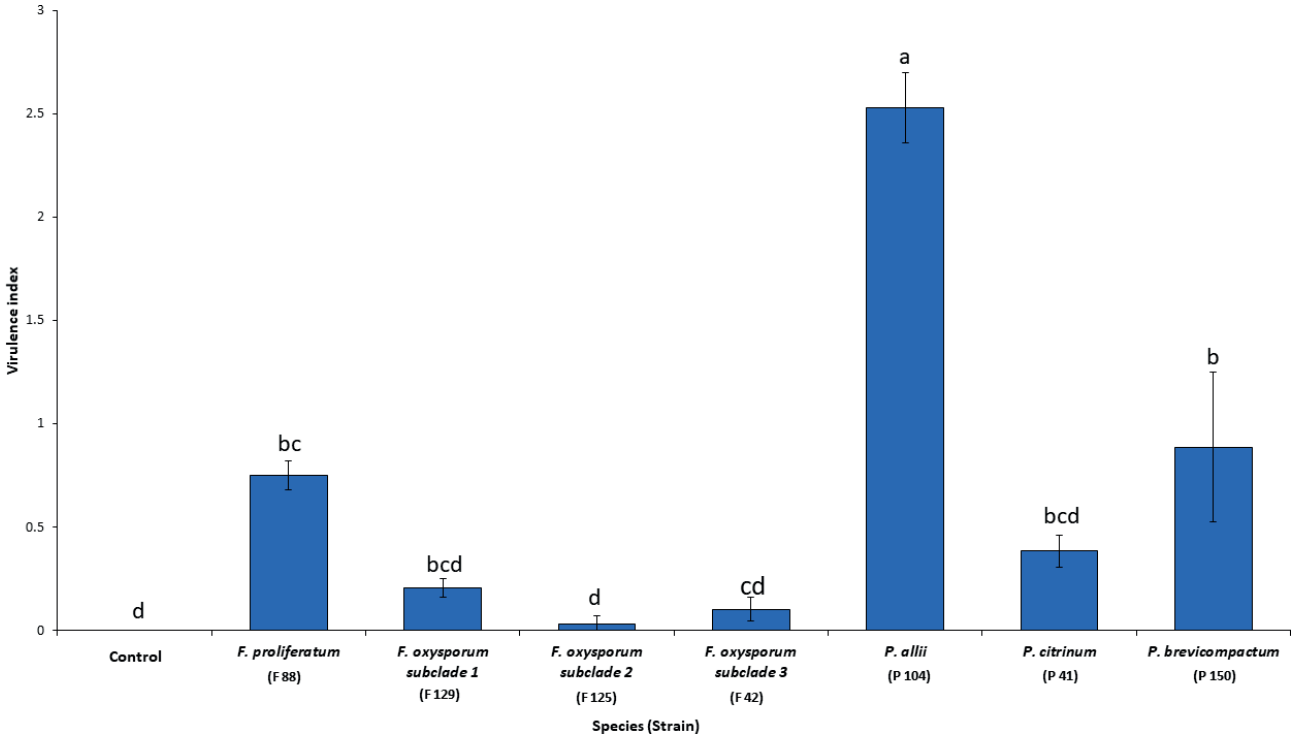

Figure 8. Mean virulence indices for *Fusarium proliferatum* (F 88), *F. oxysporum* subclade 1 (F 129), *F. oxysporum* subclade 2 (F 125), *F. oxysporum* subclade 3 (F 42), *Penicillium allii* (P 104), *P. citrinum* (P 41), and *P. brevicompactum* (P 150), on elephant garlic cloves at 30 days post inoculation. Control cloves were treated with sterile potato dextrose agar plugs. Each column represents the average (± standard error) of four biological replicates, each composed of two cloves with two wounds. Values accompanied by the same letter are not significantly different ($P \leq 0.05$), based on Tukey Honestly Significant Difference multiple comparison tests.

survey, fungi morphologically identified as *Penicillium* and *Fusarium* were isolated both from symptomatic and asymptomatic components of elephant garlic cloves.

Molecular and phylogenetic analyses confirmed the morphological identifications and allowed definition of the fungal species involved.

Penicillium was the prevalent genus, and *Penicillium* isolates were obtained from all the analyzed clove components, with low occurrence in the clove tunics, probably due to the low free water content of these tissues, making them less suitable for *Penicillium* infections (Abellana *et al.*, 2001) than the other three, more hydrated, clove components.

Among the three identified *Penicillium* species, *P. allii* predominated as isolated from all the analyzed elephant garlic clove components collected in "Val di Chiana". The strong predominance of this species was detected also in a previous survey carried out on common garlic in Argentina (Valdez *et al.*, 2009). *Penicillium allii* is the causal agent of green rot or blue mould of common garlic, and has been reported in several countries (Valdez *et al.*, 2006; Dugan, 2007; Moharam *et al.*, 2013; Gálvez and Palmero, 2021). This species is also considered the most aggressive *Penicillium* spp. affecting common garlic in the field and during storage (Overy *et al.*, 2005a; 2005b; Valdez *et al.*, 2009). *Penicillium allii* was also isolated also from soil in Egypt (Vincent and Pitt, 1989).

Penicillium citrinum and *P. brevicompactum* were the other *Penicillium* spp. isolated from cloves analyzed in the present study. *Penicillium citrinum* is of broad geographic distribution, and causes postharvest rots on a wide range of hosts (Wang *et al.*, 2014; González-Estrada *et al.*, 2017; Coutinho *et al.*, 2020; Onaebi *et al.*, 2020; Khan and Javaid, 2023). In addition, *P. citrinum* has been isolated from different substrates including soil, and has been reported as a common endophytic fungus of wheat and soybean (Samson *et al.*, 2004; Khan *et al.*, 2008). *Penicillium brevicompactum* is very widely distributed, especially because of its xerophytic nature (Pitt and Hocking, 1997). This could explain its presence only on the tunics of the elephant garlic cloves analyzed in the present study. This fungus has been reported as a weak pathogen on several fruit types (Overy and Frisvad, 2005), and was isolated from common garlic cloves in Argentina (Valdez *et al.*, 2009).

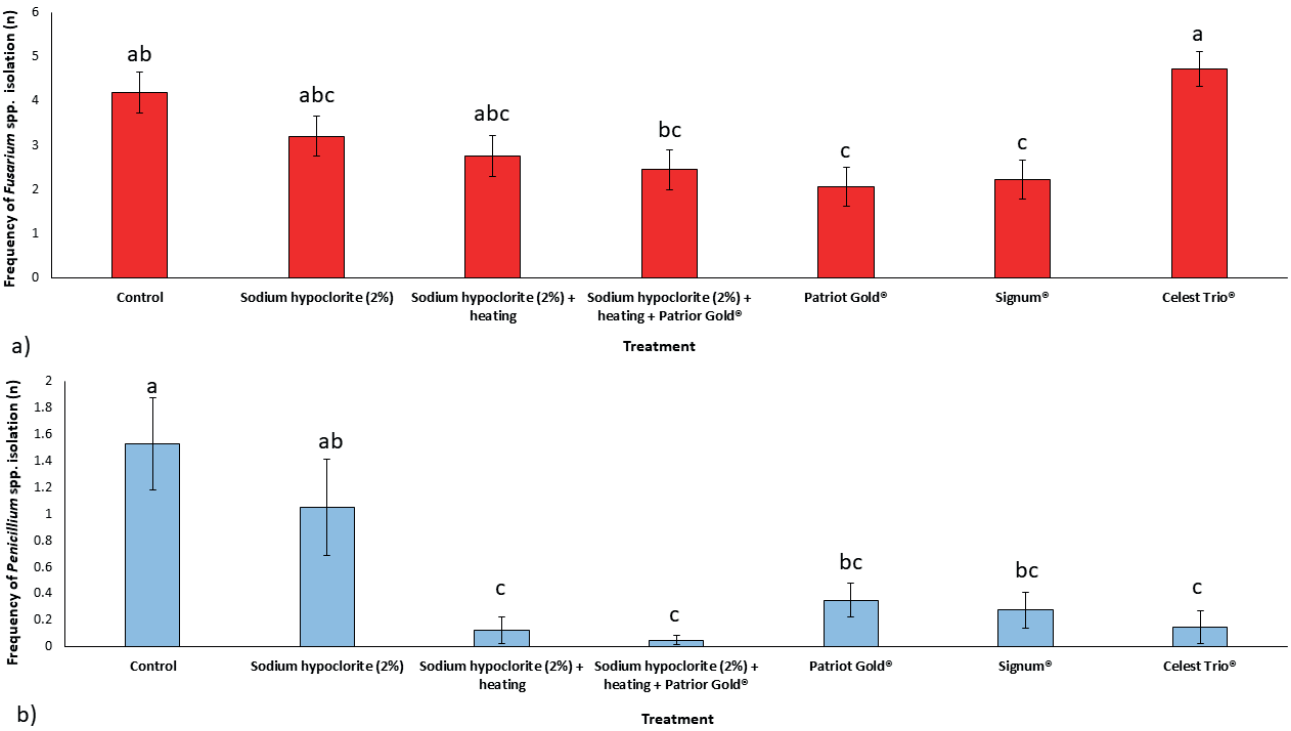

Figure 9. Frequency (n) of *Fusarium* spp. (a) and *Penicillium* spp. (b) isolations from clove components (tunics, basal plates, reserve tissues or shoots) for untreated (Control) or treated naturally infected elephant garlic cloves. Each column represents the average (± standard error) for ten cloves. Different letters indicate differences ($P \leq 0.05$), based on Tukey Honestly Significant Difference multiple comparison tests.

All *Penicillium* species isolated from elephant garlic cloves ready to be used as planting material in "Val di Chiana" have also been isolated from soil (Vincent and Pitt, 1989; Frisvad and Samson, 2004; Samson *et al.*, 2004; Khan *et al.*, 2008; Min *et al.*, 2019). Therefore, *Penicillium* inoculum could infect elephant garlic cloves from the soil, and the pathogens could further develop during storage, particularly when environmental conditions are unsuitable for bulb conservation. *Penicillium allii*, the most isolated species in the present survey, was previously classified as a "field" pathogen, and not as a "storage" pathogen, of common garlic (Valdez *et al.*, 2006). Moreover, *P. citrinum* was isolated only from cloves of a sample obtained from a field where the preceding crop was wheat, which is a commonly reported host for *P. citrinum* (Kaur and Saxena, 2023). These results indicate that the use of infected cloves as planting material and/or preceding crop residues provide or increase *Penicillium* inoculum in soil. The results also underline the importance of crop rotations that avoid cultivation of *Allium ampleoprasum* var. *holmense* after other *Allium* spp., as well as well-proven hosts of these pathogens.

Penicillium spp. were more frequently isolated than *Fusarium* spp. from elephant garlic clove components. *Fusarium* infections may have resulted from soil inoculum, this fungal genus was isolated more frequently from clove components (tunics and basal plates) in contact with the soil. The basal plates were indicated, together with roots, as the most important infection sites of *Fusarium* spp. causing *Fusarium* basal rot (FBR) (also known as *Fusarium* dry rot) on common garlic cloves (Le *et al.*, 2021). This is because FBR is also a "soil-borne" disease, and the causal agents can survive as chlamydospores or as saprophytes in crop residues (Le *et al.*, 2021). However, FBR is not only a "soil-borne" disease and the soil may not be the major reservoir of inoculum, because, for example, *F. proliferatum*, one of the FBR causal agents, does not form chlamydospores (Elmer *et al.*, 1999). *Fusarium* inoculum, from soil or from planting material, is important for causing field infections, while latently infected garlic cloves mainly contribute to post-harvest rots of *Allium* spp. (Stankovic *et al.*, 2007; Gálvez *et al.*, 2017a; Le *et al.*, 2021;), also compromising quality of planting material. This can become an additional source of inoculum in the field (Le *et al.*, 2021).

Fusarium oxysporum was the most isolated *Fusarium* species, followed by *F. proliferatum*. As reported in common garlic (Stankovic *et al.*, 2007; Mondani *et al.*, 2021a), these two *Fusarium* spp. frequently co-occur in

garlic cloves (Le *et al*., 2021; Gálvez and Palmero, 2022).

Fusarium proliferatum is a well-known FBR pathogen of common garlic and onion crops (Mahmoody, 1998; Dugan *et al*., 2003; Stankovic *et al*., 2007; Palmero *et al*., 2010; Sankar and Prasad Babu, 2012; Tonti *et al*., 2012; Fuentes *et al*., 2013; Salvalaggio and Ridao, 2013; Ignjatov *et al*., 2017; Leyronas *et al*., 2018). In most cases, *F. proliferatum* has been the predominant *Fusarium* species associated with FBR in common garlic (Chrétien *et al*., 2021; Gálvez and Palmero, 2022). In addition, *F. proliferatum* has also been reported from elephant garlic in Serbia (Ignjatov *et al*. 2019). Due to its polyphagous behaviour, *F. proliferatum* has been reported as a cosmopolitan pathogen of many important crop plants (Gálvez and Palmero, 2022). For this reason, inoculum of this fungus is likely to be present in field soils. Some hosts (maize, wheat, potato, and sunflower) can serve as inoculum sources (Molinero-Ruiz *et al*., 2011), and severe *F. proliferatum* infections can be expected in susceptible crops such as garlic types. These aspects should be considered by elephant garlic growers, to define the rotations within their cropping systems. Assessment would be worthwhile of the ability of *F. proliferatum* strains detected from elephant garlic to cause disease in other hosts. *Fusarium proliferatum* can also biosynthesize mycotoxins, such as fumonisins, that can induce toxic effects in humans (Kamle *et al*., 2019). Elephant garlic cloves, even though in small quantities, are used for human consumption, so it is important that accumulation of mycotoxins is monitored, as has already been investigated in common garlic (Tonti *et al*., 2017).

Fusarium oxysporum was also isolated in the present study with high incidence from elephant garlic cloves. This fungus has already been reported in elephant garlic in Chile (Besoain *et al*., 2002). Identifications based on *tef1α* showed that *F. oxysporum* isolates obtained in the present study were in three subclades, most closely associated with f. sp. *cepae*, f. sp. *dianthi* or f. sp. *lactucae*. However, further study is required, particularly of isolate gene sequences, to ascribe these isolates to different *formae speciales* (El-Komy *et al*., 2023). *Fusarium oxysporum* is a soil-borne pathogen, well-known as an FBR agent in different *Allium* spp. including onion, common garlic and shallot (Schwartz and Mohan, 2006; Sintayehu *et al*., 2011; Mondani *et al*., 2021a; Gálvez and Palmero, 2022). Mondani *et al*. (2021a) conducted a survey of common garlic basal plates from bulbs cultivated in Northern Italy, and showed that *F. oxysporum* was favoured by dry weather, differently from *F. proliferatum* which was favoured by rain.

Representative isolates of each *Penicillium* and *Fusarium* species were shown to be pathogenic on elephant garlic cloves. The inoculation technique adopted, as described elsewhere (Dugan *et al*., 2007; Ignjatov *et al*., 2019), is invasive to host tissues, so did not allow verification of relationships between the pathogen species and associated host symptoms. For this purpose, further study is required, including inoculating spore suspensions directly onto cloves or into soil.

In the experimental conditions used in the present study, *P. allii* was the most virulent fungus followed by *P. brevicompactum*, *F. proliferatum* and *F. oxysporum*. The greater virulence of *P. allii* in comparison to *Fusarium* spp. (Gálvez and Palmero, 2021), or other *Penicillium* spp. (Overy *et al*. 2005a and 2005b; Valdez *et al*. 2009) has been previously reported for common garlic. Also in elephant garlic cloves, *P. hirstum* had greater virulence than *F. oxysporum* (Besoain *et al*., 2002). The greater aggressiveness of *P. allii* could be attributed, as already suggested by Valdez *et al*. (2009), to the ability of this fungus to utilize enzymatic digestion of host cell wall polymers.

Appropriate disease management strategies are required for elephant garlic, but no management protocols are currently available for this "niche" crop in Italy, which is cultivated in a limited area. Farmers adapt to elephant garlic control methods for similar crops, such as common garlic, onion, or leek. Since fungal pathogens can reach the field also through infected garlic cloves used as planting material, a first step to reduce pathogen inoculum added to soil from infected planting material could be clove disinfection. The present study tested different disinfection treatments. Among these, the products Signum® and Patriot Gold® showed efficacy for control of *Penicillium* spp. and *Fusarium* spp. Instead, Celest Trio® and sodium hypochlorite (2%), combined with heat treatments, or with heating and Patriot Gold®, reduced *Penicillium* spp. only.

Several studies have assessed effectiveness of chemical treatments for reducing *Fusarium* occurrence in crops similar to elephant garlic, including common garlic. These studies demonstrated effectiveness of several fungicide active ingredients, including benomyl (Dugan *et al*., 2007), carbendazim, metalaxyl + mancozeb, tiophanate-methyl (Elshahawy *et al*., 2017), propiconazole + prochloraz, or tebuconazole (Mondani *et al*., 2021c; 2022), for reducing *F. proliferatum* and *F. oxysporum* growth *in vitro* and/or isolation frequencies *in vivo*. However, authorization for the use of some of these active ingredients (benomyl, carbendazim, propiconazole and prochloraz) has been recently revoked by the European Commission. Interest in biofungicides in crop protection has rapidly increased (Chandler *et al*., 2011). For example, *Bacillus subtilis* and *Streptomyces*

griseoviridis showed the promise for control of *F. proliferatum* comparable to that from chemicals on common garlic cloves. In contrast, *Trichoderma harzianum* + *T. gamsii*, which showed potential for reducing *in vitro* growth of *F. proliferatum* and *F. oxysporum*, was not fully confirmed for reducing disease *in vivo* (Mondani *et al.*, 2021c). However, *B. subtilis* or *T. harzianum* + *T. gamsii* based products have yet to be authorized for use on common garlic, onion, or leek in Italy, and therefore their use cannot be extended to elephant garlic. The heat treatment in the experimental conditions used in the present study did not negatively affect plant emergence from treated garlic cloves. Application of thermotherapy (using hot water) could be deleterious to emergence, if combinations of temperature and time are not carefully assessed. When this technique was assessed for common garlic, its practical application was considered to be difficult, and effectiveness could decrease if pathogen mycelium had entered host clove lesions (Palmero Llamas *et al.*, 2013). The present study recorded efficient control of *Fusarium* spp. and *Penicillium* spp. with Patriot Gold® and Signum® (both currently approved in Italy for use on common garlic, onion, or leek, and therefore potentially extendable for use on elephant garlic). Therefore, these treatments are likely to be for managing these increasingly threatening pathogens of elephant garlic cloves.

In conclusion, the present study was the first to focus on phytosanitary problems of elephant garlic cultivated in Italy, and was a preliminary assessment of possible disease management solutions. Choice of healthy, symptom/sign-free cloves remains the first step for producing healthy crops. However, since *Fusarium* and *Penicillium* were also isolated from symptom/sign-free garlic cloves, application of disinfection methods is the second, and necessary, step as common practice for elephant garlic cultivation. The preliminary, positive disease control results obtained should be further investigated and confirmed. The several current and registered active ingredients (both chemical and microbiological) could be accompanied or replaced by new solutions, making an evolving phytoiatric scenario for elephant garlic production.

ACKNOWLEDGEMENTS

The authors acknowledge "BMP CONSULENZA AZIENDALE s.a.s di Berna E. & C., Castiglione del Lago, Perugia" and "Colombaiolo & Villamaggiore Società Agricola a r.l., località l'Amorosa, Sinalunga (Siena)" for funding this research. Dr Maurizio Orfei, Mrs Maria Vittoria Consalvi, and Mr Luca Ceccarelli gave excellent technical assistance in this study.

LITERATURE CITED

Abellana M., Sanchis V., Ramos A.J., 2001. Effect of water activity and temperature on growth of three *Penicillium* species and *Aspergillus flavus* on a sponge cake analogue. *International Journal of Food Microbiology* 71: 151–157. https://doi.org/10.1016/s0168-1605(01)00596-7

Altschul S.F., Gish W., Miller W., Myers E.W., Lipman D.J., 1990. Basic local alignment search tool. *Journal of Molecular Biology* 3: 403–410. https://doi.org/10.1016/S0022-2836(05)80360-2

Ascrizzi R., Flamini G., 2020. Leek or garlic? A chemical evaluation of elephant garlic volatiles. *Molecules* 25: 2082. https://doi.org/10.3390/molecules25092082

Beccari G., Senatore M.T., Tini F., Sulyok M., Covarelli L., 2018. Fungal community, Fusarium head blight complex and secondary metabolites associated with malting barley grains harvested in Umbria, Central Italy. *International Journal of Food Microbiology* 273: 33–42. https://doi.org/10.1016/j.ijfoodmicro.2018.03.005

Beccari G., Prodi A., Senatore M.T., Balmas V., Tini F., … Covarelli L., 2020. Cultivation area affects the presence of fungal communities and secondary metabolites in Italian durum wheat grains. *Toxins* 12: 97. https://doi.org/10.3390/toxins12020097

Besoain X.A., Vejar R.A., Piontelli E.L. 2002. Principales hongos fitopatogenos asociados a bulbos almacenados de ajo elefante (*Allium ampeloprasum* var. *holmense*) de la zona de quillota y nogales (Chile). *Boletin Micologico* 17: 9–14. https://doi.org/10.22370/bolmicol.2002.17.0.433

Block E., 2011. Challenges and artefact concerns in analysis of volatile sulfur compounds. In: *Volatile Sulfur Compounds in Food* (E. Block Ed.). (pp. 35–63). *American Chemical Society*. https://doi.org/10.1021/bk-2011-1068.ch002

Bogo A., 1997. Evaluation of fungicides in the control of garlic bulb rot caused by *Penicillium* spp. *Agropecuaria Caterinense* 10: 5–6. https://doi.org/https://eurekamag.com/research/003/131/003131890.php

Borlinghaus J., Albrecht F., Gruhlke M.C.H., Nwachukwu I.D., Slusarenko A., 2014. Allicin: chemistry and biological properties. *Molecules* 19: 12591–12618. https://doi.org/10.3390/molecules190812591

Ceccanti C., Rocchetti G., Lucini L., Giuberti G., Landi M., … Guidi L., 2021. Comparative phytochemical profile of the elephant garlic (*Allium ampelo-*

prasum var. *holmense*) and the common garlic (*Allium sativum*) from the Val di Chiana area (Tuscany, Italy) before and after in vitro gastrointestinal digestion. *Food Chemistry* 338: 128011. https://doi.org/10.1016/j.foodchem.2020.128011

Chandler D., Bailey A.S., Tatchell G.M., Davidson G., Greaves J., Grant W.P., 2011. The development, regulation and use of biopesticides for integrated pest management. *Philosophical Transaction of the Royal Society* 366: 1987–1998. https://doi.org/10.1098/rstb.2010.0390

Chrétien P.L., Laurent S., Bornard I., Troulet C., El Maâtaoui M., Leyronas C., 2020. Unraveling the infection process of garlic by *Fusarium proliferatum*, the causal agent of root rot. *Phytopathologia Mediterranea* 59: 285–293. https://doi.org/10.14601/Phyto-11103

Chrétien P.L., Morris C.E., Duffaud M., Leyronas C., 2021. Aetiology of garlic rot, an emerging disease in France. *Plant Pathology* 70: 1276–1291. https://doi.org/10.1111/ppa.13394

Ciabanal I.L., Fernandez L.A., Murray A.P., Pellegrini C.N., Gallez L.M., 2021. Propolis extract and oregano essential oil as biofungicides for garlic seed cloves: in vitro assays and synergistic interaction against *Penicillium allii. Journal of Applied Microbiology* 131: 1909–1918. https://doi.org/10.1111/jam.15081

Coutinho T.C., Ferreira M.C., Rosa L.H., de Oliveira A.M., Oliveira Junior, 2020. *Penicillium citrinum* and *Penicillium mallochii*: new phytopathogens of orange fruit and their control using chitosan. *Carbohydrate Polymers* 234: 115918. https://doi.org/10.1016/j.carbpol.2020.115918

Covarelli L., Beccari G., Prodi A., Generotti S., Etruschi F., … Mañes J., 2015. *Fusarium* species, chemotype characterisation and trichothecene contamination of durum and soft wheat in an area of Central Italy. *Journal of the Science of Food and Agriculture* 95: 540–551. https://doi.org/10.1002/jsfa.6772

Crous P.W., Lombard L., Sandoval-Denis M., Seifert K.A., Schroers H.-J., … Thines M, 2021. *Fusarium*: more than a node or a foot-shaped basal cell. *Studies in Mycology* 98: 100116. https://doi.org/10.1016/j.simyco.2021.100116

Crowe F.J., 1995. Fusarium basal rot of garlic. In: *Compendium of Onion and Garlic Diseases* (Schwartz HF, Mohan SK, ed), St Paul, Minnesota, APS Press, pp. 11.

Dugan F. M., Hellier B.C., Lupien S.L., 2003. First report of *Fusarium proliferatum* causing rot of garlic bulbs in North America. *Plant Pathology* 52: 426. https://doi.org/10.1094/PDIS-94-2-0277C

Dugan F.M., 2007. Diseases and disease management in seed garlic: problems and prospects. *American Journal of Plant Science and Biotechnology* 1: 47–51.

Dugan F.M., Hellier B.C., Lupien S.L., 2007. Pathogenic fungi in garlic seed cloves from the Unites States and China, and efficacy of fungicides against pathogens in garlic germplasm in Washington State. *Journal of Phytopathology* 155: 437–445. https://doi.org/10.1111/j.1439-0434.2007.01255.x

Dugan F.M., Hellier B.C., Lupien S.L., 2011. Resistance to *Penicillium allii* in accessions from a national plant germoplasm system *Allium* collection. *Crop Protection* 30: 483–488. https://doi.org/10.1016/j.cropro.2010.12.021

El-Komy M.H., Gao X., Almasrahi A., Ibrahim Y.E., Sharafaddin A.H., Saleh A.A., Hamad Y.K., 2023. First report of basal rot of onion caused by *Fusarium oxysporum* f. sp. *cepae* in Saudi Arabia. *Plant Disease* 107: 2854. https://doi.org/10.1094/PDIS-02-23-0333-PDN

Elmer W.H., Summerell B.A., Burgess L.W., Nigh Jr. E.L., 1999. Vegetative compatibility groups in *Fusarium proliferatum* from asparagus in Australia. *Mycologia* 91: 650–654. https://doi.org/10.2307/3761251

Elshahawy I.E., Saied N.M., Morsy A.A., 2017. *Fusarium proliferatum*, the main cause of clove rot during storage, reduces clove germination and causes wilt of established garlic plants. *Journal of Plant Pathology* 99: 85–93. https://doi.org/https://www.jstor.org/stable/44280576

Felsenstein J., 1985. Confidence limits on phylogenies: An approach using the bootstrap. *Evolution* 39: 783–791. https://doi.org/10.1111/j.1558-5646.1985.tb00420.x

Frisvad J.C., Samson R.A., 2004. Polyphasic taxonomy of *Penicillium*: a guide to identification of food and airborne terverticillate Penicillia and their mycotoxins. *Studies in Mycology* 49: 1–173. https://doi.org/https://api.semanticscholar.org/CorpusID:90769261}

Fritsch R.M., Friesen N., 2002. Evolution, domestication and taxonomy. In: *Allium Crop Science: Recent Advances* (Rabinowitch H.D., Currah L., ed.),. CABI, Wallingford, pp. 5-30

Fuentes Y.M.O., Ortiz J.C.D., Chavez E.C., Castillo F.D.H., Olivas A.F., … Guerra R.R., 2013. The first report of *Fusarium proliferatum* causing garlic bulb rots in Mexico. *African Journal of Agricultural Research* 8: 570–573. https://doi.org/10.5897/AJAR12.1726

Gálvez L. M., Urbaniak, Waśkiewicz A., Stępień Ł., Palmero D., 2017a. *Fusarium proliferatum* – Causal agent of garlic bulb rot in Spain: Genetic variability and mycotoxin production. *Food Microbiology* 67: 41–48. https://doi.org/10.1016/j.fm.2017.05.006

Gálvez L., Redondas M.D., Palmero D., 2017b. In vitro and field efficacy of three fungicides against *Fusarium*

bulb rot of garlic. *European Journal of Plant Pathology* 148: 321–328. https://doi.org/10.1007/s10658-016-1091-7

Gálvez L., Palmero D., 2021. Incidence and aetiology of postharvest fungal diseases associated with bulb rot in garlic (*Allium sativum*) in Spain. *Foods* 10: 1063. https://doi.org/10.3390/foods10051063

Gálvez L., Palmero D., 2022. Fusarium dry rot of garlic bulbs caused by *Fusarium proliferatum*: a review. *Horticulturae* 8: 628. https://doi.org/10.3390/horticulturae8070628

Geiser D.M., Jimenez-Gasco M.D., Kang S.C., Makalowska I., Veeraghavan N., Ward T.J., … O'Donnel K., 2004. FUSARIUM-ID v. 1.0: A DNA sequence for identifying *Fusarium*. *European Journal of Plant Pathology* 110: 473–479. https://doi.org/10.1023/B:EJPP.0000032386.75915.a0

González-Estrada R.R., de Jesus Ascencio-Valle F., Ragazzo-Sánchez J.A., Santoyo M.C., 2017. Use of a marine yeast as a biocontrol agent of the novel pathogen *Penicillium citrinum* on Persian Lime. *Emirates Journal of Food and Agriculture* 29: 114–122. https://doi.org/10.9755/ejfa.2016-09-1273

Greathead A.S., 1978. Control of *Penicillium* decay of garlic. *California Agriculture* 6: 18.

Guenaoui C., Mang S., Figliuolo G., Naffati M., 2013. Diversity in *Allium ampeloprasum*: from small and wild to large and cultivated. *Genetic Resources and Crop Evolution* 60: 97–114. https://doi.org/10.1007/s10722-012-9819-5

Han T.S., Zheng Q.J., Onstein R.E., Rojas-Andres B.M., Hauenschild F., … Xing Y.W., 2020. Polyploidy promotes species diversification of *Allium* through ecological shifts. *New Phytologist* 225: 571–583. https://doi.org/10.1111/nph.16098

Horáková M.K., Tancik J., Barta M., 2021. *Fusarium proliferatum* causing dry rot of stored garlic in Slovakia. *Journal of Plant Pathology* 103: 997–1002. https://doi.org/10.1007/s42161-021-00883-5

Houbraken J., Samson R.A., 2011. Phylogeny of *Penicillium* and segregation of *Trichocomaceae* into three families. *Studies in Mycology* 70: 1–51. https://doi.org/10.3114/sim.2011.70.01

Ignjatov M.V., Bjelić D.D., Nokolić Z.T., Milošević D.N., Marinković J.B., … Gvozdanović-Varga J.M., 2017. Morphological and molecular identification of *Fusarium tricinctum* and *Fusarium acuminatum* as causal agents of garlic bulbs rot in Serbia. *Zbornik Matice srpske za prirode nauke* 133: 271–277. https://doi.org/10.2298/ZMSPN1733271I

Ignjatov M.V., Vlajić S.A., Milošević D.N., Nikolić Z.T., Tamindžić G.D., … , Ivanović Z.S., 2019. Identification and phylogenetic analysis of *Fusarium proliferatum* isolated from elephant garlic *Allium ampeloprasum* L. *Journal of Natural Sciences Novi Sad* 137: 49–55. https://doi.org/10.2298/ZMSPN1937049I

Johnson S.B., 2013. Blue mold of garlic. Cooperative Extension Publications, The University of Maine, Bullettin #1206 (available at https://extension.umaine.edu/publications/1206e/, accessed on 21 July, 2023).

Kamle M., Mahato D.K., Devi S., Lee K.E., Kang S.G., Kumar P., 2019. Fumonisins: impact on agriculture, food and human health and their management strategies. *Toxins* 11: 328. https://doi.org/10.3390/toxins11060328

Kaur R., Saxena S., 2023. *Penicillium citrinum*, a drought-tolerant endophytic fungus isolated from wheat (*Triticum aestivum* L.) leaves with plant growth-promoting abilities. *Current Microbiology* 80: 184. https://doi.org/10.1007/s00284-023-03283-3

Keusgen M., Fritsch R.M., Hisoriev H., Kurbonova P.A., Khassanov F.O., 2006. Wild *Allium* species (*Alliaceae*) used in folk medicine of Tajikistan and Uzbekistan. *Journal of Ethnobiology and Ethnomedicine* 2: 18. https://doi.org/10.1186/1746-4269-2-18

Khan I.H., Javaid A., 2023. *Penicillium citrinum* causing postharvest decay on stored garlic cloves in Pakistan. *Journal of Plant Pathology* 105: 337. https://doi.org/10.1007/s42161-022-01254-4

Khan S.A., Hamayun M., Yoon H., Kim H.Y., Suh S.J., … Kim J.G., 2008. Plant growth promotion and *Penicillium citrinum*. *BMC Microbiology* 8: 231. https://doi.org/10.1186/1471-2180-8-231

Kim S., Kim D.B., Jin W., Park J., Yoon W., … Yoo M., 2018. Comparative studies of bioactive organosulphur compounds and antioxidant activities in garlic (*Allium sativum* L.), elephant garlic (*Allium ampeloprasum* L.) and onion (*Allium cepa* L.). *Natural Product Research* 32: 1193–1197. https://doi.org/10.1080/14786419.2017.1323211

Kumar S., Stecher G., Tamura K., 2016. MEGA7: Molecular evolutionary genetics analysis version 7.0 for bigger dataset. *Molecular Biology and Evolution* 33: 1870–1874. https://doi.org/10.1093/molbev/msw054

Le D., Audenaert K., Haesaert G., 2021. *Fusarium* basal rot: profile of an increasingly important disease in *Allium* spp. *Tropical Plant Pathology* 46: 241–253. https://doi.org/10.1007/s40858-021-00421-9

Leyronas C., Chretien P.L., Troulet C., Duffaud M., Villeneuve F., … Hunyadi H, 2018. First report of *Fusarium proliferatum* causing garlic clove rot in France. *Plant Disease* 102: 2658. https://doi.org/10.1094/PDIS-12-20-2743-PDN

Mahmoody B., 1998. *Fusarium oxysporum* associated with garlic rot in Khorasan Province. *Iranian Journal of Plant Pathology* 34: 235–236.

Min C., Dong H., Liu X., Zhang Z., 2019. Screening and identification of a *Penicillium brevicompactum* strain isolated from the fruiting body of *Inonotus obliquus* and the fermentation production of mycophenolic acid. *Annals of Microbiology* 69: 1351–1360. https://doi.org/10.1007/s13213-019-01517-z

Ministry of Agricultural, Food and Forestry Policies, 2016. Sedicesima revisione dell'elenco nazionale dei prodotti agroalimentari tradizionali, G.U. n. 143 of June 21st, 2016, https://www.aglionevaldichiana.net/public/Documenti/Decreto_MiPAAF.pdf (accessed on 24 July 2023).

Moharam M.H.A., Farrag E.S.H., Mohamed M.D.A., 2013. Pathogenic fungi in garlic seed cloves and first report of *Fusarium proliferatum* causing cloves rot of stored bulbs in Upper Egypt. *Archives of Phytopathology and Plant Protection* 46: 2096–2103. https://doi.org/10.1080/03235408.2013.785122

Molinero-Ruiz L., Rubio-Pérez E., Gonzaléz-Dominquez E., Basallote-Ureba M.J., 2011. Alternative hosts for *Fusarium* spp. causing crown and root rot of asparagus in Spain. *Journal of Phytopathology* 159: 114–116. https://doi.org/10.1111/j.1439-0434.2010.01723.x

Mondani L., Chiusa G., Battilani P., 2021a. Fungi associated with garlic during the cropping season, with focus on *Fusarium proliferatum* and *F. oxysporum*. *Plant Health Progress* 22: 37–46. https://doi.org/10.1094/PHP-06-20-0054-RS

Mondani L., Chiusa G., Pietri A., Battilani P., 2021b. Monitoring the incidence of dry rot caused by *Fusarium proliferatum* in garlic at harvest and during the storage. *Postharvest Biology and Technology* 173: 111407. https://doi.org/10.1016/j.postharvbio.2020.111407

Mondani L., Chiusa G., Battilani P., 2021c. Chemical and biological control of *Fusarium* species involved in garlic dry rot at early crop stages. *European Journal of Plant Pathology* 160: 575–587. https://doi.org/10.1007/s10658-021-02265-0

Mondani L., Chiusa G., Battilani P., 2022. Efficacy of chemical and biological spray seed treatments in preventing garlic dry rot. *Phytopathologia Mediterranea* 61: 27–37. https://doi.org/10.36253/phyto-13103

O'Donnell K., Kistler H.C., Cigelnik E., Ploetz R.C., 1998. Multiple evolutionary origins of the fungus causing Panama disease of banana: concordant evidence from nuclear and mitochondrial gene genealogies. *Proceedings of National Academy of Sciences USA* 95: 2044–2049. https://doi.org/10.1073/pnas.95.5.2044

Onaebi N.C., Ugwuja N.F., Okoro C.A., Amujiri N.A., Ivoke U.M., 2020. Mycoflora associated with postharvest rot of onion (*Allium cepa*) and garlic (*Allium sativum*) bulbs. *Research on Crops* 21: 380–389. https://doi.org/10.31830/2348-7542.2020.064

Onofri A., Pannacci E., 2014. Spreadsheet tools for biometry classes in crop science programmes. *Communication in Biometry and Crop Science* 9: 43–45.

Overy D.P., Frisvad J.C., 2005. Mycotoxin production and post harvest storage rot of ginger (*Zingiber officinale*) by *Penicillium brevicompactum*. *Journal of Food Protection* 68: 607–609. https://doi.org/10.4315/0362-028X-68.3.607

Overy D.P., Karlshoj K., Due M., 2005a. Low temperature growth and enzyme production in *Penicillium* ser. *Corymbifera* species, casual agents of blue mould storage rot in bulbs. *Journal of Plant Pathology* 87: 57–63. https://doi.org/10.4454/jpp.v87i1.897

Overy D.P., Frisvad J.C., Steinmeier U., Thrane U., 2005b. Clarification of the agents causing blue mold storage rot upon various flower and vegetable bulbs: Implications for mycotoxin contamination. *Postharvest Biology and Technology* 35: 217–221. https://doi.org/10.1016/j.postharvbio.2004.08.001

Palmero D., De Cara M., Nosir W., Iglesias C., Garcia M., … Tello J.C., 2010. First report of *Fusarium proliferatum* causing rot of garlic bulbs in Spain. *Plant Disease* 94: 277. https://doi.org/10.1094/PDIS-94-2-0277C

Palmero Llamas D., Gálvez Patón L., García Díaz M., Gil Serna J., Benito S., 2013. The effects of storage duration, temperature and cultivar on the severity of garlic clove rot caused by *Fusarium proliferatum*. *Postharvest Biology and Technology* 78: 34–39. https://doi.org/10.1016/j.postharvbio.2012.12.003

Pitt J.I., Hocking A.D., 1997. Fungi and food spoilage, 2nd eds. London, UK: Blackie Academic and Professional.

Saitou N., Nei M., 1987. The neighbor-joining method: A new method for reconstructing phylogenetic trees. *Molecular Biology and Evolution* 4: 406–425. https://doi.org/10.1093/oxfordjournals.molbev.a040454

Salvalaggio A.E., Ridao A.D.C., 2013. First report of *Fusarium proliferatum* causing rot on garlic and onion in Argentina. *Plant Disease* 97: 556. https://doi.org/10.1094/PDIS-05-12-0507-PDN

Samson R.A., Hoekstra E.S., Frisvad J.C., 2004. Introduction to food- and airborne fungi, 7th edn. Centralbureau voor Schimmelcultures, Utrecht.

Sankar R., Prasad Babu G., 2012. First report of *Fusarium proliferatum* causing rot of garlic bulbs (*Allium sativum*) in India. *Plant Disease* 96: 290. https://doi.org/10.1094/PDIS-08-11-0649

Schwartz H.F., Mohan S.K., 2006. *Compendium of Onion and Garlic Diseases and Pests*, 2nd ed. APS Press, Minnesota, USA, p. 127.

Slow Food Foundation, 2023. Slow Food Foundation for Biodiversity Onlus, Ark of Taste, Aglione della Chiana, https://www.fondazioneslowfood.com/it/arca-del-gusto-slow-food/aglione-della-chiana/ (accessed on 14th September 2023).

Sintayehu A., Sakhuja P.K., Fininsa C., Ahmed S., 2011. Management of fusarium basal rot (*Fusarium oxysporum* f. sp. *cepae*) on shallot through fungicidal bulb treatment. *Crop Protection* 5: 560–565. https://doi.org/10.1016/j.cropro.2010.12.027

Southwood M.J., Viljoen A., Mostert L., Rose L.J., McLeod A., 2012. Phylogenetic and biological characterization of *Fusarium oxysporum* isolates associated with onion in South Africa. *Plant Disease* 96: 1250–1261. https://doi.org/10.1094/PDIS-10-11-0820-RE

Stankovic S., Levic J., Petrovic T., Logrieco A., Moretti A. 2007. Pathogenicity and mycotoxin production by *Fusarium proliferatum* isolated from onion and garlic in Serbia. *European Journal of Plant Pathology* 118: 165–172. https://doi.org/10.1007/s10658-007-9126-8

Tamura K., Nei M., Kumar S., 2004. Prospects for inferring very large phylogenies by using the neighbor-joining method. *Proceedings of the National Academy of Sciences USA* 101: 11030–11035. https://doi.org/10.1073/pnas.0404206101

Taylor A., Vágány V., Jackson A.C., Harrison R.J., Rainoni A., Clarkson J.P., 2016. Identification of pathogenicity-related genes in *Fusarium oxysporum* f.sp. *cepae*. *Molecular Plant Pathology* 17: 1031–1047. https://doi.org/10.1111/mpp.12346

Terzaroli N., 2015. Caratterizzazione genetica dell'Aglione (*Allium ampeloprasum*) della Val di Chiana (Bachelor thesis). University of Perugia.

Terzaroli N., Caproni L., 2020. "Aglione della Val di Chiana", a white gentle giant. *Landraces*, 23.

Terzaroli N., Marconi G., Russi L., Albertini E., 2022. Phenotypic and genetic characterization of "Aglione della Valdichiana": population structure and genetic relationship analysis of a white gentle giant. *Scientia Horticulturae* 293: 110673. https://doi.org/10.1016/j.scienta.2021.110673

Tonti S., Dal Prà M., Nipoti P., Prodi A., Alberti I., 2012. First report of *Fusarium proliferatum* causing rot of stored garlic bulbs (*Allium sativum* L.) in Italy. *Journal of Phytopathology* 160: 761–763. https://doi.org/10.1111/jph.12018

Tonti S., Mandrioli M., Nipoti P., Pisi A., Gallina Tuschi T., Prodi A., 2017. Detection of fumonisins in fresh and dehydrated commercial garlic. *Journal of Agricultural and Food Chemistry* 16: 7000–7005. https://doi.org/10.1021/acs.jafc.7b02758

Tuscany Region, 2016. Aggiornamento per l'anno 2016 dell'elenco dei prodotti agroalimentari tradizionali della Toscana, Decreto Esecutivo Regione Toscana 1569, 04/04/2016, https://www.aglionevaldichiana.net/public/Documenti/Decreto_Regione_Toscana.pdf (accessed on 25 July 2023).

Umbria Region, 2020. Legge Regionale 12/2015, Tutela delle Risorse Genetiche Autoctone di Interesse Agrario, Aglione, Numero Iscrizione 69, 16/12/2020, https://biodiversita.umbria.parco3a.org/risorsa/aglione/#5

Valdez J.G., Makuch M.A., Ordovini A.F., Masuelli R.W., Overy D.P., Piccolo R.J., 2006. First report of *Penicillium allii* as a field pathogen of garlic (*Allium sativum*). *Plant Pathology* 55: 583. https://doi.org/10.1111/j.1365-3059.2006.01411.x

Valdez J.G., Makuch M.A., Ordovini A.F., Frisvad J.C., Overy D.P., … Piccolo R.J., 2009. Identification, pathogenicity and distribution of *Penicillium* spp. isolated from garlic in two regions in Argentina. *Plant Pathology* 58: 352–361. https://doi.org/10.1111/j.1365-3059.2008.01960.x

Vincent M.A., Pitt J.I., 1989. *Penicillium allii*, a new species from Egyptian garlic. *Mycologia* 81: 300–303. https://doi.org/https://doi.org/10.2307/3759715

Visagie C.M., Houbraken J., Frisvad J.C., Hong S.B., Klaassen C.H.W., … Samson RA 2014. Identification and nomenclature of the genus *Penicillium*. *Studies in Mycology* 78: 343–371. https://doi.org/10.1016/j.simyco.2014.09.001

Wang K., Jin P., Han L., Shang H., Tang S., Rui H., … Zheng Y., 2014. Methyl jasmonate induces resistance against *Penicillium citrinum* in Chinese bayberry by priming of defense responses. *Postharvest Biology and Technology* 98: 90–97. https://doi.org/10.1016/j.postharvbio.2014.07.009

Phytopathologia Mediterranea
The international journal of the
Mediterranean Phytopathological Union

Firenze University Press
www.fupress.com/pm

New or Unusual Disease Reports

Mixed infections of Tomato yellow leaf curl New Delhi virus and a '*Candidatus* Phytoplasma asteris' strain in zucchini squash in Italy

Giuseppe PARRELLA*, Elisa TROIANO

Institute for Sustainable plant Protection of National Research Council (IPSP-CNR), Piazzale Enrico Fermi 1, 80055 Portici (NA), Italy
*Corresponding author. E-mail: giuseppe.parrella@ipsp.cnr.it

Summary. A new disease syndrome of zucchini squash was observed in Southern Italy, in 2018 and again in 2020. Affected plants were severely stunted and leaves were bent downwards, small, stiff, thick, leathery, and had interveinal chloroses. In addition, flowers were virescent and fruits were deformed and often cracked. Disease incidence was 20 and 30% in two different zucchini cultivations in Campania region (Southern Italy). Tomato yellow leaf curl New Delhi virus (ToLCNDV) was detected in eight samples, by loop-mediated isothermal amplification–based (LAMP) kit and by PCR and Sanger sequencing of the AV1 gene. Phytoplasmas were detected in the same samples using nested PCR assays with primer pairs P1/P7 and R16F2n/R16R2. Phytoplasma associations in plant samples were confirmed using specific primers for the multilocus genes *SecY*, *tuf* and *rp*. Sequence comparison of multilocus genes and phylogenetic analyses of the 16S rDNA gene confirmed the association of a phytoplasma strain closely related to '*Candidiatus* Phytoplamsa asteris'. This is the first report of mixed infections of ToLCNDV and a putative '*Ca*. Phytoplamsa asteris' strain in zucchini, associated with a new Squash-Phytoplasma-Begomovirus (SqPB) disease syndrome.

Keywords. Aster yellows phytoplasma, ToLCNDV, *Cucurbita pepo,* mixed infection.

OPEN ACCESS

Citation: G. Parrella, E. Troiano (2024) Mixed infections of Tomato yellow leaf curl New Delhi virus and a '*Candidatus* Phytoplasma asteris' strain in zucchini squash in Italy. *Phytopathologia Mediterranea* 63(1): 73-78. doi: 10.36253/phyto-15110

Accepted: March 14, 2024

Published: April 29, 2024

Data Availability Statement: All relevant data are within the paper and its Supporting Information files.

Competing Interests: The Author(s) declare(s) no conflict of interest.

Editor: Arnaud G Blouin, Institut des sciences en production végétale IPV, DEFR, Agroscope, Nyon, Switzerland.

ORCID:
GP: 0000-0002-0412-4014
ET: 0000-0001-7755-4915

INTRODUCTION

Tomato leaf curl New Delhi virus (ToLCNDV), a bipartite begomovirus, was first reported to infect tomato in 1995 in India (Padidam *et al.*, 1995). During the last 20 years ToLCNDV has emerged as an important pathogen, and has spread rapidly in *Cucurbitaceae* in the Mediterranean area, where zucchini crops have been most affected. The disease caused by ToLCNDV is often epidemic, thanks to the presence of its efficient vector, the whitefly *Bemisia tabaci* (Bertin *et al.*, 2018; Parrella *et al.*, 2018; Panno *et al.*, 2019; Bertin *et al.*, 2021). ToLCNDV-infected zucchini squash plants showed typical symptoms, including stunting, severe leaf-curling, yellow mosaic and vein swelling of young leaves, rough skin and reduced size of fruit. Some of these symptoms are similar to those associated with phytoplasma infections.

Figure 1. The previously unreported Squash-Phytoplasma-Begomovirus (SqPB) disease syndrome that was observed on zucchini plants doubly infected with tomato leaf curl New Delhi virus (ToLCNDV) and a phytoplasma related to 16Sr-IB strain. A) yellowish young leaves and virescence of the flowers; B) deformed and cracked fruits with virescent flowers, compared to a healthy fruit and flower (on the left).

In 2018, during field monitoring for cucurbit viruses, an unusual syndrome was observed on zucchini squash plants in a field in Campania region (southern Italy). This syndrome was observed again in 2020, in a zucchini field located approx. 100 km from the 2018 observation. Symptoms consisted of severe stunting of the affected plants, while leaves were bent downwards, stiff, thicker than normal, with leathery texture, and showed interveinal chloroses and reduced leaf area. Young leaves were slightly chlorotic (yellowish) (Figure 1A). These symptoms were like those previously associated with ToLCNDV on zucchini in southern Italy (Panno *et al.*, 2019). However, additional symptoms were observed during fruit set including reductions in fruit size, and fruits were also deformed and often cracked. Flowers were virescence, which could be attributed to phytoplasma infections (Figure 1B). These field observations implied simultaneous infections of ToLCNDV and an unknown phytoplasma. This syndrome was first observed on zucchini plants in Italy, which is referred to as Squash-Phytoplasma-Begomovirus (SqPB).

MATERIALS AND METHODS

Two 1000 m^2 zucchini fields, one in 2018 and one in 2020, both with diseased plants and located in the Campania region of southern Italy, were selected for sample collection and analysis of disease incidence. The two fields were 100 km apart. The percentage incidences of SqPB was assessed by counting the number of plants with SqPB symptoms out of total number of plants observed in each field, using the following formula:

$$\% \text{ disease incidence} = \frac{\text{No. of symptomatic plants}}{\text{No. of plants observed}} \times 100$$

One SqPB diseased plant was randomly collected within each of four 1 m^2 plots on a diagonal transect across each of the two 1000 m^2 zucchini fields. Thus, four symptomatic SqPB plants and four asymptomatic plants were chosen from each field for laboratory analyses. Samples (one leaf per plant) were analyzed by double antibody sandwich ELISA with a commercial kit (Bioreba AG) for cucumber mosaic virus (CMV) and by indirect plate trapped antigen ELISA for potyviruses (potygroup test). ToLCNDV testing was carried out first, using a specific commercial loop-mediated isothermal amplification–based (LAMP) kit (Enbiotech). Total DNA was extracted from virescent flowers of the eight symptomatic plants following previously described methods (Parrella *et al.*, 2008). Nucleic acid samples diluted in TE buffer [10 mM Tris-HCl, 1 mM EDTA (pH 8.0)] to give a final concentration of 20-60 ng μL^{-1} were employed in PCR reactions, as described by Schaff *et al.* (1992). For ToLCNDV detection by PCR, the specific primer pair for the AV1 gene was used, as described by Parrella *et al.* (2018). For phytoplasmas detection, direct PCR amplification was carried out using the universal primer pair P1/P7 (Deng and Hiruki, 1991; Schneider *et al.*, 1995) to amplify the 16S rDNA, the spacer region and part of the 23S region, followed by nested-PCR with primers R16F2n/R16R2 (Gundersen and Lee, 1996) on P1/P7 amplicons diluted 1:30, and following procedure described previously (Parrella *et al.*, 2008; Parrella *et*

al., 2014). The AYsecYF1/AYsecYR1 primers (Lee *et al.*, 2006) were used to amplify the *secY* gene, the fTufu/rTufu primers (Schneider and Gibb, 1997) to amplify the *tuf* gene, and the rpF1/rpR1 (Lim and Sears, 1992) to amplify the *rp* gene, in direct PCR assays. Positive and negative controls, including a no template control, were included in all ELISA and PCR assays. The potyvirus-positive control were the isolate PAC-1 of BYMV (Parrella and Lanave, 2009), and the phytoplasma positive control was the isolate CATA-IT1 of Catharanthus roseus 16Sr-IB phytoplasma (Parrella *et al.*, 2008). Amplicons of the ToLCNDV AV1 gene and of each of the four phytoplasma genes from each positive plant sample were purified using the Wizard® SV Gel and PCR Clean-Up System (Promega), and were then directly Sanger sequenced twice on both directions. Multiple sequence alignments of 16S rDNA from different *Candidatus* Phytoplasma species (*Ca.* P.) and of the AV1 gene from ToLCNDV-ES/ToLCNDV-In isolates were conducted using Muscle (Edgar, 2004) implemented in MEGA11. Phylogenetic trees were constructed using the best fit model for each alignment, using the maximum likelihood (ML) method in the MEGA11 (Tamura *et al.*, 2021) with 500 bootstrap replicates. The trees were drawn to scale, with branch lengths measured as the number of substitutions per site.

RESULTS AND DISCUSSION

Incidence of the SqPB was estimated at 20% in the field inspected in 2018, and at 30% in the second field inspected in 2020. No positive reactions were observed for all the samples analyzed by ELISA for the search of CMV and potyviruses. All eight SqPB syndrome leaf samples tested positive to ToLCNDV by LAMP, while the eight symptomless samples tested negative for ToLCNDV. The presence of ToLCNDV was further confirmed in the eight positive samples, using the ToLCNDV AV1 gene PCR assay. The nucleotide sequences of AV1 gene amplicon

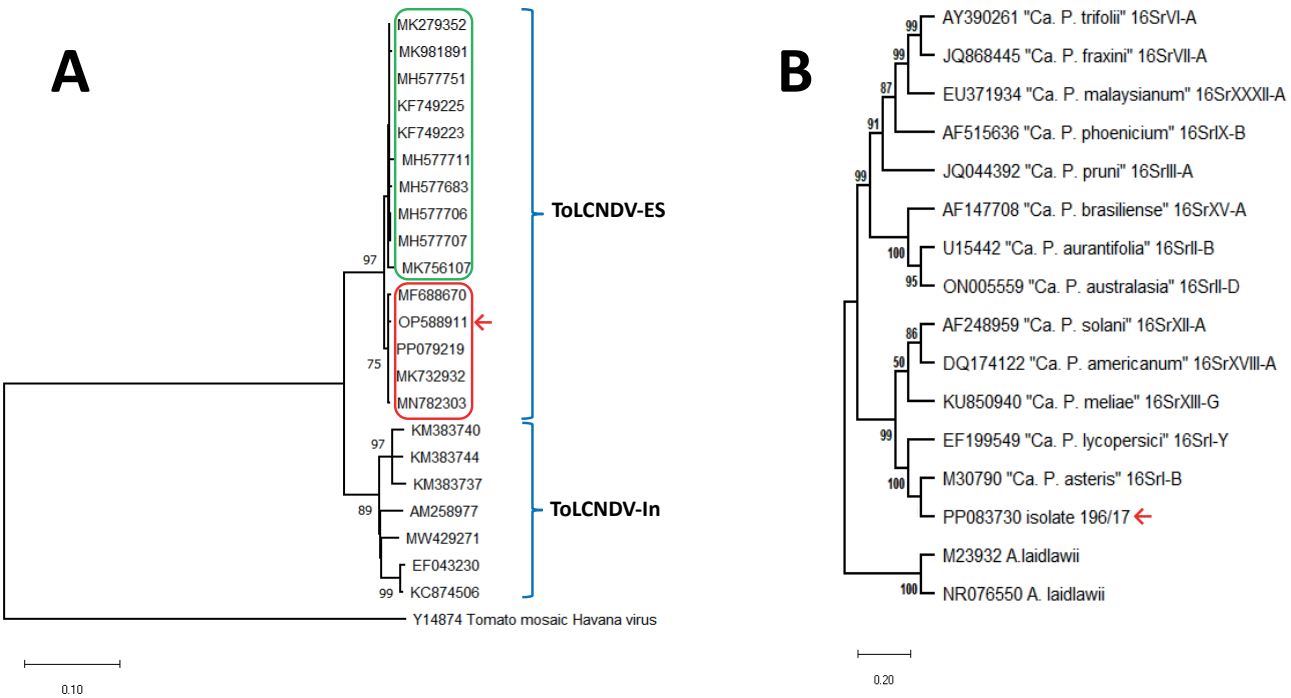

Figure 2. A) Phylogenetic analyses based on ToLCNDV coat protein gene of different virus isolates from the Mediterranean area (ToLCNDV-ES) and Asia (ToLCNDV-In). Evolutionary analyses were conducted in MEGA 11 (Tamura *et al.*, 2021), using the Maximum Likelihood method and Tamura-Nei model (Tamura and Nei, 1993), with 500 bootstrap replicates. The percentage of trees in which the associated taxa clustered together is shown next to the branches for values >70%. The ToLCNDV isolate from double-infected zucchini (indicated in the tree with a red arrow) groups together with four other isolates identified in the same Italian region (Campania) belonging to the subgroup I (red box), as described by Troiano and Parrella (2023), and within the ToLCNDV-ES major clade. The green box groups the ToLCNDV isolates belonging to subgroup II (isolates from Spain and Lazio, central Italy) within the ToLCNDV-ES major clade. B) Phylogenetic tree based on phytoplasma 16S rDNA, using the Maximum Likelihood method and Tamura-3 parameter model (Tamura and Nei, 1993), with 500 bootstrap replicates. The tree shows relationships among '*Candidatus* Phytoplasma' species (*Ca.* P.). GenBank accession numbers are specified in the tree together with ribosomal group or subgroup indications (the position of the phytoplasma isolate is indicated with a red arrow).

obtained from the eight symptomatic plants were identical. A BLASTN search showed that they were also identical (100% nucleotide similarity) to the sequence of the ToLCNDV Italian isolate Caa-164/16 from pepper (MK732932), which belongs to the ToLCNDV-ES subgroup I (Troiano and Parrella, 2023). This was confirmed by the phylogenetic analyses (Figure 2A). The 1049 bp sequence was submitted to NCBI (GenBank Acc. No. PP079219).

Amplicons of the expected size for the 16S rDNA, *tuf*, *SecY* and *rp* gene assays were produced only from all eight plants showing the SqPB syndrome. Sanger sequences were 100% identical among each gene and 99-100% identical to the related sequences of '*Ca*. P. asteris' strain RP166 (CP055264), a phytoplasma in the 16SrI-B Aster yellows group and associated with rapeseed phyllody (Cho *et al*., 2020). This was confirmed by the phylogenetic analyses (Figure 2B). Sequences of each gene were submitted to NCBI (accession nos. PP083730 for 16S rDNA; PP079220 for *SecY*; PP079221 for *tuf*; PP079222 for *rp*).

Mixed infections of phytoplasmas and begomoviruses have been reported in different vegetable crops from other countries. These reports include: in tomato and pepper in Mexico (Cardenas-Conejo *et al*., 2010; Lebsky *et al*., 2011); in chickpea, eggplant, tomato, pepper and *Withania somnifera* in India (Swarnalatha and Reddy, 2014; Singh *et al*., 2015; Venkataravanappa *et al*., 2018; Reddy *et al*., 2021; Tiwari *et al*., 2022); in common bean in Cuba (Zamora *et al*., 2021); in tomato in Saudi Arabia (Sohrab *et al*., 2016); and in many ornamental crops (Ahmad and Khan, 2021). The present study results represent the first evidences of mixed infections of the whitefly-transmitted *Begomovirus* ToLCNDV and a 16SrI-B group related phytoplasma in diseased zucchini squash, and in Italy. The presence of both pathogens in zucchini squash in Campania it not surprising, since ToLCNDV infects zucchini in the region and '*Ca.* P. asteris' is widespread in Italy (Panno *et al*., 2019).

The effects of possible interactions between viruses and phytoplasmas have not yet been studied in detail in mixed infections. Phytoplasmas belonging to the aster yellows group are probably one of the most diverse and widespread groups (Lee and Davis, 2000). ToLCNDV has also become an endemic virus on cucurbits grown in countries in the Mediterranean Basin, partly due to the invasion into new areas of its efficient vector, the whitefly *Bemisia tabaci* (Panno *et al*., 2019; Bertin *et al*., 2018). Generalized yellowing caused by ToLCNDV infections in zucchini could be attractive to different sucking insects, including the leafhoppers that transmit phytoplasmas (Shi *et al*., 2020). Conversely, if '*Ca*. P. asteris' causes yellowing in zucchini squash, this could further attract ToLCNDV infectious whiteflies (Johnston and Martini, 2020). Mixed infections may enhance disease severity and yield losses compared to those of single infections. Hence, interactions between phytoplasmas and viruses should be studied in more detail, especially in vegetable crops and from epidemiological and pathogens interaction viewpoints.

ACKNOWLEDGEMENTS

This research was supported by the Campania Region, Italy (Plan of Phytosanitary Action 2018-2020).

LITERATURE CITED

Ahmad A., Khan A.A. 2021. Association of phytoplasma and begomovirus with some ornamental plants: a review. *Plant Archives* 21: 350–355.

Bertin S., Luigi M., Parrella G., Giorgini M., … Tomassoli L. 2018. Survey of the distribution of *Bemisia tabaci* (Hemiptera: Aleyrodidae) in Lazio region (Central Italy): a threat for the northward expansion of the Tomato leaf curl New Delhi virus (*Begomovirus*: Geminiviridae) infection. *Phytoparasitica* 46: 171–182.

Bertin S., Parrella G., Nannini M., Guercio G., Troiano E., Tomassoli L., 2021. Distribution and genetic variability of *Bemisia tabaci* cryptic species (Hemiptera: Aleyrodidae) in Italy. *Insects* 12: 521.

Cardenas-Conejo Y., Arguello-Astorga G., Poghosyan A., Hernandez-Gonzalez J., Lebsky V., … Vega-Peña, 2010.First report of *Tomato yellow leaf curl virus* co-infecting pepper with *Tomato chino La Paz virus* in Baja California Sur, Mexico. *Plant Disease*, 94: 1266.

Cho S.T., Zwolińska A., Huang W., Wouters R.H.M., Mugford S.T., … Kuo C.H. 2020. Complete genome sequence of "*Candidatus* Phytoplasma asteris" RP166, a plant pathogen associated with rapeseed phyllody disease in Poland. *Microbiology Resources Announcement* 9: e00760-20.

Deng S., Hiruki C. 1991. Amplification of 16S rRNA genes from culturable and nonculturable Mollicutes. *Journal of Microbiology Methods* 14: 53–61.

Edgar R.C., 2004. MUSCLE: multiple sequence alignment with high accuracy and high throughput, *Nucleic Acids Research* 32: 1792–1797.

Gundersen D.E., Lee I.M. 1996. Ultrasensitive detection of Phytoplasmas by nested-PCR assays using two universal primer pairs. *Phytopathologia Mediterranea* 35: 114–151.

Johnston N., Martini X. 2020. The influence of visual and olfactory cues in host selection for *Bemisia tabaci* biotype B in the presence or absence of *Tomato Yellow Leaf Curl Virus*. *Insects* 11: 115.

Lebsky V., Hernández-González, Arguello-Astorga G., Cardenas-Conejo Y., Poghosyan A. 2011. Detection of phytoplasmas in mixed infection with begomoviruses: a case study of tomato and pepper in Mexico. *Bulletin of Insectology* 64 (Supplement): S55–S56.

Lee I.M., Davis R.E. 2000. Aster yellows. In: *Encyclopedia of Plant Pathology (*Maloy OC, Murray TD., ed.), New York, Wiley, pp 60–63.

Lee I.-M., Zhao Y., Bottner K.D. 2006. SecY gene sequence analysis for finer differentiation of diverse strains in the aster yellows phytoplasma group. *Molecular and Cellular Probes* 20: 87–91.

Lim P.O., Sears B.B. 1992. Evolutionary relationships of a plant-pathogenic mycoplasma-like organism and *Acholeplasma laidlawii* deduced from two ribosomal protein gene sequences. *Journal of Bacteriology* 174: 2606–2611.

Padidam M., Beachy R.N., Fauquet C.M. 1995. Tomato leaf curl geminivirus from India has a bipartite genome and coat protein is not essential for infectivity. *Journal of General Virology* 76: 25–35.

Panno S., Caruso A.G., Troiano E., Luigi M., … Davino S. 2019. Emergence of tomato leaf curl New Delhi virus in Italy: estimation of incidence and genetic diversity. *Plant Pathology* 68: 601–608.

Parrella G., Lanave C. 2009. Identification of a new pathotype of Bean yellow mosaic virus (BYMV) infecting blue passion flower and some evolutionary characteristics of BYMV. *Archives of Virology* 154: 1689–1694.

Parrella G., Paltrinieri S., Botti S., Bertaccini A. 2008. Molecular identification of phytoplasmas from virescent ranunculus plants and from leafhoppers in Southern Italian crops. *Journal of Plant Pathology* 90: 537–543.

Parrella G., Paltrinieri S., Contaldo N., Vitale M.R., Bertaccini A. 2014. Characterization of 'Candidatus Phytoplasma asteris' strains associated with periwinkle virescence in Southern Italy. *Phytopathogenic Mollicutes* 4: 53–58.

Parrella G., Troiano E., Formisano G., Accotto G.P., Giorgini M. 2018. First report of *Tomato leaf curl New Delhi virus* associated with severe mosaic of pumpkin in Italy. *Plant Disease* 102: 459–460.

Reddy M.G., Baranwal V.K., Sagar D., Rao G.P. 2021. Molecular characterization of chickpea chlorotic dwarf virus and peanut witches' broom phytoplasma associated with chickpea stunt disease and identification of new host crops and leafhopper vectors in India. *3 Biotech* 11: 112.

Schaff D., Lee I.-M., Davis R.E. 1992. Sensitive detection and identification of mycoplasma-like organisms by polymerase chain reaction. *Biochemical and Biophysical Research Communications* 186: 1503–1509.

Schneider B, Seemüller E, Smart CD and Kirkpatrick BC. 1995. Phylogenetic classification of plant pathogenic mycoplasma-like organisms or phytoplasmas. In: *Molecular and Diagnostic Procedures in Mycoplasmology* (Razin S., Tully J.G., ed.), San Diego, CA, Academic press, pp. 369–380.

Schneider B., Gibb K.S. 1997. Sequence and RFLP analysis of the elongation factor *Tu* gene used in differentiation and classification of phytoplasmas. *Microbiology* 143: 3381–3389.

Shi L, He H, Yang G, Huang H, Vasseur L, You M. 2020. Are yellow sticky cards and light traps effective on tea green leafhoppers and their predators in Chinese tea plantations? *Insects* 12: 14.

Singh J., Singh A., Kumar P., Rani A., Baranwal V.K., Sirohi A., 2015. Evidence of a mixed infection of Candidatus Phytoplasma trifolii and a Begomovirus in Eggplan (*Solanum melongena*). *Journal of Pure and Applied Microbiology* 9: 663–670.

Sohrab S.S., Yasir M., El-Kafrawy S.A., Abbas A. T., Mousa M.A.A., Bakhashwain A.A. 2016. Association of tomato leaf curl sudan virus with leaf curl disease of tomato in Jeddah, Saudi Arabia. *VirusDisease* 27: 145–153.

Swarnalatha P., Reddy M. K. 2014. Duplex PCR for simultaneous detection of Begomovirus and Phytoplasma from naturally infected tomato. *Pest Management in Horticultural Ecosystems* 20: 59–68.

Tamura K., Nei M. 1993. Estimation of the Number of Nucleotide Substitutions in the Control Region of Mitochondrial DNA in Humans and Chimpanzees. *Molecular Biology and Evolution* 10: 512–526.

Tamura K., Stecher G., Kumar S., 2021. MEGA11: Molecular Evolutionary Genetics Analysis version 11. *Molecular Biology and Evolution* 38: 3022–3027.

Tiwari N.N., Jain R. K., Prajapati M.R., Singh J., Srivastava S., Tiwari A.K., Marcone C. 2022. Evidence of mixed infection of phytoplasma and begomovirus associated with *Withania somnifera* and *Capsicum annum* plants from Uttar Pradesh, India. *Archives of Phytopathology and Plant Protection* 55: 2146–2157.

Troiano E., Parrella G. 2023. First report of tomato leaf curl New Delhi virus in *Lagenaria siceraria* var. longissima in Italy. *Phytopathologia Mediterranea* 62: 17–24.

Venkataravanappa V., Prasanna H.C., Lakshminarayana C.N., Reddy M.K. 2018. Molecular detection and

characterization of phytoplasma in association with begomovirus in eggplant. *Acta Virologica* 62: 246–258.

Zamora L., Quiñones M., Acosta K., Piñol B., Santos M.E., … Arocha Y. 2021. Molecular characterization of '*Candidatus* Phytoplasma asteris' and a *Bean golden yellow mosaic virus* isolate present in mixed infection in common bean in Cuba. *Revista de Protección Vegetal* 36: 1–9.

Phytopathologia Mediterranea
The international journal of the
Mediterranean Phytopathological Union

Firenze University Press
www.fupress.com/pm

Research Papers

Reactions of *Citrullus amarus* and *Cucumis metuliferus* to *Meloidogyne chitwoodi*, *Meloidogyne enterolobii* and *Meloidogyne luci*

Aïda Magdalena FULLANA[1], Carla MALEITA[2,3], Duarte SANTOS[2,3], Isabel ABRANTES[3], Francisco Javier SORRIBAS[1], Ariadna GINÉ[1,*]

[1] *Department of Agri-Food Engineering and Biotechnology (DEAB), Barcelona School of Agri-Food and Biosystems Engineering (EEABB), Universitat Politècnica de Catalunya, BarcelonaTech (UPC), Castelldefels, Spain*
[2] *University of Coimbra, Chemical Engineering and Renewable Resources for Sustainability (CERES), Department of Chemical Engineering, Rua Sílvio Lima, Pólo II – Pinhal de Marrocos, 3030-790 Coimbra, Portugal*
[3] *University of Coimbra, Centre for Functional Ecology - Science for People & the Planet (CFE), Associate Laboratory Terra, Department of Life Sciences, Calçada Martim de Freitas, 3000-456 Coimbra, Portugal*
*Corresponding author. E-mail: ariadna.gine@upc.edu

Summary. *Meloidogyne chitwoodi*, *M. enterolobii,* and *M. luci* are present in some EU countries, with restricted distributions, and plant resistance can be used to manage these nematodes. Two pot experiments were conducted under controlled conditions for 56 d to assess the host suitability of two potential rootstocks, *Cucumis metuliferus* BGV11135 and *Citrullus amarus* BGV5167, to one isolate of each nematode. The susceptible cucumber (*Cucumis sativus*) 'Dasher II', watermelon (*Citrullus lanatus*) 'Sugar Baby' and tomato (*Solanum lycopersicum*) 'Coração-de-Boi' were included for comparisons. A histopathological study using confocal-laser microscopy was also conducted 15 d after nematode inoculations. In the pot test, the rootstocks showed lower numbers of galls, egg masses, and eggs per plant than their susceptible ones. Reproduction indices of the rootstocks varied from immune to moderately resistant, depending on the isolate-rootstock combination. In the histopathological study, *M. enterolobii* and *M. luci* induced similar numbers of giant cells (GC) per feeding site in all germplasms. However, GC volumes and numbers of nuclei in rootstocks were lower than in the susceptible germplasms. GCs induced by *M. chitwoodi* were only detected in susceptible cucumber. These results emphasize the potential of *C. metuliferus* and *C. amarus* as effective, eco-friendly strategies for managing root-knot nematodes, and show the complex these host-pathogen interactions.

Keywords. Histopathology, plant resistance, root-knot nematodes, rootstocks.

OPEN ACCESS

Citation: A.M. Fullana, C. Maleita, D. Santos, I. Abrantes, F.J. Sorribas, A. Giné (2024) Reactions of *Citrullus amarus* and *Cucumis metuliferus* to *Meloidogyne chitwoodi*, *Meloidogyne enterolobii* and *Meloidogyne luci*. *Phytopathologia Mediterranea* 63(1): 79-90. doi: 10.36253/phyto-15108

Accepted: March 20, 2024

Published: April 29, 2024

Data Availability Statement: All relevant data are within the paper and its Supporting Information files.

Competing Interests: The Author(s) declare(s) no conflict of interest.

Editor: Thomas A. Evans, University of Delaware, Newark, DE, United States.

ORCID:
AMF: 0000-0001-5190-3478
CM: 0000-0003-1616-3632
DS: 0000-0003-4948-7473
IA: 0000-0002-8761-2151
FJS: 0000-0001-7465-7353
AG: 0000-0002-3598-4818

INTRODUCTION

Plant-parasitic nematodes (PPN) have significant economic impacts on agriculture (Jones *et al.*, 2013), leading to diminished crop yields qual-

ity (Elling, 2013). *Meloidogyne* spp., commonly known as root-knot nematodes (RKN), are obligate sedentary endoparasites of roots of many plant species, and are responsible for approx. half of crop yield losses attributed to PPN (Bent *et al*., 2008). In a compatible host, the RKN trigger formation of multinucleated giant cells (GC), from which the nematodes obtain the nutrients for development. RKN induce formation of host root galls, disrupting the uptake of water and nutrients and causing nonspecific symptoms in aerial plant parts, including stunting, nutrient deficiency, epinasty, and plant death, at high nematode population densities in soil. Disease severity depends on soil nematode population density at sowing or transplanting, and on host species and cultivar, cropping season, soil texture and presence of potential nematode antagonists (Sorribas *et al.,* 2020). Conversely, when compatibility between the host plant and the nematode is suboptimal, GCs often have inhibited growth, characterized by presence of multiple vacuoles, sparse nuclei, or cytoplasmic collapse. Another distinctive feature frequently observed is the absence of fluorescence in histopathological images, due to the probable accumulation of phenolic compounds surrounding the GCs, indicating hypersensitive responses to nematode infections (Phan *et al*., 2018; Expósito *et al*., 2020; Fullana *et al*., 2023). This defensive response results in suppression of nematode infection and reproduction, and, in some cases, increases in proportions of males in the populations (Ye *et al*., 2017).

Of the approx. 100 RKN species described to date, *Meloidogyne arenaria*, *M. incognita, M. javanica* (tropical species), and *M. hapla* (temperate species), are responsible for most yield crop losses attributed to *Meloidogyne* spp. (Jones *et al.,* 2013). However, other RKN species, such as *M. chitwoodi, M. enterolobii* and *M. luci,* are gaining importance, because of their high pathogenicity in several economically important crops despite their limited global distributions (Castagnone-Sereno, 2012; Elling, 2013; Maleita *et al*., 2022). *Meloidogyne chitwoodi* and *M. enterolobii* have been added to the EPPO A2 list of pests recommended for regulation as quarantine pests (EPPO, 2023a), and *M. luci* has been added to the EPPO Pest Alert List (EPPO, 2017). In Europe, populations of *M. chitwoodi* have been reported in Belgium, France, Germany, the Netherlands and Portugal in 2016 (EPPO, 2016). Currently, however, 17 other countries, including Spain, have been included (EPPO 2023b). The distribution of *M. enterolobii* is more limited than that of other *Meloidogyne* species, having been reported in Belgium, France, Italy, the Netherlands, Portugal and Switzerland (EPPO, 2023c). *Meloidogyne luci* is present in Greece, Italy, Portugal, Serbia, Slovenia and Turkey (EPPO, 2023d). Despite these restricted distributions, legislative measures have been implemented to eradicate these nematodes, and prevent their introduction into regions where they are absent. This emphasizes the need for increased surveillance and control measures against these emerging nematode species.

RKN control has traditionally relied on fumigant and non-fumigant nematicides. However, use of most of these have been prohibited or restricted, due to harmful environmental, human, and/or animal effects. In response, the European Union has adopted new policies that promote the use of integrated nematode management strategies, which prioritize environmentally friendly and safe approaches reflected in Directive 2009/128/CE and the European Green Deal. Plant resistance plays a key role in the available control strategies, because it suppresses nematode infection and/or reproduction (Roberts, 2002). Resistance is cost-effective, prevents nematode reproduction and crop yield losses (Sorribas *et al*., 2005), and its effect is extended to following susceptible crops (Ornat *et al*., 1997; Hanna, 2000). Commercially available resistant vegetable cultivars or rootstocks for tropical RKN species are limited to the *Solanaceae* and *Cucurbitaceae* including tomato, pepper, eggplant and watermelon. However, some of the minor and temperate RKN species can reproduce on these plants, or their reproductive capacity is unknown.

Meloidogyne chitwoodi, M. enterolobii and *M. hapla* can reproduce on tomato carrying the *Mi1.2* resistance gene and pepper germplasm carrying the *N* resistance gene (Brown *et al*., 1997; Koutsovoulos *et al.,* 2020). In addition, virulent isolates of *M. luci* able to overcome resistance conferred by the tomato *Mi1.2* gene have been reported (Aydinli *et al*., 2019). In cucurbits, the experimental melon rootstocks *Cucumis metuliferus* BGV11135 display resistance to *M. arenaria*, *M. incognita* and *M. javanica* (Expósito *et al*., 2018, and 2019), as well as *Citrullus amarus*, a commercial watermelon rootstock (García-Mendívil *et al.,* 2019; Waldo *et al.,* 2023). Additionally, three accessions of *C. metuliferus* 'Kino' exhibit resistance to *M. enterolobii*, *M. incognita* race 1, and *M. javanica* (Pinheiro *et al.,* 2019). Waldo *et al.* (2023) also evaluated 108 different accessions of *C. amarus*, and some of these were resistant to *M. enterolobii*. Nevertheless, there is currently no available knowledge about the host suitability of *C. metuliferus* and *C. amarus* for the emerging RKN species *M. chitwoodi* and *M. luci.*

Histopathological studies conducted with laser scanning confocal microscopy have shown that GCs in resistant germplasms are less voluminous and have fewer

nuclei than those in susceptible germplasm (Expósito *et al.,* 2020; Fullana *et al.,* 2023). The aim of the present study was to determine host suitability of *C. metuliferus* BGV11135 and *C. amarus* BGV5167 accessions for isolates of *M. chitwoodi, M. enterolobii,* and *M. luci.* Histopathological studies of each plant germplasm-RKN isolate combination were also carried out.

MATERIALS AND METHODS

Nematode inocula

Inocula consisted of second-stage juveniles (J2) of *M. chitwoodi* (PtCh), *M. enterolobii* (PtEn), and *M. luci* (PtL1) isolates selected from the RKN NEMATOlab collection (CFE, University of Coimbra) (Maleita *et al.*, 2021). The isolates were maintained on the susceptible tomato (*Solanum lycopersicum*) cultivar 'Coração-de-Boi' (Vilmorim-Mikado Ibérica, Alicante, Spain; Maleita *et al.*, 2022), in a growth chamber maintained at 24 ± 2°C and 16 h light 8 h dark daily cycle. One week before nematode inoculations, nematode egg masses were hand-picked and placed in Baermann funnels to allow J2 emergence. After 24 h, the emerged J2 were discarded, and the remaining J2 were collected daily and kept at 4°C until the beginning of the experiment, for a maximum of 5 d. Biochemical electrophoretic analyses of non-specific esterase enzymes were carried out to confirm the *Meloidogyne* species (Pais *et al.*, 1986).

Plant material

Seeds of the *C. metuliferus* BGV11135 and *C. amarus* BGV5167 (COMAV-UPV, Valencia, Spain) were used in this study. The cucumber (*Cucumis sativus*) 'Dasher II' (Seminis Seeds) and the watermelon (*Citrullus lanatus*) 'Sugar Baby' (Batlle Seeds) were used as cultivars susceptible to tropical RKN species for comparisons (Giné *et al.*, 2014; López- Gómez *et al.*, 2014). The susceptible tomato (*S. lycopersicum*) 'Coração-de-Boi' was included as a control, to assess the viability of the nematode inocula. Seeds were germinated in Petri dishes with sterile filter paper soaked with sterile distilled water at 24 ± 1°C for 3 d in the dark. After germination, seedlings were transplanted (one per pot) into 50 cm^3 pots containing a sterile mixture (1:1:2) of sandy loam soil, sand and a germination substrate (Siro Germinação bio®). This substrate contains 2 $kg{\cdot}m^{-3}$ of NPK 9-2-2. The seedlings were kept in a growth chamber for 3 weeks at 24 ± 2°C and a 16 h light 8 h dark daily cycle.

Host suitability

Plants were transplanted into 200 cm^3 capacity pots containing the soil mixture described above, and were each inoculated with 200 J2. The nematode inoculum was distributed in each pot into two 2 cm holes, located 1 cm away from the plant stem and 2 cm deep in the soil. Each plant germplasm-RKN isolate combination was repeated 10 times, and the experiment was conducted twice.

The plants were maintained in controlled climate chamber at 25 ± 2°C and 60% relative humidity with a 16 h light 8 h dark daily cycle for 56 d. The plants were watered at 2 d intervals, and were fertilized once each week with NUTREA 12-4-6 (Genyen, Crop Solutions), a liquid fertilizer containing 5% N, 8% P and 10% K. At the end of the experiment, plant roots were carefully washed free of soil with tap water, and were then immersed in a phloxine B (0.0015%) solution for 15 min to stain and visualize the nematode egg masses (Holbrook *et al.*, 1983). The number of root galls and egg masses per plant were counted to estimate nematode penetration (galls) and infectivity (egg masses). Nematode eggs were extracted from each whole root system by blending maceration in a 1% NaOCl solution, using the procedure outlined by Hussey and Barker (1973), eggs were counted to estimate the final nematode population densities (Pf). Nematode fertility was calculated as the number of eggs per egg mass per plant, and reproduction index (RI), as the percentage of reproduction of a given *Meloidogyne* isolate in the resistant germplasm relative to that in the susceptible germplasm [RI = (Pf in resistant germplasm/Pf in susceptible germplasm) × 100]. Levels of resistance were estimated according to the RI values, as immune (RI = 0), highly resistant (RI < 1%), resistant (1% ≤ RI < 10%), moderately resistant (10% ≤ RI < 25%), slightly resistant (25% ≤ RI < 50%), or susceptible (RI ≥ 50%), based on the scale of Hadisoeganda and Sasser (1982).

Histopathology

Fifteen plants of each plant germplasm (described above) were transplanted into 200 cm^3 capacity pots containing sterilized sand, and were maintained under the conditions described above. After 7 d, each susceptible plant germplasm-RKN isolate combination was inoculated with 200 J2, and each expected resistant plant germplasm-RKN isolate combination was inoculated with 600 J2, using the procedure described above. Each plant germplasm-RKN isolate combination was repeated five times. Fifteen days after nematode inoculation, five root systems

of each RKN isolate-plant combination were washed free of subtrate, and were then fixed and rinsed following the procedure of Expósito *et al.* (2020). Images were acquired using a laser scanning confocal microscope (LSM 710 Axio Observer Z1 microscope with QUASAR detection unit; ZEN Black software) using a Plan-Neofluar 10×/0.3 objective, and Argon/2 (488 nm) and HeNe633 (633 nm) lasers, all of which are components from Carl Zeiss. Volumes were acquired with Z-stacks with a step size of 10 µm. The volumes and numbers of nuclei per GC, the numbers of GCs, and the volumes and numbers of nuclei per feeding site were determined using ImageJ and the TrakEM2 ImageJ plugin (ImageJ, version 1.50). This study was conducted once.

Data analyses

Statistical analyses were carried out using GraphPad Prism 7.00 (GraphPad Software). The normality of the data distributions and homogeneity of variances were determined with non-transformed or $\log_{10}$ (x+1) transformed data for parametric or non-parametric analyses. The nonparametric Mann-Whitney test was used to compare penetration (number of galls per plant), infectivity (number of egg masses per plant), reproduction (number of eggs per plant), and fecundity (number of eggs per egg mass) between the experimental repetitions. When significant differences ($P \leq 0.05$) were observed, the values for each replicate were presented separately. Additionally, each parameter was compared between susceptible and the expected resistant germplasm of the same plant genus, or between paired comparisons of tomato plants and each of the susceptible cucurbit germplasms, by Student's t-test ($P \leq 0.05$) when the data exhibited a normal distribution or Mann-Whitney test ($P \leq 0.05$) if it did not. In addition, nonparametric Kruskal-Wallis analyses and Dunn's test ($P \leq 0.05$) were used to compare each parameter between RKN isolate by plant germplasm combinations.

The numbers of nuclei per feeding site and GCs per feeding site, the volume of each GC, and the number of nuclei per GC from the histopathological study were compared ($P \leq 0.05$), between expected resistant and susceptible germplasms per plant genus, as well as the paired comparisons between tomato plants and each of the susceptible cucurbit germplasms. Data were compared using Student's t-test if the data fitted normal distributions; otherwise, the nonparametric Mann-Whitney test was used. In addition, nonparametric Kruskal-Wallis analysis and Dunn's test ($P \leq 0.05$) were used to compare each parameter among the RKN isolate by plant germplasm combinations.

RESULTS

Host suitability

Although general trends were observed, statistically significant differences ($P < 0.05$) were found between the experiments, results for each experiment are presented separately (Table 1). Second-stage juveniles of all RKN isolates penetrated the roots of each plant germplasm, leading to the formation of galls (Table 1). Among the susceptible germplasms, *M. chitwoodi* produced fewer ($P < 0.05$) galls on the cucurbit than on the tomato plants, while no differences ($P > 0.05$) were found between *M. enterolobii* and *M. luci*. Among the resistant germplasms, all the RKN isolates induced fewer ($P < 0.05$) galls than the susceptibles (Table 1). For nematode reproduction, all the RKN isolates developed until the adult female stage producing eggs, in all germplasms, except for *M. chitwoodi* in *C. metuliferus* (Table 1). Fewer ($P < 0.05$) egg masses per plant were produced in the resistant germplasms than in the susceptible germplasms of the same plant genus, except for *M. chitwoodi* in *Citrullus* spp. (Table 1). Concerning the levels of resistance of *C. amarus* to the RKN isolates, performed as resistant to *M. luci* (RI = 4.3 and 4.3%) in both experiments, and resistant or moderately resistant to *M. enterolobii* (RI = 6.7 and 12.2%) and *M. chitwoodi* (RI = 5.3 and 19.1%), depending on the experiment. Meanwhile, *C. metuliferus* was immune to *M. chitwoodi* (RI = 0), highly resistant to resistant to *M. enterolobii* (RI = 0.3 and 3.8%), and resistant to *M. luci* (RI = 1.6 and 1.8%).

Regarding the RKN isolates, *M. chitwoodi* produced fewer ($P < 0.05$) egg masses and eggs per plant on tomato plants than the other RKN isolates. *Meloidogyne luci* reproduced means of 5.5 and 11.3 more times in tomato than *M. chitwoodi* in experiment 1, and 2.6 and 1.7 more times than *M. enterolobii* in experiment 2 (Table 1). In *C. sativus*, *M. chitwoodi* produced fewer ($P < 0.05$) egg masses and eggs per plant than *M. enterolobii* and *M. luci*, which were not different for the numbers of eggs per egg mass in the second experiment. For *C. metuliferus*, *M. chitwoodi* induced fewer ($P < 0.05$) root galls than the other RKN isolates, but no reproduction was detected. In *Citrullus* spp., *M. enterolobii* produced more ($P < 0.05$) egg masses (4.0 to 112.9 times more in *C. lanatus*; 5.3 to 42.0 times more in *C. amarus*) and eggs per plant (4.3 to 515.0 times more in *C. lanatus*; 6.8 to 680.0 times more in *C. amarus*) than the other RKN isolates (Table 1).

Histopathology

Fifteen d after nematode inoculations, only the *M. enterolobii* and *M. luci* isolates were able to infect the

Table 1. Number of galls, nematode egg masses and eggs per plant, and number of eggs per egg mass of *Meloidogyne chitwoodi, M. enterolobii* or *M. luci*, in susceptible plants of *Solanum lycopersicum* 'Coração-de-Boi', *Cucumis sativus* 'Dasher II', and *Citrullus lanatus* 'Sugar Baby', or *Cucumis metuliferus* BGV11135 or *Citrullus amarus* BGV5167 rootstocks 56 d after inoculations with 200 second-stage juveniles per pot, in a climatic chamber in the two experiments [a].

	Meloidogyne species	Plant species	Galls	Egg masses per plant	Eggs per plant (10^2)	Egg per egg mass	Reproduction index (%)[b]	Resistance level [c]
First experiment	*M. chitwoodi*	*S. lycopersicum*	>100 A	22 ± 4.0 C	74 ± 6.7 C	486 ± 111 A		
		C. sativus	59 ± 6 B * †	1.8 ± 0.6 B †	0.9 ± 0.2 B †	23 ± 5 B †		
		C. metuliferus	7 ± 1 C	0 ± 0	0 ± 0	nc	0	I
		C. lanatus	28 ± 9 B * †	0.9 ± 0.4 B †	2.0 ± 0.4 C * †	120 ± 10 A †		
		C. amarus	8 ± 1 C	0.1 ± 0.1 B	0.01 ± 0.01 B	nc	5.3	R
	M. enterolobii	*S. lycopersicum*	>100 A	42 ± 2.3 B	144 ± 9.5 B	346 ± 22 A		
		C. sativus	>100 A *	34 ± 2.3 A * †	44 ± 3.7 A * †	136 ± 16 A †		
		C. metuliferus	25 ± 2 B	0.8 ± 0.3 A	1.7 ± 1.4 A	179 ± 136 A	3.8	R
		C. lanatus	>100 A *	36 ± 3.0 A *	102 ± 9.0 A * †	295 ± 28 A		
		C. amarus	50 ± 5 B	4.2 ± 1.7 A	6.8 ± 2.5 A	191 ± 56 A	6.7	R
	M. luci	*S. lycopersicum*	>100 A	96 ± 4.5 A	382 ± 24.1 A	431 ± 25 A		
		C. sativus	>100 A *	34 ± 2.3 A * †	36 ± 2.2 A * †	112 ± 10 A †		
		C. metuliferus	53 ± 3 A	0.3 ± 0.2 A	0.7 ± 0.5 A	218 ± 43 A	1.8	R
		C. lanatus	>100 A *	9 ± 2.0 B * †	24 ± 5.6 B * †	242 ± 50 A †		
		C. amarus	79 ± 5 A	0.8 ± 0.3 B	1.0 ± 0.6 AB	157 ± 106 A	4.3	R
Second experiment	*M. chitwoodi*	*S. lycopersicum*	>100 A	27 ± 3.0 B	57 ± 7.3 C	221 ± 30 C		
		C. sativus	37 ± 2 B * †	5.6 ± 1.8 B †	5.6 ± 0.3 B †	90 ± 25 C †		
		C. metuliferus	20 ± 1 B	0 ± 0	0 ± 0	nc	0	I
		C. lanatus	33 ± 3 B * †	0.7 ± 0.4 B †	0.8 ± 0.5 C †	114 ± 39 B †		
		C. amarus	13 ± 2 C	0.2 ± 0.2 B	0.2 ± 0.2 B	nc	19.1	MR
	M. enterolobii	*S. lycopersicum*	>100 A	105 ± 9.0 A	380 ± 33.5 B	393 ± 55 B		
		C. sativus	>100 A *	34 ± 5.0 A * †	224 ± 39.3 A * †	801 ± 172 A *		
		C. metuliferus	39 ± 5 A	0.3 ± 0.2 A	0.6 ± 0.4 A	200 ± 16 B	0.3	HR
		C. lanatus	>100 A *	79 ± A 7.0 * †	412 ± 26.9 A *	548 ± 50 A †		
		C. amarus	66 ± 6 A	8.3 ± 1.5 A	50 ± 10.4 A	603 ± 70 A	12.2	MR
	M. luci	*S. lycopersicum*	>100 A	121 ± 6.0 A	647 ± 22.5 A	544 ± 26 A		
		C. sativus	>100 A *	36 ± 4.0 A * †	160 ± 23.0 A * †	442 ± 42 B		
		C. metuliferus	25 ± 2 A	0.4 ± 0.2 A	2.6 ± 2.1 A	510 ± 162 A	1.6	R
		C. lanatus	>100 A *	7 ± 2.0 B * †	27 ± 7.3 B * †	371 ± 65 AB †		
		C. amarus	50 ± 5 B	0.6 ± 0.2 B	1.1 ± 0.5 B	222 ± 89 B	4.3	R

[a] Data are means ± standard errors of ten replicates. Data in each column followed by different letters are significantly different ($P < 0.05$) between root-knot nematode (RKN) isolates for a given plant germplasm, according to Dunn's test. Data for each column and each RKN isolate followed by * indicate significant differences ($P < 0.05$) between germplasms of the same genus, and by † indicate differences ($P < 0.05$) between *Solanum lycopersicum* and *Cucumis sativus* or *Citrullus lanatus*, as shown by Student's t tests or Mann-Whitney tests. nc = Not calculated. [b] Reproduction index: percentage of the eggs produced in the resistant germplasm compared with those produced in the susceptible germplasm. [C] Resistance level: I = immune (RI = 0), HR = highly resistant (RI < 1%), R = resistant (1% ≤ RI ≤ 10%), MR = moderately resistant (10% < RI ≤ 25%), SR = slightly resistant (25% < RI ≤ 50%) or S = susceptible (RI > 50%), as categorized by Hadisoeganda and Sasser (1982).

roots of all the assessed plant germplasms (Table 2; Figures 1 to 4). *Meloidogyne chitwoodi* only infected tomato and cucumber roots (Table 2; Figures 1 and 4). Despite *M. chitwoodi* J2 being observed inside the roots of *C. metuliferus* and *C. lanatus,* no GCs were induced (Figure 4, b and c); therefore, comparisons were only valid between tomato and cucumber. The number and volume of GCs per feeding site and the number of nuclei per GC and per feeding site did not differ ($P > 0.05$) between the tomato and cucumber plants (Table 2).

Meloidogyne enterolobii induced a similar ($P > 0.05$) number of GCs in *C. metuliferus* and cucumber. However, the volumes of the GCs in *C. metuliferus* were six times less ($P < 0.05$) than in cucumber, resulting in a 9.5-fold reduction ($P < 0.05$) in the total volume of GCs per feeding site. The number of nuclei per GC and per

Table 2. Number of giant cells per nematode feeding site (GC·fs^{-1}), number of nuclei per giant cells (N·GC^{-1}), number of nuclei per feeding site (N·fs^{-1}), giant cell volume (GCV) and giant cell volume per feeding site (GCV·fs^{-1}), in *Solanum lycopersicum* 'Coração-de-Boi', *Cucumis sativus* 'Dasher II' and *Citrullus lanatus* 'Sugar Baby' plants, and *Cucumis metuliferus* BGV11135 and *Citrullus amarus* BGV5167 rootstocks, 15 d after nematode inoculations with 200 or 600 second-stage juveniles per pot [a], in susceptible or rootstocks respectively.

Meloidogyne species	Plant species	GC·fs^{-1}	N·GC^{-1}	N·fs^{-1}	GCV (μm^3 10^{-5})	GCV·fs^{-1} (μm^3 10^{-5})
M. chitwoodi	*S. lycopersicum*	5 ± 1.0 A	14 ± 3.2 B	44 ± 8.8 B	8 ± 1.1 B	26 ± 3.0 B
	C. sativus	4 ± 0.2 A	9 ± 1.7 B	29 ± 6.4 C	5 ± 0.9 C	22 ± 3.4 B
	C. metuliferus	na	na	na	na	na
	C. lanatus	na	na	na	na	na
	C. amarus	na	na	na	na	na
M. enterolobii	*S. lycopersicum*	5 ± 0.8 A	26 ± 3.1 A	131 ± 6.7 A	14 ± 1.9 A B	70 ± 7.8 A
	C. sativus	9 ± 0.9 A	20 ± 1.7 A *	181 ± 8.3 A *	12 ± 1.8 B *	114 ± 23.1 A *
	C. metuliferus	5 ± 0.8 A	7 ± 1.5 A	33 ± 5.6 B	2 ± 0.6 A	12 ± 2.0 A
	C. lanatus	5 ± 0.7 A	17 ± 2.8 A *	79 ± 10.7 A * †	40 ± 13.8 A * †	170 ± 32.8 A * †
	C. amarus	6 ± 1.7 A	5 ± 0.4 A	28 ± 3.2 A	3 ± 0.4 A	20 ± 3.0 A
M. luci	*S. lycopersicum*	4 ± 0.4 A	30 ± 5.2 A	138 ± 31.2 A	19 ± 4.7 A	87 ± 24.1 A B
	C. sativus	6 ± 0.4 A	16 ± 2.1 A †	89 ± 14.7 B	33 ± 5.5 A * †	181 ± 29.6 A * †
	C. metuliferus	9 ± 0.8 A	9± 1.4 A	59 ± 7.3 A	3 ± 0.8 A	15 ± 2.6 A
	C. lanatus	5 ± 0.5 A	22 ± 2.9 A *	112 ± 8.7 A *	12 ± 1.9 B *	65 ± 9.8 B *
	C. amarus	5 ± 0.7 A	7 ± 0.3 A	35 ± 3.3 A	5 ± 0.2 A	22 ± 1.8 A

[a] Data are means ± standard errors for five replicates. Data in the same column followed by different letters are significantly different ($P < 0.05$) between root-knot nematode (RKN) isolates by a given plant germplasm, according to Dunn's test. Data in each column and for each RKN isolate followed by * are significantly different ($P < 0.05$) between germplasms of the same genus. † indicates differences ($P < 0.05$) between *Solanum lycopersicum* and *Cucumis sativus* or *Citrullus lanatus*, according to Student's t or Mann-Whitney tests. na = No available data because no infection was observed.

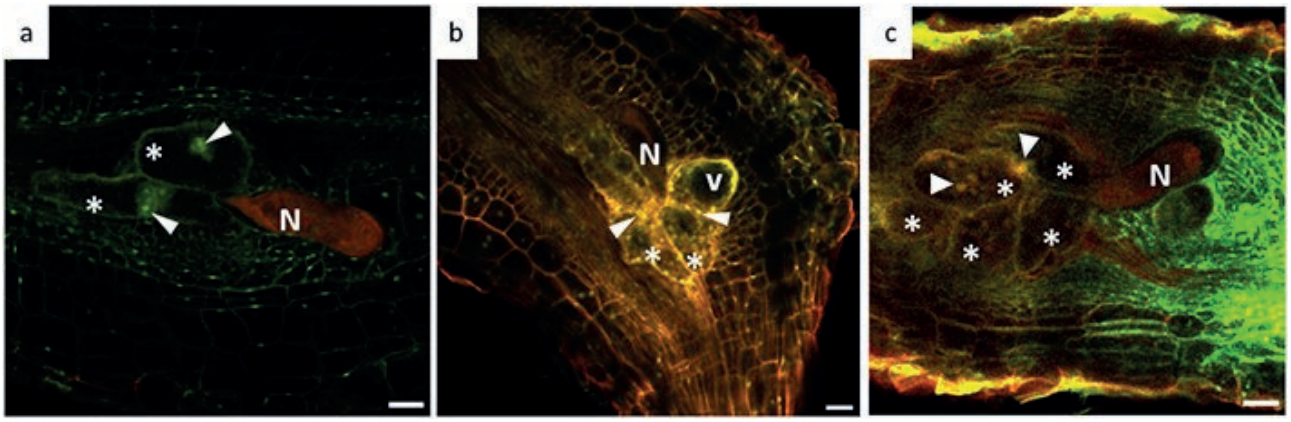

Figure 1. Laser scanning confocal microscope images of the infection sites of *Meloidogyne chitwoodi* (a), *Meloidogyne enterolobii* (b) and *Meloidogyne luci* (c), 15 dafter inoculation, in *Solanum lycopersicum* 'Coração-de-Boi'. Nematode (N); vacuoles (v); giant cells (asterisks); and some nuclei (white arrowheads) are indicated. Scale bars = 50 μm.

feeding site were 2.9 and 5.5 times greater ($P < 0.05$) in cucumber than in *C. metuliferus* (Table 2). Similar results were observed in watermelon. Although the nematodes induced similar ($P > 0.05$) numbers of GCs per feeding site in both *Citrullus* spp., the volumes per GC were 13.3 greater in *C. lanatus* and 8.5 times greater ($P < 0.05$) than in *C. amarus*. The numbers of nuclei per GC were 3.4 greater, and per feeding site were 2.8 greater ($P < 0.05$).

Meloidogyne luci induced a similar ($P > 0.05$) numbers of GCs in *C. metuliferus* and cucumber, but the GC volumes in *C. metuliferus* were 11 times less ($P < 0.05$) than in cucumber, resulting in a 12.1-fold reduction (*P*

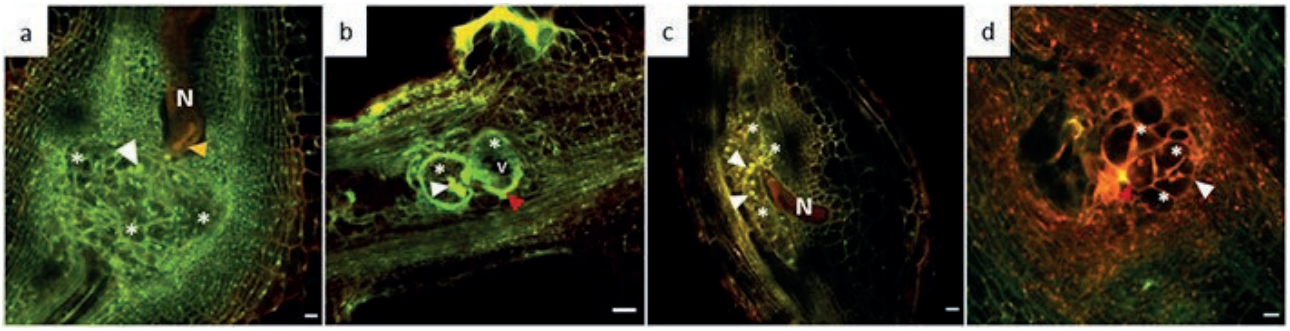

Figure 2. Laser scanning confocal microscope images of infection sites of *Meloidogyne enterolobii*, 15 d after inoculation, in *Cucumis sativus* 'Dacher II' (a), *Cucumis metuliferus* BGV11135 (b), *Citrullus lanatus* 'Sugar Baby' (c) or *Citrullus amarus* BGV5167 (d). Nematodes (N); vacuoles (v); giant cells (asterisks); some nuclei (white arrowheads); necrosed areas (red arrowheads); and a nematode oesophageal median bulb (yellow arrowhead) are indicated. Scale bars = 50 µm.

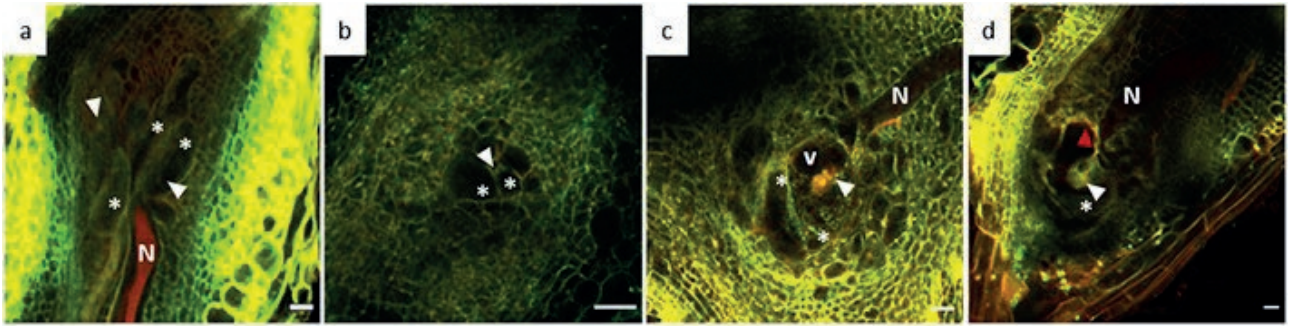

Figure 3. Laser scanning confocal microscope images of infection sites of *Meloidogyne luci* 15 d after inoculation in *Cucumis sativus* 'Dacher II' (a), *Cucumis metuliferus* BGV11135 (b), *Citrullus lanatus* 'Sugar Baby' (c), or *Citrullus amarus* BGV5167 (d). Nematodes (N); giant cells (asterisks); some nuclei (white arrowheads); and necrosed area (red arrowhead) are indicated. Scale bars = 50 µm.

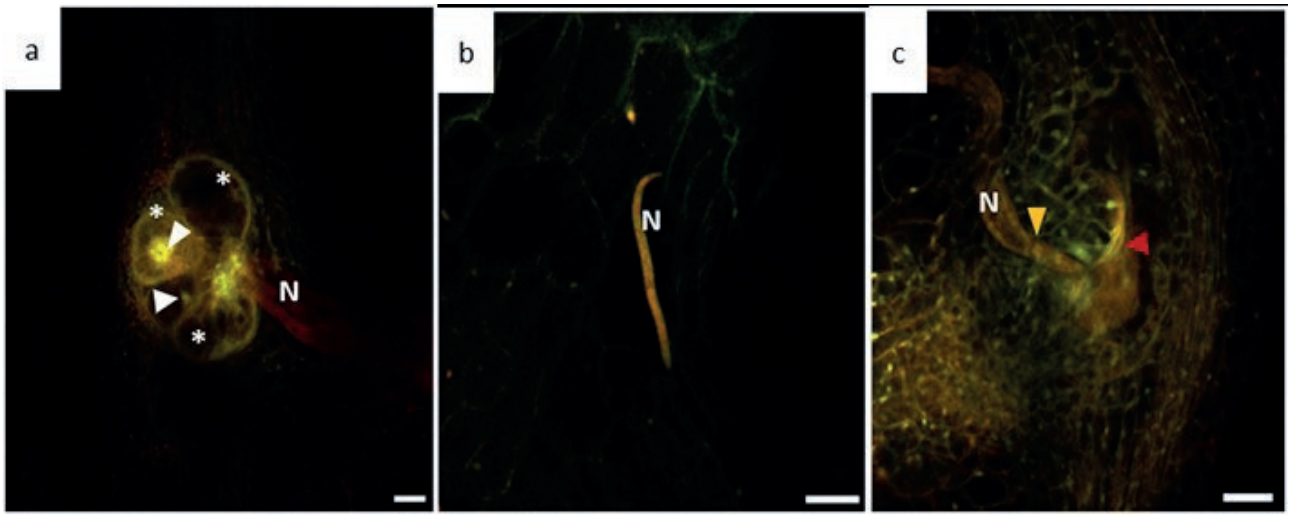

Figure 4. Laser scanning confocal microscope images of *Meloidogyne chitwoodi* infection sites, 15 d after inoculation in the cucumbers *Cucumis sativus* 'Dacher II' (a), *Cucumis metuliferus* BGV11135 (b), watermelon *Citrullus lanatus* 'Sugar Baby' (c), or *Citrullus amarus* BGV5167 (d). Nematodes (N); giant cells (asterisks); some nuclei (white arrowheads); necrosed area (red arrowhead), and an oesophageal median bulb (yellow arrowhead) are indicated. Scale bars = 50 µm.

< 0.05) in total volume of GC per feeding site. However, the numbers of nuclei per GC and per feeding site did not differ ($P > 0.05$) (Table 2). In both *Citrullus* species, *M. luci* induced similar numbers ($P > 0.05$) of GCs, but GC volumes and numbers per feeding site in *C. amarus* were 2.5 and 3 times less ($P < 0.05$) than in in *C. lanatus*. In addition, 3.1 times fewer nuclei per GC ($P < 0.05$) and 3.2 times fewer feeding sites were observed in *C. amarus* than in *C. lanatus*.

The majority of GCs induced by *M. enterolobii* and *M. luci* in *C. metuliferus* and *C. amarus* were almost empty, with few or no nuclei and with some necrotic areas compared to those in the respective susceptible plant germplasm (Figure 2 b and d, Figure 3 b and d).

Of the different RKN isolates, *M. enterolobii* induced formation of GCs that were 3.3 more voluminous ($P < 0.05$) than *M. luci* in *C. lanatus,* which resulted in a total mean GC volume per feeding site that was 2.6 times greater ($P < 0.05$). Nevertheless, no differences ($P > 0.05$) were observed in *C. amarus*. The numbers of nuclei per GC and per feeding site induced by *M. enterolobii* and *M. luci* in both *Citrullus* spp. did not differ ($P > 0.05$), but the numbers of nuclei per feeding site differed ($P < 0.05$) in *Cucumis* spp. (Table 2). Specifically, the number of nuclei per feeding site induced by *M. enterolobii* was 2 times greater in *C. sativus* and 0.56 times greater in *C. metuliferus,* compared to those induced by *M. luci* (Table 2). *Meloidogyne enterolobii* induced the formation of 1.8 times more GC volume ($P < 0.05$) in *S. lycopersicum* than *M. chitwoodi,* resulting in 2.7 more GC volume per feeding site ($P < 0.05$).

DISCUSSION

The main objective of this study was to determine host suitability of *C. metuliferus* BGV11135 and *C. amarus* BGV5167 for the nematodes *M. chitwoodi*, *M. enterolobii* and *M. luci*, to provide insights into the potential use of these rootstocks for melon and watermelon crops, and to provide this information to assist management of RKN species. Previous studies have reported resistance of some *C. metuliferus* accessions to *M. incognita, M. arenaria, M. hapla, M. javanica* and *M. enterolobii* (Walters *et al*., 2006; Ye *et al.,* 2017; Pinheiro *et al.,* 2019), and that of *C. amarus* to *M. arenaria, M. enterolobii, M. incognita* and *M. javanica* (García-Mendívil *et al.,* 2019; Waldo *et al.,* 2023). The present paper is the first report on levels of resistance of *C. metuliferus* and *C. amarus* to *M. chitwoodi* and *M. luci*. In addition, cucumber may be included as a potential plant host of *M. chitwoodi*, because this nematode reproduced in this plant species, as in watermelon which is listed as a plant host (EPPO, 2023b).

The results of the present study have shown that the levels of resistance of *C. metuliferus* ranged from immune (RI = 0) to *M. chitwoodi*, highly resistant (RI < 1%) to resistant (1% ≤ RI < 10%) to *M. enterolobii*, and resistant to *M. luci*. *Citrullus amarus* ranged from resistant to moderately resistant (10% ≤ RI ≤ 25%) to *M. chitwoodi* and *M. enterolobii*, and resistant to *M. luci*.

Several resistance mechanisms of *C. metuliferus* against RKN have been proposed, affecting root penetration, feeding site formation, nematode development, and sex differentiation (Fassuliotis, 1970; Walters *et al.,* 2006). Xie *et al.* (2022) reported the emission of 18 volatiles by the roots of the CM3 accession of *C. metuliferus*, which had repellent effects on *M. incognita*. In the present study, substantial reductions of J2s root penetration of all the RKN isolates were observed, compared to that in cucumber, and only a low proportion of J2 achieved the adult female stage laying eggs (0% for *M. chitwoodi,* 2% for *M. enterolobii* and 1.1% for *M. luci*; averaged over two experiments). Some studies comparing the transcriptome of *C. metuliferus* and cucumber plants inoculated with *M. incognita* have proposed putative resistance mechanisms (Ling *et al.,* 2017; Ye *et al.,* 2017; Li *et al.,* 2021). Ling *et al.* (2017) attributed resistance to differential expression in two host gene clusters related to cytoskeletons and RNA processing. Ye *et al.* (2017) attributed resistance to induction of phenylalanine ammonia-lyase and peroxidase activities after infection together with the expression of genes related to biosynthesis of phenylpropanoids and plant hormone signalling. Li *et al.* (2021) attributed resistance to upregulation of genes related to the Ca^{2+} signalling pathway at early stages of *M. incognita* infection, as well as the salicylic acid and jasmonate signalling pathways. In all these cases, nematode penetration and root infection were reduced, and nematode development was delayed. According to the present study results, the resistance mechanisms of *C. metuliferus* were highly effective against *M. chitwoodi*, because less J2 were able to penetrate, compared to *M. enterolobii* and *M. luci,* and no J2 reached the adult female stage. The histopathological analysis showed that *C. metuliferus* was not infected at 15 d after *M. chitwoodi* inoculation, and those that infected cucumber plants produced less voluminous GCs with a low numbers of nuclei per GC and per feeding site than did the other studied RKN species. For *M. enterolobii* and *M. luci,* reductions in nematode infection and reproduction were detected in *C. metuliferus* in comparison with cucumber, but J2, which were able to infect, to develop until the female stage and reproduce,

produced a similar number of eggs per egg mass than in cucumber (except for *M. enterolobii* in the second experiment). However, a reduction in female fertility of *M. incognita* on *C. metuliferus* has been reported previously (Ye *et al.*, 2017; Expósito *et al.,* 2020). This result is important, because it could be an indicator of adaptation of a given percentage of individuals that could reproduce and increase populations after repeated cultivation. The present histopathological study showed some differences from previous studies regarding the *C. metuliferus-M. incognita* relationship (Ye *et al.*, 2017; Expósito *et al.,* 2020), in which fewer nuclei per cell and per feeding site were reported.

Resistance of *C. amarus* to tropical *Meloidogyne* spp. has been attributed to its high root fibrosity in comparison with that of other cucurbits (Thies and Levi, 2007; Thies *et al.*, 2015; García-Mendivil *et al.,* 2019). Waldo *et al.* (2023) suggested that resistance to *M. enterolobii* is modulated by 11 single-nucleotide polymorphisms. Those in the locus QTL 3.1 influence root galling and egg mass formation, while those in QTL 4.1, 4.2, and 8.1 are associated with nematode egg production. In the present study, compared with those of watermelon, J2 root penetration of all the RKN isolates was reduced, and only a low proportion of J2 achieved the adult female stage laying eggs: 1.4% for *M. chitwoodi,* 10.5% for *M. enterolobii*, and 1.1% for *M. luci* (averaged for the two experiments). Watermelon is considered a poor host for the tropical *Meloidogyne* spp. due to their reduced reproduction rates (López-Gómez *et al.*, 2014), but is a main host for *M. enterolobii* (EPPO, 2023b). This was observed in the present study, achieving levels of reproduction close to those in tomato. However, *M. enterolobii* reproduction in *C. amarus* reached 9.45% of that observed on watermelons, defining the *C. amarus* rootstock as an effective tool for managing this RKN.

Histopathological analyses revealed that neither *C. lanatus* nor *C. amarus* were infected by *M. chitwoodi* 15 d after inoculations. Reductions in the numbers of nuclei and GC volumes were observed in the combinations of remaining RKN-isolates in *C. amarus* compared with watermelon, which may affect nematode development and reproduction.

The results from the present study will provide valuable information for farmers to facilitate decision-making for implementing integrated RKN control strategies, including scenarios with a co-occurrence of RKN species and/or virulent nematode populations to specific host resistant genes. Resistance of these plant species to tropical RKN species in pot and field experiments (Ye *et al.,* 2017; García-Mendívil *et al.,* 2019), and the effectiveness for managing virulent RKN populations to the *Mi1.2* resistance gene in tomato (Expósito *et al.,* 2018; Fullana *et al.,* 2023) have been demonstrated. In addition, several accessions of *C. metuliferus* and *C. amarus* are resistant to other pathogens and diseases, such as *Fusarium oxysporum*, gummy stem blight, powdery mildew, and potyvirus (Gusmini *et al.*, 2005; Guner *et al.*, 2008; Tetteh *et al.*, 2010; Keinath *et al.*, 2019). These characteristics enhance agronomic value of these plant germoplasm. The strategic use of these rootstocks in rotations with other resistant plant germplasms can alleviate the impacts of RKN on crop yield and contribute to reducing reliance on pesticides, as has been previously reported (Expósito *et al.*, 2018; Fullana *et al.*, 2023).

ACKNOWLEDGMENTS

The UPC authors acknowledge funding from the R+D+i project AGL2017-89785-R, financed by MCIN/AEI/10.13039/501100011033 and by the FEDER and FSE (PRE2018-084265, Aïda Magdalena Fullana). In UC, this research was supported by FEDER funds through the Portugal 2020 (PT 2020), COMPETE 2020 and by the Portuguese Foundation for Science and Technology (FCT), under contracts UIDB/00102/2020, UIDP/00102/2020 (CERES), and UIDB/04004/2020 (DOI identifier 10.54499/UIDB/04004/2020), UIDP/04004/2020 (DOI identifier 10.54499/UIDP/04004/2020) (CFE); and by 'Instituto do Ambiente, Tecnologia e Vida'. Duarte Santos is funded by FCT through the grant SFRH/BD/146196/2019. The authors are also grateful to the Institut de Conservació i Millora de l'Agrodiversitat Valenciana from Universitat Politècnica de Valencia (COMAV-UPV) for providing seeds of *Cucumis metuliferus* BGV11135 and *Citrullus amarus* BGV5167. Dr Teresa Rodrigues, iLAB – Microscopy and Bioimaging Lab, a facility of the Faculty of Medicine of University of Coimbra and a member of the national infrastructure PPBI-Portuguese Platform of BioImaging (POCI-01-0145-FEDER-022122) and supported by FSE CENTRO-04-3559-FSE-000142, gave technical support with the laser scanning confocal microscopy. The NEMATO-lab members are also acknowledged for their technical laboratory assistance.

LITERATURE CITED

Aydinli G., Kurtar E.S., Mennan S., 2019. Screening of *Cucurbita maxima* and *Cucurbita moschata* genotypes for resistance against *Meloidogyne arenaria*, *M. incognita*, *M. javanica*, and *M. luci*. *Journal of Nema-*

tology 51: 2019–2057. https://doi.org/10.21307/jofnem-2019-057

Bent E., Loffredo A., McKenry M.V., Becker J.O., Borneman J., 2008. Detection and investigation of soil biological activity against *Meloidogyne incognita*. *Journal of Nematology* 40(2): 109–118.

Brown C.R., Mojtahedi H., Santo G.S., Williamson V.M., 1997. Effect of the *Mi* gene in tomato on reproductive factors of *Meloidogyne chitwoodi* and *M. hapla*. *Journal of Nematology* 29(3): 416-419.

Castagnone-Sereno P., 2012. *Meloidogyne enterolobii* (= *M. mayaguensis*): profile of an emerging, highly pathogenic, root-knot nematode species. *Nematology* 14(2): 133–138. https://doi.org/10.1163/156854111X601650

Elling A.A., 2013. Major emerging problems with minor *Meloidogyne species*. *Phytopathology* 103: 1092–1102. https://doi.org/10.1094/PHYTO-01-13-0019-RVW

EPPO, 2016. PM 7/41 (3) *Meloidogyne chitwoodi* and *Meloidogyne fallax*. *Bulletin OEPP/EPPO* 46(2): 171–189.

EPPO, 2017. EPPO Alert List: Addition of *Meloidogyne luci* together with *M. ethiopica*. EPPO Reporting Service, 2017/2018. Available at: https://gd.eppo.int/reporting/article-6186. Accessed August 05, 2023

EPPO, 2023a. EPPO Alert List 2013-10. Available at: https://www.eppo.int/ACTIVITIES/plant_quarantine/alert_list. Accessed November 03, 2023

EPPO, 2023b. *Meloidogyne chitwoodi.* EPPO global database. Available at: https://gd.eppo.int/taxon/MELGCH Accessed November 03, 2023

EPPO, 2023c. *Meloidogyne enterolobii*. EPPO global database. Available at: https://gd.eppo.int/taxon/MELGMY Accessed August 05, 2023

EPPO, 2023d. *Meloidogyne luci*. EPPO global database. Available at: https://gd.eppo.int/taxon/MELGLC Accessed August 05, 2023

Expósito A., Munera M., Giné A., López-Gómez M., Cáceres A., … Sorribas F.J., 2018. *Cucumis metuliferus* is resistant to root-knot nematode *Mi1.2* gene (a)virulent isolates and a promising melon rootstock. *Plant Pathology* 67: 1161–1167. https://doi.org/10.1111/ppa.12815

Expósito A., García S., Giné A., Escudero N., Sorribas F.J., 2019. *Cucumis metuliferus* reduces *Meloidogyne incognita* virulence against the *Mi1.2* resistance gene in a tomato-melon rotation sequence. *Pest Management Science* 75: 1902–1910. https://doi.org/10.1002/ps.5297

Expósito A., Pujolà M., Achaerandio I., Giné A., Escudero N., … Sorribas F.J., 2020. Tomato and melon *Meloidogyne* resistant rootstocks improve crop yield but melon fruit quality is influenced by the cropping season. *Frontiers Plant Science* 11: 560024-14. https://doi.org/10.3389/fpls.2020.560024

Fassuliotis G., 1970. Resistance of *Cucumis* spp. to the root-knot nematode, *Meloidogyne incognita acrita*. *Journal of Nematology* 2: 174–178.

Fullana A.M., Expósito A., Escudero N., Cunquero M., Loza-Alvarez P., … Sorribas F.J., 2023. Crop rotation with *Meloidogyne*-resistant germplasm is useful to manage and revert the (a)virulent populations of Mi1.2 gene and reduce yield losses. *Frontiers Plant Science* 14: 1133095-13. https://doi.org/10.3389/fpls.2023.1133095

García-Mendívil H.A., Munera M., Giné A., Escudero N., Picó M.B., … Sorribas F.J., 2019. Response of two *Citrullus amarus* accessions to isolates of three species of *Meloidogyne* and their graft compatibility with watermelon. *Crop Protection* 119: 208–213. https://doi.org/10.1016/j.cropro.2019.02.005

Giné A., López-Gómez M., Vela M.D., Ornat C., Talavera M., … Sorribas F.J., 2014. Thermal requirements and population dynamics of root-knot nematodes on cucumber and yield losses under protected cultivation. *Plant Pathology* 63(6): 1446–1453. https://doi.org/10.1111/ppa.12217

Guner N., Wehner T.C., Pitrat M., 2008. Overview of potyvirus resistance in watermelon. In: *Proceedings of the IXth EUCARPIA Meeting on Genetics and Breeding of* Cucurbitaceae. (M Pitrat ed.), Institut National de la Recherche Agronomique, Avignon, France, 445–451.

Gusmini G., Song R., Wehner T.C., 2005. New sources of resistance to gummy stem blight in watermelon. *Crop Science* 45(2): 582–588. https://doi.org/10.2135/cropsci2005.0582

Hadisoeganda W.W., Sasser J.N., 1982. Resistance of tomato, bean, southern pea, and garden pea cultivars to root-knot nematodes based on host suitability. *Plant Disease* 66: 145–150.

Hanna H.Y., 2000. Double-cropping muskmelons with nematode-resistant tomatoes increases yield, but mulch color has no effect. *HortScience* 35: 1213–1214. https://doi.org/10.21273/HORTSCI.35.7.1213

Holbrook C.C., Knauf D.A., Dickson D.W., 1983. A technique for screening peanut for resistance to *Meloidogyne incognita*. *Plant Disease* 57: 957–958.

Hussey R.S., Barker K.R., 1973. A comparison of methods of collecting inocula of *Meloidogyne* spp., including a new technique. *Plant Disease Report* 57: 1025–1038.

Jones J.T., Haegeman A.J., Danchin E.G., Gaur H.S., Helder J.K., … Perry R.N., 2013. Top 10 plant-parasitic nematodes in molecular plant pathology.

Molecular Plant Pathology 14: 946–961. https://doi.org/10.1111/mpp.12057

Keinath A.P., Wechter W.P., Rutter W.B., Agudelo P.A., 2019. Cucurbit rootstocks resistant to *Fusarium oxysporum f.* sp. niveum remain resistant when coinfected by *Meloidogyne incognita* in the field. *Plant Disease* 103: 1383–1390. https://doi.org/10.1094/PDIS-10-18-1869-RE

Koutsovoulos G.D., Poullet M., Elashry A., Kozlowski D.K., Sallet E., … Danchin E.G., 2020. Genome assembly and annotation of *Meloidogyne enterolobii*, an emerging parthenogenetic root-knot nematode. *Scientific Data* 7(1): 324. https://doi.org/10.1038/s41597-020-00666-0

Li X., Sun Y., Yang Y., Yang X., Xue W., … Chen S., 2021. Transcriptomic and histological analysis of the response of susceptible and resistant cucumber to *Meloidogyne incognita* infection revealing complex resistance via multiple signalling pathways. *Frontiers Plant Science* 12: 675429-675441. https://doi.org/10.3389/fpls.2021.675429

Ling J., Mao Z., Zhai M., Zeng F., Yang Y., Xie B., 2017. Transcriptome profiling of *Cucumis metuliferus* infected by *Meloidogyne incognita* provides new insights into putative defense regulatory network in Cucurbitaceae. *Scientific Reports* 7: 3544–3559. https://doi.org/10.1038/s41598-017-03563-6

López-Gómez M., Giné A., Vela M.D., Ornat C., Sorribas F.J., … Verdejo-Lucas S., 2014. Damage functions and thermal requirements of *Meloidogyne javanica* and *Meloidogyne incognita* on watermelon. *Annals of Applied Biology* 165(3): 466–473. https://doi.org/10.1111/aab.12154

Maleita C., Cardoso J.M., Rusinque L., Esteves I., Abrantes I., 2021. Species-specific molecular detection of the root knot nematode *Meloidogyne luci*. *Biology* 10*:* 775–788. https://doi.org/10.3390/biology10080775

Maleita C., Correia A., Abrantes I., Esteves I., 2022. Susceptibility of crop plants to the root-knot nematode *Meloidogyne luci*, a threat to agricultural productivity. *Phytopathologia Mediterranea* 61: 169–179. doi: 10.36253/phyto-13369

Ornat C., Verdejo-Lucas S., Sorribas F.J., 1997. Effect of the previous crop on population densities of *Meloidogyne javanica* and yield of cucumber. *Nematropica* 27: 85–90.

Pais C.S., Abrantes I., Fernandes M.F.M., Santos M.S.N.A., 1986. Técnica de electroforese aplicada ao estudo das enzimas dos nemátodes-das-galhas-radiculares, *Meloidogyne* spp. *Ciência Biológica Ecology and Systematics* 6: 19–34.

Phan N.T., Waele D., Lorieux M., Xiong L., Bellafiore S., 2018. A hypersensitivity-like response to *Meloidogyne graminicola* in rice (*Oryza sativa*). *Phytopathology* 108(4): 521–528. https://doi.org/10.1094/PHYTO-07-17-0235-R

Pinheiro J.B., Silva G.O.D., Oliveira V.R., Amaro G.B., Morais A.A.D., 2019. Prospection of genetic resistance resources to root-knot nematodes in cucurbit genotypes. *Horticultura Brasiliera* 37: 343–347. https://doi.org/10.1590/S0102-053620190314

Roberts P.A., 2002. Concepts and consequences of resistance. In: *Plant Resistance to Parasitic Nematodes* (J.L. Starr, R. Cook, J. Bridge, ed.), Wallingford, UK: CAB International, 25–41.

Sorribas F.J., Ornat C., Verdejo-Lucas S., Galeano M., Valero J., 2005. Effectiveness and profitability of the Mi-resistant tomatoes to control root-knot nematodes. *European Journal of Plant Pathology* 111: 29–38. https://doi.org/10.1007/s10658-004-1982-x

Sorribas F.J., Djian-Caporalino C., Mateille T., 2020. Nematodes. In: *Integrated pest and disease management in greenhouse crops* (M.L. Gullino, R. Albajes, P.C. Nicot, ed.), Springer Cham, Switzerland, 147–174.

Tetteh A.Y., Wehner T.C., Davis A.R., 2010. Identifying resistance to powdery mildew race 2W in the USDA-ARS watermelon germplasm collection. *Crop Science* 50(3): 933-939. https://doi.org/10.2135/cropsci2009.03.0135

Thies J.A., Levi A., 2007. Characterization of watermelon (*Citrullus lanatus* var. citroides) germplasm for resistance to root-knot nematodes. *HortScience* 42(7): 1530–1533. https://doi.org/10.21273/HORTSCI.42.7.1530

Thies J.A., Ariss J.J., Hassell R.L., Buckner S., Levi A., 2015. Accessions of *Citrullus lanatus* var. citroides are valuable rootstocks for grafted watermelon in fields infested with root-knot nematodes. *HortScience* 50: 4–8. https://doi.org/10.21273/HORTSCI.50.1.4

Waldo B.D., Branham S.E., Levi A., Wechter W.P., Rutter W.B., 2023. Distinct Genomic Loci Underlie Quantitative Resistance to *Meloidogyne enterolobii* Galling and Reproduction in *Citrullus amarus*. *Plant Disease* 107(7): 2126–2132. https://doi.org/10.1094/PDIS-09-22-2228-RE

Walters S.A., Wehner T.C., Daykin M.E., Barker K.R., 2006. Penetration rates of root-knot nematodes into *Cucumis sativus* and *C. metuliferus* roots and subsequent histological changes. *Nematropica* 36: 231–242.

Xie X., Ling J., Mao Z., Li Y., Zhao J., … Xie B., 2022. Negative regulation of root-knot nematode parasitic behavior by root-derived volatiles of wild relatives of

Cucumis metuliferus CM3. *Horticulture Research* 9: uhac051. https://doi.org/10.1093/hr/uhac051

Ye D.Y., Qi Y.H., Cao S.F., Wei B.Q., Zhang H.S., 2017. Histopathology combined with transcriptome analyses reveals the mechanism of resistance to *Meloidogyne incognita* in *Cucumis metuliferus*. *Journal of Plant Physiology* 212: 115–124. https://doi.org/10.1016/j.jplph.2017.02.002

Phytopathologia Mediterranea
The international journal of the
Mediterranean Phytopathological Union

Firenze University Press
www.fupress.com/pm

Research Papers

Grapevine pruning strategy affects trunk disease symptoms, wood pathobiome and mycobiome

Leticia MEZA[1,†], Elizabeth DEYETT[1,†], Jessica VALLANCE[2], Lucille GENDRE[4], Jadran F. GARCIA[3], Dario CANTU[3], Patrice REY[4], Pascal LECOMTE[2,*], Philippe E. ROLSHAUSEN[1,*]

[1] *Department of Botany and Plant Sciences, University of California, Riverside, 92521, U.S.A.*
[2] *INRAE, UMR 1065 SAVE, Université de Bordeaux, ISVV, CS20032, 33882 Villenave d'Ornon, France*
[3] *Department of Viticulture and Enology, University of California, Davis, CA, U.S.A.*
[4] *Bordeaux Sciences Agro, UMR 1065 SAVE, Université de Bordeaux, ISVV, CS20032, 33882 Villenave d'Ornon, France*
*Corresponding authors. E-mail: pascal.lecomte210@orange.fr; philrols@ucr.edu
[†]These authors contributed equally.

Summary. Vine training and pruning are cultural strategies that can be deployed to manage grapevine trunk diseases (GTDs). Forty-year-old commercial vineyards in the Cognac region, France, trained to either Guyot-Arcure (severe pruning) or Guyot-Poussard (minimal pruning), were studied to determine how the two systems affected trunk disease symptomatology. Effects of pruning practices on the pathobiome and mycobiome of asymptomatic grapevines were also assessed, using culture- and amplicon-based Illumina sequencing approaches. The hypothesis examined was that severe pruning of Guyot-Arcure increases trunk diseases incidence and severity, and causes higher pathogen load and microbial diversity, compared to Guyot-Poussard. Numbers of symptomatic and asymptomatic vines for the two training systems were recorded over 3 years, including numbers of vines with esca foliar symptoms, and partially unproductive and dead vines. Six asymptomatic vines from each pruning method were selected, and culturing and sequencing data were obtained from 27 samples per vine. Fungi in the *Phaeomoniellaceae*, *Togniniaceae*, and *Botryosphaeriaceae* were the most frequently identified. The data indicated that severe pruning increased risk of pathogen infections, with *Phaeomoniella chlamydospora*, *Phaeoacremonium minimum* and *Diplodia* sp. being the most commonly identified fungi. Greater numbers of dead or dying vines were recorded in the severely pruned vineyard, indicating that this strategy shortens vine longevity. Results also showed that severe pruning increased endophytic microbial diversity, and that the pruning methods influenced mycobiome community composition. This knowledge will improve recommendations to growers for practical and cost-effective ways to manage GTDs.

Keywords. Botryosphaeria canker, esca, disease management, microbiome.

OPEN ACCESS

Citation: L. Meza, E. Deyett, J. Vallance, L. Gendre, J.F. Garcia, D. Cantu, P. Rey, P. Lecomte, P.E. Rolshausen (2024) Grapevine pruning strategy affects trunk disease symptoms, wood pathobiome and mycobiome. *Phytopathologia Mediterranea* 63(1): 91-102. doi: 10.36253/phyto-14778

Accepted: March 4, 2024

Published: April 29, 2024

Data Availability Statement: All relevant data are within the paper and its Supporting Information files.

Competing Interests: The Author(s) declare(s) no conflict of interest.

Editor: Vladimiro Guarnaccia, DiSAFA - University of Torino, Italy.

ORCID:
LM: 0000-0003-3855-1302
ED: 0000-0001-6625-6381
JV: 0000-0002-5581-4453
JFG: 0000-0002-5883-4820
DC: 0000-0002-4858-1508
PR: 0000-0002-7250-0114
PL: 0000-0002-0479-0295
PER: 0000-0002-6202-680X

INTRODUCTION

Grapevines are cultivated for their fresh fruit, dried fruit, wine, and other spirits, producing more than 77 million tons annually and providing US$ 68 billion production value (Alston *et al.,* 2019; Casolani *et al.,* 2022). Grapevine Trunk Diseases (GTDs) are a significant impediment to grape production worldwide (Bois *et al.,* 2017; Gramaje *et al.,* 2018). GTDs are caused by a complex of taxonomically unrelated fungal pathogens, and vines are often affected by mixed infections of fungi (Bertsch *et al.,* 2013; Gramaje *et al.,* 2018).

Esca, Botryosphaeria canker and Eutypa dieback are among the main GTDs that affect vineyard longevity, yield of productive vines, and quality of the fruit (Kaplan *et al.,* 2016; Gispert *et al.,* 2020; Larach *et al.,* 2020; Dewasme *et al.,* 2022). *Eutypa lata* (*Diatrypaceae*) is the main causal agent of Eutypa dieback, and several taxa in the *Botryosphaeriaceae* cause Botryosphaeria canker. Both diseases have symptoms of brown to black sectorial necroses in grapevine wood, and Eutypa dieback also develop symptoms of shoot and leaf dwarfing (Rolshausen *et al*., 2006; Úrbez-Torres, 2011; Travadon *et al*., 2012; Bertsch *et al*., 2013). The *Ascomycota* fungi *Phaeomoniella chlamydospora* and *Phaeoacremonium minimum* (formerly *P. aleophilum*), and *Basidiomycota Fomitiporia mediterranea* are among the major causal agents of esca. Esca wood symptoms include black spots in trunk cross-sections and streaking in longitudinal sections but can be surrounded by pink to brown wood discolorations, and in older vines, white rot is also common. Foliar symptoms associated with esca include tiger stripe leaf patterns, wilting, and apoplexy, ranging from a few leaves to the entire vine canopies (Mugnai *et al.,* 1999; Surico, 2009; Lecomte *et al.,* 2012; Lecomte *et al.,* 2018).

Among all GTDs, the esca complex is a serious threat to grape production. A survey of European and Mediterranean vineyards by Guerin-Dubrana *et al.* (2019) indicated that esca symptoms were the most common. Wood dieback symptoms caused by Eutypa and Botryosphaeria were less frequently recorded, although incidence of Botryosphaeria canker was reported to be increasing in several countries. In France, the National Grapevine Trunk Disease Survey reported that GTDs incidence increased nationally from 3 to 13% between 2003 and 2013, with esca being the most-widespread, whereas other GTDs such as Eutypa dieback were more region-specific (Fussler *et al.,* 2008; Bruez *et al.,* 2013; Lecomte *et al.,* 2018). Esca foliar symptom expression has been shown to be erratic, linked to different amounts of annual rainfall, particularly in late spring to early summer (Calzarano *et al.,* 2018; Kraus *et al.,* 2019; Dewasme *et al.,* 2022). Recent studies that have deployed high throughput gene sequencing methods to profile the mycobiome in symptomatic and asymptomatic esca-affected grapevines have also identified the causal agents of Eutypa dieback and Botryosphaeria canker (Bruez *et al.,* 2014; Del Frari *et al.,* 2019). Co-occurrence of these pathogens in the woody tissues could also affect esca symptom expression and may explain inconsistencies of annual observations of foliar disease symptoms.

Grapevine wounds are the main entry points for GTD pathogens, so grapevines are especially susceptible to GTD infections during pruning. Wound susceptibility mainly depends on the time of pruning and the period between pruning and infection events (Munkvold and Marois, 1995). Temperature and rainfall influence wound healing processes, and the period vine susceptibility, as well as the quality and quantity of pathogen inoculum (Eskalen *et al.,* 2007; Martinez-Diz *et al.,* 2020). There are no effective curative methods or treatments for GTDs. These diseases are mainly managed using preventative strategies, among which fungicide applications to protect pruning wounds have been the most effective (Rolshausen *et al.,* 2010). Although removal of infected wood ("curettage") has been shown to reduce foliar and fruit symptoms of esca (Cholet *et al.,* 2021; Pacetti *et al.,* 2021). Growers often start protecting pruning wounds with the appearance of first GTD symptoms, when it is too late for effective disease control. Pruning wound treatment practices must be used early at vineyard establishment to provide yield benefits (Kaplan *et al.,* 2016; Gispert *et al.,* 2020; Di Marco *et al.,* 2022). The banning of sodium arsenite in Europe, that was long registered for protecting grapevine pruning wounds, left growers with no alternatives, and likely resulted in an increased of GTDs incidence (Bruez *et al.,* 2021). Many growers do not protect pruning wounds, due to costs and lack of immediate visible benefits of fungicide applications because of the long incubation period from pathogen infection to symptoms appearance (Hillis *et al.,* 2017). Implementing alternative disease prevention strategies that are affordable and time efficient would provide large benefits to viticulture industries.

Vine training and pruning have been studied as a strategy to reduce GTDs. Pruning objectives balance vine productivity with fruit quality. Attaining this balance while reducing the number and size of pruning wounds would minimize the point of entry for vascular GTD pathogens. The 'Vertical Shoot Positioned' (VSP) system that has been broadly and internationally adopted is an intensive pruning system that is more conducive to GTDs compared to minimal pruning (Gu *et al.,* 2005; Travadon *et al.,* 2016; Kraus *et al.,* 2019; Kraus *et*

al., 2022). There are different types of VSP training systems; the 'Guyot-Poussard' system, similar to cordon pruning, trains long mature arms with few large cuts close to main trunks, and can reduce esca (Lafon, 1921). In contrast, the 'Guyot-Simple' system, similar to cane-pruned vines, trains one spur on each side of each vine, and creates large cuts close to the trunk head. This system was described to be conducive of GTDs (Lecomte *et al.,* 2018). Following a survey of French vineyards, Lecomte *et al.* (2018) noted that vine training forms with longs arms (cordons) decline less rapidly than short arm training forms. However, those observations were not supported with studies in the United States of America (Gu *et al.,* 2005) and Australia (Henderson *et al.,* 2021), that measured less Eutypa dieback incidence and severity in cane-pruned vineyards than in cordon-pruned vineyards. Henderson *et al.* (2021) concluded that the spur pruning resulted in wounds that were smaller than those made by cane pruning, but the larger number of cuts made per vine resulted in greater wound area per vine. Thus, limiting the total surface wound area per vine should be taken into account when pruning vines to limit GTDs incidence. While all these comparative studies of pruning strategies have measured disease incidence and severity, only a few have attempted to assess how the strategies affected microbial community diversity and composition of grapevine wood endospheres (Travadon *et al.,* 2016; Kraus *et al.,* 2022).

The research reported here included a comparative analysis of the Guyot-Arcure and Guyot-Poussard pruning strategies that are used in most of the Cognac vineyards of France. The aim was to evaluate, over a 3-year period in a mature (> 40-year-old) commercial vineyard, the effects of vine pruning on trunk disease symptomatology, including foliar and wood symptoms and vine death. In addition, effects of these two pruning practices on vine pathobiome and mycobiome were assessed, using culture-based and amplicon-based Illumina sequencing approaches. The research hypothesis was that the severe Guyot-Arcure pruning increases disease severity and incidence and provides a gateway for increased pathogen load and microbial diversity compared to Guyot-Poussard pruning. The information generated from this study will provide knowledge for recommendations to growers on practical ways to prevent GTDs.

MATERIALS AND METHODS

Vineyard characteristics.

Two adjacent vineyards with contrasting training systems were selected. They were located near Cognac in the Charente region of southwestern France (Table 1). The vineyards of 'Ugni Blanc' on 101-14 (41B) rootstock were planted in 1972 and 1973, and one was trained as 'Guyot-Arcure' and one as 'Guyot-Poussard' (see Supplemental Figure 1A). The Guyot-Poussard training system consists of horizontal cordons with few small-to-medium-sized pruning wounds primarily concentrated at the top of the cordons, allowing permanent bilateral flow of sap in the lower vasculature of the vine cordons. In contrast, the 'Guyot-Arcure' training system consists of V-shaped cordons that are often renewed and restored, a system that requires extensive pruning. The positions of pruning wounds is not controlled, and can disrupt consistent sap flow that can lead to changes in sap routes (Lafon, 1921). The two vineyards were surveyed during 3 years from 2018-2020, and numbers of asymptomatic and symptomatic vines (foliar and wood symptoms) were recorded, as well as the numbers of dead vines. Direct comparisons between the grapevine training systems and incidence of symptomatic *versus* asymptomatic trunk diseases were assessed using Chi-square statistical

Table 1. Vine training systems (Arcure or Poussard) impact on mean grapevine trunk disease incidence and severity in three survey years.

Vineyard training System	Survey year	Percent asymptomatic vines	Mean percent symptomatic vines			
			Vines with esca foliar symptoms[c]	Partially unproductive Vines[d]	Unproductive Vines[e]	Total
Arcure[a]	2018	42.5	1.6	14.7	41.3	57.5
	2019	40.1	1.2	17.8	40.9	59.9
	2020	38.7	2.9	16.2	42.1	61.3
Poussard[b]	2018	70.4	0.7	14.9	14	29.6
	2019	66.9	0.4	18.6	14	33.1
	2020	65.9	1.7	17.9	14.5	34.1

[a] 511 total vines; [b] 692 total vines; [c] No other foliar symptoms (e.g., Eutypa) recorded; [d] re-trained vines, one arm missing, one dead-arm; [e] dead or missing.

analyses. Twelve asymptomatic vines (six of each training type), were selected for further assessment. Whole vines were uprooted during the dormant season, were numbered, and were then stored in a cold room (4°C) while awaiting processing. All vines were processed (using image analysis, tissue culturing and DNA extraction from woody tissues) within 2 weeks following sampling from the vineyards.

Image analysis of wood decay

All 12 asymptomatic vines from the two pruning methods were cut longitudinally with an upright electric chainsaw. When needed, the trunk and cordons of each vine were sectioned into smaller pieces to ensure that all wood sections were cut in the middle. All the sections were photographed using a NIKON D 3100 digital camera. The proportions (%) of necrotic surface were then evaluated from these photos using the Image J software Fiji version 2.14.0 (Schindelin *et al.,* 2012), by calculating the ratio of the areas of necroses to those of the total cross section areas (Supplementary Figure 2). To do this, each image was cleaned of impurities (e.g., markings made by the saw used to make longitudinal cuts), and the image was scaled to 5 mm. To crop each image from the background, each wood piece was manually traced, and this procedure was replicated three times for accuracy. Thereafter, a threshold for the necrotic regions was created (shown in red in Supplementary Figure 2), and additional tracing of necrosis on the wood was carried out manually as required. A binary image was then created, resulting in black background and white for necrotic tissue, and this was used to calculate proportions (%) necrosis by dividing the necrotic area by the total area of the wood section. The percentage of the necrotic area was calculated for each trunk and both arms separately, then the arms and trunk were averaged. Analysis of the distribution of values was then carried out using nonparametric Kruskal-Wallis tests, with using R software version 2.8.0 (Fox, 2005).

Grapevine processing

For each of the 12 asymptomatic grapevines, a total of 27 samples were collected that consisted of nine samples per cordon and trunk (Supplementary Figure 1B). The lengths of the trunk and the arms were measured, and then sampled at 20%, 50%, and 80% of the length of the cordons or trunk. For each spatial location, wood samples were collected from the top and bottom sections of the cordon, from approx. 1 cm beneath the bark and from the middle section of the heartwood. Similarly, wood samples were collected from the left and right sides of the trunk from approx. 1 cm beneath the bark, and from the center of the heartwood. All samples were collected with wood chisel treated between each cut with 70% ethanol and heat. For each sample, approximately 2 g of wood was collected for molecular and microbiological studies. Samples for molecular assessments were flash-frozen in liquid nitrogen and stored at -20°C, and samples for microbiological assessments were processed within the same day.

Culture-dependent analyses

Wood samples (≈ 3 × 5 × 2 mm) from all 27 sampling points on each vine were disinfected (15 sec in 3% calcium hypochlorite), and were then rinsed with twice in sterile water, and dried on sterile filter paper. For each sample, the wood fragments were placed on a malt extract agar (MEA; 20 g L^{-1} malt extract and 15 g L^{-1} agar) (five fragments per Petri dish), and the dishes were incubated at room temperature. Fungal development was then observed over a six-week period. Taxonomic classification of resulting fungi was carried out at the family level based on culture and morphological characteristics for *Botryosphaeriaceae* (Phillips *et al.*, 2013), *Diaporthaceae* (van Niekerk *et al.*, 2005), *Diatrypaceae* (Trouillas *et al.*, 2010), *Nectriaceae* (Chaverri *et al.*, 2011; Grafenhan *et al.,* 2011), *Phaeomoniellaceae* (Chen *et al.*, 2022), *Togniniaceae* (Gramaje *et al.*, 2015), or the *Basidiomycota Fomitiporia mediterranea* (Fischer *et al.*, 2005). The Identity of *Phaeoacremonium minimum* (*Togniniaceae*) and *Phaeomoniella chlamydospora* (*Phaeomoniellaceae*) was verified by PCR, using primer pairs PalQr [CGTCATCCAAGATGCCGAATAAAG]- PalQf [CGGTGGGGTTTTTACGTCTACAG] for *Pm. minimum* and PchQr [CCATTGTAGCTGTTCCAAGATCAG]- PchQf [CTCTGGTGTGTAAGTTCAATCGACTC] for *Pa. chlamydospora*, targeting the b-tubulin DNA region (Pouzoulet *et al.*, 2013). Presence or absence of each fungal group was recorded for the 27 data points for each assessed vine. The distributions for the numbers of fungal families recovered from the trunk or cordon samples were analyzed by ANOVA tests or nonparametric Kruskal-Wallis tests using the Rcmdr package of the R software version 2.8.0 (Fox, 2005). The statistical tests were carried out according to the vine training system (Arcure vs. Poussard) and were presented separately for trunk and cordons.

Culture-independent analyses

All 27 frozen wood samples from each vine were individually ground to powder with MM300 grinder (Retsch). DNA was extracted from each of the 324 wood samples (27 samples per vine from 12 grapevines), from 60 mg of wood powder, using the Indvisorb Spin Plant Mini Kit (Eurobio), according to the manufacturer's instructions. The purity of the extracted DNA was evaluated with NanoDrop One (Thermo Fisher Scientific), and was quantified with Qubit 2.0 (Thermo Fisher Scientific). Fungal ribosomal ITS regions were amplified using the forward (AAAACTTTCAACAACGGATC) and reverse (TYCCTACCTGATCCGAGGTC) GTAA primers designed by Morales-Crus *et al.* (2018). Each 25-µL PCR reaction mix contained 1 ng of DNA template, Apex 2× Taq DNA Polymerase Master Mix solution (Genesee Scientific), and 0.4 µM of each primer. The PCR program (Veriti thermal cycler, Thermo Fisher Scientific) was as follows: initial denaturation at 95°C for 3 min, followed by 37 cycles each at 95°C for 45 s, 55°C for 1 min, and 72°C for 1 min, and a final extension at 72°C for 10 min. Following PCR, amplicon sizes and uniqueness were verified using gel electrophoresis. The PCR products were cleaned using 1X Ampure XP magnetic beads (Agencourt, Beckman Coulter). DNA concentration was determined for each purified amplicon using Qubit 2.0 (Thermo Fisher Scientific). For high-throughput sequencing, equimolar amounts of all barcoded amplicons were pooled into a single sample, the total concentration of which was determined. Five hundred nanograms of pooled DNA were then end-repaired, A-tailed and single-index adapter ligated (Kapa LTP library prep kit, Kapa Biosystems). After adapter ligation, the library was completed with two consecutive 1X Ampure XP magnetic beads (Agencourt, Beckman Coulter) cleanups. The size distribution of the library was determined with the Bioanalyzer (Agilent Technologies), and was submitted for sequencing in 250-bp paired-end mode on an Illumina MiSeq (UC Davis, Genome Center DNA Technologies Core). The fungal dataset totalled 173 starting samples of the possible 324 (2 pruning types × 6 vines × 27 samples per vine), for downstream computational analyses. The reasons for the missing samples were poor quality or quantity of DNA that was not suitable for Illumina sequencing, or because the PCR yielded no products. The 173 samples included 85 for Arcure pruned vines [Arm20 = 20 samples; Arm50 = 18 samples; Arm80 = 19 samples; Trunk20 = 12 samples; Trunk50 = eight samples; Trunk80 = eight samples], and 88 for Poussard pruned vines [Arm20 = 15 samples; Arm50 = 15 samples; Arm80 = 21 samples; Trunk20 = 12 samples; Trunk50 = 14 samples; Trunk80 = 11 samples]. All sequences were submitted to the National Center for Biotechnology Information Sequence Read Archive, under the bioproject accession number PRJNA1066615.

Computational analyses.

Trimmomatic v 0.39 was used to initially clean the sequencing reads, with a sliding window of 4:19 and a minimum length of 150. The R v4.1.2 software (R Core Team, 2021) was used to carry out perform all computational analyses. Most processing for the reads was done in DADA2 v 1.16.0 (Callahan *et al.,* 2016), including further quality control sequencing filtering, dereplication, chimera identification, merging paired-end reads, and construction of Amplicon Sequence Variant (ASV) tables. Taxonomic identifications were assigned using the UNITE database v 10.5.2021 for fungal taxa. Phyloseq v 1.36.0 (McMurdie and Holmes, 2013) and ggplot2 v3.3.5 packages (Wickham, 2009) were used for much of the graphical and statistical analyses of the data. Unidentified microbes at the kingdom level were removed. Alpha diversity was measured for observed taxa within the communities. Poisson generalized linear modelling with *ad hoc* Tukey tests was used to verify statistical differences among groups. Bar charts were constructed by aggregating taxa at the family and genus levels. Samples were also constructed by tissue compartments, and were transformed to relative abundance. Bray–Curtis dissimilarity was used to calculate the compositional dissimilarities between samples. These dissimilarities were visualized with Non-metric MultiDimenstional Scaling (NMDS) plots using the Vegan package v 2.5-7. The Adonis test was used to determine the statistical significance of beta diversity.

RESULTS

The two vineyard blocks were 45 years old in the first year of the survey and showed high incidence of grapevine trunk diseases that increased in each year of the survey (Table 1). The results demonstrate how the two training systems affected GTDs incidence and severity. Arcure-pruned vines displayed greater percentage ($P < 0.0001$) of vines symptomatic for GTD than for Poussard-pruned vines, for all 3 years of the study, mostly for numbers of dead or dying vines. ImageJ analysis of the ratios of the necrotic areas to areas of total vine wood vine indicated a high percentage (70–80%) of wood decay in the asymptomatic vines, regardless of the training system (Supplementary Table 1). The decay appeared as wood discolourations, ranging from light brown to

dark black in colour with little to no white rot observed in all 12 vines (Supplementary Figures 1 and 2).

The Miseq produced appox. 24 million reads. After trimmomatic (before processing with DADA2) there were 8,672,611 reads across all the 173 starting samples. At the end of DADA2 processing, there were 7,614,009 reads remaining, keeping between 60–98% of reads in each sample through DADA2 processing. No samples had less than 15K reads for analyses. After filtering, a total of 1267 ASVs were recorded from the 173 samples. These results indicated that pruning methods affected microbial diversity richness (Figure 1) and community composition (Figure 2). Alpha diversity plots showed greater observed microbial diversity in trunks of Arcure-pruned vines than in trunks of Poussard-pruned vines [Poisson generalized linear model with Tukey; $P < 0.001$], with trend indicating greatest diversity near the heads of the trunks. In vine arms, microbial diversity differences between the two pruning types were only detected in the sections closest to the trunks (arm 20), with Arcure-pruned vines having the greatest taxa richness. Pruning practice type also affected fungal community composition both in vine arms and trunks (Adonis test $P < 0.001$).

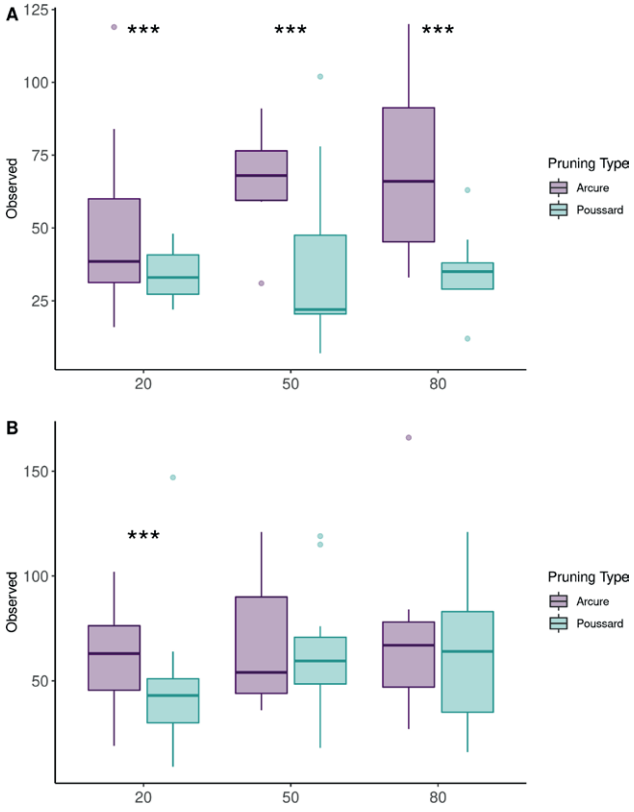

Figure 1. Alpha diversity plots indicating that microbial richness was affected by grapevine pruning practice. Boxplots represent observed diversity at the location on the vine (20%, 50% or 80%) on trunks (A) and arms (B). Statistical significance is indicated for $P < 0.001$ (***), based on Poisson generalized linear models with pairwise Tukey tests. Arcure: Arm20 = 20 samples; Arm50 = 18 samples; Arm80 = 19 samples; Trunk20 = 12 samples; Trunk50 = eight samples; Trunk80 = eight samples. Poussard: Arm20 = 15 samples; Arm50 = 15 samples; Arm80 = 21 samples; Trunk20 = 12 samples; Trunk 50 = 14 samples; Trunk80 = 11 samples.

Taxa bar plots showed that *Phaeomoniella* (*Phaeomoniellaceae*) and *Phaeoacremonium* (*Togniniaceae*) were the two main pathogen taxa infecting the grapevine trunks and arms, regardless of the pruning method. *Phaeomoniella* and *Phaeoacremonium* represented approx. 60% and 12% in relative abundance, respectively (Figure 3; Supplementary Figure 3). The PCR analyses confirmed that the pathogenic species were *Pa. chlamydospora* and *Pm. minimum*. Sequence data also indicated that the pathogen *Diplodia* (*Botryosphaeriaceae*) was also present in all grapevine sampled compartments, representing approx. 2% relative abundance (Figure 3; Supplementary Figure 3). These three families (*Phaeomoniellaceae*, *Togniniaceae*, *Botryosphaeriaceae*) with known pathogenic fungi represented 81.6% in arms and 77.8% in trunks of all the taxonomic groups in severely-pruned vines, compared with 74.4% in arms and 71% in trunks of minimally-pruned vines (See Supplementary Figure 3A). Of those, *Phaeomoniellaceae* had greater abundance in severely pruned vines than in minimally-pruned vines (See Supplementary Figure 3B).

Microbial isolations from the 324 tissue samplings from the 12 grapevines (27 sample per grapevine) confirmed, to some degree, the sequencing data. Recovery proportions were greatest for fungi in the *Phaeomoniellaceae* (44.8% recoveries), *Botryosphaeriaceae* (42.9%) and *Togniniaceae* (31.5%; Figure 4). The fourth most recovered pathogenic group were *Nectriaceae* (13%), but incidences of other pathogenic groups were low (*Diatrypaceae*, 1.2%; *Diaporthaceae*, 0.6%. *Fomitiporia mediterranea* was only isolated from one trunk sample and one arm sample from Arcure-pruned vines. Severely-pruned vines displayed greater incidence of esca-causing fungi (*Pm. minimum* and *Pa. chlamydospora*) in vine arms and trunks in comparison to the minimally-pruned vines (Figure 4). Similarly, *Botryosphaeriaceae* percent recovery was also greater in the trunks of severely- vs minimally-pruned vines, whereas the opposite was true for the vine arms.

DISCUSSION

This study was designed to gain knowledge on effects of two grapevine pruning practices on incidence

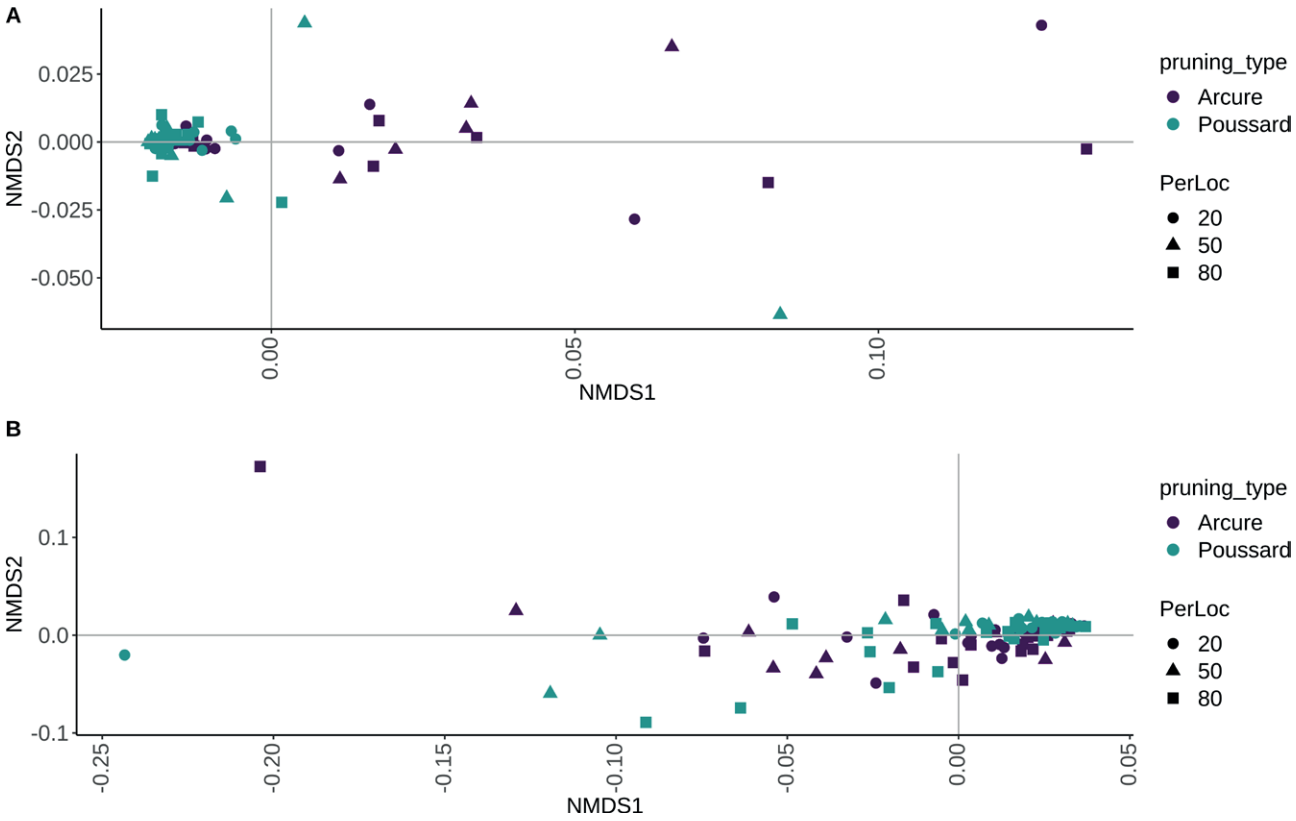

Figure 2. Bray Curtis beta diversity plots indicating that fungal beta diversity was affected by grapevine pruning practice. Each dot represents the fungal community composition of one vine sample. Points are coloured by each pruning type (Arcure vs. Poussard) and shaped for sampling location on each vine (20%, 50% and 80%) on trunks (A) and arms (B). Statistically significant *P* and R^2 values were measured by Adonis permutational multivariate analysis of variance for trunks ($P = 0.001$, $R^2 = 0.15$) or arms ($P = 0.001$, $R^2 = 0.0865$). Arcure: Arms = 57 samples; Trunks = 28 samples. Poussard: Arms = 51 samples; Trunks = 37 samples.

and severity of GTDs. In addition, effects were assessed of these pruning strategies on spatial composition and diversity of the mycobiome and pathobiome in asymptomatic grapevines. Incidence of GTD foliar symptoms in the surveyed vineyards was low for all three years of the study, although the assessed vines showed extensive wood decay, regardless of the pruning strategy applied. Leaf stripe symptoms were observed and were indicative of esca, which was confirmed with culture-dependent and independent diagnoses.

Esca has been identified as the major threat to vineyards across Mediterranean climates (Lecomte *et al.*, 2018; Guerin-Dubrana *et al.*, 2019). Community composition analysis from non-symptomatic vines indicated that GTD pathogens dominated the wood mycobiome, supporting previous data (Geiger *et al.*, 2022). *Phaeomoniella chlamydospora* and *Pm. minimum* were the dominant fungi of the wood mycobiome and pathobiome, with, respectively, 60% and 12% of relative abundance. Profiling of the wood microbiome affected by GTDs and esca using high throughput sequencing showed that *Pa. chlamydospora* is the dominant member in many viticulture areas (Morales-Cruz *et al.*, 2018; Del Frari *et al.*, 2019; Niem *et al.*, 2020; Geiger *et al.*, 2022; Kraus *et al.*, 2022; Vanga *et al.*, 2022). However, *Pm. minimum* was not always the second most prevalent pathogen reported in esca-affected vineyards, as *Fomitiporia mediterranea* was often detected. The GTAA primers that were used in the present study are specific for *Ascomycota* (Morales-Cruz *et al.*, 2018), and will not amplify *Fomitiporia* (*Basidiomycota*). Nonetheless, the presence of white wood rot was not commonly observed in the analysed vines, and *Fomitiporia* isolation was very low. This may explain the low incidence of leaf stripe symptoms observed in the two vineyards. Previous studies (Maher *et al.*, 2012; Pacetti *et al.*, 2021) have shown that incidence leaf stripe symptoms were correlated with presence of white wood rot and abundance of *F. mediterranea*.

Sequencing data indicated that fungi in the *Herpotrichiellaceae* were the third most abundant, and these

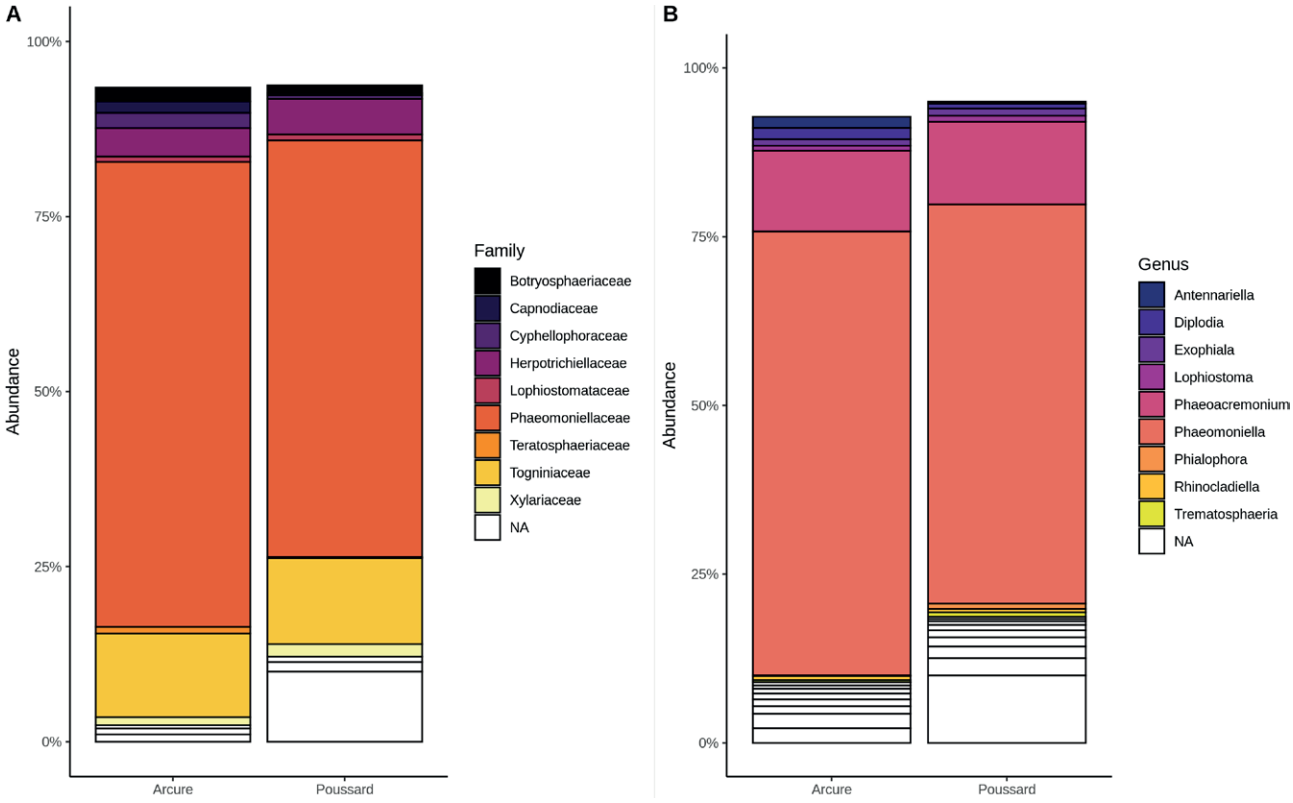

Figure 3. Taxa bar plots showing relative abundance of the top ten fungal families (panel A) and genera (panel B) inhabiting grapevine endospheres for Arcure- (n = 85) and Poussard- (n = 88) trained vines.

fungi have also been reported in other studies (Del Frari *et al.*, 2019; Vanga *et al.*, 2022). However, suspected grapevine pathogens within the *Herpotrichiellaceae* (*Phialophora*; Hawksworth *et al.*, 1976) were not re-isolated from grapevines, possibly due to their slow-growing nature or because other non-pathogenic represented this group. *Botryosphaeriaceae* (*Diplodia*) were the fourth most abundant pathogenic fungi identified, although with disparity between low relative abundance and the high recovery rates from wood samples, because of the rapid growth of these fungi in culture. Fungi within this family cause Botryosphaeria canker in a broad host range and have also been associated with esca in several studies (Bruez *et al.*, 2014; Lecomte *et al.*, 2018; Geiger *et al.*, 2022; Kraus *et al.*, 2022). Several other pathogenic fungi in the *Diatrypaceae* (*Eutypa*), *Diaporthaceae* (*Diaporthe*) and *Nectriaceae* (*Fusarium*) were also identified, but at low incidence and abundance, indicating that these fungi played marginal roles in decline of the surveyed vineyards.

Efficient management of GTDs in vineyards is achieved by early adoption of preventative measures (Kaplan *et al.*, 2016; Gispert *et al.*, 2020). Post-pruning fungicide treatment is the most effective practice, mainly because the causal agents are airborne with free water and infect vines through wounds (Rolshausen *et al.*, 2010). Adjusting the timing of pruning during dry weather conditions when pathogen inoculum is low and/or when periods of wound susceptibility are short during warm temperatures, is also recommended (Munkvold and Marois, 1995; Martinez-Diz *et al.*, 2020). However, those strategies are not always practical because the required weather conditions are not always present at pruning, or in are synchronized with the availability of field labour.

Vine training and pruning practices have been investigated for management of GTDs. Evidence suggests that severe pruning with high numbers of cuts and large wound sizes increases GTD incidence and severity (Gu *et al.*, 2005; Lecomte *et al.*, 2018). Henderson *et al.* (2021) proposed that severity of pruning is best defined by the total surface area of pruning cuts per vine, which is affected both by the number and size of wounds per vine. Incidence of esca (number of symptomatic vines) and severity (extent of wood decay) were reduced after commercial vineyards in Germany and France were con-

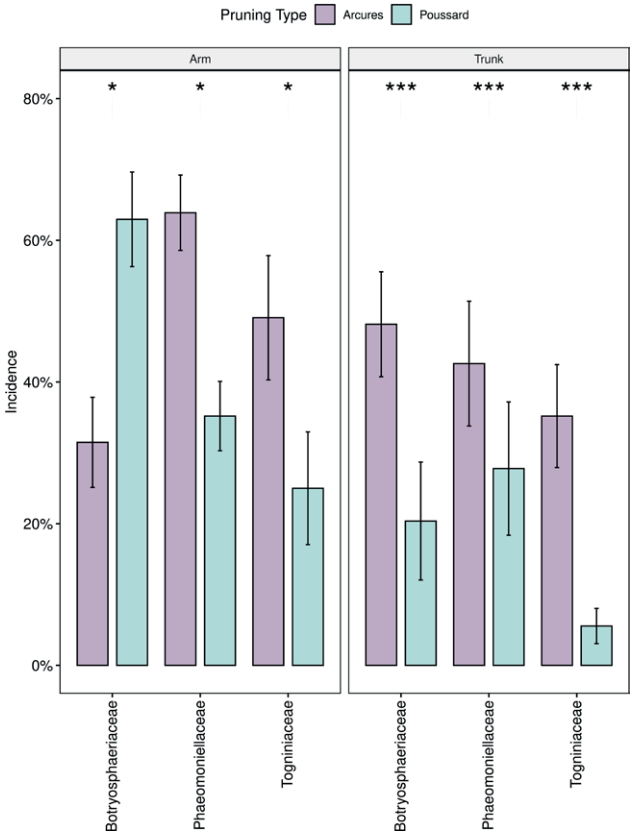

Figure 4. Statistical significant differences in percent recovery for *Phaeomoniellaceae*, *Togniniaceae*, and *Botryosphaeriaceae* fungi between Arcure- and Poussard-pruned grapevines in arms (left panel; six grapevine replicates with two arms per vine and nine data point per arm; n = 108), and trunks (right panel; six grapevine replicates with one trunk per vine and nine data points per trunk; n = 54). Standard errors are shown on the bar graph and statistical *P* values are indicated with asterisks (* P< 0.5; *** P< 0.001).

verted from intensive pruning and training systems (e.g. vertical spur position [VSP]) to minimal pruning (Travadon *et al.*, 2016; Kraus *et al.*, 2019; Kraus *et al.*, 2022). However, improved disease outcomes were only significant when these practices were adopted early in the lives of vineyards (Kraus *et al.*, 2022). Results from the present study were in line with these findings and showed a 45% decrease in vine symptoms and 75% decrease in vine mortality in minimally-pruned grapevines that could be attributed to the reduction of *Pm. minimum* and *Pa. chlamydospora* incidence from vine trunk and arm tissues. *Botryosphaeriaceae* infections were only less present in the vine arms that were severely pruned vines, highlighting the possible contrast in disease etiology for the other two pathogens. However, pruning methods did not affect internal wood decay, with all asymptomatic vines having 70–80% of necrosis in trunks and arms. Differences in the extent of wood decay between pruning practices could perhaps be better observed in younger vines. The Guyot-Poussard pruning has been shown to minimize the interruption of vine sap flow to foliage, whereas Guyot-Arcure pruning interrupts sap routes causing xylem vessel occlusion and loss of physiological function, thereby stressing vines and supporting escapathogen colonization (Lecomte *et al.*, 2018). Together, these results suggest that training methods that decrease wound surface areas per vine, but also pay attention to location of pruning by preserving integrity of continuous sap routes, reduce vine stress. These are factors that minimize the risks of GTDs infections and maximize vineyard lifespans.

The present study has also indicated that the pruning strategy affected fungal community diversity and composition of asymptomatic vines. Two studies, from France (Travadon *et al.*, 2016) and Germany (Kraus *et al.*, 2022), compared minimal pruning with spur pruning, in two cultivars, and both studies yielded inconsistent outcomes on fungal community diversity and composition. It was suggested that fungal abundance and diversity are driven both by cultivar susceptibility to wood-infecting fungi and pruning severity (Travadon *et al.*, 2016). However, in both of these studies, all the vineyards were converted from spur pruning to minimal pruning after several years, which confounded microbial composition analyses. The assemblage of the core endophytic microbiome in perennial wood of grapevines is driven by several factors, including above and below ground wound colonization (Deyett and Rolshausen, 2020; Martinez-Diz *et al.*, 2020). Because pruning methods influence the aboveground endophytic pathobiome it is also likely that it influences the entire host mycobiome, as indicated by the present study. Large-scale sampling from different geographical areas which use contrasting pruning practices will help validate these data.

In conclusion, data from this study support current knowledge that severe pruning increases the risks of GTD pathogen infections and shortens vine longevity and vineyard productivity. Additional comparative studies between intensive and minimal pruning should be carried out over long time periods (years), starting at the vineyard establishment, to increase understanding of the long-term effects of vine training systems on wood endophytic microbiome assembly dynamics and pathobiome profiles. Attention should also be paid to the severity of pruning with respect to wound surface area per vine, and how this affects vine xylem integrity and sap flow routes. This knowledge will improve grower recommendations for practical ways to effectively manage GTDs.

ACKNOWLEDGEMENTS

This study was funded by the 'Industrial chair Gtdfree', a research programme jointly supported by the French National Agency for Research (ANR) and the Hennessy Company (Cognac, France). The study was also locally supported by the Cluster of Excellence COTE (University of Bordeaux). The authors also thank the U.S. National Science Foundation Graduate Research Fellowship Program (grant number DGE-1326120) for supporting Leiticia Meza.

LITERATURE CITED

Alston J., Sambucci O. 2019. Grapes in the word economy. Pages 1-24 in: *The Grape Genome. Springer Cham*, Springer Nature, Switzerland. doi: 10.1007/978-3-030-18601-2

Bertsch C., Ramirez-Suero M., Magnin-Robert M., Larignon P., Chong J., … Fontaine F. 2013. Grapevine trunk diseases: complex and still poorly understood. *Plant Pathology* 62: 243–265.

Bois B., Zito S., Calonnec A. 2017. Climate vs grapevine pests and diseases worldwide : the first results of a global survey. *Oeno One* 51: 133-139.

Bruez E., Lecomte P., Grosman J., Doublet B., Bertsch C., … Rey P. 2013. Overview of grapevine trunk diseases in France in the 2000s. *Phytopathologia Mediterranea* 52: 262–275.

Bruez E., Vallance J., Gerbore J., Lecomte P., Da Costa J. P., … Rey P. 2014. Analyses of the temporal dynamics of fungal communities colonizing the healthy wood tissues of esca leaf-symptomatic and asymptomatic vines. *Plos One* 9.

Bruez E., Larignon P., Bertsch C., Robert-Siegwald G., Lebrun M., … Fontaine F. 2021. Impacts of Sodium Arsenite on Wood Microbiota of Esca-Diseased Grapevines. *Journal of Fungi* 7.

Callahan B.J., McMurdie P.J., Rosen M.J., Han A.W., Johnson A.J.A., Holmes S.P. 2016. DADA2: High-resolution sample inference from Illumina amplicon data. *Nature Methods* 13: 581-583.

Calzarano F., Osti F., Baránek M., Di Marco S. 2018. Rainfall and temperature influence expression of foliar symptoms of grapevine leaf stripe disease (esca complex) in vineyards. *Phytopathologia Mediterranea* 57: 488–505.

Casolani N., D'Eusanio M., Liberatore L., Raggi A., Petti L. 2022. Life cycle assessment in the wine sector: A review on inventory phase. *Journal of Cleaner Production* 379.

Chaverri P., Salgado C., Hirooka Y., Rossman A., Samuels G. 2011. Delimitation of *Neonectria* and *Cylindrocarpon* (Nectriaceae, Hypocreales, Ascomycota) and related genera with *Cylindrocarpon*-like anamorphs. *Studies in Mycology* 68: 57–78.

Chen Q., Bakhshi M., Balci Y., Broders K., Cheewangkoon R., … Crous P. 2022. Genera of phytopathogenic fungi: GOPHY 4. *Studies in Mycology* 101: 417–564.

Cholet C., Bruez É., Lecomte P., Barsacq A., Martignon T., … Gény L. 2021. Plant resilience and physiological modifications induced by curettage of Esca-diseased grapevines. *Oeno One* 55: 153–169.

Del Frari G., Gobbi A., Aggerbeck M.R., Oliveira H., Hansen L.H., Ferreira R.B. 2019. Characterization of the wood mycobiome of *Vitis vinifera* in a vineyard affected by esca. Spatial distribution of fungal communities and their putative relation with leaf symptoms. *Frontiers in Plant Science* 10.

Dewasme C., Mary S., Darrieutort G., Roby J., Gambetta G. 2022. Long-term esca monitoring reveals disease impacts on fruit yield and wine quality. *Plant Disease* 106: 3076–3082.

Deyett E., Rolshausen P. 2020. Endophytic microbial assemblage in grapevine. *Fems Microbiology Ecology* 96.

Di Marco S., Metruccio E., Moretti S., Nocentini M., Carella G., … Mugnai L. 2022. Activity of *Trichoderma asperellum* strain ICC 012 and *Trichoderma gamsii* strain ICC 080 toward diseases of esca complex and associated pathogens. *Frontiers in Microbiology* 12.

Eskalen A., Feliciano A.J., Gubler W.A. 2007. Susceptibility of grapevine pruning wounds and symptom development in response to infection by *Phaeoacremonium aleophilum* and *Phaeomoniella chlamydospora*. *Plant Disease* 91: 1100–1104.

Fischer M., Edwards J., Cunnington J., Pascoe I. 2005. Basidiomycetous pathogens on grapevine: a new species from Australia - *Fomitiporia australiensis*. *Mycotaxon* 92: 85–96.

Fox J. 2005. The R commander: A basic-statistics graphical user interface to R. *Journal of Statistical Software* 14.

Fussler L., Kobes N., Bertrand F., Mauray M., Grosman J., Savary S. 2008. A characterization of grapevine trunk diseases in France from data generated by the National Grapevine Wood Diseases Survey. *Phytopathology* 98: 571–579.

Geiger A., Karacsony Z., Golen R., Vaczy K., Geml J. 2022. The compositional turnover of grapevine-associated plant pathogenic fungal communities Is greater among intraindividual microhabitats and terroirs

than among healthy and esca-diseased plants. *Phytopathology* 112: 1029–1035.

Gispert C., Kaplan J.D., Deyett E., Rolshausen P.E. 2020. Long-term benefits of protecting table grape vineyards against trunk diseases in the California desert. *Agronomy* 10: 1895.

Grafenhan T., Schroers H., Nirenberg H., Seifert K. 2011. An overview of the taxonomy, phylogeny, and typification of nectriaceous fungi in *Cosmospora, Acremonium, Fusarium, Stilbella*, and *Volutella*. *Studies in Mycology* 68: 79–113.

Gramaje D., Mostert L., Groenewald J., Crous P. 2015. *Phaeoacremonium*: from esca disease to phaeohyphomycosis. *Fungal Biology* 119: 759–783.

Gramaje D., Urbez-Torres J.R., Sosnowski M.R. 2018. Managing grapevine trunk diseases with respect to etiology and epidemiology: current strategies and future prospects. *Plant Disease* 102: 12–39.

Gu S., Cochran R., Du G., Hakim A., Fugelsang K., … Verdegaal P. 2005. Effect of training-pruning regimes on Eutypa dieback and performance of 'Cabernet Sauvignon' grapevines. *Journal of Horticultural Science & Biotechnology* 80: 313–318.

Guerin-Dubrana L., Fontaine F., Mugnai L. 2019. Grapevine trunk disease in European and Mediterranean vineyards: occurrence, distribution and associated disease-affecting cultural factors. *Phytopathologia Mediterranea* 58: 49–71.

Hawksworth D., Gibson I., Gams W. 1976. *Phialophora parasitica* associated with disease conditions in various trees. *Transactions of the British Mycological Society* 66: 427–431.

Henderson B., Sosnowski M.R., McCarthy M.G., Scott E.S. 2021. Incidence and severity of Eutypa dieback in grapevines are related to total surface area of pruning wounds. *Australian Journal of Grape and Wine Research* 27: 87–93.

Hillis V., Lubell M., Kaplan J., Baumgartner K. 2017. Preventative disease management and grower decision making: a case study of California wine-grape growers. *Phytopathology* 107: 704–710.

Kaplan J., Travadon R., Cooper M., Hillis V., Lubell M., Baumgartner K. 2016. Identifying economic hurdles to early adoption of preventative practices: the case of trunk diseases in California winegrape vineyards. *Wine Economics and Policy* 5: 127–141.

Kraus C., Voegele R., Fischer M. 2019. The esca complex in German vineyards: does the training system influence occurrence of GLSD symptoms? *European Journal of Plant Pathology* 155: 265–279.

Kraus C., Rauch C., Kalvelage E., Behrens F., D'Aguiar D., … Fischer M. 2022. Minimal versus intensive: how the pruning intensity affects occurrence of grapevine leaf stripe disease, wood integrity, and the mycobiome in grapevine trunks. *Journal of Fungi* 8.

Lafon R. 1921. L'apoplexie: traitement préventif (Méthode Poussard), traitement curatif. Pages 35–44 in: Modifications à apporter à la taille de la vigne dans les Charentes : taille Guyot-Poussard mixte et double. Imprimerie Roumégous et Déhan, Montpellier, France.

Larach A., Torres C., Riquelme N., Valenzuela M., Salgado E., … Besoain X. 2020. Yield loss estimation and pathogen identification from Botryosphaeria dieback in vineyards of Central Chile over two growing seasons. *Phytopathologia Mediterranea* 59: 537–548.

Lecomte P., Darrieutort G., Liminana J.M., Comont G., Muruamendiaraz A., … Fermaud M. 2012. New insights into esca of grapevine: the development of foliar symptoms and their association with xylem discoloration. *Plant Disease* 96: 924–934.

Lecomte P., Diarra B., Carbonneau A., Rey P., Chevrier C. 2018. Esca of grapevine and training practices in France: results of a 10-year survey. *Phytopathologia Mediterranea* 57: 472–487.

Maher N., Piot J., Bastien S., Vallance J., Rey P., Guérin-Dubrana L. 2012. Wood necrosis in esca-affected vines: types, relationships and possible links with foliar symptom expression. *Journal International Des Sciences De La Vigne Et Du Vin* 46: 15–27.

Martinez-Diz M., Eichmeier A., Spetik M., Bujanda R., Diaz-Fernandez A., … Gramaje D. 2020. Grapevine pruning time affects natural wound colonization by wood-invading fungi. *Fungal Ecology* 48.

McMurdie P.J., Holmes S. 2013. phyloseq: an R package for reproducible interactive analysis and graphics of microbiome census data. *PLoS One* 8: e61217.

Morales-Cruz A., Figueroa-Balderas R., Garcia J.F., Tran E., Rolshausen P.E., … Cantu D. 2018. Profiling grapevine trunk pathogens in planta: a case for community-targeted DNA metabarcoding. *BMC Microbiology* 18.

Mugnai L., Graniti A., Surico G. 1999. Esca (Black measles) and brown wood-streaking: Two old and elusive diseases of grapevines. *Plant Disease* 83: 404–418.

Munkvold G.P., Marois J.J. 1995. Factors associated with variation in susceptibility of grapevine pruning wounds to infection by *Eutypa lata*. *Phytopathology* 85: 249–256.

Niem J., Billones-Baaijens R., Stodart B., Savocchia S. 2020. Diversity profiling of grapevine microbial endosphere and antagonistic potential of endophytic *Pseudomonas* against grapevine trunk diseases. *Frontiers in Microbiology* 11.

Pacetti A., Moretti S., Pinto C., Compant S., Farine S., … Mugnai L. 2021. Trunk surgery as a tool to reduce foliar symptoms in diseases of the esca complex and its influence on vine wood microbiota. *Journal of Fungi* 7.

Phillips A.J., Alves A., Abdollahzadeh J., Slippers B., Wingfield M.J., … Crous P.W. 2013. The Botryosphaeriaceae: genera and species known from culture. *Stud Mycol* 76: 51–167.

Pouzoulet J., Mailhac N., Couderc C., Besson X., Dayde J., … Jacques A. 2013. A method to detect and quantify *Phaeomoniella chlamydospora* and *Phaeoacremonium aleophilum* DNA in grapevine-wood samples. *Applied Microbiology and Biotechnology* 97: 10163–10175.

Rolshausen P., Mahoney N., Molyneux R., Gubler W. 2006. Reassessment of the species concept in *Eutypa lata*, the causal agent of eutypa dieback of grapevine. *Phytopathology* 96: 369–377.

Rolshausen P.E., Urbez-Torres J.R., Rooney-Latham S., Eskalen A., Smith R.J., Gubler W.D. 2010. Evaluation of pruning wound susceptibility and protection against fungi associated with grapevine trunk diseases. *American Journal of Enology and Viticulture* 61: 113–119.

Schindelin J., Arganda-Carreras I., Frise E., Kaynig V., Longair M., … Cardona A. 2012. Fiji: an open-source platform for biological-image analysis. *Nature Methods* 9: 676–682.

Surico G. 2009. Towards a redefinition of the diseases within the esca complex of grapevine. *Phytopathologia Mediterranea* 48: 5–10.

Travadon R., Baumgartner K., Rolshausen P., Gubler W., Sosnowski M., … Péros J. 2012. Genetic structure of the fungal grapevine pathogen *Eutypa lata* from four continents. *Plant Pathology* 61: 85–95.

Travadon R., Lecomte P., Diarra B., Lawrence D., Renault D., … Baumgartner K. 2016. Grapevine pruning systems and cultivars influence the diversity of wood-colonizing fungi. *Fungal Ecology* 24: 82–93.

Trouillas F., Urbez-Torres J., Gubler W. 2010. Diversity of diatrypaceous fungi associated with grapevine canker diseases in California. *Mycologia* 102: 319–336.

van Niekerk J., Groenewald J., Farr D., Fourie P., Halleen F., Crous P. 2005. Reassessment of *Phomopsis* species on grapevines. *Australasian Plant Pathology* 34: 27–39.

Vanga B., Panda P., Shah A., Thompson S., Woolley R., … Bulman S. 2022. DNA metabarcoding reveals high relative abundance of trunk disease fungi in grapevines from Marlborough, New Zealand. *Bmc Microbiology* 22.

Wickham H. 2009. Ggplot2: Elegant Graphics for Data Analysis. Springer, New York, USA.

Úrbez-Torres J.R. 2011. The status of Botryosphaeriaceae species infecting grapevines. *Phytopathologia Mediterranea* 50: S5–S45.

Phytopathologia Mediterranea
The international journal of the
Mediterranean Phytopathological Union

Firenze University Press
www.fupress.com/pm

Research Papers

First report of *Aspergillus* species in green pistachio of Bronte

Wanissa MELLIKECHE[1], Giulia CASINI[2], Marilita GALLO[3], Anna Maria D'ONGHIA[3], Giancarlo COLELLI[1], Alessandra RICELLI[4,*]

[1] *Dipartimento di Scienze Agrarie, degli Alimenti e dell'Ambiente, Università di Foggia, Via Napoli 25, 71122 Foggia, Italy*
[2] *Enbiotech S.r.l., Via Quarto dei Mille, 6, 90129 Palermo, Italy*
[3] *Centre International de Hautes Etudes Agronomiques Méditerranéennes Bari (CIHEAM Bari), Via Ceglie 9, 70010 Valenzano, Bari, Italy*
[4] *Istituto di Biologia e Patologia Molecolari (IBPM-CNR) P.le A. Moro 5, 00185, Roma, Italy*
*Corresponding author. E-mail: alessandra.ricelli@cnr.it

Summary. *Aspergillus* contamination of pistachios causes significant product losses and potential presence of mycotoxins, particularly aflatoxin B1 (AFB1), and ochratoxin A (OTA). These toxins, which threaten human health, are strictly monitored by most nations. Italian pistachios produced in Bronte, Sicily, have high nutritional value and unique organoleptic properties, but the extent to which they contain these contaminants is unknown. *Aspergillus* spp. isolated from Bronte pistachios (cultivar Napoletana) were assessed for their ability to synthesize OTA or AFB1. *Aspergillus* occurrence in pistachio samples was measured at 1137 cfu g^{-1} for in shell pistachios and 770 cfu g^{-1} for kernels. The predominant isolated *Aspergillus* species was *A. niger* representing 74% of section *Nigri* (black isolates) and 47% of all *Aspergillus* isolates. Within section *Flavi*, *A. flavus* comprised 83% of green isolates. Only one black isolate (identified as *A. carbonarius*) had high OTA production, but all the *A. flavus* isolates had potential to produce AFG1 and AFB1, with AFB1 produced amount ranging from 0.1 to 8498 ng mL^{-1} of culture filtrate.

Keywords. *Aspergillus niger*, *Aspergillus flavus*, *Aspergillus carbonarius*, *Aspergillus tamarii*, *Aspergillus tubingensis*, aflatoxins, ochratoxin A.

OPEN ACCESS

Citation: W. Mellikeche, G. Casini, M. Gallo, A.M. D'Onghia, G. Colelli, A. Ricelli (2024) First report of *Aspergillus* species in green pistachio of Bronte. *Phytopathologia Mediterranea* 63(1): 103-110. doi: 10.36253/phyto-14949

Accepted: March 5, 2024

Published: April 29, 2024

Data Availability Statement: All relevant data are within the paper and its Supporting Information files.

Competing Interests: The Author(s) declare(s) no conflict of interest.

Editor: Lluís Palou, Valencian Institute for Agricultural Research, Valencia, Spain.

ORCID:
WM: 0000-0001-6383-4094
GC: 0000-0001-7224-7158
AR: 0000-0002-1151-6120
GCo: 0000-0001-8619-3541
MG: 0000-0003-4981-485X
MD'O: 0000-0002-1817-4637

INTRODUCTION

Pistachio nut tree (*Pistachia vera* L.), native to the arid zones of Central and West Asia, is widely distributed across the Mediterranean region. Pistachios are one of the most highly valued nut commodities consumed raw, toasted, and salted, or as an ingredient in many foods including desserts, ice-cream, pastry, and some sausages (Arena *et al.*, 2007). Pistachios also have high nutritional value and contain phytochemical antioxidants (D'Evoli *et al.*, 2015; Sheikhi *et al.*, 2019). Pistachio trees are cultivated mainly in the United States of America, Iran, and Turkey and in the Medi-

Figure 1. Pistachio trees spontaneously growing in volcanic soil in Bronte, Sicily.

terranean countries of southern Europe and North Africa (Mandalari *et al*., 2022).

Pistachios were brought to Italy from Syria during the Roman era in the 9th Century AD (Marino and Marra, 2019). In Sicily, where agriculture was highly influenced by Arabs, pistachios became an integral part of the island's cuisine and culture. Pistachios produced in Bronte are very high-quality and particularly flavourful, due to the island's volcanic soils and climatic conditions. Pistachio trees in this area grow spontaneously on the volcanic soils (Figure 1), and are harvested once every 2 years, in September, and then dried in greenhouses. Despite their low production volume, "green pistachios of Bronte" cultivar Napoletana (also known as "Nostrale" or "Bianca") are the most expensive in the world, and are of economic importance in Italy (Wilson *et al*., 2018).

The green pistachio of Bronte was officially registered as an Italian Protected Designation of Origin (PDO) product in 2010. This designation aims to promote and protect product authenticity and characteristics, to improve economic conditions for producers in the specified areas (within 'the municipalities' of Bronte, Adrano, and Biancavilla), and to provide consumers with information about product origins and production methods (Wilson *et al*., 2018; Marino and Marra, 2019).

The quality of pistachios does not depend only on their flavor and nutritional value, but also on the absence of mycotoxins. These are secondary metabolites produced by several widespread fungi, mainly *Aspergillus* spp., *Penicillium* spp., and *Fusarium* spp. Pistachios have been associated with several types of mycotoxins including cyclopiazonic acid (Hua *et al*., 2012), and HT-2 toxin, fumonisins, ochratoxin A and aflatoxins, with this latter group being of the greatest interest on pistachios (Soares Mateus *et al*., 2021).

Aflatoxins are commonly found in pistachios, due to contaminations by green *Aspergillus* spp. (section *Flavi*), and particularly *A. flavus* and *A. parasiticus*. These species produce several aflatoxins including aflatoxin B1 (AFB1), AFB2, AFG1, and AFG2. While all of these compounds are hazardous due to their interference with the immune system, AFB1 is also characterized by the most potent mutagenic and carcinogenic activity. Therefore, it was confirmed as Group 1 agent by IARC (IARC, 2002).

In addition to aflatoxins, analyses of other varieties of pistachios found presence of ochratoxin A (OTA), which is linked to black *Aspergillus* (section *Nigri*), mainly *A. carbonarius* and *A. niger* (Fernane *et al*., 2010). OTA is a nephrotoxic, carcinogenic, teratogenic, immunotoxic and hepatotoxic mycotoxin. It is classified in Group 2B by IARC (IARC, 1993).

AFB1 and OTA are strictly regulated in many countries including those of the European Union. For pistachios intended for direct human consumption or use as food ingredients, the maximum acceptable levels are 8 μg kg^{-1} of AFB1 (with 10 μg of total aflatoxins), and 5 μg kg^{-1} of OTA (EU Reg EC 1881/2006, as amended by 165/2010).

Because of the high economic value of pistachio production and the potential for expansion of this industry in Italy, studies addressing the composition of pistachios (Tomaino *et al*., 2010) and the pathogens that could endanger pistachio production (Gusella *et al*., 2022) have increased. However, there are no reports on the presence of toxigenic *Aspergilli* in Bronte's pistachios. The present study aimed to determine the state of pistachio mycotoxin contamination, as knowledge to support the healthi-

ness of this valuable product. A survey of *Aspergillus* species on Bronte pistachios was conducted, and the potential capacity of isolated strains to produce AFB1 and OTA was evaluated.

MATERIAL AND METHODS

Sampling and isolation of fungi

Ten samples of dried pistachios (1 kg each) obtained from the area of Bronte (Catania province, Italy) were used in this study. To estimate fungal contamination levels (cfu g^{-1}) on these samples, isolations were performed by plating water spore suspensions. Fifty nuts from each sample were weighed and added to 50 mL of sterile water containing 0.1% Tween20 in a sterile Erlenmeyer flask, which was then shaken for 1 h on an orbital shaker (120 rpm), at room temperature. The resulting suspension was filtered and was used to prepare serial 10-fold dilutions.

One hundred µL of spore suspension was seeded onto three potato dextrose agar (PDA: Difco, Becton Dickinson) plates, which were incubated at 25°C and monitored daily for 7 d. Each resulting fungal colony was transferred to a new Petri dish containing PDA and was left to grow at 25°C. The total number of colonies grown on each original isolation plate was expressed as colony forming units per gram of matrix (cfu g^{-1}). For each sample, isolations were carried out from in shell pistachios (kernels and shells) and from kernels.

Identification of isolated Aspergillus *spp.*

Among the isolated fungi, *Aspergillus* isolates belonging to *Nigri* and *Flavi* sections were identified by their distinctive morphological structures, including colony characteristics and shape and size of conidia and conidiophores (Pitt and Hoking, 1997). Green isolates were tested using a LAMP assay (Mellikeche *et al.*, 2024) designed specifically for the detection of *A. flavus,* the greatest producer of AFB1. To detect *A. carbonarius*, the greatest producer of OTA, black isolates were grown on semi-selective malt extract agar, (MOA-B), containing 10 mg L^{-1} of Boscalid®, (Merck) (Samson *et al.*, 2007), on which only this species can sporulate. A LAMP assay for the detection of *A. carbonarius* (Enbiotech S.r.l.) was used to confirm identification of this fungus.

Remaining black and green isolates were divided into groups based on similarities of morphological characteristics on potato dextrose agar (PDA), czapek yeast agar (CYA), *Aspergillus* differentiation agar (ADA Difco, Becton Dickinson). Representative isolates from each group were subjected to DNA extraction (Carlucci *et al.*, 2013), and PCR assays using Calmodulin primers described by O'Donnell *et al.* (2000), followed by sequencing of the amplified regions to identify the species.

Production of AFB1 and OTA

Fungal cultures were incubated in czapek yeast broth (CDY), which is conductive to biosynthesis of aflatoxins and ochratoxin A by Aspergilli (Visagie *et al.*, 2014; Frisvad *et al.*, 2019). The cultures were grown at 24°C in the dark in static conditions, and were filtered through Whatman no. 4 filter paper, using a a vacuum pump system. Resulting filtrates were frozen at -25°C until they were used for mycotoxin analyses.

Production of OTA and AFB1 by the black and green *Aspergillus* species isolated from pistachio nuts was first qualitatively evaluated using High-Performance Thin-Layer Chromatography (HPTLC, Merck). Two mL of each culture filtrate were acidified by 0.2 mL of formic acid and then extracted using 2 mL of ethyl acetate. Each extraction was repeated twice, and the extracts were collected and concentrated under a nitrogen stream. The concentrated extracts were reconstituted with ethyl acetate to 1 mL, and then 5 µL were plated on HPTLC plates together with known amounts of the pure AFB1 and OTA as references. The eluent phase used was a mixture of toluene, ethyl acetate and formic acid (6:3:1, v/v/v).

For quantitative analyses, culture filtrates were purified using immunoaffinity columns (AflaOchra® Immuno Affinity columns, VICAM), with 20 mL of each culture filtrate used for each purification. After passage through the column, washings were each carried out with 20 mL of distilled water. Water was then eliminated from the columns by applying light pressure, and mycotoxins potentially present were eluted from the column with 1.5 mL methanol, as prescribed in the manufacturer's instructions. Each sample was then evaporated under nitrogen flow at room temperature. The dry sample was then reconstituted in 200 µL of a mixture of acetonitrile, water, acetic acid (99:99:2 v/v/v).

Mycotoxin analyses were carried out using the procedure of Solfrizzo *et al.* (1998). A stock solution (1.0 mg mL^{-1}) of OTA (Sigma) was prepared in toluene plus acetic acid (99:1, v/v). OTA calibration standard solutions for HPLC determination were prepared by dissolving appropriate amounts of stock solution in acetonitrile-water-acetic acid (99:99:2, v/v/v) to obtain final concentrations of 1 ng mL^{-1}. For AFB1, the stock solution (Sig-

ma) was prepared at 1.0 mg mL^{-1} in methanol. Calibration standard solutions for HPLC determinations were prepared by further dissolving appropriate amounts of stock solution in methanol to obtain final concentrations of 1 ng mL^{-1}. Each dried sample was resuspended in 200 µL of an acetonitrile-methanol mixture (1:1, v/v), and was analyzed using an HPLC (1260 Infinity Agilent) equipped with a diode array detector and a C18 column (Poroshell 120; 50 × 4.6 mm, 2.7 µm, Agilent). The mobile phase consisted of a mixture of acetonitrile-water-acetic acid (99:99:2, v/v/v) at a flow rate of 1 mL min^{-1}. The chromatographic runs were carried out in isocratic mode, whereby an aliquot of 10 µL, taken from 200 µL of each dissolved extract, was injected into the HPLC system. AFB1 and OTA in the samples were detected and quantified by comparing the retention times and the absorbance spectra of the authentic standards.

Each mycotoxin was quantified by measuring peak areas and comparing them with the relevant calibration curves. The Limits of Quantification (LOQ) were 2 ng for OTA and 2.5 ng for AFB1. Detection and quantification of AFB1 were carried out at 363 λ and for OTA at 333 λ, which are the relative maxima for these molecules.

RESULTS AND DISCUSSION

Isolation and evaluation of Aspergillus *occurrence in pistachios*

Most isolated fungi were identified as *Aspergillus*, comprising 95.8% of the isolates from in shell pistachios and 94.5% of the isolates from pistachio kernels. Morphological analyses of the other isolated fungi indicated they belong to the genera *Penicillium* and *Alternaria* (Figure 2). Average *Aspergillus* occurrence in kernels was 770 cfu g^{-1}. A total of 133 isolates were obtained from kernels, with the majority (78%) belonging to section *Nigri*, while only 18% were classified as section *Flavi*. Greater occurrence was recorded from in shell pistachio nuts averaging 1137 cfu g^{-1}. A total of 141 fungal isolates were obtained, with 56% of these classified as section *Nigri* and 43% as section *Flavi*.

Aspergillus species are the most prominent postharvest contaminants in pistachios. However, Bronte pistachios exhibited greater predominance of *Aspergillus* over other molds, compared to pistachios assessed in other countries. Fernane *et al.* (2010) analyzed pistachios from the Spanish market, and showed a more diverse mycoflora including *Fusarium* and *Penicillium*, with *Penicillium* surpassing prevalence of *Aspergillus*. Although section

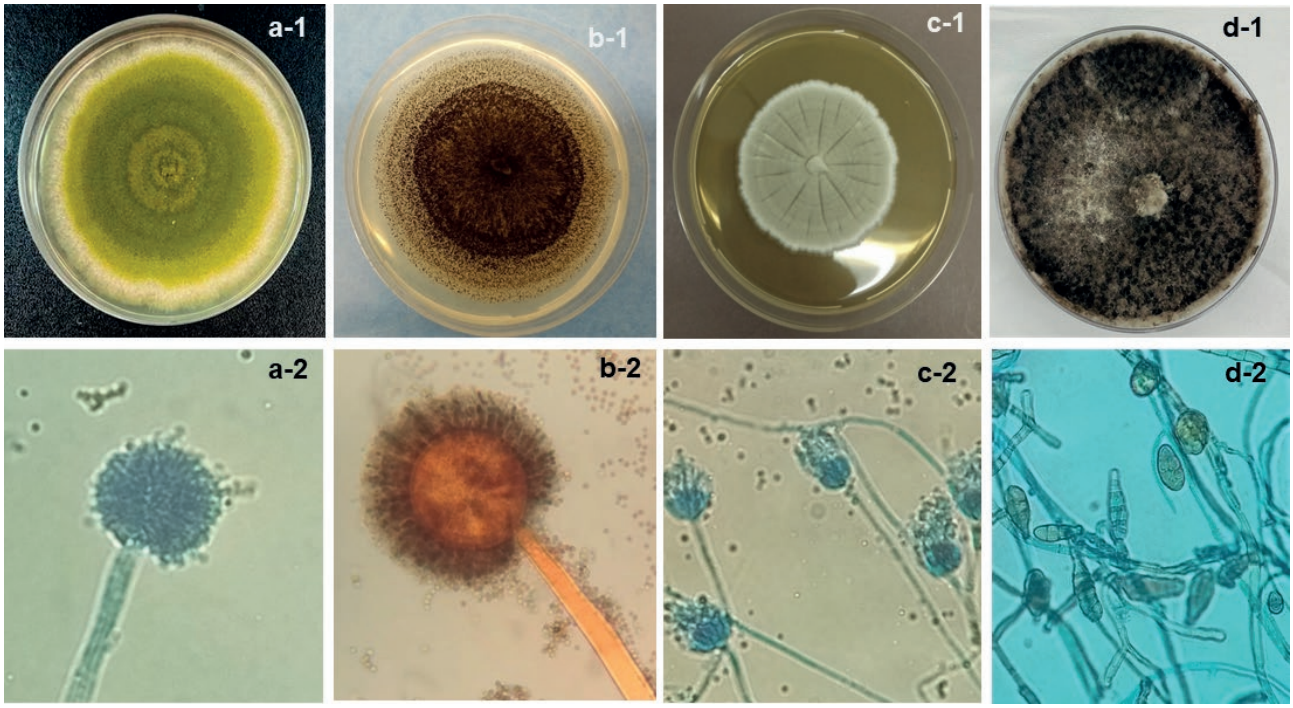

Figure 2. Fungal genera isolated from pistachio samples: a) *Aspergillus* section *Flavi* 1 colony on PDA and 2 conidiophore; b) *Aspergillus* section *Nigri* 1 colony and 2 conidiophore; c) *Penicillium* 1 colony and 2 conidiophore; d) *Alternaria* 1 colony and 2 conidiophore.

Nigri is often the most isolated among *Aspergillus* from pistachios (Doster and Michailides, 1994), greater attention is directed towards section *Flavi*. This is due to the favourable substrate provided by pistachios for the production of Aflatoxins by section *Flavi* species.

The presence of Aflatoxins is often associated with marketing and exportation issues, due to strict regulations. An example is the European ban of Iranian pistachios in 1994, due to their high aflatoxin contents (Bui-Klimke *et al.*, 2014). In Iran, Moghadam *et al.* (2020) showed green *Aspergilli* contamination in pistachio kernels ranged from 1.6×10^3 to 1.6×10^4 cfu g^{-1}. This contamination is much greater than recorded in the present study on Bronte pistachio kernels, where the average contamination was 1.3×10^2 cfu g^{-1}, and on in shell pistachios (4.9×10^2 cfu g^{-1}).

The low fungal contamination in Bronte pistachios could be due to several factors that can affect fungal growth and mycotoxin accumulation in the complex host plant-fungus-environment interactions, e.g., climatic conditions, soil type, agricultural practices, crop variety and characteristics (Kaminiaris *et al.*, 2020). The green pistachios of Bronte grow spontaneously on the volcanic soil. Therefore, agricultural practices, which often allow the introduction and spread of fungi, are practically absent. The cultivar Napoletana is possibly less prone to fungal contamination than other varieties, especially in the susceptible period of the maturity (Panahi and Khezri, 2011). However, these aspects should be verified by testing this cultivar in other Italian pistachio's growing areas.

Identification of isolated Aspergillus *spp.*

A total number of 75 green isolates were analyzed with the LAMP assay specific for *A. flavus*. Among these, 48 isolates were positive, while the remaining isolates were identified as *A. tamarii* through PCR amplification using calmodulin primers and sequencing of resulting products.

Black isolates were grown on MEA-B on which only one isolate, UPB36, sporulated and was identified as *A. carbonarius* (Figure 3a). This was further confirmed by LAMP analysis, which gave a positive result only for isolate UPB36 (Figure 3b). PCR amplifications identified the remaining isolates as *A. tubingensis* and *A. niger* which was the predominant species (74% of section *Nigri* and 47% of all sections).

The most commonly occurring *Aspergillus* species were *A. niger* and *A. flavus* belonging, respectively, to the sections *Nigri* and *Flavi* (Perrone *et al.*, 2007). On pistachios, the distribution of Aspergilli probably differs depending on the growing region and the cultivar. For instance, Khodavaisy *et al.* (2012), examined pistachios from Samandaj, Iran, and found high incidence of *A. flavus* (56.2%) followed by *A. niger* (12.5%) among all detected fungal contaminants. Moghadam *et al.* (2020) also confirmed the dominance of *Aspergillus* section *Flavi* in Iranian pistachios, with its distribution varying depending on the cultivar. However, Rahimi *et al.* (2007), assessed the contamination of pistachios from Kerman, Rafsanjan, and Isfahan, recorded greatest occurrence of *A. niger* (49%) followed by *A. flavus*

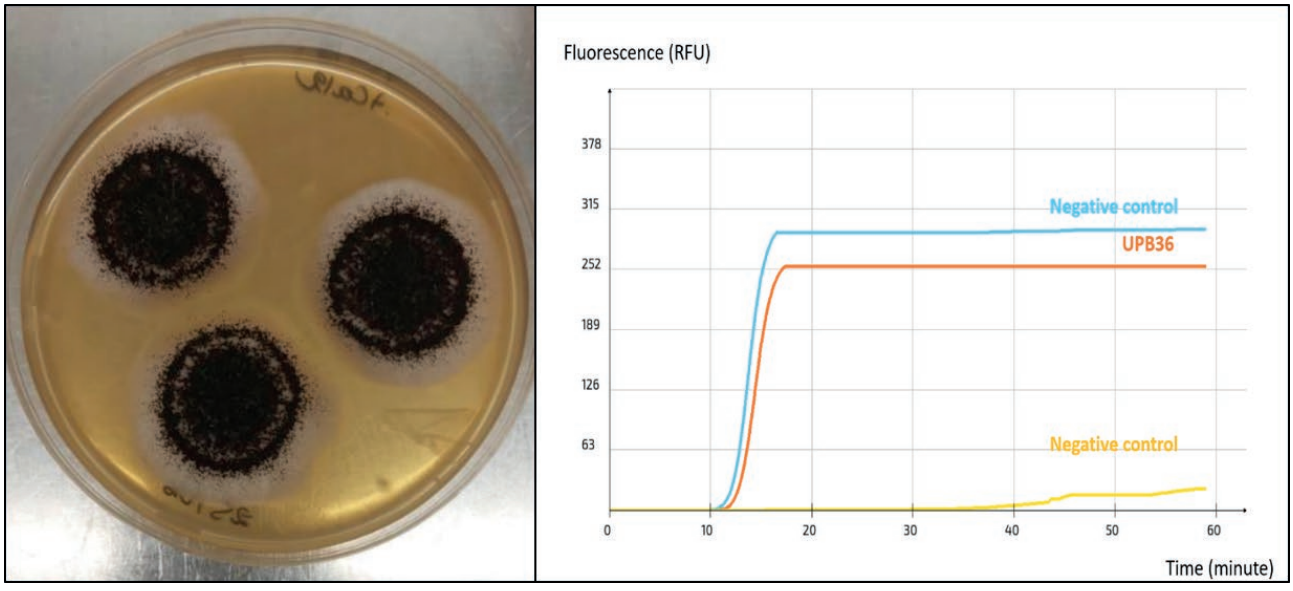

Figure 3. *Aspergillus carbonarius* UPB36 a) colonies on MEA-Boscalid. b) Positive signal with LAMP set ACS02

(33%). The present study also recorded high diversity in aspergilli associated with pistachios, with 11 species identified. This is not the case for Italian pistachios where we have detected dominance of *A. niger* (74%), and low diversity amongst aspergilli with only five species detected. The situation of Italian Bronte pistachios is more comparable to the Californian pistachios on which *A. niger* has been frequently reported as the most common species (Doster and Michailides, 1994; Bayman *et al.*, 2002).

Mycotoxin production

For the green *Aspergillus* isolates, TLC analyses showed that all *A. flavus* isolates produced AFB1 and AFG1, while *A. tamarii* isolates did not produce these mycotoxins. Therefore, HPLC analyses were carried out for all *A. flavus* isolates to confirm and quantify their AFB1 production. Some isolates of *A. tamarii* were also analyzed with HPLC, which confirmed the TLC results. HPLC analyses confirmed that all *A. flavus* isolates produced AFB1 at quantities ranging from 0.1 to 8497.8 ng mL^{-1} of culture filtrate (Table 1).

The only *A. carbonarius* isolate that produced OTA was UPB36, at an amount of 34.2 ng mL^{-1} (Table 2). For *A. niger*, TLC analyses showed that five isolates were potential OTA producers. These isolates were further analyzed with HPLC, and the ability to produce OTA was confirmed, at relatively low levels, for three of them (Table 2).

Aspergillus flavus is the species most commonly associated with aflatoxin production in pistachios. Previous studies have linked *A. flavus* strains with high potential to produce aflatoxins (Hua *et al.*, 2012; Marín *et al.,* 2012). The present study showed that in Bronte pistachios the majority of *A. flavus* isolates have high potential to produce AFB1. Previous studies have detected the presence of OTA and OTA-producing Aspergilli in pistachio samples (Fernane *et al.*, 2010; Singh *et al.*, 2023). In the present study, one *A. carbonarius* isolate produced OTA at 34.2 ng mL^{-1}, and only five *A. niger* isolates were potential OTA producers. Despite their low production, these isolates cannot be dismissed as threats to human health, due to their possession of genes for OTA production, and because this production could be triggered by the occurrence of appropriate growth conditions.

Table 1. AFB1 production in culture by green *Aspergillus* isolates.

Isolate	*Aspergillus* species	Amount (ng mL^{-1}) of AFB1
UP60	*A. flavus*	576.6
UP66	*A. flavus*	414,6
UP67	*A. flavus*	178.7
UP68	*A. flavus*	604.6
UP74	*A. flavus*	253.3
UP85	*A. flavus*	5624.8
UP86	*A. flavus*	246.6
UP87	*A. flavus*	154.0
UP88	*A. flavus*	2223.1
UP89	*A. flavus*	691.3
SP5	*A. flavus*	8497.8
SP6	*A. flavus*	6350.0
Sp7	*A. flavus*	4424.9
SP9	*A. flavus*	4247.6
SP11	*A. flavus*	4612.9
SP12	*A. flavus*	3509.7
SP22	*A. flavus*	879.9
SP27	*A. flavus*	978.6
SP30	*A. flavus*	1147.2
SP31	*A. flavus*	3927.6
SP34	*A. flavus*	1513.2
SP38	*A. flavus*	234.6
SP39	*A. flavus*	50.00
SP40	*A. flavus*	1983.8
SP42	*A. flavus*	683.9
SP44	*A. flavus*	66.0
SP64	*A. flavus*	2651.7
SP91	*A. flavus*	368.0
SP92	*A. flavus*	0.1
SP93	*A. flavus*	0.1
SP95	*A. flavus*	0.1
SP96	*A. flavus*	0.1
SP97	*A. flavus*	0.1
SP99	*A. flavus*	0.1
SP100	*A. flavus*	0.1
SP102	*A. flavus*	0.1
SP104	*A. flavus*	0.1
UP82	*A. flavus*	170.7
SP107	*A. flavus*	77.3
SP108	*A. flavus*	89.3
SP109	*A. flavus*	152.7
SP110	*A. flavus*	214.0
SP119	*A. flavus*	0.1
SP128	*A. flavus*	0.1
SP12(2)	*A. flavus*	6387.4
UP48	*A. flavus*	59.6
UP50	*A. flavus*	63.5
SP53	*A. flavus*	43.5
SP17	*A.tamarii*	0.0
SP80	*A.tamarii*	0.0
SP20	*A.tamarii*	0.0
SP25	*A.tamarii*	0.0

CONCLUSION

This is the first study of *Aspergillus* spp. contamination in green pistachios that have been produced on the

Table 2. OTA production by black *Aspergillus* isolates.

Isolate	Species	Amount (ng/mL) of OTA
UPB16	*A. niger*	0.6
UPB31	*A. niger*	1.0
UPB33	*A. niger*	0.2
UPB36	*A. carbonarius*	34.2
UP51	*A. niger*	0.0
UP55	*A. niger*	0.0

volcanic soils in Bronte, Sicily. This study estimated that *Aspergillus* occurrence in these pistachios is less than for pistachios produced in other countries. This could be related to the type of plantation, soils, climatic conditions, and/or the pistachio variety.

Mycotoxins are secondary metabolites which are produced independently from mycelium growth and sporulation. However, examination of *Aspergillus* spp. occurring on pistachios and their ability to produce mycotoxins can indicate their potential production under favorable conditions. Although the contamination of Bronte pistachios with green *Aspergillus* spp. is low, these contaminants showed high levels of production of AFB1.

These results indicate that investigations dealing with mycotoxigenic fungi developing on pistachio nuts grown in Italy should be expanded. In particular, considering areas with different envirnmental, climatic, and management conditions. It is also important that agricultural and post-harvest practices should be improved to mitigate human health risks related to mycotoxin contamination. This will help to preserve the organoleptic and nutritional qualities of these nut products.

LITERATURE CITED

Arena E., Campisi S., Fallico B., Maccarone E., 2007. Distribution of fatty acids and phytosterols as a criterion to discriminate geographic origin of pistachio seeds. *Food Chemistry* 104: 403-408. https://doi.org/10.1016/j.foodchem.2006.09.029

Bayman P., Baker J.L., Mahoney N.E., 2002. *Aspergillus* on tree nuts: incidence and associations. *Mycopathologia* 155: 161–169. https://doi.org/10.1023/a:1020419226146

Bui-Klimke T.R., Guclu H., Kensler T.W., Yuan J.M., Wu F., 2014. Aflatoxin regulations and global pistachio trade: Insights from social network analysis. *PLoS ONE* 9(3): e92149. https://doi.org/10.1371/journal.pone.0092149

Carlucci A., Raimondo M.L., Cibelli F., Phillips A.J.L., Lops F., 2013. *Pleurostomophora richardsiae*, *Neofusicoccum parvum* and *Phaeoacremonium aleophilum* associated with a decline of olives in Southern Italy. *Phytopathologia Mediterranea* 52(3): 517–527. https://doi.org/10.14601/Phytopathol_Mediterr-13526

D'Evoli L., Lucarini M., Gabrielli P., Aguzzi A., Lombardi-Boccia G., 2015. Nutritional value of Italian pistachios from Bronte (*Pistacia vera* L.), their nutrients, bioactive compounds and antioxidant activity. *Food and Nutrition Sciences* 6(14): 1267. https://doi.org/10.4236/fns.2015.614132

Doster M.A., Michailides T.J., 1994. Aspergillus molds and aflatoxins in pistachio nuts in California postharvest pathology and mycotoxins. *Phytopathology* 84: 583–590. 10.1094/Phyto-84-583

Fernane F., Cano-Sancho G., Sanchis V., Marín S., Ramos A.J., 2010. Aflatoxins and ochratoxin A in pistachios sampled in Spain: occurrence and presence of mycotoxigenic fungi. *Food Additives Contaminants Part B Surveill*. 3(3): 185–192. https://doi.org/10.1080/19440049.2010.497257.

Frisvad J.C., Hubka V., Ezekiel C.N., Hong S.B., Novakova A., and Houbraken J. 2019. Taxonomy of *Aspergillus* section *Flavi* and their production of aflatoxins, ochratoxins and other mycotoxins. *Studies in Mycology* 93: 1–63.

Gusella G., Vitale A., Polizzi G., 2022. Potential role of biocontrol agents for sustainable management of fungal pathogens causing canker and fruit rot of pistachio in Italy. *Pathogens* 11: 829. https://doi.org/10.3390/pathogens11080829

Hua S.S., McAlpin C.E., Chang P.K., Sarreal S.B., 2012. Characterization of aflatoxigenic and non-aflatoxigenic *Aspergillus flavus* isolates from pistachio. *Mycotoxin Research*. 28(1): 67–75. https://doi.org/10.1007/s12550-011-0117-4

IARC 1993. Working Group on the evaluation of carcinogenic risks to humans. Monograph Volume 56: *Some Naturally Occurring Substance: Food Items and Constituents, Heterocyclic Aromatic Amines and Mycotoxins*. Lyon, France: IARC Press, World Health Organization.

IARC 2002. Working Group on the evaluation of carcinogenic risks to humans. Monograph Volume 82: *Some Traditional Herbal Medicines, Some Mycotoxins, Naphthalene and Styrene*. Lyon, France: IARC Press, World Health Organization.

Kaminiaris M.D., Camardo Leggieri M., Tsitsigiannis D.I., Battilani P., 2020. AFLA-PISTACHIO: Development of a mechanistic model to predict the aflatoxin contamination of pistachio nuts. *Toxins* 12(7): 445. https://doi.org/10.3390/toxins12070445

Khodavaisy S., Maleki A., Hossainzade B., Rezai S., Ahmadi, F., and Ghahramani E., 2012. Occurrence of

fungal contamination in pistachio and peanut samples from retail shops in Sanandaj province, Iran. *African Journal of Microbiology Research* 6: 6781–6784. https://doi.org/10.5897/AJMR12.722

Mandalari G., Barreca D., Gervasi T., Roussell M.A., Klein B., Feeney M.J., Carughi A., 2022. Pistachio nuts (*Pistacia vera* L.): Production, Nutrients, Bioactives and Novel Health Effects. *Plants* 11(1): 18. https://doi.org/10.3390/plants11010018

Marín S., Ramos A.J., Sanchis V., 2012. Modelling Aspergillus flavus growth and aflatoxins production in pistachio nuts. *Food Microbiology* 32(2): 378–388, https://doi.org/10.1016/j.fm.2012.07.018

Marino G., Marra F.P., 2019. Horticultural management of Italian pistachio orchard systems: current limitations and future prospective. *Italus Hortus* 26 (3): 14–26. https://doi.org/10.26353/j.itahort/2019.2.1426

Mellikeche W., Ricelli A., Casini G., Gallo M., Colelli G., D'Onghia A.M. 2024. Development of Loop-Mediated Isothermal Amplification (LAMP) Assays for the Rapid Detection of Toxigenic Aspergillus flavus and A. carbonarius in Nuts. *International Journal of Molecular Sciences* 25(7): 3809. https://doi.org/10.3390/ijms25073809

Moghadam M.M., Rezaee S., Mohammadi A.H., Zamanizadeh H.R., Moradi M., 2020. A Survey on contamination of Iranian pistachio cultivars to *Aspergillus* section Flavi and Aflatoxin. *Journal of Nuts* 11(1): 13–22. https://doi.org/10.22034/jon.2020.1882572.1072

O'Donnell K., Kirenberg H.I., Cigelnik E., 2000. A multigene phylogeny of the Gibberella fujkuroi species complex detection of additional phylogenetically distinct species. *Mycoscience* 41: 61–78. https://doi.org/10.1007/BF02464387

Panahi B., Khezri M., 2011. Effect of harvesting time on nut quality of pistachio (*Pistacia vera* L.) cultivars. *Scientia Horticulturae* 129: 730–734. https://doi.org/10.1016/j.scienta.2011.05.029

Perrone G., Susca A., Cozzi G., Ehrlich K., Varga J., and Samson R.A., 2007**.** Biodiversity of *Aspergillus* species in some important agricultural products**.** *Studies in Mycology* 59(1): 53–66 https://doi.org/10.3114/sim.2007.59.07

Pitt, J.I., Hocking, A.D. 1997. Methods for isolation, enumeration and identification. In: *Fungi and Food Spoilage*. Springer, Boston, MA, USA. https://doi.org/10.1007/978-1-4615-6391-4_4

Rahimi P., Sharifnabi B., Bahar M., 2007. Detection of Aflatoxin in Aspergillus Species Isolated from Pistachio in Iran. *Journal of Phytopathology* 156(1): 15–20. https://10.1111/j.1439-0434.2007.01312.x

Samson R., Noonim P., Meijer M., Houbraken J., Frisvad J., Varga, J., 2007. Diagnostic tools to identify black aspergilli. *Studies in Mycology* 59: 129–145. https://doi.org/10.3114/sim.2007.59.13

Sheikhi A., Mirdehghan S.H., Ferguson L., 2019. Extending storage potential of de-hulled fresh pistachios in passive-modified atmosphere. *Journal of the Science of Food and Agriculture* 99(7): 3426–3433. https://doi.org/10.1002/jsfa.9560

Singh P., Jaime R., Puckett R.D. Lake J., Papangelis A., and Michailides T., 2023. Ochratoxin A contamination of California pistachios and identification of causal agents. *Plant Disease* https://doi.org/10.1094/PDIS-06-23-1233-RE

Soares Mateus A.R., Barros S., Pena A., Sanches Silva A. 2021. Mycotoxins in Pistachios (*Pistacia vera* L.): Methods for Determination, Occurrence, Decontamination. *Toxins* 13(10): 682. https://doi.org/10.3390/toxins13100682

Solfrizzo M., Avantaggiato G., Visconti A., 1998. Use of various clean-up procedures for the analysis of ochratoxin A in cereals. *Journal of Chromatography* 815: 67–73. https://doi.org/10.1016/s0021-9673(98)00271-4

Tomaino A., Martorana M., Arcoraci T., Monteleone D., Giovinazzo C., Saija A., 2010. Antioxidant activity and phenolic profile of pistachio (*Pistacia vera* L., variety Bronte) seeds and skins. *Biochimie* 92(9): 1115–1122. https://doi.org/10.1016/j.biochi.2010.03.027

Visagie C.M., Varga J., Houbraken J., Meijer M., Kocsub S., and Samson R.A. 2014. Ochratoxin production and taxonomy of the yellow aspergilli (Aspergillus section Circumdati). *Studies in Mycology* 78: 1–61. http://dx.doi.org/10.1016/j.simyco.2014.07.001

Wilson J.S., Petino G., Knudsen D.C., 2018. Geographic context of the green pistachio of Bronte, a protected designation of origin product. *Journal of Maps* 14(2): 144–150. https://doi.org/10.1080/17445647.2018.1438318

Phytopathologia Mediterranea
The international journal of the
Mediterranean Phytopathological Union

Firenze University Press
www.fupress.com/pm

Short Notes

Characterization and pathogenicity of *Pleurostoma richardsiae* causing decline of mango trees in Southern Italy

Giuseppa Rosaria LEONARDI, Dalia AIELLO*, Giorgio GUSELLA, Giancarlo POLIZZI

Dipartimento di Agricoltura, Alimentazione e Ambiente, University of Catania, 95123, Via S. Sofia 100, Catania, Italy
*Corresponding author. E-mail: dalia.aiello@unict.it

Summary. Mango trees (*Mangifera indic*a) showing symptoms of twig and branch dieback, internal wood necroses, and decline, were surveyed in an orchard in Palermo province (Eastern Sicily, Italy). A *Pleurostoma*-like fungus was consistently isolated from symptomatic wood tissues. Based on morphology and phylogenetic analysis of ITS and *tub2* sequences, the fungus was identified as *Pleurostoma richardsiae*. A pathogenicity test was conducted by inoculating stems of 2-year-old mango seedlings with mycelium plugs and conidium suspensions of a representative isolate. Two months after inoculation, necrotic lesions were observed around the inoculation points, and *P. richardsiae* was reisolated from the necrotic tissues. This is the first report of *P. richardsiae* causing dieback and decline of mango trees.

Keywords. Fungal diseases, *Mangifera indica*, wood necrosis, twig dieback, phylogeny.

Citation: G.R. Leonardi, D. Aiello, G. Gusella, G. Polizzi (2024) Characterization and pathogenicity of *Pleurostoma richardsiae* causing decline of mango trees in Southern Italy. *Phytopathologia Mediterranea* 63(1): 111-118. doi: 10.36253/phyto-15104

Accepted: March 23, 2024

Published: May 13, 2024

Data Availability Statement: All relevant data are within the paper and its Supporting Information files.

Competing Interests: The Author(s) declare(s) no conflict of interest.

Editor: Luisa Ghelardini, University of Florence, Italy.

ORCID:
GRL: 0000-0002-4676-5100
DA: 0000-0002-6018-6850
GG: 0000-0002-0519-1200
GP: 0000-0001-8630-2760

Mango (*Mangifera indic*a L.; *Anacardiaceae*) is a fruit tree crop that is native to India and Southeast Asia (Mukherjee, 1953). Mango is widely cultivated especially in tropical and subtropical regions. In recent years, its cultivation has increased in the Mediterranean basin, due to the popularity of the fruit among European consumers and good productivity, and adaptability of the species to different environments. In Italy, the cultivation of subtropical crops is mainly concentrated in the coastal regions of Sicily (Palermo, Messina, and Catania provinces), where climate and soil conditions are suitable (Lauricella *et al.,* 2017). The growing interest in the mango fruit is due to their high content of bioactive compounds beneficial for human nutrition and health, which makes it attractive for direct consumption and useful for food and pharmaceutical industries (Maharaj *et al.,* 2022; García-Mahecha *et al.,* 2023).

In Italy, few pre- and post-harvest fungal diseases of mango have been reported. The most production-limiting diseases include canker and shoot blight caused by *Botryosphaeriaceae* spp. (Aiello *et al.,* 2022), and fruit decay and stem-end rot caused by *Colletotrichum* spp. (Ismail *et al.,* 2015). Stem-end rot of fruit caused by *Neofusicoccum* spp. has also been occasion-

Figure 1. Decline of mango trees 'Glenn' grafted on 'Gomera 3', caused by *Pleurostoma richardsiae* in an orchard located in Bagheria (Palermo, Italy). (a) Dieback of twigs and branches showing necroses of inner wood tissues. (b) Severe dieback of a mango tree.

ally observed (Ismail *et al.,* 2013a). Leaf spots caused by *Pestalotiopsis uvicola* and *P. clavispora* (Ismail *et al.,* 2013b), and wilt caused by *Verticillium dahliae* (Ahmed *et al.,* 2014), have also been reported.

Since 2021, dieback of twigs and branches was observed on 6-year-old mango trees ('Glenn' grafted on 'Gomera 3' rootstocks) during surveys of mango orchards in Bagheria (Palermo province, Italy). Affected trees had declining vegetation vigour during the year, followed by rapid dieback of twigs and branches, often leading to tree death (Figure 1). During a survey in May 2023, examination of cross-sections of branches and twigs of declining and low vigour trees revealed irregular, brown to black wood necroses, co-occurring in some cases with black spots and reddish-brown to black streaking of the inner wood tissue (Figure 2). Further observations detected canopy thinning and dry leaves hanging from the twigs. The sudden decline observed after years of slow and stunted growth made disease incidence variable, with few plants showing dieback at each season, and disease incidence based on these symptoms was approx. 10%.

Twigs and branches showing internal necroses were randomly collected from five plants, and were kept in plastic bags and taken to a laboratory for pathogen isolation and further analyses. Small wood fragments (3 × 3 × 3 mm, n = 160) from the margins of necrotic or apparently healthy tissues were surface sterilized in a 1.2% sodium hypochlorite solution for 60 s, and then rinsed once in sterile distilled water for 60s. The fragments were air dried in a laminar-flow cabinet on sterile paper, placed on potato dextrose agar (PDA, Lickson) amended with lactic acid (APDA; containing 1 mL L^{-1} of 98% [vol/vol] lactic acid), and were then incubated at approx. 25°C under natural light for 10 d. One type of fungal colony consistently grew from the symptomatic mango tissues, with isolation frequency of 60 to 72%. From twelve representative *Pleurostoma*-like colonies, single-conidium isolates were obtained, and were stored in the collection of the Dipartimento di Agricoltura, Alimentazione e Ambiente, section Patologia Vegetale, University of Catania.

Two representative isolates (CP23, CP28) were grown on acidified Malt Extract Agar (AMEA) at 25 ± 1°C for 21 d in the dark, to study colony morphology

Figure 2. Details of symptoms on a mango tree 'Glenn'. (a to d) Cross-sections of branches and twigs of declining trees with irregular, brown to black wood necroses. (e) Cross-section of a twig showing reddish-brown to black streaking in the inner wood tissue. (f) Longitudinal section of branch showing internal wood necrosis.

(texture, density, obverse and reverse colour, and margin), according to Vijaykrishna *et al.* (2004). Mycelium samples were mounted on microscope slides in lactic acid. Lengths and widths of conidia (n = 30) were measured at 100× magnification, using a Zeiss Axiolab 5 microscope and Zeiss Axiocam 208 color, using the software Zen Core (v.35.96.03000), and average dimensions and length/width ratios of the dimension means were calculated.

Colonies grown on AMEA for 20 d had white to off-white cottony appearance in the centres, with outwardly decreasing aerial hyphae extending to light grey, slightly uneven colony margins, as reported by Lawrence *et al.* (2021). The colonies produced two distinct types of conidia. One type were brown subglobose to spherical and thick-walled, with dimensions (min, average, max; length/width ratio ± standard error of the mean) of (1.5–) 2.2 (–3.1) × (1.5–) 2.0 (–2.8) µm; 1.1 ± 0.03. The other types were hyaline, cylindrical to oblong ellipsoidal, and thin-walled, with dimensions (4.5–) 5.3 (–6.8) × (1.8–) 2.6 (–3.5) µm; 2.4 ± 0.08.

All collected fungal isolates were grown on PDA for 14 d, and mycelium was then removed with a sterile scalpel. Genomic DNA was extracted using the Wizard Genomic DNA Purification Kit (Promega Corporation). The obtained DNA was stored at 4°C for further analyses. Two gene regions were amplified and sequenced. The internal transcriber spacer region (ITS) of the nuclear ribosomal RNA operon was amplified with the primers ITS5 and ITS4 (White *et al.,* 1990), and the primers Bt2a and Bt2b were used for the partial beta tubulin gene (*tub2*) (Glass and Donaldson, 1995). PCRs were carried out in a total volume of 25 µL, using One Taq® 2X Master Mix with Standard Buffer (BioLabs), according to the manufacturer's instructions. PCR conditions were set as follows: 30 s at 94°C; 35 cycles, each of 30 s at 94°C, 1 min at 52°C, and 1 min at 68°C; and 5 min at 68°C. PCR products were visualized on 1% agarose gels (90 V for 40 min) stained with GelRed® Nucleic Acid GelStain (Biotium), were purified, and then sequenced in both directions by Macrogen Inc. (Seoul, South Korea). The obtained forward and reverse DNA

Table 1. Fungal isolates from mango used in phylogenetic analysis. Isolates in bold font were obtained in the present study.

Fungal species	Isolate ID	Host	Location	GenBank accession number[b]	
				ITS	*tub2*
Calosphaeria africana	CBS 120870[a]	*Prunus armeniaca*	South Africa	EU367444	EU367464
Calosphaeria pulchella	CBS 115999[a]	*Prunus avium*	France	EU367451	KT716476
Flabellascus tenuirostris	CBS 138680[a]	*Fagus sylvatica*	Czech Republic	KT716466	KT716488
Jattaea algeriensis	STEU-6201[a]	*Prunus salicina*	South Africa	EU367446	EU367466
Jattaea ribicola	CBS 139779[a]	*Ribes petraeum*	Austria	KT716463	KT716480
Phaeoacremonium minimum	CBS 246.91[a]	*Vitis vinifera*	Yugoslavia	AF017651	AF246811
Phaeoacremonium novae-zelandiae	CBS 110156[a]	*Cupressus macrocarpa*	New Zeland	KF764572	DQ173110
Pleurostoma ochraceum	CBS 131321[a]	*Homo sapiens*	Sudan	JX073270	JX073271
Pleurostoma ootheca	CBS 115329[a]	Unknown	Thailand	MH862984	JX073272
Pleurostoma repens	CBS 294.39[a]	*Pinus* sp.	FL, USA	NR_135925	JX073273
Pleurostoma richardsiae	CBS 270.33[a]	Unknown	Sweden	AY179948	AY579334
P. richardsiae	EFA 317B	*Vitis* sp.	Spain	KX036522	KX036523
P. richardsiae	pr_GRAP	*Vitis vinifera*	Brazil	MG966406	MH053437
P. richardsiae	pr_OLIV	*Olea europaea*	Brazil	MG966416	MH053439
P. richardsiae	KARE488	*Prunus domestica*	Tulare County, CA	MT645621	MT734998
P. richardsiae	KARE1566	*Olea europaea*	San Joaquin County, CA	MT645625	MT735002
P. richardsiae	CP12	*Mangifera indica*	Bagheria (Sicily, Italy)	PP001252	PP025884
P. richardsiae	CP15	*Mangifera indica*	Bagheria (Sicily, Italy)	PP001253	PP025885
P. richardsiae	CP22	*Mangifera indica*	Bagheria (Sicily, Italy)	PP001254	PP025886
P. richardsiae	CP23	*Mangifera indica*	Bagheria (Sicily, Italy)	PP001255	PP025887
P. richardsiae	CP28	*Mangifera indica*	Bagheria (Sicily, Italy)	PP001256	PP025888
P. richardsiae	CP30	*Mangifera indica*	Bagheria (Sicily, Italy)	PP001257	PP025889
P. richardsiae	CP31	*Mangifera indica*	Bagheria (Sicily, Italy)	PP001258	PP025890
P. richardsiae	CP32	*Mangifera indica*	Bagheria (Sicily, Italy)	PP001259	PP025891
P. richardsiae	CP33	*Mangifera indica*	Bagheria (Sicily, Italy)	PP001260	PP025892
P. richardsiae	CP35	*Mangifera indica*	Bagheria (Sicily, Italy)	PP001261	PP025893
P. richardsiae	CP36	*Mangifera indica*	Bagheria (Sicily, Italy)	PP001262	PP025894
P. richardsiae	CP37	*Mangifera indica*	Bagheria (Sicily, Italy)	PP001263	PP025895

[a] Isolates linked to type specimens.
[b] ITS = internal transcribed spacer; *tub2* = beta-tubulin.

sequences were assembled, edited and aligned using MEGA X (Kumar *et al.,* 2018). All sequences of the ITS and *tub2* gene regions obtained were deposited in the National Centre of Biotechnology Information (NCBI) GenBank database (Table 1).

The obtained sequences were first compared with those available in GenBank. BLASTn searches of ITS and *tub2* sequences showed 99% similarity with the sequences of *Pleurostoma richardsiae* (Nannf.) Réblová & Jaklitsch (*Pleurostomataceae*, *Calosphaeriales*) isolate CBS 270.33 (GenBank accession No. MT153151.1), and 100% similarity with *P. richardsiae* isolate KARE1881 (GenBank accession No. MT735027.1). Phylogenetic analysis based on Maximum Parsimony (MP) was conducted on a concatenated dataset of ITS and *tub2,* including a total of 29 taxa, based on Lawrence *et al.* (2021). Multiple alignment was conducted in MEGA X. Maximum Parsimony analysis was carried out using Phylogenetic Analysis Using Parsimony (PAUP*) version 4.0a (Swofford, 2002), and *Phaeoacremonium minimum* CBS 246.91 and *Phaeoacremonium novae-zelandiae* CBS 110156 were used as the outgroups. The MP parameters were set as follows: heuristic search function and tree bisection and reconstruction (TBR) as branch swapping algorithms, with the branch swapping option set on "best trees" only. Gaps were treated as "missing", the characters unordered and of equal weight, and Maxtrees were limited to 100. MP scores including tree length (TL), consistency index (CI), retention index (RI), and rescaled consistency index (RC) were calculated. A total of 1,000 bootstrap replicates were performed to test the robustness of the tree topology. The MP analysis of the

combined dataset showed that of 1574 total characters, 512 were parsimony informative, 268 were parsimony-uninformative, and 794 were constant. In total, 100 trees were retained. Tree scores were: TL = 1874, CI = 0.688, RI = 0.649, and RC = 0.446. The MP analysis showed that the isolates from Bagheria clustered within the group of *P. richardsiae*, with strong support (bootstrap support 100) (Figure 3).

To assess pathogenicity of *P. richardsiae*, isolate CP28 was inoculated onto 2-year-old potted healthy plants of mango 'Gomera 3', which were maintained in a growth chamber at 25 ± 1°C with a 12 h photoperiod. The stem of each plant was surfaced disinfected with 70% ethanol and wounded with a sterilised 5 mm diam. cork borer. Agar plugs (5 mm diam.) taken from 30-d-old fungal cultures growing on AMEA at 25 ± 1°C, or 20 µL of conidium suspension (1×10^5 conidia mL^{-1}), were placed into each stem wound. A total of six plants were inoculated, with three plants per inoculation method and two inoculation sites per plant along the stem. Control plants were inoculated with AMEA plugs and sterile distilled water. After inoculation, the wounds were sealed with Parafilm®, and the plants were maintained at 25 ± 1°C in a growth chamber. After 2 months, bark was removed with a sterile blade, and lengths of lesions (upward and downward from inoculation points) were measured, and means were calculated. Re-isolations were carried out (as described above) to determine fulfilment of Koch's postulates, and proportions (%) of *Pleurostoma*-like colonies were determined.

Pathogenicity tests confirmed that *P. richardsiae* was pathogenic to mango trees, causing reddish-brown to black necrotic lesions in the wood of all the inoculated plants, and these lesions were visible 2 months after inoculation (Figure 4, b and c). Control plants did not show any symptoms, except those due to wound oxidation (Figure 4, a and d). Mean lesion length from *P. richardsiae* isolate CP28 was 2.25 ± 1.29 from conidium suspension inoculations, and 2.85 ± 0.47 cm from mycelium plug inoculations. Re-isolation frequency was 80%, and these fungal colonies matched the originally inoculated *P. richardsiae* isolate as indicated by colony and conidium morphology.

Pleurostoma richardsiae has been reported from many countries as the cause of diseases in important crops. The fungus is a severe vascular pathogen of olive in Brazil, California, Croatia, Greece, Italy, Spain and South Africa (Carlucci *et al.,* 2013; Nigro *et al.,* 2013; Markakis *et al.,* 2017; Ivic *et al.,* 2018; Canale *et al.,* 2019; Spies *et al.,* 2020; Agustí-Brisach *et al.,* 2021; Lawrance *et al.,* 2021; van Dyk *et al.,* 2021). This fungus was also

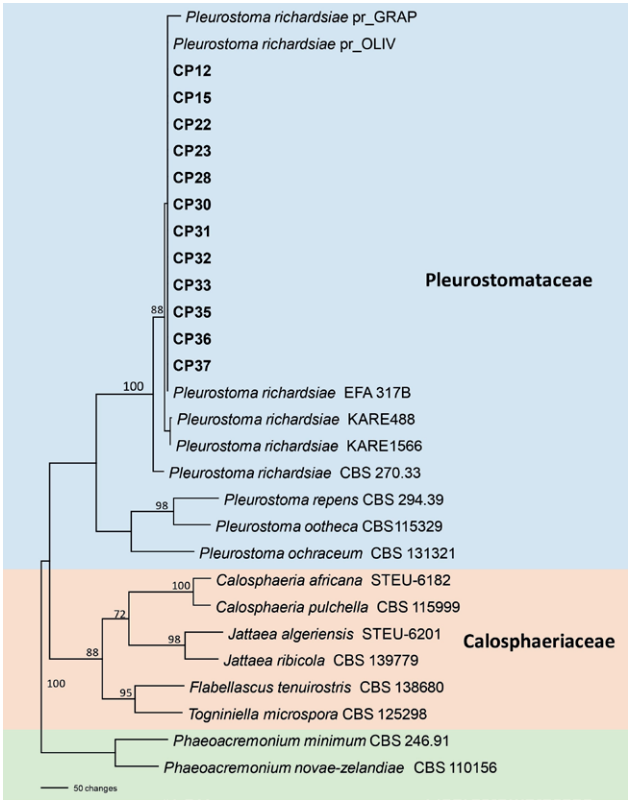

Figure 3. A parsimonious tree generated from maximum parsimony analysis of the two-gene (ITS + *tub2*) combined dataset. Numbers beside the clades represent parsimony bootstrap values from 1,000 replicates. Isolates in bold font were obtained in the present study. The bar indicates the number of nucleotide changes.

reported as a pathogen of grapevine in Brazil, California, Italy, Spain, and South Africa (Halleen *et al.,* 2007; Rolshausen *et al.,* 2010; Carlucci *et al.,* 2015; Pintos Varela *et al.,* 2016; Canale *et al.,* 2019). It was sometimes isolated from esca-affected vines, although its role in the disease has not yet been confirmed (White *et al.,* 2011). Avocado and nut crops have also been reported to be hosts of this pathogen (Olmo *et al.,* 2015; Markakis *et al.,* 2017; Sohrabi *et al.,* 2020). Several species of *Botryosphaeriaceae*, several *Phaeoacremonium* spp. and *Fomitiporia mediterranea*, have been isolated with *P. richardsiae* from woody tissues of grapevine (Pintos Varela *et al.,* 2016; Raimondo *et al.,* 2019), almond (Sohrabi *et al.,* 2020), and olive (Spies *et al.,* 2020; van Dyk *et al.,* 2021), showing the same symptoms. However, only *P. richardsiae* was isolated from symptomatic twig and branch tissues of mango trees in the present study.

This is the first report of *P. richardsiae* causing disease on mango trees. Future epidemiological studies are needed to assess the presence of *P. richardsiae* in mango

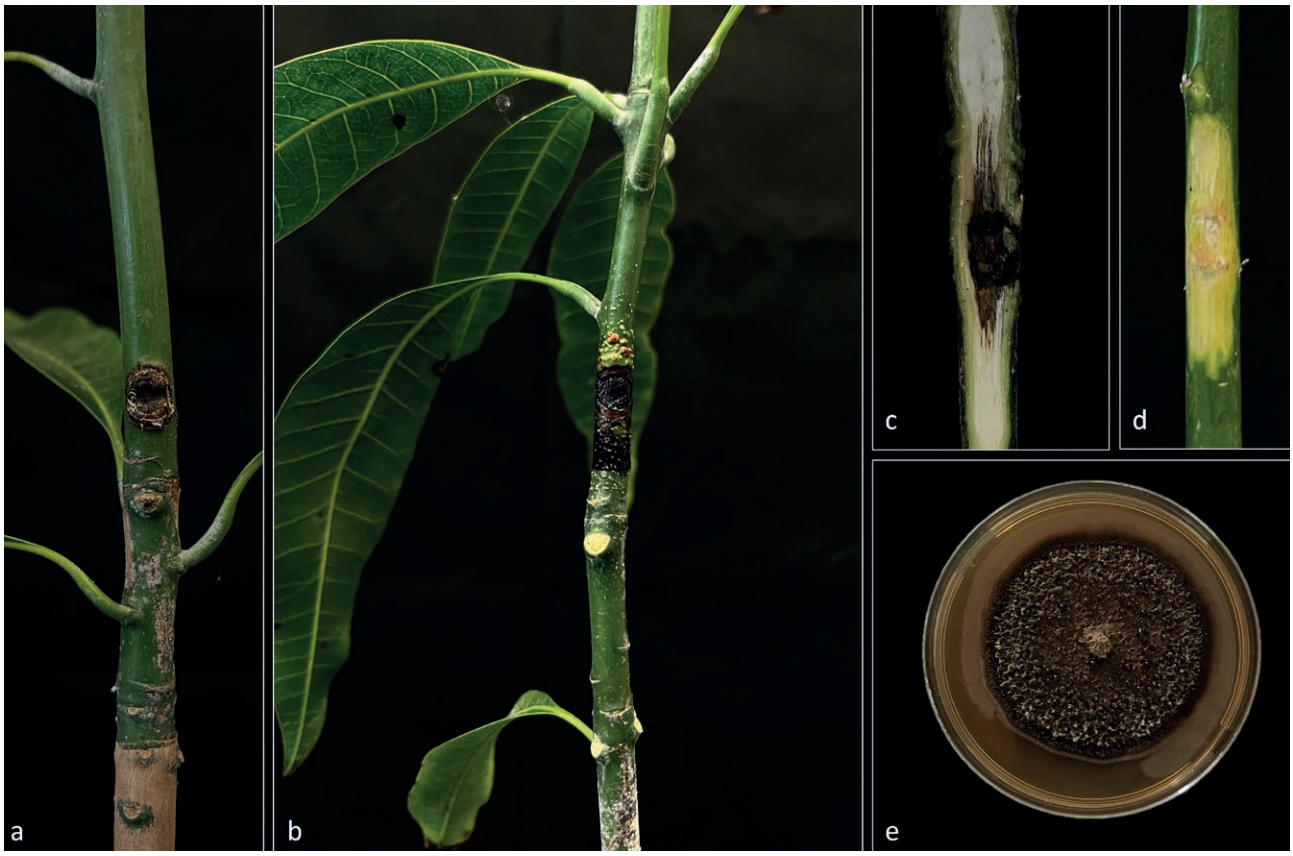

Figure 4. Pathogenicity test on mango seedlings 'Gomera 3'. (a) Agar plug inoculation control. (b) Stem inoculated with *Pleurostoma richardsiae* isolate CP28, showing a brown to black lesion. (c) An internal lesion produced by *P. richardsiae* isolate CP28 around the inoculation point. (d) Internal tissue of a control stem with no symptoms around the agar inoculation point. (e) Colony of *P. richardsiae* isolate CP22 grown on acidified malt extract agar for 30 d at 25°C.

orchards in other areas of Italy, and to evaluate possible effects of climate change on the emergence of new pathogen-host interactions. It is known that climate change may alter plant physiology and increase susceptibility to disease, and may also widen plant pathogen host ranges (Guarnaccia *et al.,* 2023; Joachin *et al.,* 2023). To date, *Botryosphaeriaceae* that cause canker and shoot blight of plants are considered the most damaging trunk pathogens for mangoes in Italy (Aiello *et al.,* 2022). The present record of severe damage of mango caused by *P. richardsiae* deserves attention for the risks it could pose to this important fruit tree crop.

FUNDING

Programma Ricerca di Ateneo MEDIT-ECO UNICT 2023–2024 Linea 2-University of Catania (Italy); Starting Grant 2020, University of Catania (Italy); Fondi di Ateneo 2023–2024, University of Catania (Italy), Linea Open Access. Research Project 201–62018, University of Catania 5A722192134.

DATA AVAILABILITY

Nucleotide sequences from this study are deposited in NCBI GenBank with the accession numbers reported in the paper text.

LITERATURE CITED

Agustí-Brisach C., Jiménez-Urbano J.P., Raya M.C., López-Moral A., Trapero A., 2021. Vascular fungi associated with branch dieback of olive in superhigh-density systems in southern Spain. *Plant Disease* 105: 797–818. https://doi.org/10.1094/PDIS-08-20-1750-RE

Ahmed Y., Cirvilleri G., D'Onghia A.M., Yaseen T., 2014. First report of Verticillium wilt of mango (*Mangifera*

indica) caused by *Verticillium dahliae* in Italy. *Plant Disease* 98: 1156. https://doi.org/10.1094/PDIS-02-14-0130-PDN

Aiello D., Guarnaccia V., Costanzo M.B., Leonardi G.R., Epifani F., … Polizzi G., 2022. Woody canker and shoot blight caused by Botryosphaeriaceae and Diaporthaceae on mango and litchi in Italy. *Horticulturae* 8: 330. https://doi.org/10.3390/horticulturae8040330

Canale M.C., Nunes Nesi C., Falkenbach B.R., Hunhoff Da Silva C.A., Brugnara E.C., 2019. *Pleurostomophora richardsiae* associated with olive tree and grapevine decline in southern Brazil. *Phytopatologia Mediterranea* 58: 201–205. https://doi.org/10.13128/Phytopathol_Mediterr-23357

Carlucci A., Raimondo M.L., Cibelli F., Phillips A.J.L., Lops F., 2013. *Pleurostomophora richardsiae*, *Neofusicoccum parvum* and *Phaeoacremonium aleophilum* associated with a decline of olives in southern Italy. *Phytopathologia Mediterranea* 52: 517–527. https://doi.org/10.14601/Phytopathol_Mediterr-13526

Carlucci A., Cibelli F., Lops F., Phillips A.J.L., Ciccarone C., Raimondo M.L., 2015. *Pleurostomophora richardsiae* associated with trunk diseases of grapevines in southern Italy. *Phytopatologia Mediterranea* 54: 109–123. https://doi.org/10.14601/Phytopathol_Mediterr-15257

García-Mahecha M., Soto-Valdez H., Carvajal-Millan E., Madera-Santana T.J., Lomelí-Ramírez M.G., Colín-Chávez C., 2023. Bioactive compounds in extracts from the agro-industrial waste of mango. *Molecules* 28(1): 458. https://doi.org/10.3390/molecules28010458

Glass N.L., Donaldson G.C., 1995. Development of primer sets designed for use with the PCR to amplify conserved genes from filamentous ascomycetes. *Applied Environmental Microbiology* 61: 1323–1330. https://doi.org/10.1128/aem.61.4.1323-1330.1995

Guarnaccia V., Kraus C., Markakis E.A., Alves A., Armengol J., … Gramaje D., 2023. Fungal trunk diseases of fruit trees in Europe: pathogens, spread and future directions. *Phytopathologia Mediterranea* 61: 563–599. https://doi.org/10.36253/phyto-14167

Halleen F., Mostert L., Crous P.W., 2007. Pathogenicity testing of lesser-known vascular fungi of grapevines. *Australasian Plant Pathology* 36: 277–285. https://doi.org/10.1071/AP07019

Ismail A.M., Cirvilleri G., Lombard L., Crous P.W., Groenewald J.Z., Polizzi G., 2013a. Characterisation of *Neofusicoccum* species causing mango dieback in Italy. *Journal of Plant Pathology* 95: 549–557. https://doi.org/10.4454/JPP.V95I3.008

Ismail A.M., Cirvilleri G., Polizzi G., 2013b. Characterisation and pathogenicity of *Pestalotiopsis uvicola* and *Pestalotiopsis clavispora* causing grey leaf spot of mango (*Mangifera indica* L.) in Italy. *European Journal of Plant Pathology* 135: 619–625. https://doi.org/10.1007/s10658-012-0117-z

Ismail A.M., Cirvilleri G., Yaseen T., Epifani F., Perrone G., Polizzi G., 2015. Characterisation of *Colletotrichum* species causing anthracnose disease of mango in Italy. *Journal of Plant Pathology* 97: 167–171. https://doi.org/10.4454/JPP.V97I1.011

Ivic D., Tomic Z., Godena S., 2018. First report of *Pleurostomophora richardsiae* causing branch dieback and collar rot of olive in Istria, Croatia. *Plant Disease* 102: 2648. https://doi.org/10.1094/PDIS-04-18-0669-PDN

Joachin J., Kritzell C., Lagueux E., Luecke N.C., Crawford K.M., 2023. Climate change and plant-microbe interactions: water-availability influences the effective specialization of a fungal pathogen. *Fungal Ecology* 66: 101286. https://doi.org/10.1016/j.funeco.2023.101286

Kumar S., Stecher G., Li M., Knyaz C., Tamura K., 2018. MEGA X: Molecular evolutionary genetics analysis across computing platforms. *Molecular Biology and Evolution* 35: 1547–1549. https://doi.org/10.1093/molbev/msy096

Lauricella M., Emanuele S., Calvaruso G., Giuliano M., D'Anneo A., 2017. Multifaceted health benefits of *Mangifera indica* L. (mango): the inestimable value of orchards recently planted in Sicilian rural areas. *Nutrients* 9(5): 525. https://doi.org/10.3390/nu9050525

Lawrence D.P., Nouri N.T., Trouillas F.P., 2021. Pleurostoma decline of olive trees caused by *Pleurostoma richardsiae* in California. *Plant Disease* 105(8): 2149–2159. https://doi.org/10.1094/PDIS-08-20-1771-RE

Maharaj A., Naidoo Y., Dewir Y.H., Rihan H., 2022. Phytochemical screening and antibacterial and antioxidant activities of *Mangifera indica* leaves. *Horticulturae* 8: 909. https://doi.org/10.3390/horticulturae8100909

Markakis E.A., Kavroulakis N., Ntougias S., Koubouris G.C., Sergentani C.K., Ligoxigakis E.K., 2017. Characterization of fungi associated with wood decay of tree species and grapevine in Greece. *Plant Disease* 101: 1929–1940. https://doi.org/10.1094/PDIS-12-16-1761-RE

Mukherjee S.K., 1953. Origin, distribution and phylogenetic affinities of the species of *Mangifera indica* L. *Journal of the Linnean Society of London, Botany* 55: 65–83. https://doi.org/10.1111/j.1095-8339.1953.tb00004.x

Nigro G., Boscia D., Antelmi I., Ippolito A., 2013. Fungal species associated with a severe decline of olive

in southern Italy. *Journal of Plant Pathology* 95: 668. https://doi.org/10.4454/JPP.V95I3.034

Olmo D., Armengol J., León M., Gramaje D., 2015. Pathogenicity testing of lesser-known fungal trunk pathogens associated with wood decay of almond trees. *European Journal of Plant Pathology* 143: 607–611. https://doi.org/10.1007/s10658-015-0699-3

Pintos Varela G., Redondo Fernandez V., Aguin Casal O., Ferreiroa Martinez V., Mansilla Vazquez J.P., 2016. First report of *Pleurostoma richardsiae* causing grapevine trunk disease in Spain. *Plant Disease* 100: 2168. https://doi.org/10.1094/PDIS-05-11-0429

Raimondo M.L., Carlucci A., Ciccarone C., Sadallah A., Lops F., 2019. Identification and pathogenicity of lignicolous fungi associated with grapevine trunk diseases in southern Italy. *Phytopathologia Mediterranea* 58(3): 639–662. https://doi.org/10.14601/Phyto-10742

Rolshausen P.E., Urbez-Torres J.R., Rooney-Latham S., Eskalen A., Smith R.J., Gubler W.D., 2010. Evaluation of pruning wound susceptibility and protection against fungi associated with grapevine trunk diseases. *American Journal of Enology and Viticulture* 61: 113–119. https://doi.org/10.5344/ajev.2010.61.1.113

Sohrabi M., Mohammadi H., León Santana M., Armengol F.J., Banihashemi Z., 2020. Fungal pathogens associated with branch and trunk cankers of nut crops in Iran. *European Journal of Plant Pathology* 157(2): 327–351. https://doi.org/10.1007/s10658-020-01996-w

Spies C.F.J., Mostert L., Carlucci A., Moyo P., Van Jaarsveld W.J., … Halleen F., 2020. Dieback and decline pathogens of olive trees in South Africa. *Persoonia* 45: 196–220. https://doi.org/10.3767/persoonia.2020.45.08

Swofford D.L., 2002. PAUP*: Phylogenetic analysis using parsimony (and other methods), version 4.0a165. Sinauer Associates, Sunderland, Massachusetts, USA.

van Dyk M., Spies C.F., Mostert L., van der Rijst M., du Plessis I.L., … Halleen F., 2021. Pathogenicity testing of fungal isolates associated with olive trunk diseases in South Africa. *Plant Disease* 105: 4060–4073. https://doi.org/10.1094/PDIS-08-20-1837-RE

Vijaykrishna D., Mostert L., Jeewon R., Gams W., Hyde K.D., Crous P.W., 2004. *Pleurostomophora*, an anamorph of *Pleurostoma* (*Calpshaeriales*), a new anamorphs genus morphologically similar to *Phialophora*. *Studies in Mycology* 50: 387–395. https://edepot.wur.nl/28946

White T.J., Bruns T., Lee S.J.W.T., Taylor J.L., 1990. Amplification and direct sequencing of fungal ribosomal RNA genes for phylogenetics. In: *PCR Protocols: a Guide to Methods andAapplications* (M.A. Innis, D.H. Gelfand, J.J. Sninsky, T.J. White, ed.), Academic Press, New York, 315–321. https://doi.org/10.1016/B978-0-12-372180-8.50042-1

White C.L., Halleen F., Mostert L., 2011. Symptoms and fungi associate with esca in South African vineyards. *Phytopathologia Mediterranea* 50: S236–S246. https://doi.org/10.14601/Phytopathol_Mediterr-8983

Phytopathologia Mediterranea
The international journal of the
Mediterranean Phytopathological Union

Firenze University Press
www.fupress.com/pm

Research Papers

Evaluation of fungicides for management of *Botryosphaeriaceae* associated with dieback in Australian walnut orchards

Stella ANTONY[1,2,*], Christopher C. STEEL[1,2], Benjamin J. STODART[1,2], Regina BILLONES-BAAIJENS[2,3], Sandra SAVOCCHIA[1,2]

[1] *Faculty of Science and Health, School of Agricultural, Environmental and Veterinary Sciences, Charles Sturt University, Locked Bag 588, Wagga Wagga, NSW 2678, Australia*
[2] *Gulbali Institute, Charles Sturt University, Locked Bag 588, Wagga Wagga, NSW 2678, Australia*
[3] *Current address: Affinity Labs, Australian Wine Research Institute, Adelaide, South Australia*
*Corresponding author. E-mail: astella@csu.edu.au

Summary. Dieback of fruiting spurs, stems and branches of walnut trees (*Juglans regia* L.), caused by *Botryosphaeriaceae*, is widespread in walnut orchards in Australia. Five species of *Botryosphaeriaceae* (*Diplodia seriata*, *Dothiorella omnivora*, *Neofusicoccum macroclavatum*, *N. parvum*, and *Spencermartinsia viticola*) were recovered from the Australian walnut orchards in a previous study, with *D. seriata* and *N. parvum* being the most prevalent. The present study evaluated inhibitory effects of ten fungicides on mycelium growth of those five species and on conidium germination of *D. seriata* and *N. parvum*. It investigated the preventative and curative efficacy of selected fungicides on disease incidence in glasshouse and field trials. *In vitro* experiments showed that nine of the fungicides reduced mycelium growth, and all ten inhibited conidium germination, but to varying extents. Tebuconazole, prochloraz manganese chloride, fluazinam, fludioxonil and pyraclostrobin were the most effective for inhibiting mycelium growth (EC_{50} < 0.14 µg a.i. mL^{-1}), whereas pyraclostrobin, fluxapyroxad, fluopyram, penthiopyrad and tebuconazole were the most effective for inhibiting conidium germination (EC_{50} < 2.2 µg a.i. mL^{-1}). *In planta* experiments with five fungicides confirmed that preventative treatments had greater efficacy than curative treatments. A field trial with four commercial fungicide formulations demonstrated that tebuconazole and tebuconazole + fluopyram provided protection of walnut trees for the longest period. The field trial also confirmed the efficacy of pyraclostrobin and the inhibitory effect of fluazinam. This study is the first in Australia to evaluate fungicides in different classes and with different modes of action for efficacy against *Botryosphaeriaceae* recovered from walnut orchards in Australia, and provides a wider selection of active ingredients for a fungicide rotation programme than that which is currently available to the Australian walnut industry.

Keywords. Dieback, *Diplodia seriata*, *Juglans regia*, *Neofusicoccum parvum*.

OPEN ACCESS

Citation: S. Antony, C.C. Steel, B.J. Stodart, R. Billones-Baaijens, S. Savocchia (2024) Evaluation of fungicides for management of *Botryosphaeriaceae* associated with dieback in Australian walnut orchards. *Phytopathologia Mediterranea* 63(1): 119-135. doi: 10.36253/phyto-14957

Accepted: April 1, 2024

Published: May 13, 2024

Data Availability Statement: All relevant data are within the paper and its Supporting Information files.

Competing Interests: The Author(s) declare(s) no conflict of interest.

Editor: Anne-Sophie Walker, Bioger, Inrae, Thiverval-Grignon, France.

ORCID:
SA: 0000-0002-8406-3564
CCS: 0000-0001-6126-880X
BJS: 0000-0002-3184-7998
RB-B: 0000-0001-9902-8684
SS: 0000-0001-7768-4170

INTRODUCTION

Australia has a young and expanding walnut industry. In recent years, yield losses caused by dieback of fruiting spurs, stems and branches has become widespread in walnut (*Juglans regia* L.) orchards, and *Botryosphaeriaceae* fungi have been implicated in the dieback syndromes. A first systematic survey conducted in 2019–2020 covered 14 orchards, representing all the major walnut-growing regions of Australia (Riverina in New South Wales, Adelaide Hills and Riverland regions in South Australia, the east coast of Tasmania, all of Victoria, and south-west Western Australia), and recovered five species of *Botryosphaeriaceae* from walnut tissues. The survey identified *Diplodia seriata* and *Neofusicoccum parvum* as the most prevalent species, constituting 93% of all isolates analysed by DNA sequencing. Pathogenicity studies confirmed the two prevalent species to be the most virulent among the five species, with *N. parvum* more virulent than *D. seriata* (Antony *et al*., 2023a). No published research has been conducted on control strategies for these pathogens in walnuts in Australia.

Symptoms of dieback, cankers, blight and fruit rot caused by *Botryosphaeriaceae* have been reported in walnut orchards in a number of countries, including Chile (Díaz *et al.,* 2018; Luna *et al.,* 2022), China (Yu *et al.,* 2015; Li *et al.,* 2016; Zhang *et al.,* 2017; Li *et al.,* 2023), the Czech Republic (Eichmeier *et al.,* 2020), Egypt (Haggag *et al.,* 2007), Greece (Rumbos, 1987), Iran (Abdollahzadeh *et al.,* 2013; Sohrabi *et al.,* 2020), Italy (Frisullo *et al.,* 1994; Gusella *et al.,* 2021), Korea (Cheon *et al.,* 2013), Spain (López-Moral *et al.,* 2020), Turkey (Kara *et al.,* 2021; Yildiz *et al.,* 2022), and the United States of America (Trouillas *et al*., 2010; Michailides *et al.,* 2012; Chen *et al.,* 2013; Chen *et al.,* 2014). Eighteen species of *Botryosphaeriaceae* from six genera have been recovered from walnut orchards in these countries. Economic losses caused by these pathogens has been estimated to be significant, although it is difficult to separate losses caused by other pathogens such as the *Diaporthe* spp. that cause similar symptoms (Moral *et al.,* 2019). *Botryosphaeriaceae* reduce yields by killing walnut tree branches, immature fruit, and wood, and by infecting nut (Hasey and Michailides, 2016). If dieback is not controlled, yield losses are likely to become more significant with successive harvests, and can lead to total crop failures (Michailides *et al.,* 2012).

Research on fungicide efficacy for control of these pathogens has not included *Botryosphaeriaceae* isolates recovered from Australia, despite well-established knowledge that plant pathogens evolve differently in different environments (van Niekerk *et al*., 2004; Slippers and Wingfield, 2007). A review of previous studies on fungicide efficacy against *Botryosphaeriaceae* in crops other than walnut and in other regions showed high variability in results, indicating that it is not possible to draw generalisations on the efficacy of the fungicides across crops and regions. Even within the same region and crop, fungicide efficacy has been found to vary between species of *Botryosphaeriaceae* (Bester *et al*., 2007; Amponsah *et al*., 2012; Pitt *et al*., 2012). Therefore, fungicide application programmes should be built on an understanding of incidence and prevalence of the target pathogens of specific hosts, in specific regions. Further research is required to assess the efficacy of fungicides for management of dieback in walnuts under Australian conditions.

No fungicides are currently registered in Australia for the control of *Botryosphaeriaceae* in walnuts, although two minor use chemical permits for formulations of pyraclostrobin [Fungicide Action Resistance Committee (FRAC) 11] and a mixture of tebuconazole (FRAC 3) plus fluopyram (FRAC 7) have been approved by the Australian Pesticides and Veterinary Medicines Authority (APVMA). This reliance on only two fungicides, with a total of three active ingredients (a.i.) that have single-site modes of action, may increase the potential risk for development of fungicide resistance among target pathogens, and is inadequate for development and implementation of a sustainable fungicide programme. Although there are no published reports of fungicide resistance developing in *Botryosphaeriaceae* associated with walnuts, reduced sensitivity of these fungi to multiple fungicides has been reported in other crops. In California, while comparing the baseline sensitivity to tebuconazole of *Botryosphaeria dothidea* populations from pistachio, Ma *et al.* (2002) identified an isolate with low sensitivity to tebuconazole. Their study also showed a shift towards greater tebuconazole EC_{50} values in orchards that had consecutive years of multiple applications of this fungicide. Similar studies in China identified emergence of tebuconazole resistance in populations of *B. dothidea* from apple orchards (Fan *et al*., 2016). This was attributed to use of consecutive multiple applications of tebuconazole for over 10 years. Likewise, resistance to pyraclostrobin has been reported to be common among *Lasiodiplodia theobromae* populations from mango in China (He *et al*., 2021; Yang *et al*., 2021). Decreased sensitivity to fluopyram has been reported in different host-pathogen systems including *Alternaria alternata* on pistachio (Avenot *et al*., 2014; Avenot *et al*., 2019) and *Botrytis cinerea* on strawberry (Amiri *et al*., 2014), after only a few years of field applications. Therefore, these resistance-prone fungicides should be used in the walnut orchards in Australia only with appropriate fungicide resistance management strategies in place.

One strategy to prevent development of fungicide resistance in pathogens is the alternation and/or combinations of contact and systemic fungicides, and inclusion of multi-site fungicides (Denman *et al*., 2004; Brent and Hollomon, 2007). Incorporating a.i. from different chemical groups with different modes of action in rotation programme, or using the fungicides in mixtures, is likely to reduce over-exposure of pathogens to only a few a.i. This could be achieved by considering the fungicides already in use in various horticultural crops to control fungal diseases, and identifying the most promising candidates that are effective against the prevalent *Botryosphaeriaceae* present in Australian walnut orchards.

Experiments were conducted to evaluate selected fungicides from different classes and modes of action, for their abilities to: (i) reduce *in vitro* mycelium growth of five species of *Botryosphaeriaceae* recovered from walnut orchards in Australia; (ii) inhibit *in vitro* conidium germination of the two most prevalent pathogens *D. seriata* and *N. parvum*; (iii) control infections by these fungi in glasshouse experiments on detached stems and glasshouse-grown walnut plants; and (iv) evaluate effective field durations of preventative and curative action that the fungicides have against the most virulent species, *N. parvum*.

MATERIALS AND METHODS

Efficacy of fungicides against in vitro *mycelium growth of fungal isolates*

Ten active ingredients from different chemical groups (Table 1) were identified for this experiment. Fungicides banned in the European Union and not

Table 1. Fungicides tested in this study.

Active ingredient (a.i.)	Chemical class, Mode of action[b]	FRAC code, Risk of fungicide resistance development[b]	Trade name and formulation used in *in vivo* experiments and in the field
Boscalid[a]	Carboxamide SDHI, single site	FRAC 7, medium to high	Only a.i. was used *in vitro*
Captan	Phthalimide Respiration inhibitor, multi-site	M04, low	Only a.i. was used *in vitro*
Fluazinam	Pyrrole, 2,6-initroanilines Energy synthesis disruptor, multi-site	FRAC 29, low	Emblem®, Nufarm Australia, 500 g L^{-1} fluazinam
Fludioxonil	Phenylpyrrole Osmoregulation inhibitor, single site	FRAC 12, low to medium	Geoxe®, Syngenta Australia, 500 g Kg^{-1} fludioxonil
Fluopyram[a]	Pyridinyl ethyl benzamide SDHI, single site	FRAC 7, medium to high	Only a.i. was used *in vitro*
Fluxapyroxad[a]	Carboxamide SDHI, single site	FRAC 7, medium to high	Only a.i. was used *in vitro*
Penthiopyrad[a]	Carboxamide SDHI, single site	FRAC 7, medium to high	Only a.i. was used *in vitro*
Prochloraz manganese chloride	Imidazole DMI, multi-site	FRAC 3, medium	Octave®, Bayer Crop Science, Australia, 500 g Kg^{-1}
Pyraclostrobin[a]	Methoxycarbamate QoI, single site	FRAC 11, high	Cabrio®[c], BASF Australia, 250 g L^{-1} pyraclostrobin
Tebuconazole[a]	Triazole DMI, single site	FRAC 3, medium	Orius®, ADAMA Agricultural Solutions Ltd, Australia, 200 g L-1 tebuconazole
Tebuconazole + Fluopyram[a]	DMI + SDHI	FRAC 3 + FRAC 7	Luna Experience®[c], Bayer Crop Science, Australia, 200 g L^{-1} tebuconazole + 200 g L^{-1} fluopyram

[a] Used in California for control of Botryosphaeria dieback in walnuts.
[b] Source: https://www.frac.info/
[c] Minor use chemical permit approved by the Australian Pesticides and Veterinary Medicines Authority for control of Botryosphaeria dieback in walnuts.
DMI = Demethylation Inhibitors (FRAC 3).
QoI = Quinone outside Inhibitors (FRAC 11).
SDHI = Succinate Dehydrogenase Inhibitors (FRAC 7).

approved by APVMA were excluded. The concentrations of each a.i. assessed were 0, 0.001, 0.01, 0.1, 1.0, or 10 mg L^{-1}. Efficacy of these concentration/a.i. combinations were tested on nine *Botryosphaeriaceae* isolates obtained from walnut orchards in Australia during the study of Antony *et al*. (2023a). The isolates tested included three isolates each of *D. seriata* and *N. parvum,* and one isolate each of *Dothiorella omnivora, N. macroclavatum* and *Spencermartinsia viticola*. For the two prevalent species, *D. seriata* and *N. parvum*, the three most virulent isolates (DS04, DS15, and DS27 of *D. seriata*; NP03, NP05 and NP18 of *N. parvum*) were selected based on a detached stem assay conducted previously (Antony *et al*., 2023a). For the other three fungi, one isolate per species was included since the total available isolates belonging to those species was only four.

Technical grade fungicide active ingredients were used in this experiment. Since some have low solubility in water (e.g., solubility of prochloraz mc in water is 34.4 mg L^{-1}. https://www.epa.govt.nz/), acetone, classified as a solvent (https://www.ncbi.nlm.nih.gov/) was used to dissolve them, as described by Pitt *et al*. (2012). For these fungicides, each a.i. was dissolved in 100% acetone, adjusted to a 10 mg L^{-1} stock solution, and diluted to: 1.0 mg L^{-1}, 0.1 mg L^{-1}, 0.01 mg L^{-1}, or 0.001 mg L^{-1}. Experimental controls contained acetone alone. These were used to prepare potato dextrose agar (PDA; Oxoid Ltd) plates amended with each a.i. After sterilization (121°C for 20 min), the medium was allowed to cool to 50°C, and acetone containing required amounts of each a.i. was added to the PDA to produce the required fungicide concentrations. In all batches of amended media, including the control, the final acetone concentration was adjusted to 0.1% v/v. These media were mixed, then poured into 9-cm diam. Petri plates and left to cool to room temperature.

The fungicide-amended PDA plates were each inoculated with a 5 mm diam. mycelium disc taken from the margin of an actively growing 3-d-old culture of each selected isolate that was previously cultured on PDA. For each isolate/fungicide/concentration combination three replicate plates were prepared. Within each fungicide/species combination, the inoculated PDA plates were arranged in a totally randomised design, and were incubated at 25°C in the dark. After incubation for 48 h, the mycelium growth in each plate was quantified by measuring the colony across two perpendicular diameters, and calculating the average diameter. Inhibition was then calculated by subtracting mean colony diameters from those of the nil fungicide experimental controls. Percent growth inhibition relative to the control was determined using the formula:

$$\text{Inhibition (percent)} = [(C\text{-}T)/C] \times 100$$

where C = average colony diameter on the control plate, and T = average colony diameter on the fungicide-amended plate.

Inhibition data were fitted to fungicide concentrations for each isolate and fungicide. The data were normalised by logarithmic transformation for fungicide concentrations, and the probit values were used for the inhibition data. The EC_{50} value for each fungicide/isolate concentration was calculated using R Statistical Software (v4.2.2; R Core Team 2022). Means were back transformed to the original scale. The experiment was repeated twice, and the EC_{50} values obtained in the three rounds of experiments were tested for homogeneity of variance using Levene's test. Since the Levene statistics were not significant (P = 0.172, indicating equality of variances), analysis of variance (ANOVA) was applied to the EC_{50} values to determine statistically significant differences between variables. A Generalised Linear Model (GLM) univariate analysis in IBM SPSS Statistics for Windows (Version 27.0. Armonk, New York: IBM Corp) was applied, and means were separated using Tukey's HSD test at $P < 0.05$.

Effects of fungicides on in vitro *conidium germination*

The same ten a.i. evaluated for the mycelium growth inhibition were tested for their effects on conidium germination of *D. seriata* and *N. parvum*. The same isolates of *D. seriata* and *N. parvum* used in the experiment described above were used to prepare conidium suspensions (10^4 conidia mL^{-1}) of the two species. To prepare the mixed isolate conidium suspension, an equal volume of filtered conidium suspension from each of the three selected isolates was combined in a sterile tube, as described by Antony *et al*. (2023b). Each a.i. was dissolved in acetone (as described above), and was then mixed with sterile distilled water (SDW) at twice the designated concentration so that, when mixed with an equal volume of conidium suspension or SDW, the resultant solution would achieve the designated concentration. For each germination evaluation, 100 µL of the mixed isolate conidium suspension was added to 100 µL of each a.i. solution, or 100 µL of SDW for the experimental control treatments. To establish the germination test for each fungicide/concentration/conidium suspension combination, three 50 µL drops were placed onto each of three replicate glass slides. Each slide was placed on a water moistened filter paper in a Petri plate, which was then sealed with parafilm to maintain high humidity. The plates were then arranged in a completely randomised

design, and incubated at 25°C in the dark. After 24 h of incubation, germination of 100 conidia was assessed within randomly selected microscope fields of view (×40 magnification) from each droplet. A conidium was considered to have germinated if the length of the germ tube was greater than half the length of the conidium. The percent germination inhibition data relative to the controls were calculated for each microscope slide, and the values were used to determine the EC_{50} for each fungicide and species, as described above for inhibition of mycelium growth. The experiment was repeated twice, and the EC_{50} values were investigated as described above.

Evaluation of fungicides: detached stem assays

Based on the efficacy of the a.i. for *in vitro* inhibition of mycelium growth and conidium germination, and considering their chemical classes and modes of action, six a.i. were selected for further assessment of their preventative and curative effects against *D. seriata* and *N. parvum* infections (Table 1). For five chemicals, (tebuconazole, pyraclostrobin, prochloraz mc, fluazinam and fludioxonil), commercial formulations that each had the individual a.i. as the only active constituent were used. The sixth fungicide was a mixture of two a.i., tebuconazole and fluopyram, and has a minor use permit approved by the APVMA for use in management of Botryosphaeria dieback in walnuts in Australia (Permit Number – PER91994. https://portal.apvma.gov.au/permits).

Asymptomatic 1-year-old dormant stems of walnut trees 'Chandler' were collected in winter from an orchard in Victoria, Australia. The stems were each pruned at the apical end and separately placed into 125 mL capacity plastic tubes filled with water. Two mixed isolate conidium suspensions were prepared with the three isolates each of *D. seriata* and *N. parvum* described above. The fungicides were mixed at label rates according to manufacturer recommendations. Since the commercial formulations contained additive required for dispersion in water, they were directly mixed with SDW, and then applied using 125 mL capacity spray bottles fitted with calibrated nozzles. For the preventative treatments, the stems were 'pruned and treated' immediately with 200 µL of the selected fungicide, and SDW was applied for the control treatment. On day 1, 3, or 7 post treatment, wounds of the stems were moistened by spraying with SDW and then each inoculated with 20 µL of a mixed isolate conidium suspension containing ~500 conidia of either *D. seriata* or *N. parvum*, using a micropipette. For the curative treatments, the stems were 'pruned and inoculated' immediately with a mixed isolate conidium suspension of either *D. seriata* or *N. parvum*. The inoculated pruning wounds were then sprayed with the selected fungicides at label rates, on either day 1, 3, or 7 post inoculation. For experimental control treatments, both positive (inoculated + no fungicide, designated "IC") and negative (non-inoculated + no fungicide, designated "NIC") controls were established without any fungicide application.

Each treatment was allocated to five walnut stems per replicate, and the experiment was set up with five replicates in a randomised complete block experimental design (RCBD), which was maintained in a glasshouse at ambient temperature of 17–25°C. The stems were assessed for lesion development 6 weeks after inoculation. The bark of each stem was peeled, and any internal and external lesions measured using a digital calliper. Wood segments excised from lesion margins were surface sterilised by soaking in 2% (v/v) sodium hypochlorite for 2 min, followed by rinsing twice in SDW. Fungal re-isolations were made by plating these wood segments onto PDA, to confirm Koch's postulates. After confirming homogeneity of variances, lesion lengths were analysed using univariate analysis as for the experiments described above.

Evaluation of fungicides using glasshouse plants

Of the six fungicides evaluated on detached walnut stems, five (tebuconazole, tebuconazole + fluopyram, pyraclostrobin, prochloraz mc, and fluazinam) were also tested on green walnut shoots, and four (tebuconazole, tebuconazole + fluopyram, pyraclostrobin, and fluazinam) were tested on 1-year-old stems of potted walnut plants 'Chandler', grown under glasshouse conditions. Both the preventative and curative efficacy of the fungicides against *D. seriata* and *N. parvum* were assessed on 1-year-old host stems; however, due to the limited availability of plants and considering industry requirements at that time for curative protection of young trees post-pruning for form training, only curative effects of five fungicides were assessed on green walnut shoots.

In the green shoot experiment, each treatment was assigned to three replicate plants in a RCBD. Three green shoots of similar thickness were identified on each plant. The shoots were tip pruned at ~12–15 cm from the basal ends, and were each immediately inoculated with 20 µL of a mixed isolate conidium suspension containing ~500 conidia of either *N. parvum* or *D. seriata*. Following inoculation, each treated shoot was covered with a transparent plastic bag for 24 h to reduce evaporation of the conidium suspension. Twenty-four hours after pruning and inoculation, wounds were sprayed with the selected fungicides mixed at label rates. Positive and negative

control stems were not given any fungicide spray. The plants were maintained in the glasshouse at ambient temperature of 17–25°C. The shoots were assessed for lesion development as described (above) for the detached stem assay 8 months after inoculation. Fungal re-isolations from lesion margins and analysis of lesion lengths were carried out as described above.

The experiment on 1-year-old stems was set up with four replicate potted walnut plants 'Chandler', grown under glasshouse conditions. Two stems of similar size were identified on each plant, one for a preventive treatment and the other for the corresponding curative treatment. For the curative treatments, inoculations and treatments were applied as described (above) in the green shoot experiment. For the preventive treatments, the stems were 'pruned and immediately treated' with the selected fungicides. The control stems were treated with SDW. Twenty-four hours after pruning and treatment, inoculations were carried out with mixed isolate conidium suspensions of *N. parvum* and *D. seriata* as described (above) for the detached stem assays. The inoculated plants were maintained in a glasshouse at ambient temperature of 17–25°C. The stems were assessed for lesion development 12 months after inoculation, as described (above) in the green shoot experiment. Fungal re-isolations from lesion margins and analyses of lesion lengths were carried out as described above. Fungal re-isolations were also carried out from 10 mm beyond each lesion margin, at 5 mm above the base of the closest side shoot and 5 mm below the node of the closest side shoot, to monitor pathogen progression beyond each dieback.

Field evaluation of fungicides

A field trial was established to evaluate the four most promising fungicides against *N. parvum* in walnut, as indicated from the *in vitro* and *in vivo* experiments, and to assess the duration of fungicide efficacy from preventative and curative treatments. The field trial was conducted from June 2022 to May 2023 in a commercial walnut orchard located in New South Wales (NSW), Australia. Efficacy of the fungicide treatments tebuconazole, tebuconazole + fluopyram, pyraclostrobin, or fluazinam were compared to an experimental control treatment of SDW, for providing preventative and curative protection, with six application timings, three of which were preventative and three were curative. The trial was established as a RCBD, with six replications, in 20-year-old walnut trees 'Chandler' with no observable disease symptoms. Within a replicate, each treatment was allotted to a tree, and in each tree, six 1-year-old stems were tagged for the allotted treatment.

For the preventative treatments, as in the glasshouse experiments, the identified stems were pruned and the treatments were immediately applied to the pruning wounds, using a paintbrush. A 20 µL mixed isolate conidium suspension of *N. parvum* (~500 conidia) was applied to each wound with a micropipette at either day 1, 7 or 14 post 'pruning and treatment'. For the experimental control treatment, stems were treated with SDW immediately after pruning, and then inoculated as described for the other preventative treatments. For the curative treatments, immediately after pruning the stems, the wounds were each inoculated with a 20 µL mixed isolate conidium suspension of *N. parvum* containing ~500 conidia. The fungicide treatments were applied either at day 1, 3 or 7 post 'pruning and inoculation'. For the positive experimental control (IC), stems were inoculated with conidium suspension of *N. parvum,* and no fungicide treatment was applied post inoculation. For the negative experimental control (NIC), stems were inoculated with SDW, and no further fungicide treatment was applied. Twelve months after inoculation, the treated stems were harvested for assessment of lesion development. Lesion lengths were measured, and fungal re-isolations were attempted from the margins of the lesions to confirm Koch's postulates.

Levene's test of equal variances applied to lesion length data confirmed homogeneity of variances. Differences in treatment effects were then investigated by ANOVA of lesion lengths, by applying a univariate analysis in IBM SPSS Statistics for Windows, as for the experiments described above. For the three preventative treatments, disease inhibition was calculated by subtracting mean lesion lengths of the fungicide treatments from those of the SDW treatments, at the corresponding inoculation times. The mean percent control (MPC) was then calculated using the formula:

$$\text{MPC on day X inoculation} = [(IC_X\text{-}T_X)/IC_X] \times 100$$

where X = 1, 7, or 14; IC_X = lesion length corresponding to day X inoculation post SDW treatment; T_X = lesion length corresponding to day X inoculation post fungicide treatment.

For the curative treatments, MPC was calculated using the formula:

$$\text{MPC of day X treatment} = [(IC\text{-}T_X)/IC] \times 100$$

where X = 1, 3, or 7; IC = lesion length of the inoculated control; T_X = lesion length corresponding to day X treatment with fungicide.

RESULTS

Efficacy of fungicides against in vitro *mycelium growth of fungal isolates*

The fungicides varied in their effectiveness for inhibiting mycelium growth of the five fungi tested, with mean EC_{50} values for the species ranging from 0.004 to 154.6 mg a.i. L^{-1}. Captan gave the greatest mean EC_{50}, which was ~15 times greater than the maximum concentration of 10 mg L^{-1} used in this experiment. To remove the influence of this value for assessing the efficacy of the other fungicides, captan was not included in the statistical analysis presented in Table 2. The EC_{50} values for the individual treatments that were obtained in the three rounds of the experiment did not differ significantly ($F = 1.952$, $DF = 2$, $P = 0.146$), so the data were combined. Logarithmic transformation was applied to normalise the data for further analyses of variance, and the results were back transformed to original scale. Mean effects of the fungicides across pathogen species were calculated to evaluate the relative efficacy of the fungicides on the species present in the Australian walnut orchards. Similarly, pathogen species means across fungicides were calculated to assess the relative sensitivity of each pathogen to the fungicides tested.

An ANOVA of the EC_{50} values indicated that five fungicides (fluazinam, tebuconazole, fludioxonil, prochloraz, and pyraclostrobin) were the most effective, and they were similar in their inhibitory effects on mycelium growth, forming a homogenous group according to Tukey's HSD test at $P < 0.05$ (Table 2). Fluopyram and penthiopyrad were next in their effectiveness, followed by fluxapyroxad. Boscalid was moderately effective, as shown by the dose required for effective inhibi-

Table 2. Mean EC_{50} values for selected technical grade fungicide active ingredients (a.i.) for inhibition of *in vitro* mycelium growth of five *Botryosphaeriaceae* species.

Fungicide	Mean EC_{50} (mg a.i. L^{-1}) values[a] and standard error within parentheses					
	Botryosphaeriaceae species					Fungicide mean effect[b]
	Diplodia seriata	*Dothiorella omnivora*	*Neofusicoccum macroclavatum*	*N. parvum*	*Spencermartinsia viticola*	
Boscalid	11.378	0.627	29.128	28.325	0.106	13.913 d
	(0.44)	(0.02)	(0.69)	(0.48)	(0.07)	(3.41)
Fluazinam	0.005	0.002	0.007	0.007	0.001	0.004 a
	(0.0004)	(0.0001)	(0.001)	(0.0003)	(0.001)	(0.001)
Fludioxonil	0.013	0.032	0.016	0.011	0.001	0.015 a
	(0.0004)	(0.0002)	(0.001)	(0.0001)	(0.001)	(0.01)
Fluopyram	3.092	0.017	2.681	2.214	0.021	1.609 b
	(0.06)	(0.001)	(0.06)	(0.10)	(0.001)	(0.35)
Fluxapyroxad	4.711	0.023	5.586	4.252	0.02	2.915 c
	(0.32)	(0.01)	(0.05)	(0.67)	(0.002)	(0.65)
Penthiopyrad	4.238	0.051	2.181	2.033	0.024	1.705 b
	(0.22)	(0.02)	(0.27)	(0.24)	(0.004)	(0.43)
Prochloraz	0.015	0.030	0.030	0.005	0.0002	0.016 a
	(0.002)	(0.0001)	(0.01)	(0.0001)	(0.004)	(0.004)
Pyraclostrobin	0.105	0.072	0.082	0.385	0.008	0.131 a
	(0.01)	(0.002)	(0.01)	(0.01)	(0.01)	(0.04)
Tebuconazole	0.004	0.028	0.009	0.005	0.001	0.009 a
	(0.0001)	(0.0001)	(0.001)	(0.001)	(0.001)	(0.003)
Species mean[c]	2.616 y	0.096 x	4.413 z	4.142 z	0.020 x	
	(0.72)	(0.01)	(0.75)	(0.71)	(0.04)	

[a] EC_{50} = mean concentration (mg L^{-1}) of fungicide at which mycelium growth is inhibited by 50%.
[b] Data pooled across species, to provide mean EC_{50} values for fungicide efficacy.
[c] Data pooled across fungicides to provide mean EC_{50} values for species sensitivity.
Fungicide effects on the prevalent species *D. seriata* (A, B, C and D) and *N. parvum* (P, Q, R and S) were significantly different ($P < 0.001$). Fungicide mean effects (a, b, c and d) were significant ($P < 0.001$). For species, the mean effects (x, y and z) were significant ($P < 0.001$). Values within each row or column followed by the same letter are not significantly different ($P > 0.05$), according to Tukey's HSD test.

tion of mycelium growth. Intra-species variation was not significant for *D. seriata* or *N. parvum*, so only the species means are presented in Table 2. The species effect was significant ($P < 0.001$), with the five species falling into three groups. *Spencermartinsia viticola* (EC_{50} = 0.020 mg L^{-1}) and *Do. omnivora* (EC_{50} = 0.096 mg L^{-1}) were similar (P=0.724), and were the most sensitive to the fungicides, followed by *D. seriata* (EC_{50} = 2.616 mg L^{-1}). *Neofusicoccum macroclavatum* (EC_{50} = 4.413) and *N. parvum* (EC_{50} = 4.142) had similar sensitivities to the fungicides (P=0.208), and *Neofusicoccum* spp. had lower sensitivities to the fungicides than *D. seriata*.

Effects of fungicides on in vitro *conidium germination*

The *in vitro* experiment assessing conidium germination was repeated twice, and the EC_{50} values obtained in the three rounds did not differ significantly (P=0.79), so the data were combined for further analyses. The fungicides varied in their effectiveness for inhibiting conidium germination of *D. seriata* and *N. parvum*, with their mean fungicide EC_{50} values ranging from 0.21 to 9.00 mg a.i. L^{-1} (Table 3).

Pyraclostrobin was the most effective fungicide ($P < 0.001$), giving the lowest mean EC_{50} of 0.21 mg L^{-1}, followed by fluopyram, fluxapyroxad, penthiopyrad and tebuconazole with mean EC_{50}s between 1.26 and 2.15 mg a.i. L^{-1}. Boscalid (EC_{50} = 5.53 mg L^{-1}) and captan (EC_{50} = 6.33 mg L^{-1}) were similar (P=0.052), and next in their effectiveness. Prochloraz mc, fluazinam and fludioxonil were similar (P=0.983), and had greater mean EC_{50}s, between 8.76 and 9.00 mg a.i. L^{-1}, indicating lower efficacy compared to the other fungicides. The fungi differed in their sensitivities to the fungicides, with *N. parvum* showing lower sensitivity than *D. seriata* ($P < 0.001$) (Table 3).

Evaluation of fungicides: detached stem assay

All the fungicide treatments, both preventative and curative, were effective for reducing mean lesion lengths compared to the experimental controls. The fungi differed significantly in their sensitivities to the fungicides, with *N. parvum* having lower sensitivity than *D. seriata* ($P < 0.001$). All the preventative fungicide treatments reduced lesion lengths ($P < 0.001$) compared to the corresponding inoculated controls treated with SDW. All six fungicides reduced the lesion length on day 1 post treatment, to sizes similar to the NIC (Figure 1a). The later inoculations on day 7 post treatment resulted in lesions that were longer than the NIC, and the two tebuconazole formulations and prochloraz mc gave greater

Table 3. Mean EC_{50}s for selected technical grade fungicide active ingredients (a.i.) for *in vitro* inhibition of conidium germination of *Diplodia seriata* and *Neofusicoccum parvum*.

Fungicide	Mean EC_{50} (mg a.i. L^{-1}) values[a] and standard error (SE)					
	Diplodia seriata		*Neofusicoccum parvum*		Fungicide mean effect[b]	
	Mean and SE		Mean and SE		Mean and SE	
Boscalid	4.78 C	0.21	6.28 S	0.24	5.53 d	0.37
Captan	5.40 C	0.23	7.04 S	0.18	6.22 d	0.39
Fluazinam	7.69 D	0.18	9.86 T	0.20	8.76 e	0.50
Fludioxonil	8.11 D	0.23	9.64 T	0.22	8.88 e	0.37
Fluopyram	1.18 AB	0.23	1.35 Q	0.24	1.26 b	0.15
Fluxapyroxad	1.22 B	0.22	1.50 Q	0.13	1.36 b	0.13
Penthiopyrad	1.29 B	0.23	1.85 QR	0.24	1.57 bc	0.19
Prochloraz mc	8.67 D	0.21	9.33 T	0.24	9.00 e	0.20
Pyraclostrobin	0.17 A	0.12	0.24 P	0.12	0.21 a	0.08
Tebuconazole	1.43 B	0.22	2.87 R	0.20	2.15 c	0.35
Species mean effect[c]	3.99 x	0.59	5.00 y	0.68		

[a] EC_{50} = mean concentration (mg L^{-1}) of fungicide at which conidium germination was inhibited by 50%.
[b] Data pooled across species to provide mean EC_{50} values for fungicide efficacy.
[c] Data pooled across fungicides to provide mean EC_{50} values for species sensitivity.
Fungicide effects on *D. seriata* (A, B, C and D) and *N. parvum* (P, Q, R, S and T) were significant ($P < 0.001$). Fungicide mean effects (a, b, c, d and e) were significant ($P < 0.001$). For species, the mean effects (x and y) were significant ($P < 0.001$). Values within each row or column followed by the same letter are not significantly different ($P < 0.05$) according to Tukey's HSD test.

efficacy for lesion size reduction than the other three fungicides (Figure 1a).

Among the curative treatments, as for the preventative treatments, application of the fungicides 1 d post inoculation reduced lesion lengths that were similar ($P > 0.05$) to those from the NIC (Figure 1b). The two tebuconazole formulations applied at day 3 post inoculation gave similar efficacy, and reduced the lesion lengths to those similar to the NIC. Treatments on day 7 post inoculation, however, resulted in lesions that were longer ($P < 0.05$) than the NIC (Figure 1b). The other four fungicides gave various levels of efficacy when applied on days 3 or 7 post inoculation. Fludioxonil and fluazinam applied on day 7 resulted in the longest lesions compared to the corresponding treatments of the other four fungicides. However, those lesions were smaller ($P < 0.05$) than those from the inoculated control.

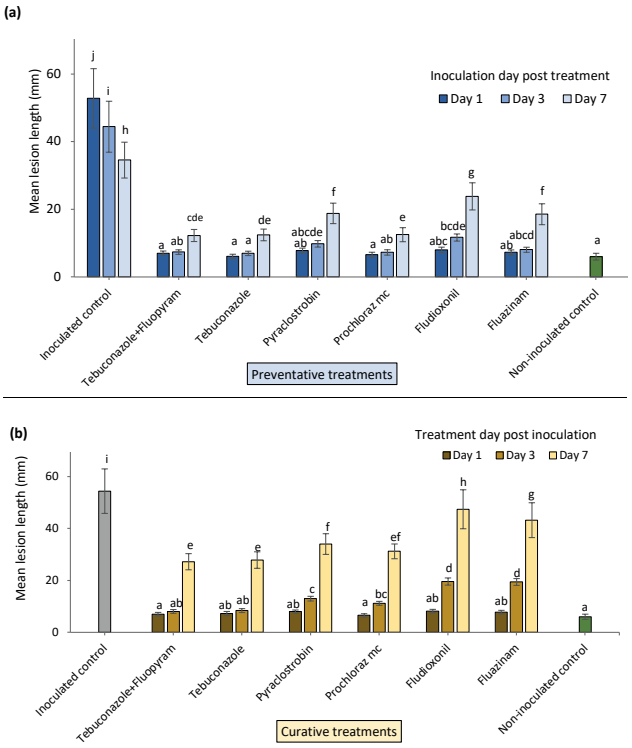

Figure 1. Mean lesion lengths caused by Botryosphaeria dieback pathogens on 1-year-old detached walnut stems after applications of six different fungicide products. (a) Preventative treatments with the fungicides, with inoculation of either *Diplodia seriata* or *Neofusicoccum parvum* at 1, 3 or 7 d after fungicide treatment. (b) Curative treatments with the fungicides, applied at 1, 3 or 7 d post inoculation with *D. seriata* and *N. parvum*. The error bars indicate standard errors of the means. Different letters associated with the means indicate differences ($P < 0.05$), according to Tukey's HSD test.

Evaluation of fungicides on glasshouse-grown plants

On green shoots of glasshouse plants, all five fungicides applied as curative treatments reduced the lesion lengths for both pathogen species, compared to the inoculated controls. The two tebuconazole formulations gave greater efficacy ($P < 0.05$) than pyraclostrobin (Figure 2). Prochloraz mc and fluazinam were not different ($P > 0.05$) from the other three fungicides for reducing lesion lengths (Figure 2). However, none of the treatments reduced the lesion lengths to the size of the NIC. Pathogen recovery from lesion margins was 17% from the fluazinam treatment and zero for the other four fungicide treatments.

On 1-year-old stems of glasshouse plants, the effects of fungicides as preventative treatments for reducing the lesion lengths were statistically significant ($P < 0.001$)

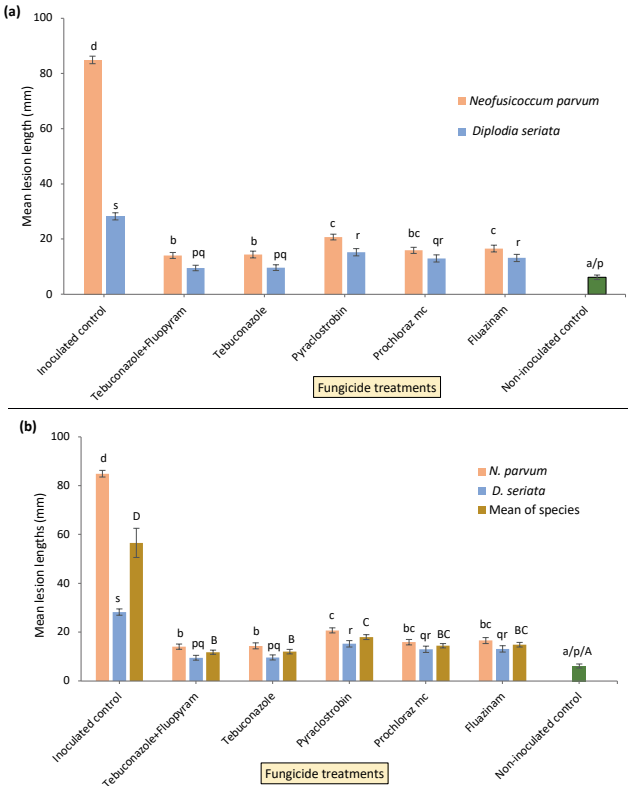

Figure 2. Mean lesion lengths caused by Botryosphaeria dieback pathogens on green shoots of glasshouse plants after curative fungicide treatments, applied 24 h after inoculations with conidium suspensions of *Neofusicoccum parvum* and *Diplodia seriata*. Figure 2a presents the effects of curative treatments on *N. parvum* and *D. seriata*. Figure 2b includes the mean effects of curative treatments on infections caused by the two pathogens. Error bars indicate standard errors of the means. Different letters on the bars (a, b, c and d for *N. parvum*; p, q, r and s for *D. seriata*; A, B, C and D for means of species) indicate differences ($P < 0.05$), according to Tukey's HSD test.

when compared to the controls inoculated with both pathogen species. The tebuconazole and fluazinam formulations had the greatest preventative efficacy, reducing lesion lengths to those similar from the NIC (Figure 3). Mean pathogen recovery from the lesion margins was zero for all the four preventative fungicide treatments.

The curative effects of the fungicides, applied 24 h post inoculation, were also statistically significant ($P < 0.001$), reducing the lengths of lesions resulting from inoculations with both fungi compared with the inoculated controls (Figure 3b). Although the four fungicides had similar curative effects ($P < 0.05$), none of the treatments reduced mean lesion lengths to those from the NIC. Mean pathogen recovery from the lesion margins was zero for all four fungicide treatments. For both the preventative and curative applications, fungal re-isolations from the three sites beyond lesion margins indicated that pathogen recovery from plant side shoots was zero, which indicates fungicide efficacy, but these isolations varied between zero and 25% from the main stems. Due to small sample sizes, these data were not further statistically analysed.

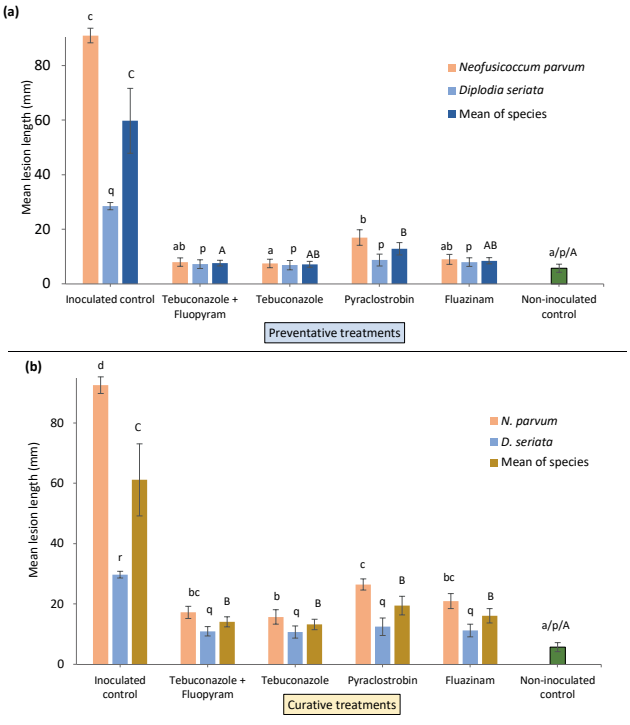

Figure 3. Mean lesion lengths caused by Botryosphaeria dieback pathogens on 1-year-old stems of glasshouse plants. (a) Preventative treatments with the fungicides, applied 24 h before inoculations with conidium suspensions of either *Diplodia seriata* or *Neofusicoccum parvum*. (b) Curative treatments with the fungicides, applied 24 h post inoculation with *D. seriata* and *N. parvum*. The error bars indicate standard errors of the means. Different letters associated with the means (a, b, c and d for *N. parvum*; p, q and r for *D. seriata*; A, B and C for means of species) indicate differences ($P < 0.05$), according to Tukey's HSD test.

Field evaluation of fungicides

All four fungicides provided preventative and curative protection of walnut trees against *N. parvum*, but for different periods and with different efficacies. Among the preventative treatments, the fungicides gave similar inhibitory effects ($P > 0.05$) on lesions caused by day 1 and day 7 inoculations (Figure 4a). The two tebuconazole formulations and pyraclostrobin were more effective for reducing lesions caused by day 14 inocula-

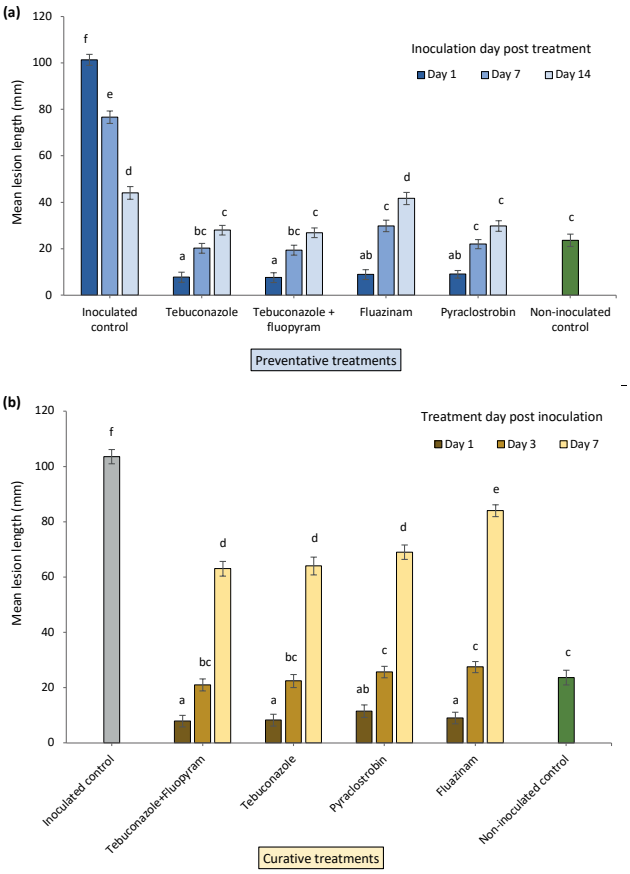

Figure 4. Mean lesion lengths caused by Botryosphaeria dieback pathogens on 1-year-old attached walnut stems in the field, after applications of four different fungicide products. (a) Preventative treatments with the fungicides, applied at 1, 7 or 14 d before inoculation with *Neofusicoccum parvum*. (b) Curative treatments with the fungicides, applied at 1, 3 or 7 d post inoculation with *N. parvum*. The error bars indicate standard errors of the means. Different letters associated with the means indicate differences ($P < 0.05$), according to Tukey's HSD test.

Table 4. Mean percent reductions in walnut tree dieback lesion lengths after conidium inoculations with *Neofusicoccum parvum* on pruned stems treated with different preventative or curative fungicide applications.

Fungicides	Reduction in lesion length compared to the control (%) Mean Percent Control and Standard Error (SE)											
	Preventative treatment						Curative treatment					
	Day 1		Day 7		Day 14		Day 1		Day 3		Day 7	
	Mean and SE		Mean and SE		Mean and SE		Mean and SE		Mean and SE		Mean and SE	
Fluazinam	91 a	2.09	61 b	3.23	05 d	3.99	91 a	2.07	73 c	2.00	19 e	2.12
Pyraclostrobin	91 a	1.62	71 b	2.58	32 c	4.79	89 ab	2.25	75 c	2.05	33 d	2.60
Tebuconazole	92 a	2.13	74 b	2.75	36 c	3.01	92 a	2.12	78 bc	2.35	38 d	3.20
Tebuconazole+fluopyram	93 a	2.08	75 b	2.80	39 c	3.85	92 a	2.08	80 bc	2.15	39 d	2.64

tions compared to fluazinam, which resulted in lesions similar ($P > 0.05$) to those from SDW treatment (Figure 4a). This indicates that fluazinam did not have any preventative effects on *N. parvum* at day 14. Among the curative treatments, the four fungicides were again similar in their effects when applied on day 1 or 3, and reduced the lesion lengths ($P < 0.05$) compared to the inoculated control (Figure 4b). The tebuconazole and pyraclostrobin formulations applied as curative treatments on day 7 were similar in their effects for reducing lesion lengths, and were more effective than fluazinam ($P < 0.05$; Figure 4b).

The preventative and curative treatments of the four fungicides were similarly effective, reducing mean lesion lengths by 89 to 93%, when time between treatment and inoculation was 1 d (Table 4). With increased time between treatment and inoculation, efficacy of the curative treatments reduced sooner than from the preventative treatments. Differences in efficacy of the fungicides also became apparent. The two tebuconazole formulations and the pyraclostrobin formulation had greater efficacy for a longer period than fluazinam. The preventative treatments were more effective for longer periods than the curative treatments, irrespective of the fungicide.

Neofusicoccum parvum was re-isolated from all inoculated controls treated with SDW. From the non-inoculated controls 20% pathogen recovery was recorded, which indicated presence of background *N. parvum* infections in the field. Pathogen recovery from lesion margins was zero for all preventative and curative treatments, when the time between treatment and inoculation was 24 h. When this time increased, pathogen recovery also increased, with curative treatments showing greater pathogen recovery than the preventative treatments. For fluazinam, pathogen recovery for later inoculations and later treatments was greatest, and varied between 35 and 90% compared to the corresponding results from treatments with the other three fungicides, that varied between 15 and 60%.

DISCUSSION

This study identified potential fungicides from different chemical classes and modes of action that could be incorporated into sustainable disease management for Botryosphaeria dieback in walnuts. In determining the efficacy of the selected fungicides, the study considered their inhibitory effects on both mycelium growth and conidium germination of the pathogen. Although natural field infections are instigated from conidia, inhibiting mycelium growth is also essential for effective disease control. Tebuconazole, fluopyram, pyraclostrobin, fluazinam, fludioxonil, fluxapyroxad, penthiopyrad, and prochloraz were effective for controlling mycelium growth and conidium germination of the assessed walnut pathogens, with EC_{50} values between 0.004 and 2.15 mg a.i. L^{-1}. These fungicides belong to seven different chemical classes, have five different modes of action, including single-site and multi-site inhibitors, and thus provide a wider selection for a fungicide rotation programme than that currently available to the Australian walnut industry. These fungicides were also among those tested and endorsed for efficacy in apple (Song *et al*., 2018), almond (Olmo *et al*., 2017), avocado (Twizeyimana *et al*., 2013), blueberry (Latorre *et al*., 2013; Tennakoon *et al*., 2019), and grapevine (Savocchia *et al*., 2005; Bester *et al*., 2007, Amponsah *et al*., 2012; Pitt *et al*., 2012).

Captan was also identified in this study as a possible candidate for management of Botryosphaeria dieback of walnuts. As a multi-site contact fungicide, this compound is at low risk for the development of fungicide resistance. Although captan *in vitro* inhibited mycelium growth at a relatively high concentration, it effectively

inhibited conidium germination of *D. seriata* (EC_{50} = 5.40 mg L^{-1}) and *N. parvum* (EC_{50} = 7.04 mg L^{-1}) with a mean EC_{50} of 6.22 mg L^{-1}. This result is consistent with those from previous studies on almond and blueberry that have reported high EC_{50} values for captan on *Botryosphaeriaceae* mycelium inhibition but lower values for inhibition of conidium germination (Olmo *et al*., 2017; Tennakoon *et al*., 2019). In Australia, captan is approved for use in pistachios for control of anthracnose (caused by *Colletotrichum acutatum*), and in almonds for control of anthracnose, blossom blight (*Monolinia laxa*), shot hole (*Wilsonomyces carpophilum*), and nut scab (*Cladosporium carpophilum*). Therefore, captan may provide disease management options when *Botryosphaeriaceae* spore populations and/or spore dispersal are high within nut orchards. Furthermore, incorporating a moderately effective fungicide in fungicide rotations is an anti-resistance strategy, since it reduces selection pressure on fungal pathogen populations (Brent and Hollomon, 2007).

The fungicides tested in the present study varied in their inhibitory effects on mycelium growth and conidium germination of pathogens causing Botryosphaeria dieback. Tebuconazole was the most effective for inhibiting mycelium growth of the pathogens, whereas its efficacy was less (ranked fifth of the ten fungicides studied) for reducing conidium germination. In contrast, pyraclostrobin was the most effective against conidium germination, but only fifth for reducing mycelium growth. Previous studies on management of *Botryosphaeriaceae* species in grapevine and blueberries in New Zealand have also reported that fungicides effective in reducing mycelium growth of pathogens generally did not perform well as inhibitors of conidium germination, and *vice versa* (Amponsah *et al*., 2012; Tennakoon *et al*., 2019). Although there was variation in the levels of efficacy among the fungicides, both pyraclostrobin and tebuconazole were among the top five fungicides for inhibition of both conidium germination and mycelium growth, confirming their important potential roles in Botryosphaeria dieback management programmes for walnut.

Tebuconazole and prochloraz, the two DMI fungicides assessed in this study, were among the top three compounds for inhibition of pathogen mycelium growth, but had less efficacy against conidium germination. Torres *et al*. (2013) reported that mycelia were more sensitive to DMIs than were conidia, in *Diplodia* and *Neofusicoccum* spp. associated with Botryosphaeria canker of grapevine. This response is attributed to the generic mode of action of the DMI fungicides, that inhibit sterol biosynthesis in fungi in the formation of cell membranes. This mode of action may be more effective against mycelium extension than for inhibition of conidium germination (Tennakoon *et al*., 2019).

The *in vitro* assessments of conidium germination showed that *N. parvum* was less sensitive than *D. seriata* to all the ten assessed fungicides. This result indicates a risk to the walnut industry, since *N. parvum* is one of the two most prevalent pathogens recovered from the Australian walnut orchards. This fungus caused lesions on green shoots and 1-year-old stems of glasshouse plants that were three times larger than those caused by *D. seriata*. This is similar to results from studies in major walnut-growing countries including Chile (Luna *et al*., 2022), China (Yu *et al*., 2015), Spain (López-Moral *et al*., 2020), and the United States of America (Chen *et al*., 2014), where *N. parvum* is considered one of the most aggressive pathogens causing walnut tree cankers and dieback. However, *N. parvum* was isolated only from two walnut-growing regions of Australia, New South Wales and Victoria both in southeastern Australia (Antony *et al*., 2023a). Furthermore, *N. macroclavatum*, isolated from a walnut orchard in southwestern Western Australia (Antony *et al*., 2023a), was similar to *N. parvum* in its sensitivity to these fungicides. Disease management programmes in these regions should take account of this occurrence, and ongoing monitoring is necessary for presence and/or absence of *Neofusicoccum* spp. in all walnut-growing regions of Australia.

The fungicides assessed in this study included one QoI (pyraclostrobin), two DMIs (prochloraz, tebuconazole) and four SDHIs (boscalid, fluopyram, fluxapyroxad, penthiopyrad), chemical classes that have been implicated in widespread development of fungicide resistance among target organisms. For instance, a study during 2010 to 2012 in strawberry fields in Florida found that 87% of the *B. cinerea* isolates tested were resistant to pyraclostrobin (Amiri *et al*., 2013). Resistance at this high level would mean complete failure of disease control and complete crop loss. In Australia, pyraclostrobin (QoI) and tebuconazole (DMI) were first approved by the APVMA in 2017 for disease management in walnut orchards (Lang and Simpson, 2018), pyraclostrobin for controlling Botryosphaeria dieback and tebuconazole for managing apical necrosis (*Alternaria* spp. and *Fusarium* spp.). Since then, the Australian walnut industry has used multiple applications of these two fungicides in each growing season for 5 years, until a mixture of fluopyram and tebuconazole was approved in 2022. Resistances to QoI and DMI fungicides have been reported in other crops following field applications over 2 years for QoIs and 7 years for DMIs (Brent and Hollomon, 2007). Therefore, field application of pyraclostrobin and tebuconazole for more than 7 years warrants careful monitoring for any changes

in pathogen sensitivity to these fungicides. The present study did not determine whether reduced efficacy of pyraclostrobin in the glasshouse and field experiments, compared to the tebuconazole formulations, was due to multiple applications of pyraclostrobin in commercial walnut orchards over the previous 6 years. Establishing baseline sensitivity data of the *Botryosphaeriaceae* spp. recovered from Australian walnut orchards, for fungicides to be included in rotation programmes, is an aspect requiring further research.

This study found that efficacy of the mixture of fluopyram (SDHI) and tebuconazole gave similar efficacy to formulation containing only tebuconazole. After a comprehensive review of experimental and modelling evidence, van den Bosch *et al*. (2014) supported use of fungicide mixtures containing chemicals with different modes of action as a resistance management strategy, even if the individual components belonged to at-risk categories for resistance development. However, use of mixtures with SDHIs requires careful monitoring for emergence of cross-resistance to other SDHIs. Cross-resistance patterns between boscalid and other SDHIs including fluopyram have been reported in other crops, and a fluopyram-resistant isolate of *A. alternata* showing cross resistance to other SDHIs was detected in pistachios (Avenot *et al*., 2014; Avenot *et al*., 2019). Shifts in sensitivity to SDHI constituents of fungicide mixtures should be monitored. Even with constituents other than SDHIs, it is possible that applications over successive years may lead to the survival of *Botryosphaeriaceae* isolates with high levels of resistance to the constituent fungicides. Therefore, strategies beyond using mixtures of at-risk fungicides are important for maintaining effective fungicide application programmes.

The detached stem assays, glasshouse experiments and field trial outlined here consistently showed that all the fungicides assessed were more effective when applied as preventative treatments than as curative treatments. This is similar to the results of Díaz and Latorre (2013), who found that regardless of the fungicide and application method, the treatments applied 24 h before inoculations with grapevine trunk disease pathogens gave better protection than treatments applied 24 h post-inoculation. The field trial also showed that the tebuconazole, tebuconazole + fluopyram and pyraclostrobin formulations gave high preventative efficacy for 7 d, and high curative efficacy for 3 d. The preventative efficacy was moderate for 14 d and curative efficacies were also moderate but only for 7 d. The present study used artificial inoculations with high numbers (~500) of conidia in the field experiment. In the natural inoculation processes, host wounds may not be exposed to this amount of inoculum, so under field conditions with natural inoculation in commercial orchards, tebuconazole, tebuconazole + fluopyram and pyraclostrobin may have better preventative and curative efficacy for longer periods (e.g. 2 weeks of preventative protection and 1 week of curative protection).

Periods of preventative and curative efficacy should be considered in light of host wound susceptibility periods, as has been reported to be greatest during the first week following wounding (Antony *et al*., 2023b). Therefore, an application of one of the three fungicides within 3 to 7 d following wounding may provide protection against *Botryosphaeriaceae* pathogens for 2 weeks. Similarly, for the multi-site contact fungicide fluazinam, an application within 3 d post wounding may provide effective protection for 1 week. These conclusions align with those from studies on grapevines (Sosnowski *et al*., 2017; Ayres *et al*., 2022). In field trials in California, Michailides *et al*. (2016) confirmed that most of the fungicides tested had long-term effects for reducing Botryosphaeria dieback in walnuts. However, the long-term effect may depend upon whether the fungicide has systemic or contact activity, and on the prevailing weather conditions such as rainfall at the time of fungicide application that may dilute or wash the fungicides off plant surfaces. These factors should be considered when identifying times for host pruning and fungicide applications.

This study has shown that the fungicides assessed as preventative and curative treatments in the glasshouse experiment prevented pathogen progression beyond the host lesion margins. Colonisation of *Botryosphaeriaceae* beyond lesion edges has been reported in previous studies in walnut, leading to recommendations that, to ensure the complete removal of infected wood, at least approx. 5 cm of the wood beyond the lesion edges should be removed (Michailides *et al*., 2016; Moral *et al*., 2019). For the isolates of *N. parvum* used in the present study, Antony *et al*. (2023b) have previously shown that in glasshouse plants, colonisation distances during 12 months on 1-year-old stems were up to 44 mm beyond lesion edges. In the present study, zero pathogen re-isolation at 5 mm and 10 mm beyond lesion edges 12 months after inoculations indicates that, when the time between treatment and pathogen exposure is less than 24 h, the assessed fungicides prevented further *Botryosphaeriaceae* colonisation, indicating efficacy of the treatments as wound protectants.

Although all the ten active ingredients assessed in this study were effective for inhibiting conidium germination of the pathogens, only four (tebuconazole, tebuconazole + fluopyram, pyraclostrobin, fluazinam) were tested under field conditions, and variations were

observed in duration of efficacy between fluazinam and the other fungicides. Developing an effective fungicide rotation programme will require establishment of the protective and curative efficacy periods for the other fungicides that were assessed in the present study.

While this study evaluated efficacy of fungicides for inhibition of *in vitro* mycelium growth for all five fungi recovered from Australian walnut orchards, further experiments on effects on conidium germination, detached stems, and glasshouse plants targeted only the two prevalent species, *D. seriata* and *N. parvum*. These two fungi were also the most virulent among the species recovered from Australian walnut orchards, with *N. parvum* more virulent than *D. seriata,* so these fungi were the focus of the study. Considering the intra-species variation in virulence among the isolates of these species on various types of walnut tissue (Antony *et al*., 2023b), to ensure the validity of the results for informing fungicide management strategies for the Australian walnut industry, three isolates were used for each prevailing pathogen. However, for the field experiment, *N. parvum* was selected because of its aggressiveness and potential for damaging productivity of the Australian walnut industry in Victoria and New South Wales. While the national survey recovered *N. parvum* from two states, *D. seriata* was recovered from all the walnut-growing regions in five Australian states. Further field trials are required, particularly for *D. seriata* and in walnut-growing regions of South Australia, where all the isolates recovered were identified as *D. seriata* (Antony *et al*., 2023a).

This study investigated efficacy of fungicides for reducing disease incidence on wounds created by tip pruning of walnut stems, since infections by the *Botryosphaeriaceae* are primarily through host wounds (Slippers and Wingfield, 2007; Adaskaveg *et al*., 2022). The present study has provided useful recommendations for protection of walnut trees from Botryosphaeria dieback when specific orchard activities (e.g., hedge pruning, tree training, canopy management) are employed that cause injuries to trees. There are also other factors that could contribute to disease pressure in walnut orchards. These include: latent infections by *Botryosphaeriaceae* (Slippers and Wingfield, 2007), internal infections from previous season's infected fruits that lead to invasion of pathogens into host spurs through peduncles (Michailides *et al*., 2014; Adaskaveg *et al*., 2017), and ability of *N. parvum* to penetrate non-wounded green tissues (Antony *et al.,* 2023a). To address these issues, development of integrated disease management is warranted, which incorporates rotational fungicide programmes with biological control agents, along with cultural and crop management strategies, including orchard hygiene, appropriately timed tree training practices and selection of disease-resistant cultivars.

ACKNOWLEDGEMENTS

The authors are grateful to: Charles Sturt University for funding this research through the Australian Government's Research Training Program; Gulbali Institute for funding this publication, the Australian Walnut Industry Association for its contribution to research operating funds, and to the walnut producer Stahmann Webster for access to the walnut orchard for the field experiment and for contributing to associated operating funds. Dr Michael D Lang provided valuable comments on the manuscript of this paper.

LITERATURE CITED

Abdollahzadeh J., Zare R., Phillips A.J.L., 2013. Phylogeny and taxonomy of *Botryosphaeria* and *Neofusicoccum* species in Iran, with description of *Botryosphaeria scharifii* sp. nov. *Mycologia* 105(1): 210–220. https://doi.org/10.3852/12-107

Adaskaveg J.E., Buchner R., Browne G.T., Gubler W.D., Michailides T.J., … Bostock R.M., 2017. Botryosphaeria and Phomopsis cankers. University of California Agriculture and Natural Resources (UCANR) Publication 3471. Accessed April 3, 2023 from https://www2.ipm.ucanr.edu/agriculture/walnut/Botryosphaeria-Dieback/

Adaskaveg J.E., Michailides T.J., Eskalan A., 2022. *Fungicides, Bactericides, Biocontrols, and Natural Products for Deciduous Tree Fruit and Nut, Citrus, Strawberry, and Vine Crops in California*. University of California Agriculture and Natural Resources. Accessed April 3, 2023 from http://ipm.ucanr.edu/PDF/PMG/fungicidefficacytiming.pdf

Amiri A., Heath S.M., Peres N.A., 2013. Phenotypic characterization of mixed fungicide resistance in *Botrytis cinerea* isolates from strawberry fields in Florida. *Plant Disease* 97(3): 393–401. https://doi.org/10.1094/pdis-08-12-0748-re

Amiri A., Heath S.M., Peres N.A., 2014. Resistance to fluopyram, fluxapyroxad, and penthiopyrad in *Botrytis cinerea* from strawberry. *Plant Disease* 98(4): 532–539. https://doi.org/10.1094/pdis-07-13-0753-re

Amponsah N.T., Jones E.E., Ridgway H.J., Jaspers M.V., 2012. Evaluation of fungicides for the management of botryosphaeriaceous dieback diseases of grapevines in New Zealand. *Pest Management Science* 68: 678–683. https://doi.org/10.1002/ps.2309

Antony S., Billones-Baaijens R., Stodart B.J., Steel C.C., Lang M.D., Savocchia S., 2023a. Incidence and distribution of Botryosphaeriaceae species associated with dieback in walnut orchards in Australia. *Plant Pathology* 72(3): 610–622. https://doi.org/10.1111/ppa.13685

Antony S., Billones-Baaijens R., Steel C.C., Stodart B.J., Savocchia S., 2023b. Pathogenicity and progression of Botryosphaeriaceae associated with dieback in walnut orchards in Australia. *European Journal of Plant Pathology.* Published online November 13, 2023. Print forthcoming. https://doi.org/10.1007/s10658-023-02794-w

Avenot H.F., van den Biggelaar H., Morgan D.P., Moral J., Joosten M., Michailides T.J., 2014. Sensitivities of baseline isolates and Boscalid-resistant mutants of *Alternaria alternata* from pistachio to fluopyram, penthiopyrad, and fluxapyroxad. *Plant Disease* 98: 197-205. https://doi.org/10.1094/pdis-04-13-0459-re

Avenot H.F., Luna M., Michailides T.J., 2019. Phenotypic and molecular characterization of resistance to the SDHI fungicide fluopyram in populations of *Alternaria alternata* from pistachio orchards in California. *Crop Protection* 124: 104838. https://doi.org/https://doi.org/10.1016/j.cropro.2019.05.032

Ayres M.R., Billones-Baaijens R., Savocchia S., Scott E.S., Sosnowski M.R., 2022. Critical timing of fungicide application for pruning wound protection to control grapevine trunk diseases. *Australian Journal of Grape and Wine Research* 28(1): 70–74. https://doi.org/10.1111/ajgw.12517

Bester W., Crous P.W., Fourie P.H., 2007. Evaluation of fungicides as potential grapevine pruning wound protectants against *Botryosphaeria* species. *Australasian Plant Pathology* 36(1): 73–77. https://doi.org/10.1071/AP06086

Brent K.J., Hollomon D.W., 2007. *Fungicide Resistance in Crop Pathogens: How Can it Be Managed?* Fungicide Resistance Action Committee (FRAC) Monograph No 1, second revised edition, FRAC. Accessed April 3, 2023 from https://www.frac.info/docs/default-source/publications/monographs/monograph-1.pdf?sfvrsn=8&sfvrsn=8

Chen S.F., Fichtner E., Morgan D.P., Michailides T.J., 2013. First report of *Lasiodiplodia citricola* and *Neoscytalidium dimidiatum* causing death of graft union of English walnut in California. *Plant Disease* 97(7): 993. https://doi.org/10.1094/PDIS-10-12-1000-PDN

Chen S.F., Morgan D.P., Hasey J.K., Anderson K., Michailides T.J., 2014. Phylogeny, morphology, distribution, and pathogenicity of *Botryosphaeriaceae* and *Diaporthaceae* from English walnut in California. *Plant Disease* 98(5): 636–652. https://doi.org/10.1094/PDIS-07-13-0706-RE

Cheon W., Kim Y.S., Lee S.G., Jeon Y.H., Chun I.-J., 2013. First report of branch dieback of walnut caused by *Neofusicoccum parvum* in Korea. *Plant Disease* 97(8): 1114–1114. https://doi.org/10.1094/pdis-12-12-1137-pdn

Denman S., Crous P.W., Sadie A., Wingfield M.J., 2004. Evaluation of fungicides for the control of *Botryosphaeria protearum* on *Protea magnifica* in the Western Cape Province of South Africa. *Australasian Plant Pathology* 33(1): 97–102. https://doi.org/10.1071/AP03080

Díaz G.A., Latorre B.A., 2013. Efficacy of paste and liquid fungicide formulations to protect pruning wounds against pathogens associated with grapevine trunk diseases in Chile. *Crop Protection* 46: 106–112. http://dx.doi.org/10.1016/j.cropro.2013.01.001

Díaz G.A., Latorre B.A., Ferrada E., Gutiérrez M., Bravo F., Lolas M., 2018. First report of *Diplodia mutila* causing branch dieback of English walnut cv. Chandler in the Maule region, Chile. *Plant Disease* 102(7): 1451. https://doi.org/10.1094/PDIS-11-17-1860-PDN

Eichmeier A., Pecenka J., Spetik M., Necas T., Ondrasek I., … Gramaje D., 2020. Fungal trunk pathogens associated with *Juglans regia* in the Czech Republic. *Plant Disease* 104(3): 761–771. https://doi.org/10.1094/PDIS-06-19-1308-RE

Fan K., Wang J., Fu L., Li X., Zhang Y., … Qu J., 2016. Sensitivity of *Botryosphaeria dothidea* from apple to tebuconazole in China. *Crop Protection* 87: 1–5. https://doi.org/10.1016/j.cropro.2016.04.018

Frisullo S., Lops F., Sisto D., Trombetta N.M. 1994. Pathogenic fungi in southern Italy. X. *Botryosphaeria ribis* Grossenb. et Duggar. on walnut. *Informatore Fitopatologico* 44(2): 61–64. Retrieved from https://www.cabdirect.org/cabdirect/abstract/19942309565

Gusella G., Giambra S., Conigliaro G., Burruano S., Polizzi G., 2021. Botryosphaeriaceae species causing canker and dieback of English walnut (*Juglans regia*) in Italy. *Forest Pathology* 51(1): e12661. https://doi.org/10.1111/efp.12661

Haggag W.M., Abou Rayya M.S. M., Kasim N.E., 2007. First report of a canker disease of walnut caused by *Botryodiplodia theobromae* in Egypt. *Plant Disease* 91(2): 226–226. https://doi.org/10.1094/PDIS-91-2-0226B

Hasey J., Michailides T.J., 2016. The latest on managing Bot canker and blight in walnut – 2016 Research Updates. *Sacramento Valley Orchard Source*. University of California Agriculture and Natural Resources. Retrieved

November 10, 2022, from https://www.sacvalleyorchards.com/walnuts/diseases/the-latest-on-managing-bot-canker-and-blight-in-walnut-2016-research-updates/

He R., Yang Y., Hu Z., Xue R., Hu Y., 2021. Resistance mechanisms and fitness of pyraclostrobin-resistant isolates of *Lasiodiplodia theobromae* from mango orchards. *PLoS One* 16(6): e0253659. https://doi.org/10.1371/journal.pone.0253659

Kara M., Soylu E.M., Soylu S., Uysal A., Kurt, Ş., 2021. First report of *Neofusicoccum parvum* causing branch dieback on *Juglans regia* in Turkey. *Journal of Plant Pathology* 103(1): 335–335. https://doi.org/10.1007/s42161-020-00662-8

Lang M.D., Simpson J.E., 2018. *Description and Management of Premature Fruit Drop in Walnuts*. Sydney, Australia: Hort Innovation; 2018. Report No.: WN13002. DOI: ISBN 978 0 7341 4380 8

Latorre B.A., Torres R., Silva T., Elfar K., 2013. Evaluation of the use of wound-protectant fungicides and biological control agents against stem canker (*Neofusicoccum parvum*) of blueberry. *Ciencia e Investigación agraria* 40(3): 537–545. https://doi.org/10.4067/S0718-16202013000300007

Li G., Liu F., Li J., Liu Q., Chen S.F., 2016. Characterization of *Botryosphaeria dothidea* and *Lasiodiplodia pseudotheobromae* from English walnut in China. *Journal of Phytopathology* 164(5): 348–353. https://doi.org/10.1111/jph.12422

Li C., Zhang M., Wei S., Yang Z., Pan X., 2023. Study of walnut brown rot caused by *Botryosphaeria dothidea* in the Guizhou Province of China. *Crop Protection* 163: 106118. https://doi.org/https://doi.org/10.1016/j.cropro.2022.106118

López-Moral A., Lovera M., Raya M.D.C., Cortés-Cosano N., Arquero O., Trapero A., Agustí-Brisach C., 2020. Etiology of branch dieback and shoot blight of English walnut caused by Botryosphaeriaceae and *Diaporthe* species in Southern Spain. *Plant Disease* 104(2): 533–550. https://doi.org/10.1094/PDIS-03-19-0545-RE

Luna I.J., Besoain X., Saa S., Peach-Fine E., Morales F.C., … Ashworth V.E., 2022. Identity and pathogenicity of Botryosphaeriaceae and Diaporthaceae from *Juglans regia* in Chile. *Phytopathologia Mediterranea* 61(1): 79–94. https://doi.org/10.36253/phyto-12832

Ma Z., Morgan D.P., Felts D.G., Michailides T.J., 2002. Sensitivity of *Botryosphaeria dothidea* from California pistachio to tebuconazole. *Crop Protection* 21: 829–835. https://doi.org/10.1016/S0261-2194(02)00046-7

Michailides T.J., Chen S.F., Coates W., Morgan D.P., Puckett R.D., … Bentley W., 2012. *Managing Anthracnose Blight and Botryosphaeria and Phomopsis Cankers of Walnut: Part I - Botryosphaeriaceae and Phomopsis Cankers of Walnuts*. Walnut Research Reports Database. Retrieved April 3, 2023, from 2012 Managing Anthracnose Blight and Botryosphaeria and Phomopsis Cankers of Walnut Part 1: Botryosphaeriaceae and Phomopsis Cankers of Walnut | Fruit & Nut Research & Information Center (ucdavis.edu)

Michailides T.J., Morgan D.P., Felts D.G., Hasey J., Puckett R.D., …Coates W., 2014. *Managing Botryosphaeria/Phomopsis Canker and Blight and Anthracnose Blight of Walnut in California*. Walnut Research Report 2014. Accessed April 3, 2023 from 2014 Managing Botryosphaeria/Phomopsis Canker and Blight and Anthracnose Blight of Walnut in California | Fruit & Nut Research & Information Center (ucdavis.edu)

Michailides T.J., Morgan D.P., Felts D.G., Luo Y., Puckett R.D., … Cunningham, C., 2016. *Epidemiology and Management of Botryosphaeria/Phomopsis Canker and Blight and Anthracnose Blight of Walnut in California*. Accessed April 3, 2023 from https://fruitsandnuts.ucdavis.edu/collaborators/california-walnut-board/reports/2016/2016-epidemiology-and-management

Moral J., Morgan D., Michailides T.J., 2019. Management of Botryosphaeria canker and blight diseases of temperate zone nut crops. *Crop Protection* 126. https://doi.org/10.1016/j.cropro.2019.104927

Olmo D., Gramaje D., Armengol J., 2017. Evaluation of fungicides to protect pruning wounds from Botryosphaeriaceae species infections on almond trees. *Phytopathologia Mediterranea* 56(1): 77–86. https://doi.org/10.14601/Phytopathol_Mediterr-19428

Pitt W.M., Sosnowski M.R., Huang R., Qiu Y., Steel C.C., Savocchia S., 2012. Evaluation of fungicides for the management of Botryosphaeria canker of grapevines. *Plant Disease* 96(9): 1303–1308. https://doi.org/10.1094/PDIS-11-11-0998-RE

Rumbos I.C., 1987. Twig and branch dieback of walnut trees induced by *Botryosphaeria ribis*. *Plant Pathology* 36(4): 602–605. https://doi.org/10.1111/j.1365-3059.1987.tb02281.x

Savocchia S., Laurent E.N., Stodart B.J., Steel C.C., 2005. Botryosphaeria canker and sensitivity to fungicides *in vitro*. *43rd Annual Congress of South African Society for Plant Pathology, 23–26 January, 2005,* Hartenbos, South Africa, p. 88 (2005).

Slippers B., Wingfield M.J., 2007. Botryosphaeriaceae as endophytes and latent pathogens of woody plants: Diversity, ecology and impact. *Fungal Biology Reviews* 21: 90–106. https://doi.org/10.1016/j.fbr.2007.06.002

Sohrabi M., Mohammadi H., León, M., Armengol J., Banihashemi Z., 2020. Fungal pathogens associated with branch and trunk cankers of nut crops in Iran. *European Journal of Plant Pathology* 157(2): 327–351. https://doi.org/10.1007/s10658-020-01996-w

Song Y., Li L., Li C., Lu Z., Men X., Chen F, 2018. Evaluating the sensitivity and efficacy of fungicides with different modes of action against *Botryosphaeria dothidea*. *Plant Disease* 102(9): 1785. https://doi.org/10.1094/PDIS-01-18-0118-RE

Sosnowski M.R., Savocchia S., Ayres M.R., Billones-Baaijens R., 2017. Practical management of grapevine trunk diseases. Accessed April 3, 2023 from https://www.wineaustralia.com/getmedia/8937f16f-d2a8-4152-947d-6a9ca873feab/Final-Report-SAR-1205_1

Tennakoon K.M.S., Ridgway H.J., Jaspers M.V., Langford G., Jones E.E., 2019. Evaluation of fungicide efficacy against *Neofusicoccum* species causing dieback disease of blueberries in New Zealand. *Australasian Plant Pathology* 48(1): 75–84. https://doi.org/10.1007/s13313-018-0565-9

Torres C., Latorre B.A., Undurraga P., Besoain X., 2013. Evaluation of DMI fungicides against species of *Diplodia* and *Neofusicoccum* associated with Botryosphaeria canker of grapevine. *Ciencia e Investigación Agraria* 40(1): 131–138. https://doi.org/10.4067/S0718-16202013000100011

Trouillas F.P., Úrbez-Torres J.R., Peduto F., Gubler W.D., 2010. First report of twig and branch dieback of English walnut (*Juglans regia*) caused by *Neofusicoccum mediterraneum* in California. *Plant Disease* 94(10): 1267–1267. https://doi.org/10.1094/pdis-06-10-0412

Twizeyimana M., McDonald V., Mayorquin J.S., Wang D.H., Na F., … Eskalen A., 2013. Effect of fungicide application on the management of avocado branch canker (formerly Dothiorella canker) in California. *Plant Disease* 97(7): 897–902. https://doi.org/10.1094/PDIS-06-12-0518-RE

van den Bosch F., Paveley N., van den Berg F., Hobbelen P., Oliver R., 2014. Mixtures as a fungicide resistance management tactic. *Phytopathology* 104(12): 1264–1273. https://doi.org/10.1094/PHYTO-04-14-0121-RVW

van Niekerk J.M., Crous P.W., Groenewald J.Z., Fourie P.H., Halleen F., 2004. DNA phylogeny, morphology and pathogenicity of *Botryosphaeria* species on grapevines. *Mycologia* 96(4): 781–798. https://doi.org/10.1080/15572536.2005.11832926

Yang Y., Dong G., Wang M., Xian X., Wang J., Liang X., 2021. Multifungicide resistance profiles and biocontrol in *Lasiodiplodia theobromae* from mango fields. *Crop Protection* 145: 105611. https://doi.org/https://doi.org/10.1016/j.cropro.2021.105611

Yildiz A., Benlioglu S., Benlioglu K., Korkom Y., 2022. Occurrence of twig blight and branch dieback of walnut caused by Botryosphaeriaceae species in Turkey. *Journal of Plant Diseases and Protection* 129(3): 687–693. https://doi.org/10.1007/s41348-022-00591-x

Yu Z., Tang G., Peng S., Chen H., Zhai M., 2015. *Neofusicoccum parvum* causing canker of seedlings of *Juglans regia* in China. *Journal of Forestry Research* 26(4): 1019–1024. https://doi.org/10.1007/s11676-015-0130-0

Zhang M., Zhang Y.K., Geng Y.H., Zang R., Wu H.Y., 2017. First report of *Diplodia seriata* causing twig dieback of English walnut in China. *Plant Disease* 101: 1036. https://doi.org/10.1094/PDIS-04-16-0458-PDN

Phytopathologia Mediterranea
The international journal of the
Mediterranean Phytopathological Union

Firenze University Press
www.fupress.com/pm

Research Papers

Bacillus velezensis B63 and chitosan control root rot, improve growth and alter the rhizosphere microbiome of geranium

Tarek R. ELSAYED[1], Nadia A.M. EL-SAID[2], Fatmah A. SAFHI[3], Nour El-Houda A. REYAD[4,*]

[1] *Microbiology Department, Faculty of Agriculture, Cairo University, Giza, Egypt*
[2] *Medicinal and aromatic plants Department, Horticulture Research Institute, Agriculture Research Center, Giza, Egypt*
[3] *Department of Biology, College of Science, Princess Nourah bint Abdulrahman University, P.O. Box 84428, Riyadh 11671, Saudi Arabia*
[4] *Plant Pathology Department, Faculty of Agriculture, Cairo University, Giza, Egypt*
*Corresponding author. E-mail: nouralhoda.ryad@agr.cu.edu.eg

Summary. The root rot complex of geranium plants caused by *Rhizoctonia solani* and *Macrophomina phaseolina* is a major threat, and control of these pathogens predominantly relies on chemicals. This study explored multifaceted applications of *Bacillus velezensis* (strain B63) and chitosan, assessing their biocontrol efficacy against root rot, and their subsequent effects on rhizosphere communities. Strain B63 was antagonistic to *R. solani* and *M. phaseolina*. Under field conditions, greatest efficacy was obtained with strain B63 (36% and 33% disease reductions in, respectively, two growing seasons), chitosan soaking + foliar spray 0.2% (CSF 0.2%) (33 and 27% reductions), and 0.1% chitosan soaking + foliar spray (CSF 0.1%) (33 and 26% reductions). These treatments also changed rhizosphere microbiota, as shown by numbers of colony-forming units (CFU) and 16S rRNA gene microbiome analyses. Concomitant with rhizosphere shifts, essential oil yields and composition were positively affected, as shown by gas chromatography analyses. Chitosan soaking + foliar spray 0.2% increased concentrations of citronellol (1.36-fold), geraniol (1.37-fold), citronellyl formate (1.54-fold), and geranyl formate (1.94-fold) in geranium essential oil, compared with the experimental controls. Strain B63 also increased these essential oils by 1.04- to 1.27-fold. B63 also enhanced eugenol levels by 1.35-fold. Treatments with B63 were more effective than chitosan in improving the geranium plant morphological parameters (plant height, numbers of branches, biomass). These results show that *B. velezensis* strain B63 treatments have potential for enhancing yields and product quality from geranium plant under root rot infection.

Keywords. Antagonistic bacteria, soil suppressiveness, marker genes, hydrodistillation, nitrogen fixation.

OPEN ACCESS

Citation: T.R. Elsayed, N.A.M. El-Said, F.A. Safhi, N.El-Houda A. Reyad (2024) *Bacillus velezensis* B63 and chitosan control root rot, improve growth and alter the rhizosphere microbiome of geranium. *Phytopathologia Mediterranea* 63(1): 137-154. doi: 10.36253/phyto-15093

Accepted: April 21, 2024

Published: May 13, 2024

Data Availability Statement: All relevant data are within the paper and its Supporting Information files.

Competing Interests: The Author(s) declare(s) no conflict of interest.

Editor: Ilaria Pertot, Centro Agricoltura, Alimenti, Ambiente, University of Trento, Italy.

ORCID:
TRE: 0000-0002-1272-6453
NAME-S: 0009-0004-1485-7045
FAS: 0000-0002-0533-614X
NE-HAR: 0000-0001-8048-3636

INTRODUCTION

Plant rhizosphere microbiomes play critical roles by promoting nutrient uptake, modulating plant immunity, suppressing pathogens, and controlling diseases (Olanrewaju and Babalola, 2022). Plants communicate with soil microbial communities through the exudation of a wide variety of compounds, boosting beneficial symbioses, modifying soil chemical and physical features, and inhibiting growth of plant pathogens. Plant roots secrete 5 to 21% of all photosynthetically fixed carbon in their rhizospheres (Simon and Haichar, 2019). Pathogenic microorganisms in soil can trigger plant immunity by modulating the root metabolism to engage root microbiota to stimulate plant defense and resistance to pathogens (Hou *et al*., 2021; Lyu and Smith, 2022). This has been illustrated in research by Liu *et al.* (2017), who discovered that when cucumber roots were attacked by *Fusarium oxysporum*, tryptophan was released and functioned as a signal to attract *Bacillus amyloliquefaciens*, which then protected cucumber from the pathogen. Wang *et al.* (2019) also demonstrated positive effects of lactic and hexanoic acids in tomato root exudates on the growth of *Bacillus cereus*, and reduction of host infection by *Ralstonia solanacearum*. Carrión *et al*. (2019) demonstrated that *Rhizoctonia solani* incited proliferation of *Chitinophaga*, *Flavobacterium*, and *Pseudomonas* spp. in sugar beet rhizospheres by activating their biosynthetic gene clusters to eliminate the fungal pathogen. A new hypothetical concept (the 'cry for help') has been proposed where plants under stress recruit beneficial microbiomes recruitment, and this protects them from detrimental effects, and can provide an array of growth-promoting benefits (Ali *et al*., 2023). Changes in rhizosphere microbiome composition could predict whether plants remain healthy or become infected by pathogens (Gu *et al*., 2022).

Geranium (*Pelargonium graveolens* L'Hér.) is a widely cultivated medicinal aromatic plant, which is extensively used for its essential oil (Narnoliya *et al*., 2019). Egypt, the second-largest producer and exporter of geranium oil after China, also holds second place following Reunion Island for the quality of its oil (Narnoliya *et al*., 2019). Geranium plants grown in Egypt are susceptible to several plant pathogens, including oomycetes and fungi. These include *Fusarium semitectum*, *Rhizoctonia solani*, *Macrophomina phaseolina*, and *Pythium ultimum*, which can cause significant damage and yield losses (Dewidar *et al*., 2019). This root rot complex (Yu *et al*., 2023) causes symptoms of rotted stems and roots, wilting or yellowing leaves, browning or blackening of the xylem vessels, and plant death (Prasad *et al*., 2008). While fungi attack geranium roots, early plant symptoms are often indistinct. As infections progress these can cause severe reductions in crop yields (Coque *et al*., 2020).

Different strategies have been developed to control root rot diseases, including cultural, physical, biological, and chemical control methods (Williamson-Benavides and Dhingra, 2021). Employing microbial antagonists and natural antifungal substances to improve soil suppressiveness and enhance plant defensive priming is a promising approach to controlling soil-borne fungal pathogens (Elsayed *et al*., 2020).

The success of introducing microorganisms for plant disease control is dependent on their adaptation and survival within host rhizospheres. Choosing the best microbial strain is critical, as it has direct impact on colonization density and effectiveness. *Bacillus*, a heterotrophic saprophyte, is common in soil and aquatic habitats, particularly in soils, where it exists as latent spores at temperatures near 0°C, allowing these bacteria to resist adverse environmental conditions (Maslennikova *et al*., 2023). *Bacillus velezensis*, particularly strains GB03, QST 713, FZB42, and D747, has commercial potential for disease biocontrol and host plant growth promotion (Vallejo, 2023). These bacteria directly combat infections through competition and antagonism, and indirectly support plant defenses and growth by stimulating production of protective chemicals (Chen *et al*., 2023).

Application of natural compounds is also useful for managing plant pathogens (Azmana *et al*., 2021). The macromolecules chitin and chitosan have been used in plant disease management. Chitosan is a natural polysaccharide found in the exoskeletons of crustaceans, insect cuticles, and fungus cell walls (Piras *et al.,* 2015). Chitosan has several agricultural applications, including promoting plant growth, eliciting plant resistance to biotic and abiotic stresses, and activation of symbiotic signalling between plants and beneficial microorganisms (Li *et al.,* 2020). This compound induces defense-related enzymes, accumulation of defense-related secondary metabolites, and increases nitrogen metabolism enzymes (Román-Doval *et al.,* 2023). Chitosan also creates physical barriers around pathogen penetrations and inhibits pathogen spread in host plants (El Hadrami *et al.,* 2010).

Previous studies have indicated successful control of *R. solani* and *M. phaseolina* using *Bacillus* spp. and chitosan. However, effects of *Bacillus* and chitosan on *R. solani* and *M. phaseolina*, and on bacterial soil microbiota, and geranium physiological and biochemical responses have not been defined. The purpose of the present study was to determine the influence of *B. velezensis* B63 and chitosan on soil microbiota and on geranium morphological and physiological parameters.

MATERIALS AND METHODS

Bacillus velezensis *(B63) and culture conditions*

Bacillus velezensis B63, known for its antibacterial and antifungal activities (Elsayed *et al*., 2020; Reyad *et al.,* 2022), was obtained from Dr Tarek R. Elsayed, Microbiology Department, Faculty of Agriculture, Cairo University, Giza, Egypt. The strain was cultivated in an Erlenmeyer flask containing 50 mL of Luria-Bertani broth (10 g of tryptone, 5 g of yeast extract, 10 g of NaCl, and 1 liter of distilled water. The pH was adjusted to 7.0 with 1 N NaOH) (Bertani 1951), and was incubated in a rotary shaker at 30°C. After 24 h, the bacterial cells were centrifuged (4500 g for 10 min); the pellet was then washed three times in sterile 0.85% NaCl, and the cell density was adjusted to OD_{600} = 1.0 (approx. 10^8 CFU mL^{-1}) in 0.85%. NaCl.

Chitosan preparation

One gram of Chitosan (crab shell, Sigma Chemical) was dissolved in 40 mL of distilled water containing 9 mL of 1 M acetic acid. Sodium acetate was used to adjust the pH to 6.0. Chitosan Solutions of 0.05%, 0.1%, and 0.2% chitosan were prepared from this stock solution (Anusuya and Sathiyabama, 2014).

Bacterial in vitro *antifungal activity against* Rhizoctonia solani *and* Macrophomina phaseolina

Rhizoctonia solani and *M. phaseolina* isolated from rotted geranium roots were obtained from our previous work (Reyad *et al*., 2022).

The antagonistic effect of the bacterium (*B. velezensis* B63) on *R. solani* and *M. phaseolina* was carried out *in vitro* using dual-culture plate assays. Potato dextrose agar (PDA) plates were inoculated with a 6-mm diam. actively growing *R. solani* and *M. phaseolina* cultures that separately placed on one side of the plate. A loop of the B63 bacterial suspension (10^8 CFU mL^{-1}) was streaked at opposite sides of the plate. Control plates were cultured only with the fungal pathogens. The plates were then incubated at 25°C for *R. solani* or 30°C for *M. phaseolina*. Three replicates were used for each treatment. Upon complete mycelial growth in any treatment plate, the radial growth of the fungi in the control and treatment plates was measured and inhibition percentages were calculated as follows:

$$I\% = C\text{-}d/C \times 100$$

where: C is the mycelium radial growth of the fungus in control; d: is the mycelium radial growth of the fungus in the treatment.

Field experiment design

Field experiments were carried out in two consecutive years (2019–2020 and 2020–2021), in a field located at the Medicinal and Aromatic Plants Department Farm, Horticulture Research Institute, Agricultural Research Center, El-Qanater El-Khayreya, Qalyubia, Egypt (30° 11'36.9"N, 31°7'55.43"E). From this field, terminal cuttings (lengths = 20 cm) from healthy geranium plants were obtained from a 2-year-old geranium plant.

The experimental setup consisted of the following nine treatments (with respective abbreviations used hereafter):

1. Control plants (CK)
2. Plants treated with Topsin-M fungicide (TM)
3. Plants pre-treated with chitosan at 0.05% (CS 0.05%)
4. Plants pre-treated with chitosan at 0.1% (CS 0.1%)
5. Plants pre-treated with chitosan at 0.2% (CS 0.2%)
6. Plants pre-treated and sprayed with chitosan at 0.05% (CSF 0.05%)
7. Plants pre-treated and sprayed with chitosan at 0.1% (CSF 0.1%)
8. Plants pre-treated and sprayed with chitosan at 0.2% (CSF 0.2%)
9. Plants treated with *B. velezensis* strain B63 (10^8 CFU mL^{-1})

The plant pre-treatments were applied, respectively, using Topsin-M fungicide at the recommended dose (2 g L^{-1}), chitosan solution at 0.05%, 0.1% or 0.2%, and a suspension of *B. velezensis* strain B63 (10^8 CFU mL^{-1}), by soaking cuttings in the treatments for 30 min. The control treatment cuttings were soaked in water. The treated cuttings were then planted on 15 November in both 2019 and 2020. Chitosan spraying treatments and additional treatments with *B. velezensis* strain B63 (soil drench) (treatments from 6 to 9 above) were each applied three times: the first application was carried out 45 d after planting, the second was carried out 1 month later, and the third was applied 30 d after the second application. Strain B63 (treatment 9 above) was applied as a soil drench at the same three times.

Each experiment plot consisted of 4 rows, each of 5 m length with 60 cm spacing between the rows. The plants in the rows were at 25 cm spacings. Three replicates were used for each treatment. Chemical fertilizers (NPK) and other agricultural practices were applied as recommended for conventional geranium crop culture.

Plant morphology and disease assessment

Two cuts (the first on 15 May, the second on 15 October, in each of 2020 and 2021) were taken from the geranium plants in the trials. Plant heights, numbers of branches, and plant fresh and dry weights (g) were assessed from each plant cut.

Disease symptoms became visible only after the first cut in each trial, and disease development was assessed on 15 October in each year, as percentages of plant mortality.

Geranium essential oil yields and gas chromatography analyses

The essential oil percentage was obtained by hydrodistillation using a Clevenger-type apparatus (British Pharmacopoeia, 1963). The percentages and yields (mL) of essential oil per plant were calculated for three replicates.

For essential oil composition analysis, samples from the second-cut field harvest from the 2020–2021 trial were analyzed using Gas–liquid chromatography (GLC) in the Laboratory of the Medicinal and Aromatic Plants Research Department, Horticulture Research Institute, using Ds Chrom 6200 GC with a flame ionization detector to separate volatile oil components. The chromatograph apparatus has a capillary column composed of BPX-5.5% phenyl (equiv.) polysilphenylene-siloxane (30 m × 0.25 mm ID × 0.25 µm film). The temperature program ramp increased at a rate of 10°C min^{-1} from 70°C to 200°C. The gas flow rates were nitrogen at 1 mL min^{-1}, hydrogen at 30 mL min^{-1}, and air at 330 mL min^{-1}. Temperature of the detector was 300°C, and of the injector was and 250°C. The GC chromatogram and analysis report for each sample were used to identify the percentage of the main components of each essential oil.

Microbiological analyses

Sampling and sample preparation

At the end of each trial (October 15), the geranium plants were cut. After removing loosely attached soil, rhizosphere soil was extracted from each sample. Five grams of roots from each sample were placed in a sterile Stomacher bag and mixed with 45 mL of sterile NaCl for 60 sec at medium speed with a Stomacher 400 blender. The Stomacher mixing process was repeated three times to obtain each root cell suspension.

Estimation of numbers of viable bacteria and fungi

Tenfold serial dilutions of the microbial suspensions in sterile 0.85% NaCl obtained (as described above) were plated onto plate count agar (PCA) for estimations of total viable bacteria, or potato dextrose agar (PDA) supplemented with tetracycline (50 mg mL^{-1}) for estimations of total viable fungi. Numbers of bacterial colony forming units (CFUs) were determined after 3 d incubation at 28°C, and fungal CFUs were determined after 5 d incubation at 25°C, respectively, and were calculated per g root fresh weight.

Total community DNA extraction from geranium rhizosphere samples

To address issues related to accuracy and cost, a sampling strategy was used where different random samples were selected from each experimental treatment group.

Total community DNA (TC-DNA) was extracted from 250 mg of rhizosphere soil samples from each treatment (two replicates each). The DNeasy Power Soil kit (Qiagen) was used for the extractions according to the manufacturer's protocol. TC-DNA was diluted (1:5) using Tris-EDTA and stored at -20°C. The integrity and quality of the extracted TC-DNA were confirmed using agarose gel electrophoresis and a Nanodrop 2000 spectrophotometer (Thermo Fisher Scientific).

Quantification of total bacteria in TC-DNA using the 16S rRNA gene

The total numbers of bacteria with 16S rRNA gene copy numbers were estimated in TC-DNA from rhizosphere samples using universal primers (Eub338 and Eub518), according to Fierer *et al*. (2005). A real-time PCR detection system (Step One Plus Real-Time PCR System, Thermo Fisher Scientific) was used. Real-time PCR was carried out using HOT FIREPol® EvaGreen® qPCR Mix Plus (Solis BioDyne) in a final volume of 20 µL for each sample. The real-time PCR conditions used were: an initial activation step at 95°C for 12 min, followed by 40 cycles each of denaturation at 95°C for 30 s, annealing at 60°C for 1 min, and extension at 72°C for 1 min, and a final elongation step at 72°C for 5 min. The specific primer sequences used in this experiment are listed in Table S1.

Illumina MiSeq sequencing and analyses of 16S rRNA gene amplicons

From the sampling strategy described above, six DNA samples were analyzed using the MiSeq platform (Illumina) to target the V3–V4 region of the 16S rRNA gene (Illumina, 2013), following the manufacturer's instructions. The raw sequence reads in the FASTQ format were uploaded to the Galaxy online platform through the public server at usegalaxy.org for Bioinformatic analyses. The analyses were carried out using the default parameters within the standard operating procedure (SOP) designed for MiSeq data. The forward and reverse FASTQ files were paired with a minimum overlap length of 50 bp, maximum mismatches of 15, and a minimum quality of 30. Reads were filtered, and sequences were filtered primarily on the basis of quality. Chimera sequences were eliminated using the Chimera Search device. Operational taxonomic units (OTUs) were chosen at a cutoff level of 0.03. The representative sequences of the OTUs were selected primarily on the basis of the greatest abundance within each cluster. Taxonomic classification was determined using the Greengenes classifier. An OTU table was obtained and analyzed using STAMP software 2.1. for analysis of community composition. Sequences were deposited at the public repository Sequence Read Archive (SRA) under the accession numbers AMN40334118 to SAMN40334121, and the Bioproject accession number PRJNA1085764.

PCR-based detection of genes encoding plant growth-promoting functions

PCR was conducted on the extracted TC-DNA to amplify marker genes indicative of soil fertility and suppressiveness. These include the *nifH* gene responsible for producing dinitrogenase reductase, the *ituD* gene related to iturin A production, the *bacC* gene related to the bacitracin biosynthesis, and the *fenD* gene responsible for the fengycin antifungal antibiotic. These genes can be used to assess soil health and disease suppressiveness. Detailed primer sequences for these genes are shown in Table S1.

Field experiment design and data analyses

The experiment was complete randomized block design with three replicates for each treatment. ANOVA was used to analyze plant mortality percentages and growth parameters, and means were compared using the least significant difference test at $P \leq 0.05$. Statistical analyses were carried out using the MSTAT-C statistical package. Plant mortality percentage data were arc sin transformed before carrying out ANOVA to produce approximately constant variances. Stacked column and principal component analysis (PCA) based on MiSeq sequencing data was carried out using Origin pro-2021 version software.

RESULTS

Antifungal activity of Bacillus velezensis *B63*

In vitro, *B. velezensis* B63 inhibited ($P \leq 0.05$) *R. solani* and *M. phaseolina*. Mean mycelial radial growth diameters were 90 mm (± 0.0) for the experimental control, 51.0 mm (± 0.58) for *M. phaseolina* (by 43% reduction) and 56.0 mm (± 2.52) for *R. solani* (by 38% reduction).

Field experiments

Under field conditions, all treatments decreased ($P \leq 0.05$) disease development (percent mortality) of geranium plants, especially in 2019–2020 season. The greatest plant mortality reduction was recorded from the treatments of *B. velezensis* B63, chitosan soaking + foliar spray 0.2% (CSF 0.2%), chitosan soaking + foliar spray 0.1% (CSF 0.1%), and chitosan 0.2% soaking alone (CS 0.2%). These treatments caused 36% (*B. velezensis* B63), 33% (CSF 0.2%), 33% (CSF 0.1%), and 31% (CS 0.2%) reductions ($P \leq 0.05$) in plant mortality, compared to the control treatment in the 2019–2020 season (Table 1).

All the treatments except *B. velezensis* B63, chitosan soaking + foliar spray 0.2% (CSF 0.2%) and chitosan soaking + foliar spray 0.1% (CSF 0.1%) gave plant mortality that was similar ($P > 0.05$) to the experimental control but still gave low mortalities compared with the control. Plant mortality from *B. velezensis* B63, chitosan soaking + foliar spray 0.2% (CSF 0.2%) and chitosan soaking + foliar spray 0.1% (CSF 0.1%) reduced ($P \leq 0.05$) by, respectively, 33%, 27%, and 26% compared to the control treatment (Table 1).

The least effective treatment was chitosan 0.05% soaking alone (CS 0.05%). This treatment decreased the plant mortality percentage from 77% to 65% (by 16.12% reduction: $P \leq 0.05$) and from 80.90% to 76.01% (by 6.04% reduction) for the first and second seasons, respectively, compared to the control treatment (Table 1).

Table 1. Mean mortality proportions from root rot (at 6 months after a first cut) for geranium plants receiving different treatments in field trials carried out in 2019–2020 and 2020–2021.

Treatment [a]	2019–2020 trial		2020–2021 trial	
	Mortality (%)	Trans.*	Mortality (%)	Trans.*
CK	94.17 ± 3.33†	77.03 a	97.5 ± 0.00	80.90 a
TM	70.83 ± 8.82	57.95 bc	83.33 ± 8.30	67.71 abc
CS 0.05%	80.83 ± 6.67	64.61 b	92.92 ± 4.58	76.01 a
CS 0.1%	70.83 ± 3.33	57.39 bc	88.33 ± 4.58	71.12 ab
CS 0.2%	64.17 ± 6.67	53.44 c	83.33 ± 8.30	67.71 abc
CSF 0.05%	80.83 ± 6.67	64.61 b	88.33 ± 4.58	71.12 ab
CSF 0.1%	60.83 ± 8.82	51.52 c	74.17 ± 9.58	60.11 bc
CSF 0.2%	60.83 ± 6.67	51.35 c	73.75 ± 5.00	59.42 bc
B63	57.5 ± 2.89	49.33 c	65.83 ± 2.60	54.24 c
Prob>F	0.003	0.002	0.009	0.010

[a] CK = Control; TM = Topsin-M; CS = Chitosan soaking; CSF = Chitosan soaking and spraying; B63 = *B. velezensis*.
*Values accompanied by the same letter are not significantly different ($P > 0.05$).
± † standard error; Trans = arc sin transformed value.

Effects of treatments on geranium plant morphology

At both cuts in the two seasons, all treatments increased the geranium parameters compared with the control treatments. *Bacillus velezensis* B63 gave the greatest increases ($P \leq 0.05$) in plant height, numbers of branches, and fresh and dry weights compared with the control (Table 2).

In 2019–2020 at the first cut, plants treated with *B. velezensis* B63 had mean plant heights that were 1.35-fold greater than the controls, mean branch numbers 1.56-fold greater, and fresh weights 3.44-fold greater than the controls (Table 2). At the second cut, mean plant heights from this treatment were 1.34-fold greater than the controls, and equivalent branch numbers were increased by 1.54-fold and fresh weights by 2.74-fold (Table 2). Plant dry weights were also increased by 2.85-fold at both cuts (Table 2).

In 2020–2021, for the first cut, the *B. velezensis* B63 treatment also increased ($P \leq 0.05$) plant height by 1.84-fold, branch numbers by 2.29-fold, fresh biomass by 6.37-fold, and dry biomass by 6.63-fold (Table 2). From the second cut, these increases were 1.65-fold, 2.33-fold, 4.85-fold, and 5.04-fold (Table 2).

Treatment application methods affected the activity of chitosan for improving geranium growth. In most cases, the greatest increases in plant parameters from chitosan treatments were from chitosan soaking + foliar spray (CSF 0.2%). In 2019–2020 at the first cut, this treatment increased ($P \leq 0.05$) plant height by 1.32-fold, number of branches by 1.52-fold, fresh biomass by 2.30-fold, and dry biomass by 2.08-fold. These parameters also increased ($P \leq 0.05$) at the second cut by 1.30-fold (plant height), 1.38-fold (number of branches), 2.43-fold (fresh biomass), and 2.53-fold dry biomass) (Table 2).

The same trend was observed in 2020–2021, where the chitosan soaking + foliar spray 0.2% (CSF 0.2%) treatment increased ($P \leq 0.05$), at the first cut, means of plant height by 1.76-fold, number of branches by 2.12-fold, fresh biomass by 5.05-fold, and dry biomass by 5.26-fold. At the second cut, these four parameters increased by 1.60-fold, 2.06-fold, 3.96-fold and 4.12-fold (Table 2).

Chitosan 0.05% soaking alone (CS 0.05%) was the least effective treatment, but still gave consistent and statistically significant ($P \leq 0.05$) enhancement of geranium growth parameters across both seasons and cuts, compared to the control treatments. In 2019–2020, for the first cut, plants treated with chitosan 0.05% soaking alone (CS 0.05%) had 1.02-fold increased ($P \leq 0.05$) mean plant height, 1.20-fold increased numbers of branches, 1.36-fold increased fresh biomass, and 1.13-fold increased dry biomass. For the second cut, these parameters increased by 1.20-fold, 1.08-fold, 1.72-fold and 1.72-fold (Table 2).

The same trend was observed in 2020–2021, chitosan 0.05% soaking alone (CS 0.05%) increased ($P \leq 0.05$) plant growth parameters across both cuts (Table 2). Mean plant height increased by 1.33-fold at the first cut and by 1.21-fold at the second cut. Similarly, at the first cut, branch numbers increased by 1.53-fold, and fresh biomass by 1.50-fold, and at the second cut these parameters increased by 1.38-fold and 1.19-fold. Dry biomass also increased by 1.38-fold at the first cut and by 1.24-fold at the second, compared to the control treatment.

Geranium essential oil yields and gas chromatography analyses

Essential oil contents

All the experimental treatments affected essential oil production by the geranium plants, as shown in Table 3. During the 2019-2020 season, at the first cut, significant increases ($P \leq 0.05$) in essential oil contents (1.27-fold) and yields (4.36-fold) were recorded from the *B. velezensis* B63 treatment, compared to the controls. At the second cut elevated essential oil contents (1.29-fold) from *B. velezensis* B63 and (1.27-fold) from chitosan 0.2% (CSF 0.2%) were recorded, but essential oil yield was significantly greater (3.54-fold: $P \leq 0.05$) only for B63 compared to the control. Topsin-M fungicide and

Table 2. Mean plant heights, numbers of branches, and herbage fresh and dry weights, for two cuts of geranium plants where different treatments were applied in two field trials carried out in 2019–2020 and 2020–2021.

Treatment [a]	First cut				Second cut			
	Plant height (cm)	No. branches/ plant	Herb FW g/plant	Herb DW g/plant	Plant height (cm)	No. branches/ plant	Herb FW g/plant	Herb DW g/plant
2019–2020 trial								
CK	46.00±0.00† e	08.33±0.33 e	378.67±9.87 h	191.00±0.00 h	48.67±0.67 h	08.00±0.00 f	666.00±6.56 i	326.34±3.21 i
TM	54.00±0.58 d	10.67±0.33 cd	559.33±9.21 f	286.33±5.33 f	56.00±0.58 g	10.67±0.33 bc	976.67±5.90 h	498.10±3.01 h
CS 0.05%	47.00±0.00 e	10.00±0.58 d	516.00±3.06 g	215.00±3.06 g	58.33±0.33 f	08.67±0.33 ef	1143.00±3.79 g	560.07±1.86 g
CS 0.1%	57.00±1.15 c	12.00±0.00 b	710.67±4.06 e	353.00±4.16 d	60.67±0.33 e	09.33±0.33 de	1240.00±4.58 f	620.00±2.29 f
CS 0.2%	58.00±0.00 c	12.00±0.00 b	700.33±6.64 e	322.67±3.28 e	61.33±0.33 d	10.00±0.00 cd	1405.00±4.58 e	716.55±2.34 e
CSF 0.05%	60.33±0.88 d	11.00±0.00 c	759.33±5.21 d	368.00±4.16 c	62.00±0.00 c	10.67±0.33 bc	1497.67±1.76 d	763.81±0.90 d
CSF 0.1%	61.33±0.88 ab	12.00±0.00 b	815.00±5.69 c	387.67±3.71 b	62.67±0.33 bc	10.33±0.33 bc	1566.00±2.89 c	798.66±1.47 c
CSF 0.2%	60.67±0.33 ab	12.67±0.33 ab	869.67±7.22 b	396.67±0.88 b	63.33±0.33 b	11.00±0.00 b	1618.00±3.51 b	825.18±1.79 b
B63	62.00±0.00 a	13.00±0.00 a	1303.67±18.32 a	544.00±3.51 a	65.00±0.00 a	12.33±0.33 a	1825.33±3.38 a	930.92±1.73 a
Prob>F	<0.0001	<0.0001	<0.0001	<0.0001	<0.0001	<0.0001	<0.0001	<0.0001
2020–2021 trial								
CK	32.33±1.20 g	5.67±0.33 f	194.00±3.46 h	95.06±1.70 h	51.00±0.58 i	6.00±0.00 g	162.67±0.88 i	79.71±0.43 i
TM	40.33±0.33 f	9.00±0.00 e	276.00±8.19 g	135.24±4.01 g	56.67±0.33 h	7.00±0.00 f	177.33±0.67 h	88.67±0.33 h
CS 0.05%	43.00±0.00 e	8.67±0.33 e	268.67±1.45 g	131.65±0.71 g	61.67±0.33 g	9.00±0.00 e	194.33±0.67 g	99.11±0.34 g
CS 0.1%	48.33±0.88 d	10.67±0.33 d	389.00±6.08 f	198.39±3.10 f	68.67±0.33 f	10.33±0.33 d	342.00±0.58 f	174.42±0.29 f
CS 0.2%	49.67±0.33 cd	11.33±0.33 c	682.00±1.73 e	347.82±0.88 e	71.67±0.88 e	11.33±0.33 c	390.33±1.20 e	199.07±0.61 e
CSF0.05%	51.00±0.58 c	12.00±0.00 b	752.67±3.93 d	383.86±2.00 d	74.67±0.33 d	12.00±0.00 b	438.00±3.21 d	223.38±1.64 d
CSF 0.1%	55.67±0.33 b	12.00±0.00 b	822.00±5.77 c	419.22±2.94 c	79.33±0.33 c	12.00±0.00 b	599.33±0.88 c	305.66±0.45 c
CSF 0.2%	57.00±0.58 b	12.00±0.00 b	979.67±6.96 b	499.63±3.55 b	81.67±0.67 b	12.33±0.33 b	644.00±1.53 b	328.44±0.78 b
B63	59.33±0.33 a	13.00±0.00 a	1236.67±7.62 a	630.70±3.89 a	84.33±0.33 a	14.00±0.00 a	788.33±0.33 a	402.05±0.17 a
Prob>F	<0.0001	<0.0001	<0.0001	<0.0001	<0.0001	<0.0001	<0.0001	<0.0001

[a] CK = Control; TM = Topsin-M; CS = Chitosan soaking; CSF = Chitosan soaking and spraying; B63 = *B. velezensis*.
Means in each row accompanied by the same letter are not significantly different ($P < 0.05$); ± † standard errors.

Table 3. Mean essential oil contents in geranium plants harvested in two cuts each in 2019–2020 or 2020–2021, after different experimental treatments were applied.

Treatment [a]	First cut		Second cut	
	Mean essential oil content (%)	Mean essential oil yield (mL plant^{-1})	Mean essential oil content (%)	Mean essential oil yield (mL plant^{-1})
2019–2020				
Control	0.200±0.000† d	0.757±0.020 h	0.310±0.000 e	2.065±0.020 h
TM	0.237±0.003 c	1.324±0.032 f	0.353±0.007 d	3.451±0.061 g
CS 0.05%	0.200±0.000 d	1.032±0.006 g	0.363±0.003 cd	4.153±0.026 f
CS 0.1%	0.237±0.003 c	1.682±0.016 e	0.380±0.000 b	4.712±0.017 e
CS 0.2%	0.247±0.003 ab	1.728±0.381 e	0.383±0.006 b	5.386±0.055 d
CSF0.05%	0.240±0.000 bc	1.822±0.013 d	0.380±0.000 b	5.691±0.007 c
CSF 0.1%	0.247±0.003 ab	2.011±0.041 c	0.370±0.006 c	5.794±0.085 c
CSF 0.2%	0.243±0.003 bc	2.116±0.034 b	0.393±0.003 a	6.364±0.040 b
B63	0.253±0.003 a	3.302±0.018 a	0.400±0.000 a	7.301±0.014 a
Prob>F	<0.0001	<0.0001	<0.0001	<0.0001
2020–2021				
Control	0.140±0.000 e	0.272±0.005 h	0.160±0.000 g	0.260±0.001 h
TM	0.233±0.003 d	0.644±0.023 g	0.247±0.003 de	0.437±0.005 g
CS 0.05%	0.243±0.003 c	0.654±0.012 g	0.237±0.003 f	0.460±0.006 g
CS 0.1%	0.267±0.003 a	1.038±0.028 f	0.240±0.000 ef	0.821±0.001 f
CS 0.2%	0.240±0.000 cd	1.637±0.004 e	0.253±0.003 cd	0.989±0.014 e
CSF0.05%	0.240±0.000 cd	1.806±0.009 d	0.250±0.000 d	1.095±0.008 d
CSF 0.1%	0.243±0.003 c	2.001±0.040 c	0.260±0.000 bc	1.558±0.002 c
CSF 0.2%	0.253±0.003 b	2.482±0.038 b	0.267±0.003 b	1.717±0.023 b
B63	0.260±0.000 ab	3.215±0.020 a	0.307±0.003 a	2.418±0.025 a
Prob>F	<0.0001	<0.0001	<0.0001	<0.0001

[a] TM = Topsin-M; CS = Chitosan soaking; CSF = Chitosan soaking and spraying; B63 = *B. velezensis*
Means in each row accompanied by the same letter are not different ($P > 0.05$)
± † standard errors.

chitosan 0.05% soaking alone (CS 0.05%) gave the least increases in oil content and yield from both cuts. During 2020-2021, the first cut showed significant ($P \leq 0.05$) increases in essential oil contents. Chitosan 0.1% soaking alone (CS 0.1%) and *B. velezensis* B63 treatments gave the greatest increases in essential oil contents by, respectively, 1.91-fold and 1.86-fold, compared to the control. Also, *B. velezensis* B63 induced an 11.82-fold increase in mean essential oil yield. At the second cut, the greatest significant increases in essential oil content (1.92-fold) and yield (9.3-fold) were recorded from the *B. velezensis* B63 treatment.

Essential oil components

Gas chromatography (GC) analyses of geranium essential oils (Figure 1) showed that the concentrations of the main components of geranium plants treated with chitosan soaking + foliar spray (CSF 0.2%) increased by 1.36-fold for citronellol, 1.37-fold for geraniol, 1.54-fold for citronellyl formate, and 1.94-fold for geranyl formate, compared to the experimental controls. *Bacillus velezensis* B63 treatment also increased these components but to lesser extents. The increases were 1.04-fold for citronellol, 1.07-fold for geraniol, 1.27-fold for citronellyl formate, and 1.17-fold for geranyl formate. In addition, the *B. velezensis* B63 treatment increased the concentration of eugenol by 1.35-fold compared to the controls.

Geranium rhizosphere bacterial communities

The dominant bacteria (more than 10% relative abundance) in the geranium rhizospheres from plants treated with *B. velezensis* B63, chitosan soaking + foliar spray 0.2% (CSF 0.2%) and untreated controls belonged to two major phyla, *Proteobacteria*, and *Actinobacteria*

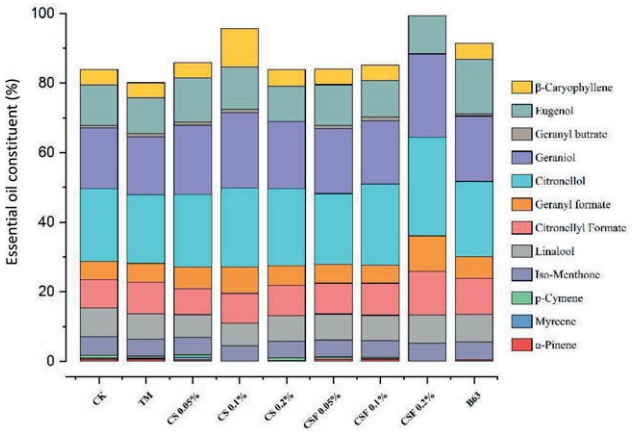

Figure 1. Mean proportions (%) of essential oils in geranium plants to which different experimental treatments were applied.

(Figure 2). *Acidobacteria* was also dominant in rhizospheres of plants treated with *B. velezensis* B63. A total of 106,061 bacterial sequences were detected from the three treatments. The greatest number of bacterial sequences (38,165; Figure S1) was obtained after chitosan treatment, while the lowest number (1,760) was detected from the *B. velezensis* B63 treatment. The control treatment gave 29,809 sequences. The bacterial sequences were affiliated with 19 phyla, 41 classes, 70 orders, 147 families, and 218 genera. The most prevalent genera (more than 3% relative abundance) detected from the control treatment were classified as *Agrobacterium*, *Kaistobacter*, and unclassified *Rhizobiales*. The most prevalent genera detected from the *B. velezensis* B63 treatment were *Kaistobacter*, *Agrobacterium*, unclassified Acidobacteria iii1-15, *Comamonadaceae* and *Rhizobiales*. Bacteria from the genera *Kaistobacter*, *Gemmata*, unclassified Acidobacteria iii1-15, and *Bacillales* were the most prevalent from the chitosan treatment (Table S2).

The chitosan soaking + foliar spray 0.2% (CSF0.2%) and *B. velezensis* B63 treatments induced increases in abundance of some minor genera of bacteria in the soil. These included *Sinorhizobium*, WD2101, unclassified *Gaiellaceae*, *Micrococcales*, *Rhodospirillaceae*, *Chthoniobacteraceae*, and *Myxococcales* compared to the control. Bacteria in *Enterobacteriaceae*, *Rhodoplanes*, *Balneimonas*, *Paracoccus*, *Gemmataceae*, and *Acidimicrobiales* increased under chitosan soaking + foliar spray 0.2% treatment (CSF 0.2%), compared to the *B. velezensis* B63 and control treatments. *Agrobacterium*, *Planctomyces*, *Sphingomonas*, *Devosia*, and several other genera decreased from the chitosan soaking + foliar spray 0.2% (CSF0.2%) treatment compared to the *B. velezensis* B63 and control. Conversely, the *B. velezensis* B63 treatment reduced the abundance of *Paracoccus*, *Planctomyces*, and several other taxa compared to the chitosan soaking + foliar spray 0.2% (CSF 0.2%) and control treatments (Table S1).

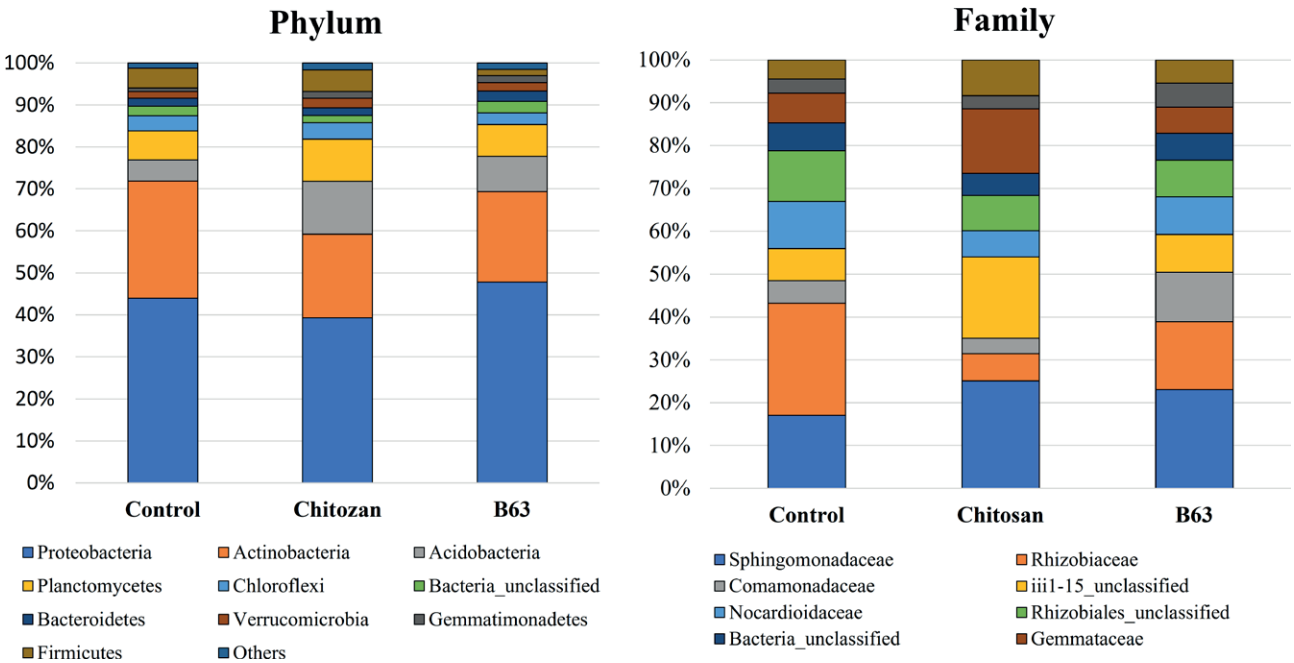

Figure 2. Microbial community compositions of geranium rhizospheres, based on MiSeq sequencing data, in response to treatment with chitosan soaking + foliar spray 0.2% (CSF 0.2%) or inoculation with *B. velezensis* B63 compared to the untreated experimental controls.

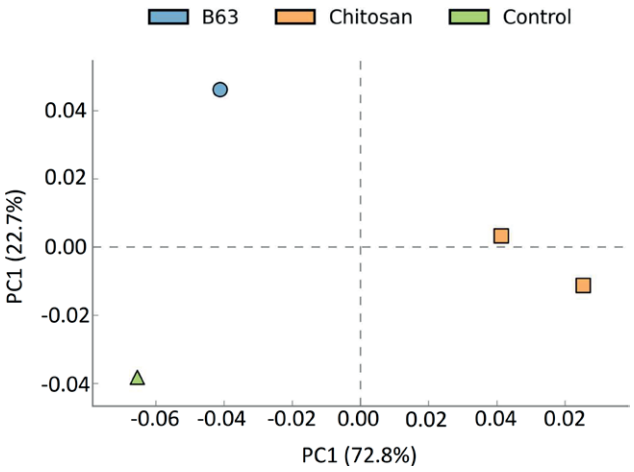

Figure 3. PCA analysis based on MiSeq sequencing data, showing separation between the microbial community compositions of the geranium rhizospheres for plants treated with chitosan soaking + foliar spray 0.2% (CSF 0.2%) or inoculation with *B. velezensis* B63 compared to experimental controls.

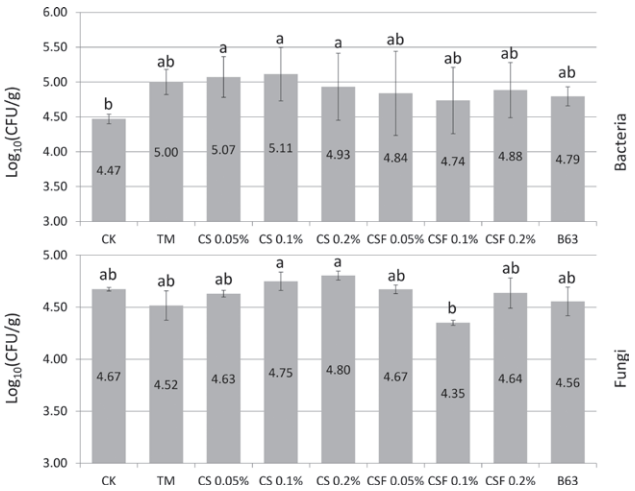

Figure 4. The total viable bacterial and fungal counts represented as Log_{10} (colony forming units/g root fresh mass). CK = Control; TM = Topsin-M; CS= Chitosan soaking; CSF = Chitosan soaking and spraying; B63 = *B. velezensis*; bars with the similar letter are not significantly different ($p \leq 0.05$).

Principle component analysis (PCA) based on the relative abundance of all bacterial OTUs obtained from geranium rhizospheres showed three distinct clusters. The first included samples from plants treated with chitosan soaking + foliar spray 0.2% (CSF 0.2%), while both *B. velezensis* B63 and control plants had diverse microbial community compositions (Figure 3).

Assessments of numbers of colony forming units (CFUs) from the geranium rhizospheres using plate count agar showed that total numbers of bacteria and fungi were not different ($P > 0.05$) between different samples (Figure 4). However, all samples from the experimental treatments tended to have greater numbers of microorganisms than the control.

The overall number of bacteria increased ($P \leq 0.05$) by 1.13-fold, 1.14-fold and 1.10-fold for Chitosan 0.05%, 0.1% and 0.2% soaking alone (CS0.05%, CS0.1% and CS0.2%) treatments, respectively, compared with the control. The other treatments did not significantly change bacterial counts compared to the control ($P > 0.05$), although they still gave greater counts than the control (Figure 4).

Figure 4 also shows that, except for the chitosan soaking + foliar spray 0.1% (CSF 0.1%) treatment, the overall number of fungi did not change ($P > 0.05$) with any of the tested treatments compared to the control. Despite this, the chitosan 0.1% and 0.2% soaking alone (CS 0.1% and CS 0.2%) treatments increased total fungal counts (1.02-fold from CS 0.1% and 1.03-fold from CS 0.2%), compared to the control, but this increase was not significantly different ($P > 0.05$). The chitosan soaking + foliar spray 0.2% (CSF 0.2%) treatment gave the lowest significant decrease in total fungal count compared to the control treatment.

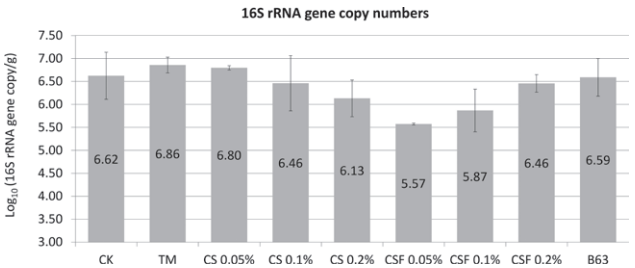

Figure 5. Real time PCR quantifications of total bacteria in TC-DNA based on 16S rRNA gene copy numbers resulting in geranium rhizosphere soil after application of different experimental treatments. CK = Control; TM = Topsin-M; CS = Chitosan soaking; CSF = Chitosan soaking and spraying; B63 = *B. velezensis*. ($P > 0.05$).

In addition to bacterial and fungal counts, 16S rRNA gene copy numbers in the geranium rhizospheres were assessed as indicators of microbial population density. However, no significant differences ($P > 0.05$) were detected between treatments. The geranium rhizosphere 16S rRNA gene copies were in the range of 5.57 to 6.86 Log_{10} copies g^{-1} of root fresh mass. Specifically, except the Topsin-M fungicide and chitosan 0.1% soaking alone (CS 0.1%) treatments, the 16S rRNA gene copies from all the treatments were less than in the control treatment (Figure 5).

Chitosan 0.05% soaking alone (CS 0.05%) gave the lowest numbers of 16S rRNA gene copies (5.57 Log_{10}

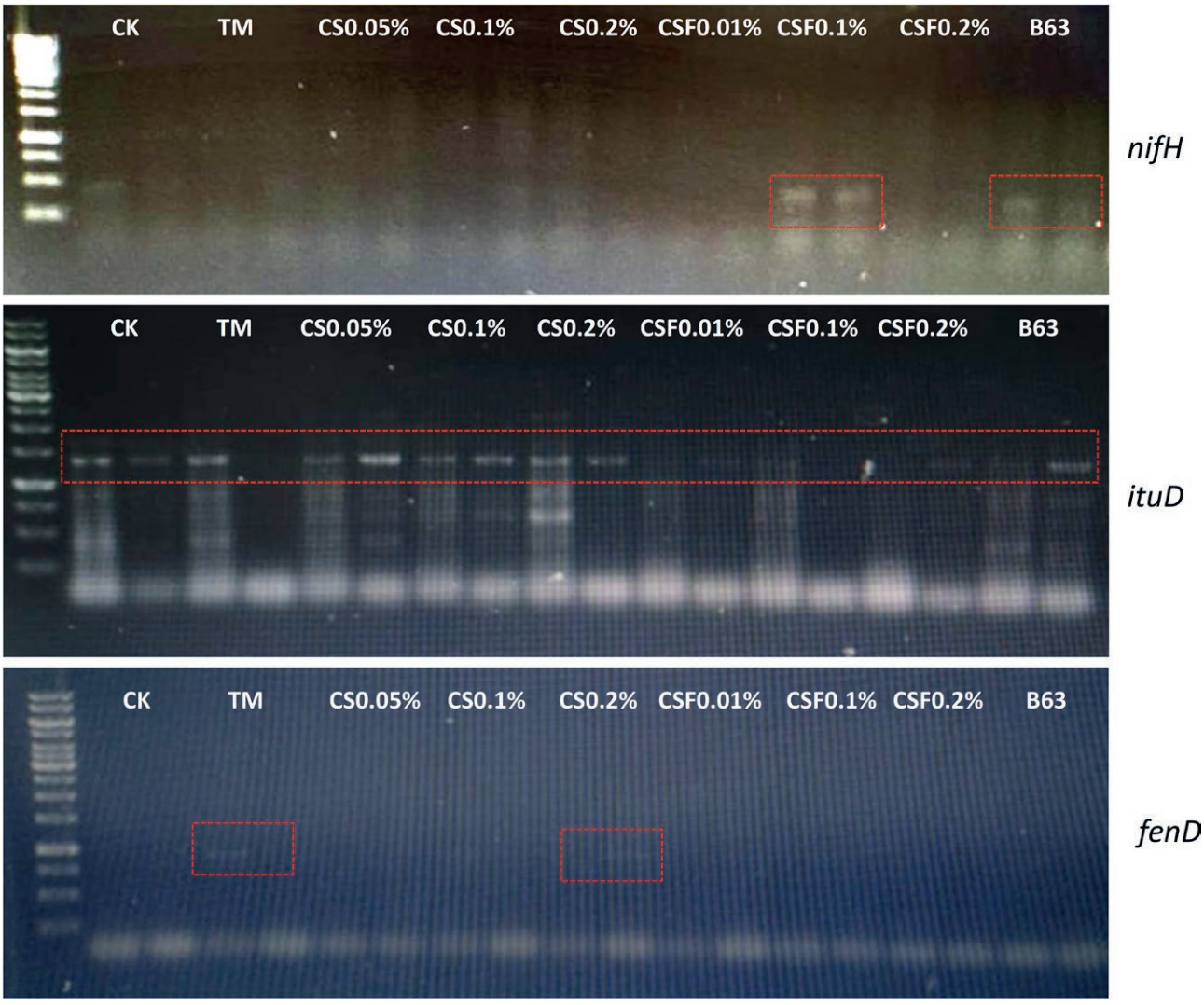

Figure 6. PCR-based detection of genes encoding plant growth promoting related functions.

copies g^{-1} of root fresh weight), followed by chitosan soaking + foliar spray (CSF 0.1%) treatment (5.87 Log_{10} copies g^{-1} of root fresh weight). Greatest numbers gene copies were recorded from the Topsin-M fungicide and chitosan 0.1% soaking alone (CS 0.1%) treatments (6.86 and 6.80 Log_{10} copies g^{-1} of root fresh weight respectively) (Figure 5).

PCR-based detection of genes encoding plant growth promoting related functions

The *nifH* gene encoding the nitrogenase reductase indicates the presence of nitrogen-fixing bacterial populations that were detected in total community DNA extracted from each rhizosphere sample. Our results showed a relatively higher band intensity for the *nifH* gene amplified from CSF 0.1 TC-DNA, followed by B63-treated plants. The *ituD* gene was detected in all treatments, at least in one of the two replicates. Only Topsin-M and SC 0.2 showed a weak *fenD* gene band (Figure 6).

DISCUSSION

A growing body of literature recognizes the importance of biological control agents and biostimulants as sustainable approaches to managing plant pathogens, particularly with increasing concern about the use of synthetic fungicides (Stukenbrock and Gurr, 2023). Bio-

control agents and biostimulants offer effective solutions for plant disease management, as they have proven efficiency for management of several diseases caused by fungi (Meena *et al.,* 2022).

The present study has shown that *B. velezensis* B63 treatment had a growth-promoting effects on geranium plants and fungicidal effects on plant pathogenic fungi. This outcome corroborates results from a previous study (Reyad *et al.,* 2022), which showed that *B. velezensis* B63 had antifungal and plant growth-promoting properties. Chitosan similarly exerted positive effects, although less pronounced than those from B63. The application of *B. velezensis* B63 and chitosan significantly influenced the soil microbial communities, reduced progression of root rot, as indicated by lower plant mortality rates, and promoted geranium growth and production of essential oils. These treatments increased geranium yields and enhanced plant quality.

Previous studies have demonstrated decreased root rot in plants treated with bioagents. For example, Gao *et al*. (2022) showed that *B. subtilis* and *B. velezensis* reduced the incidence of Fusarium root rot in *Astragalus membranaceus*. Similarly, Wang *et al*. (2023) reported that *B. velezensis* B19 was highly antagonistic to *Panax notoginseng* (Sanqi) root rot. Maslennikova *et al.* (2023) found that a mix of *B. subtilis* and *B. amyloliquefaciens* suppressed *R. solani*, and improved the physiology of potato plants. El Hadrami *et al*. (2010) and Liu *et al*. (2016) showed that chitosan played a major role in enhancing plant resistance to diseases.

In the present study, effects of *B. velezensis* B63 and chitosan on geranium root rot development were expressed as plant mortality rates across two growing seasons, and this showed that several treatments decreased plant mortality in the 2019-2020 field experiment. The most effective treatments were *B. velezensis* B63, chitosan soaking + foliar spray 0.2% or 0.1% (CSF 0.2% and 0.1%), and chitosan 0.2% soaking alone (CS 0.2%). These treatments resulted in mortality reductions of 36% for *B. velezensis* B63, 33% for CSF 0.2%, 33% for CSF 0.1%, and 31% for CS 0.2% treatment, compared to untreated experimental controls. In contrast, during the second season (2020-2021), only treatments involving *B. velezensis* B63, CSF 0.2%, and CSF 0.1% reduced plant mortality by, respectively, 33%, 27% and 26%, compared to controls. Other treatments did not differ significantly from the control. The least effective treatment over both seasons was chitosan 0.05% soaking alone (CS 0.05%), which gave a smaller reduction in geranium mortality of 16% in 2019-2020 and 6% in 2020-2021, relative to the control plants. These results indicate that chitosan efficacy was dose dependent. The observed difference in treatment efficacy, especially for chitosan treatments, may also have been due to different climatic conditions prevailing during the two growth seasons.

Bacillus velezensis B63 also strongly suppressed *in vitro* growth of *R. solani* and *M. phaseolina*. Suppression of *R. solani* and *M. phaseolina* by specific microorganisms has been associated with the formation of secondary metabolites that are toxic to the pathogens, such as siderophore bacteriocins, and cyanide (Lahlali *et al.,* 2022). The strain B63 was found to produce secondary metabolites related to biological control, including bacilysin, macrolactin, bacillaene, bacillibactin, surfactin, and fengycin, (Helal *et al*., 2022). Surfactin is important for motility, signalling, and biofilm formation as well as surface colonization (Hafeez *et al*., 2019; Helal *et al*., 2022; Reyad *et al.,* 2022).

In the present study, *B. velezensis* B63 and chitosan applications reduced geranium root rot and also improved the morphometric parameters of field-grown geranium plants during the growing seasons, including plant height, number of branches, and mass per plant. Other studies have confirmed that *Bacillus* can promote plant growth (Fan *et al*. 2018), directly or indirectly (Yánez-Mendizábal and Falconí, 2018). For example, *B. velezensis* (CE 100) effectively promoted growth of seedlings of Japanese cypress (*Chamaecyparis obtusa* Endlicher), by secreting lytic enzymes (Moon *et al*., 2021). Similarly, Zhao *et al.* (2016) demonstrated that application of *B. velezensis* (GB03) increased the growth of the traditional Chinese herbal plant *Codonopsis pilosula*. Khan *et al*. (2020), reported that *B. velezensis* Lle-9 had broad-spectrum antifungal and plant growth promotion activity. The ability of *B. velezensis* B63 to improve the geranium growth may be attributed to its plant growth-promoting traits such as nitrogen fixation and phosphate solubilization (Reyad *et al.,* 2022).

The significant influence of chitosan on agromorphological characteristics observed in the present study is comparable to previous results for sweet basil (Ghasemi Pirbalouti *et al.,* 2017), *Mentha piperita* L. (Ahmad *et al*., 2019; Da Silva *et al.,* 2021), Carla (*Momordica charantia* L.) (Sharifi-Rad *et al.,* 2020), *Amaranthus hybridus* L. (Berliana *et al.,* 2020), and Moringa (*Moringa oleifera* L.) (Zubair *et al*., 2021). These comparable results could be attributed to chitosan stimulation of production of plant hormones such as auxins and cytokinins, which promote cell elongation and division, and increase plant growth. Enhanced transportation of nitrogen in functional leaves also supports plant growth and development and enhances plant quality attributes by increasing protein synthesis and chlorophyll production (Mazrou *et al.,* 2021). In contrast to the present results, Kahromi and

Khara (2021) found that foliar application of chitosan did not affect biomass of *Dracocephalum kotschy*. A possible explanation for this could be differences in application methods, application time, and the different plant species (Kahromi and Khara, 2021).

Photosynthesis rate is important for plant productivity and is dependent on mineral nutrient uptake (Evans 2013; Li *et al.* 2023). Nutrient uptake determines chlorophyll content in leaves and photosynthetic functioning. Increased photosynthesis then increases accumulation of carbohydrates and secondary metabolites in medicinal plants (Swamy and Rao, 2009). Growing evidence also indicates that plant-microbe interactions influence the quantity and types of secondary metabolites produced by plants, ultimately affecting overall plant yields. This has created interest in the application of biostimulants to cultivated medicinal and aromatic plants using natural methods (Kıtır Sen and Duran, 2023). Concentration and composition of essential oils (Eos) in plants also have ecological significance. For example, increased EO production can be a defense mechanism against microbes (Orhan *et al*., 2012).

In the present study, applications of chitosan and *B. velezensis* B63 improved geranium essential oil yield. Specifically, *B. velezensis* strain B63 treatment gave the greatest percentage of essential oil content and greatest yield. Increased levels of essential oil in plants treated with *B. velezensis* may explain their enhanced resistance to root rot infections in the field observed in this study. This aligns with previous research demonstrating the potent antimicrobial properties of plant essential oils, making them valuable biocontrol agents against plant pathogens (Raveau *et al*., 2020). The high oil yields observed in *B. velezensis*-treated plants could be due to plant growth promotion, particularly from phosphate solubilization. Nitrogen and phosphorus are crucial elements for medicinal plants as they contribute to precursor structures of essential oils (Dehsheikh *et al*., 2020). Kıtır Sen and Duran (2023) also reported that *B. subtilis* and *B. megaterium* led to increased yields of Izmir thyme. Other reports have shown that chitosan can increase essential oil content of thyme (Emami Bistgani *et al.,* 2017), *Origanum vulgare* (Bharti *et al.,* 2013), and *Matricaria chamomilla* L. (chamomile) (Mazrou *et al*., 2021).

Chitosan soaking + foliar spray 0.2% (CSF 0.2%) and *B. velezensis* B63 also increased production of the secondary metabolites citronellol, geraniol, citronellyl formate, and geranyl formate in geranium essential oil. This bacterium strain also increased production of eugenol. These results are similar to those from previous studies, indicating that foliar chitosan applications at 0.01% promoted accumulation of artemisinin in *Artemisia annua* (Lei *et al*., 2011) and β-caryophyllene in basil (*Ocimum basilicum* L.) (Antoniazzi and Deschamps, 2006). Similarly, chitosan boosted *in vitro* saponin accumulation in *Panax ginseng* (Chamkhi *et al.,* 2021), and rosmarinic acid and quercetin in *Dracocephalum kotschyi* (Kahromi and Khara, 2021). Bacteria also release molecules that can be elicitors, inducing metabolic alterations in host plants, including accumulation of secondary metabolites. For example, *B. subtilis* uses lipoproteins such as surfactins and fengycins as elicitors to activate host plants (Chamkhi *et al*., 2021).

Rhizosphere microbiomes promote plant nutrient uptake, modulate plant immunity, suppress pathogens, and control diseases (Olanrewaju and Babalola, 2022). Ali *et al*. (2023) described the "cry for help" theory of plant responses. Plants exposed to stress actively recruit specific microorganisms to provide protection from detrimental effects. Changes in rhizosphere microbiome composition could indicate whether plants stay healthy or become infected by pathogens (Gu *et al.,* 2022). No previous research has been published on the influence of *B. velezensis* B63 and chitosan treatments on the geranium rhizosphere microbiome. The present study showed that *B. velezensis* B63 and chitosan soaking + foliar spray 0.2% (CSF 0.2%) were effective treatments for reducing geranium root rot and improving plant yields, as well as changing rhizosphere microbiome structure, including CFU and 16S rRNA gene analyses. Focus on bacterial community aims to provide insight into biological control mechanisms active in the rhizosphere. Direct quantification of pathogenic fungi can provide valuable information, but the objective was to elucidate the intricate relationships between rhizosphere bacteria and fungi, as well as host plant ability to interact with and respond to these microorganisms. By examining changes in bacterial populations, the study indirectly inferred effects on pathogenic fungi, to provide an understanding of the complex interactions involved in plant health and disease resistance.

The most obvious result from this analysis was that after treating geranium plants with *B. velezensis* B63 and chitosan soaking + foliar spray, the amounts of *Kaistobacter* showed 2-fold increases. This genus is known to have several important ecological roles, including heavy metal accumulation and bioremediation of polluted sites (Garbini *et al.,* 2022), and provision of abiotic stress tolerance and plant growth promotion (dos Santos Lopes *et al.,* 2021). Studies have also shown that *Kaistobacter* spp. can enhance plant nutrient uptake and improve resistance to pathogens (Chen *et al*., 2020). There was also a 2.3-fold and 1.4-fold increase in the amounts of bacteria in the unclassified Acidobacteria iii1–15 due to chi-

tosan treatment, and a 1.4-fold increase from *B. velezensis* B63 treatment. *Acidobacteria* are active in the rhizosphere, where they break down complex carbohydrates from plants, and have genes for extracellular peptidases, which help to release ammonium during nitrogen cycling. Additionally, these bacteria can contribute to the plant growth (Pinho *et al*., 2020). Chitosan and *B. velezensis* B63 treatments also increased the abundance of *Gemmata*, by, respectively, 2.20-fold and 1.11-fold. According to Li *et al*. (2022), *Gemmata* promote plant growth and have important roles in cucumber growth.

Chitosan and *B. velezensis* B63 treatments also induced increases in abundance of some minor bacterial genera in field soil. Various members of these groups may have crucial roles in regulating plant growth and development (Srivastava *et al*., 2022). Some of these bacteria have been identified as beneficial for plants in other pathosystems. *Rhodoplanes* and the nitrogen uptake-related *Sinorhizobium*, could provide benefits through regulation of root development, upholding hormonal balance, facilitating mobilization and acquisition of nutrients, and suppressing disease in host plants (Srivastava *et al*., 2022). Increases in these microorganisms in soil were associated with enhanced growth and development of geranium plants.

Numbers of bacterial colony-forming units (CFUs) were generally greater in all experimental treatment soil samples than in the control samples. For fungi, some changes were observed across treatments. Despite the general decrease in fungal CFU counts, application of chitosan at the tested concentrations increased fungal counts. In addition, elucidating the microbial community structure, 16S rRNA gene copy numbers indicated the density of the communities. The copy numbers were generally elevated across all treatments. Chitosan concentrations, when applied through soaking or spraying, varied markedly, indicating that the application method affected the structure of the bacterial community in geranium rhizospheres. Application of *B. velezensis* B63 resulted in considerably reduced 16S rRNA gene copy numbers, indicating an alteration in the constitution of the microbial community. Application of chitosan and inoculation with the B63 strain caused dominance of bacterial populations carrying genes associated with soil fertility (e.g., *nifH*), and disease suppression (*ituD* and *FenD*) in geranium rhizospheres. High intensity of *nifH* was recorded in plants treated with chitosan soaking + foliar spray and with *B. velezensis* B63. Biological nitrogen fixation converts nitrogen into ammonia, which is biologically usable, and is also produced through soil mineralization. The *nifH* gene is commonly used as a marker for the molecular analyses of nitrogen-fixing microorganisms. In the present study, the increase in *nifH* was consistent with the results of Liu *et al*. (2022), who reported that the copy numbers of the N_2-fixing gene *nifH* increased in watermelon rhizospheres after *Burkholderia vietnamiensis* B418 inoculation.

CONCLUSIONS

The bacterium *B. velezensis* B63 had antagonistic activity against *Rhizoctonia solani* and *Macrophomina phaseolina in vitro*. This organism also reduced damage of geranium plants during growing season more than chitosan. Both treatments led to changes in composition of the soil microbiota. Numbers of bacteria fixing nitrogen and nutrient uptake increased. This was accompanied by increases in geranium plant morphometric and physiological parameters (essential oil composition), and increases in essential oil yields. These results indicate that the chitosan and the beneficial bacterium B63 could be effective for plant disease control. The increased essential oil production and improved plant growth and yield observed in this study were likely due to the attractiveness of geranium root exudates to antimicrobial and plant growth promoting (PGP) bacterial communities (*Kaistobacter, Agrobacterium, Gemmata*, *Rhodoplanes, Sinorhizobium*, and unclassified *Acidobacteria* iii1-15) around the plant roots. Further research is required to identify the specific types of beneficial bacteria involved in this interaction, and to determine how they are influenced by root exudates under stress of pathogen infections.

ACKNOWLEDGMENTS

The authors are grateful to the Department of Plant Pathology and the Department of Microbiology, the Faculty of Agriculture, and Cairo University for supplying some of the equipment and facilities to complete this work. Thanks also to Princess Nourah bint Abdulrahman University for supporting this study through Princess Nourah bint Abdulrahman University Researchers Supporting Project number (PNURSP2024R318), Princess Nourah bint Abdulrahman University, Riyadh, Saudi Arabia

FUNDING

This research was funded by Princess Nourah bint Abdulrahman University Researchers Supporting Project number (PNURSP2024R318), Princess Nourah bint Abdulrahman University, Riyadh, Saudi Arabia

AUTHOR CONTRIBUTIONS

Conceptualization, N.E.-H.A.R., N.A.M.E and T.R.E.; methodology, N.E.-H.A.R., N.A.M.E and T.R.E.; software, N.E.-H.A. R and T.R.E.; validation, N.E.-H.A.R.; formal analysis, N.E.-H.A.R.; investigation, N.E.-H.A.R., N.A.M.E.; resources, N.A.M.E.; data curation, N.E.-H.A.R.; funding acquisition, N.E.-H.A.R., N.A.M.E and F.A.S.; writing—original draft preparation, N.A.M.E., T.R.E. and F.A.S.; writing, review and editing, N.E.-H.A.R. All authors have read and agreed to the published version of the manuscript.

LITERATURE CITED

Ahmad B., Jaleel H., Shabbir A., Khan M.M.A., Sadiq Y., 2019. Concomitant application of depolymerized chitosan and GA modulates photosynthesis, essential oil and menthol production in peppermint (*Mentha piperita* L.) *Scientia Horticulturae* 246: 371–379. https://doi.org/10.1016/j.scienta.2018.10.031

Ali S., Tyagi A., Bae H., 2023. Plant Microbiome: An ocean of possibilities for improving disease resistance in plants. *Microorganisms* 11: 392. https://doi.org/10.3390/microorganisms11020392

Antoniazzi N., Deschamps C., 2006. Análise de crescimento de duas cultivares de cevada após tratamentos com elicitores e fungicidas. *Ciência Rural* 36: 1065–1071 doi:10.1590/S0103-84782006000400004

Anusuya S., Sathiyabama M., 2014. Effect of chitosan on rhizome rot disease of turmeric caused by *Pythium aphanidermatum*. *International Scholarly Research Notices* 305349. https://doi.org/10.1155/2014/305349

Azmana M., Mahmood S., Hilles A.R., Rahman A., Arifin M.A.B, Ahmed S., 2021. A review on chitosan and chitosan-based bionanocomposites: Promising material for combatting global issues and its applications. *International Journal of Biological Macromolecules* 185: 832–848. https://doi.org/10.1016/j.ijbiomac.2021.07.023

Berliana A.I., Kuswandari C.D., Retmana B.P., Putrika A., Purbaningsih S., 2020. Analysis of the potential application of chitosan to improve vegetative growth and reduce transpiration rate in *Amaranthus hybridus*. In: IOP Conference Series: Earth and Environmental Science. Life and Environmental Sciences Academics Forum 2018, 1st November 2018, West Java, Indonesia 481: 012021, 2020. https://doi.org/10.1088/1755-1315/481/1/012021

Bertani G., 1951. Studies on lysogenesis. I. The mode of phage liberation by lysogenic *Escherichia coli*. *Journal of Bacteriology* 62(3): 293–300. https://doi.org/10.1128/JB.62.3.293-300.1951

Bharti V., Vasudeva N., Duhan J.S., 2013. Bacteriostatic and fungistatic activities of *Oreganum vulgare* extract and volatile oil and interaction studies in combination with antibiotics and antifungal agents against food poisoning pathogens. *International Food Research Journal* 20(3): 1457–1462.

British Pharmacopoeia, 1963. *Determination of Volatile Oils in Drugs*. The pharmaceutical press, London, WCI.

Carrión V.J., Perez-Jaramillo J., Cordovez V., Tracanna V., De Hollander M., … Mohanraju P., 2019. Pathogen-induced activation of disease-suppressive functions in the endophytic root microbiome. *Science* 366: 606–612. https://doi.org/10.1126/science. aaw9285

Chamkhi I., Benali T., Aanniz T., 2021. Plant-microbial interaction: The mechanism and the application of microbial elicitor induced secondary metabolites biosynthesis in medicinal plants. *Plant Physiology and Biochemistry* 167: 269–295. https://doi.org/ 10.1016/J.PLAPHY.2021.08.001

Chen J., Mo L., Zhang Z., Nan J., Xu D., … Bao Y., 2020. Evaluation of the ecological restoration of a coal mine dump by exploring the characteristics of microbial communities. *Applied Soil Ecology*. 147: 103430. https://doi.org/10.1016/J.APSOIL.2019.103430.

Chen E., Chao S., Shi B., Liu L., Chen M., …Wu H., 2023. *Bacillus velezensis* ZN-S10 reforms the rhizosphere microbial community and enhances tomato resistance to TPN. *Plants* 12: 3636. https://doi.org/10.3390/plants12203636

Coque J.J.R., Álvarez-Pérez J.M., Cobos R., González-García S., Ibáñez A.M., … Calvo-Peña C., 2020. Advances in the control of phytopathogenic fungi that infect crops through their root system. In: *Advances in Applied Microbiology* (G.M. Gadd, S. Sariaslani, ed.), Academic Press, Cambridge, MA, USA, 123–170. https://doi.org/10.1016/bs.aambs.2020.01.003

Da Silva E. A., De Paula A. C. C. F. F., Silva V. N. B., De Alvarenga A. A., Bertolucci, S. K. V., 2021. Biostimulating effect of chitosan and acetic acid on the growth and profile of the essential oil of *Mentha arvensis* L. *Industrial Crops and Products* 171: 113987. https://doi.org/10.1016/j.indcrop.2021.113987

Dehsheikh A. B., Sourestani M. M., Zolfaghari M., Enayatizamir N., 2020. Changes in soil microbial activity, essential oil quantity, and quality of Thai basil as response to biofertilizers and humic acid. *Journal of Cleaner Production* 256: 120439. https://doi.org/10.1016/j.jclepro.2020.120439

Dewidar A., Kenawy A., Ghebrial E., 2019. influence of different garlic treatments on controlling basal stem rot, root rot and infection by broomrape in Geranium plants. *Egyptian Journal of Phytopathology* 47: 347–366.

dos Santos Lopes M.J., Dias-Filho M.B., Gurgel E.S.C., 2021. Successful plant growth-promoting microbes: inoculation methods and abiotic factors. *Frontiers in Sustainable Food Systems* 5: 606454. https://doi.org/10.3389/FSUFS.2021.606454

El Hadrami A., Adam L.R., El Hadrami I., Daayf F., 2010. Chitosan in plant protection. *Marine Drugs* 4: 968–987. https://doi.org/10.3390/MD8040968

Elsayed T.R., Jacquiod S., Nour E., Sørensen S.J., Smalla K., 2020. Biocontrol of bacterial wilt disease through complex interaction between tomato plant, antagonists, the indigenous rhizosphere microbiota, and *Ralstonia Solanacearum*. *Frontiers in Microbiology* 10. https://doi.org/10.3389/FMICB.2019.02835

Emami Bistgani Z., Siadat S.A., Bakhshandeh A., Ghasemi Pirbalouti A., Hashemi M., 2017. Interactive effects of drought stress and chitosan application on physiological characteristics and essential oil yield of *Thymus daenensis* Celak. *The Crop Journal* 5: 407–415. https://doi.org/10.1016/J.CJ.2017.04.003

Evans J.R., 2013. Improving Photosynthesis. *Plant Physiology* 162: 1780–1793. https://doi.org/10.1104/pp.113.219006

Fan B., Wang C., Song X., Ding, X., Wu L., … Borriss R., 2018. *Bacillus velezensis* FZB42 in 2018: The Gram-Positive Model Strain for Plant Growth Promotion and Biocontrol. *Frontiers in Microbiology* 9: 2491. https://doi.org/10.3389/fmicb.2018.02491

Fierer N., Jackson J.A., Vilgalys R., Jackson R.B., 2005. Assessment of soil microbial community structure by use of taxon-specific quantitative PCR Assays. *Applied and Environmental Microbiology* 7: 4117–4120 https://doi.org/10.1128/AEM.71.7.4117-4120.2005

Gao Y., Zhang Y., Zheng Z., Wu X., Dong X., Hu Y., Wang X., 2022. Agricultural Jiaosu: An eco-friendly and cost-effective control strategy for suppressing Fusarium root rot disease in *Astragalus membranaceus*. *Frontiers in Microbiology* 13. https://doi.org/10.3389/fmicb.2022.823704

Garbini G.L., Grenni P., Rauseo J., Patrolecco L., Pescatore T., … Caracciolo A.B., 2022. Insights into structure and functioning of a soil microbial community amended with cattle manure digestate and Sulfamethoxazole. *Journal of Soils and Sediments* 22: 2158–2173. https://doi.org/10.1007/s11368-022-03222-y

Ghasemi Pirbalouti A., Malekpoor F., Salimi A., Golparvar A.R., 2017. Exogenous application of chitosan on biochemical and physiological characteristics, phenolic content and antioxidant activity of two species of basil (*Ocimum ciliatum* and *Ocimum basilicum*) under reduced irrigation. *Scientia Horticulturae* 217: 114–122 https://doi.org/10.1016/J.SCIENTA.2017.01.031

Gu Y., Banerjee S., Dini-Andreote F., Xu Y., Shen Q., Jousset A., Wei Z., 2022. Small changes in rhizosphere microbiome composition predict disease outcomes earlier than pathogen density variations. *International Society for Microbial Ecology Journal* 16: 2448–2456. https://doi.org/10.1038/s41396-022-01290-z

Hafeez F. Y., Naureen Z., Sarwar A., 2019. Surfactin: an emerging biocontrol tool for agriculture sustainability. In: *Plant Growth Promoting Rhizobacteria for Agricultural Sustainability* (A. Kumar, V. Meena, ed.). Springer, Singapore, 203–213. https://doi.org/10.1007/978-981-13-7553-8_10

Helal D. S., El-Khawas H., Elsayed T. R., 2022. Molecular characterization of endophytic and ectophytic plant growth promoting bacteria isolated from tomato plants (*Solanum lycopersicum* L.) grown in different soil types. *Journal of Genetic Engineering and Biotechnology* 20(1): 79. https://doi.org/10.1186/s43141-022-00361-0

Hou S., Wolinska K. W., Hacquard S., 2021. Microbiota-root-shoot-environment axis and stress tolerance in plants. *Current Opinion in Plant Biology* 62: 102028. https://doi.org/10.1016/j.pbi.2021.102028

Illumina2013. 16S Metagenomic Sequencing Library Preparation. Preparing 16S Ribosomal RNA Gene Amplicons for the Illumina MiSeq System 2013 Available at: support/documents/documentation/ https://support.illumina.com/content/dam/illumina-chemistry_documentation/16 s/16s-metagenomic-library-prep-guide-15044223-b.pdf. Accessed April 05, 2013.

Kahromi S., Khara J., 2021. Chitosan stimulates secondary metabolite production and nutrient uptake in medicinal plant *Dracocephalum Kotschyi*. *Journal of the Science of Food and Agriculture* 9: 3898–3907. https://doi.org/10.1002/jsfa.11030

Khan M.S., Gao J., Xuqing C., Mingfang Z., Fengping Y., …, Zhang X., 2020. The endophytic bacteria *Bacillus Velezensis* Lle-9, isolated from *Lilium leucanthum*, Harbors antifungal activity and plant growth-promoting effects. *Journal of Microbiology and Biotechnology* 30(5): 668–680. https://doi.org/10.4014/jmb.1910.10021

Kıtır Şen N., Duran, A., 2023. A new approach on essential oil production of *Origanum onites* L.: Microbial fertilization and microwave extraction. *Heliyon* 9: e20211. https://doi.org/10.1016/j.heliyon.2023.e20211

Lahlali R., Ezrari S., Radouane N., Kenfaoui J., Esmaeel Q., …, Barka E.A., 2022. Biological control of plant pathogens: A global perspective. *Microorganisms* 10: 596. https://doi.org/10.3390/microorganisms10030596

Lei C., Lei C., Ma D., Pu G., Qiu X., …, Liu B., 2011. Foliar application of chitosan activates artemisinin biosynthesis in *Artemisia Annua* L. *Industrial Crops and Products* 1: 176–182. https://doi.org/10.1016/j.indcrop.2010.10.001

Li K., Ronge X., Song L., Pengcheng L., 2020. Chitin and chitosan fragments responsible for plant elicitor and growth stimulator. *Journal of Agricultural and Food Chemistry* 44: 12203–12211. https://doi.org/10.1021/ACS.JAFC.0C05316

Li Y.-T., Gao H.-Y., Zhang Z.-S., 2023. Effects of environmental and non-environmental factors on dynamic photosynthetic carbon assimilation in leaves under changing light. *Plants* 12(10): 2015. https://doi.org/10.3390/plants12102015

Li Z., Zheng Y., Li Y., Cheng X., Huang S., Yang X., Qin Y., 2022. Genotype-specific recruitment of rhizosphere bacteria from sandy loam soil for growth promotion of *Cucumis sativus* var. *hardwickii*. *Frontiers in Microbiology* 13: 910644. https://doi.org/10.3389/fmicb.2022.910644

Liu X., Zhang S., Jiang Q., Bai Y., … Ding W., 2016. Using community analysis to explore bacterial indicators for disease suppression of tobacco bacterial wilt. *Scientific Reports* 6: 36773. https://doi.org/10.1038/srep36773

Liu Y., Chen L., Wu, G., Feng H., Zhang G., … Zhang R., 2017. Identification of root-secreted compounds involved in the communication between cucumber, the beneficial *Bacillus amyloliquefaciens*, and the soil-borne pathogen *Fusarium oxysporum*. *Molecular Plant-Microbe Interactions Journal* 30: 53–62. https://doi.org/10.1094/MPMI-07-16-0131-R

Liu M., Philp J., Wang Y., Hu J., Wei Y., …, Denton M.D., 2022. Plant Growth-promoting Rhizobacteria *Burkholderia vietnamiensis* B418 inhibits root-knot nematode on watermelon by modifying the rhizosphere microbial community. *Scientific Reports* 1: 8381. https://doi.org/10.1038/s41598-022-12472-2

Lyu D., Smith D. L., 2022., The root signals in rhizospheric inter-organismal communications. *Frontiers in Plant Science*, 13: 1064058. https://doi.org/10.3389/fpls.2022.1064058

Maslennikova V.S., Tsvetkova V.P., Shelikhova E.V., Selyuk M.P., Alikina T.Y., … Dubovskiy I.M., 2023. *Bacillus subtilis* and *Bacillus amyloliquefaciens* mix suppresses Rhizoctonia disease and improves rhizosphere microbiome, growth and yield of potato (*Solanum tuberosum* L.). *Journal of Fungi* 9: 1142. https://doi.org/10.3390/jof9121142

Mazrou R., Ali E., Hassan S., Hassan F.A. 2021., Pivotal role of chitosan nanoparticles in enhancing the essential oil productivity and antioxidant capacity in *Matricaria chamomilla* L. *Horticulture* 12: 114–122. https://doi.org/10.3390/horticulturae7120574

Meena M., Yadav G., Sonigra P., Nagda A., Mehta T.N., …, Harish Marwal A., 2022., Role of elicitors to initiate the induction of systemic resistance in plants to biotic stress. *Plant Stress* 5: 100103. https://doi.org/10.1016/j.stress.2022.100103

Moon J.H., Won S.J., Maung C.E.H., Choi J.H., Choi S.I., …, Ahn Y.S., 2021., *Bacillus velezensis* CE 100 inhibits root rot diseases (*phytophthora* spp.) and promotes growth of Japanese Cypress (*Chamaecyparis obtusa* Endlicher) seedlings. *Microorganisms* 4: 821. https://doi.org/10.3390/MICROORGANISMS9040821

Narnoliya L.K., Jadaun J.S., Singh S.P., 2019. The phytochemical composition, biological effects and biotechnological approaches to the production of high-value essential oil from geranium. In: Essential Oil Research: Trends in Biosynthesis, Analytics, Industrial Applications and Biotechnological Production (Malik S. ed.). Springer, 327–352

Olanrewaju O.S., Babalola O.O., 2022. The rhizosphere microbial complex in plant health: A review of interaction dynamics. *Journal of Integrative Agriculture* 21(8): 2168–2182. https://doi.org/10.1016/S2095-3119(21)63817-0

Orhan I.E., Ozçelik B., Kartal M., Kan Y., 2012. Antimicrobial and antiviral effects of essential oils from selected Umbelliferae and Labiatae plants and individual essential oil components, *Turkish Journal of Biology* 36(3): 239–246. https://doi.org/10.3906/biy-0912-30.

Pinho, D., Barroso, C., Froufe, H., Brown, N., Vanguelova, …, Denman, S., 2020. Linking Tree Health, Rhizosphere Physicochemical Properties, and Microbiome in Acute Oak Decline. *Forests* 11(11): 1153. https://doi.org/10.3390/f11111153

Piras A.M., Maisetta G., Sandreschi S., Gazzarri M., Bartoli C., … Batoni G., 2015. Chitosan nanoparticles loaded with the antimicrobial peptide Temporin B exert a long-term antibacterial activity *in vitro* against clinical isolates of *Staphylococcus epidermidis*. *Frontiers in Microbiology* 6: 372. https://doi.org/10.3389/FMICB.2015.00372

Prasad D., Singh K.P., Kumar J., 2008. Root Rot and wilt complex of rose-scented Geranium (*pelargonium Graveolens*) in Uttarakhand. *Indian Phytopathology* 61(3): 365–366.

Raveau R., Fontaine J., Lounès-Hadj Sahraoui A.L., 2020. Essential oils as potential alternative biocontrol products against plant pathogens and weeds: A review. *Foods* 9(3): 365. https://doi.org/10.3390/foods9030365

Reyad N. E. H. A., Elsayed T. R., Naguib D. M., Azoz, S. N., 2022. Biocontrol of root rot in Geranium with antimycotic rhizobateria. *Rhizosphere* 24: 100607. https://doi.org/10.1016/j.rhisph.2022.100607

Román-Doval R., Tenorio-Barajas A.Y., Gomez-Sánchez A., Valencia-Lazcano A.A., 2023. Chitosan: properties and its application in agriculture in context of molecular weight. *Polymers* 15: 2867 https://doi.org/10.3390/polym15132867

Sharifi-Rad R., Esmaeilzadeh Bahabadi S., Samzadeh-Kermani A., Gholami M., 2020. The effect of non-biological elicitors on physiological and biochemical properties of medicinal plant *Momordica charantia* L. *Iranian Journal of Science and Technology, Transactions A: Science* 44: 1315–1326 https://doi.org/10.1007/s40995-020-00939-8

Simon L., Haichar Z., 2019. Determination of Root Exudate Concentration in the Rhizosphere Using 13C Labeling. *Bio-Protocol Journal* 9(9): e3228. https://doi.org/10.21769/BioProtoc.3228

Srivastava A.K., Das A.K., Jagannadham P.T.K., Bora P., Ansari F.A., Bhate R., 2022. Bioprospecting Microbiome for Soil and Plant Health Management Amidst Huanglongbing Threat in Citrus: A Review. *Frontiers in Plant Science* 13: 858842. https://doi.org/10.3389/fpls.2022.858842

Stukenbrock E.H., Gurr S., 2023. Address the growing urgency of fungal disease in crops. *Nature* 617(7959): 31–34. https://doi.org/10.1038/d41586-023-01465-4

Swamy K.N., Rao S.S.R., 2009. Effect of 24-epibrassinolide on growth, photosynthesis, and essential oil content of *Pelargonium graveolens* (l.) Herit. *Russian Journal of Plant Physiology* 56: 616–620. https://doi.org/10.1134/S1021443709050057

Vallejo L., 2023. The future of *Bacillus Amyloliquefaciens* based formulations looks promising interview with Liliana Vallejo from BASF. Accessed November 11, 2023, from https://news.agropages.com/News/Detail-45350.htm

Wang N., Wang L., Zhu K., Hou S., Chen L., … Guo JH., 2019. Plant root exudates are involved in *Bacillus cereus* AR156 mediated biocontrol against *Ralstonia solanacearum*. *Frontiers in Microbiology* 10: 98. https://doi.org/10.3389/fmicb.2019.00098

Wang C., Zhao X., Wu K., Liang C., Liu J., … Zhang W., 2023. Isolation and characterization of *Bacillus velezensis* strain B19 for biocontrol of *Panax notoginseng* root rot. *Biological Control* 185: 105311. https://doi.org/10.1016/j.biocontrol.2023.105311

Williamson-Benavides B.A., Dhingra A., 2021. Understanding root rot disease in agricultural crops. *Horticulturae* 7(2): 33. https://doi.org/10.3390/horticulturae7020033

Yánez-Mendizábal V., Falconí C.E., 2018. Efficacy of *Bacillus* spp. to biocontrol of anthracnose and enhance plant growth on *Andean lupin* seeds by lipopeptide production. *Biological Control* 122: 67–75. https://doi.org/10.1016/j.biocontrol.2018.04.004

Yu H., Yang F., Hu C., Yang X., Zheng A., … Lv M., 2023. Production status and research advancement on root rot disease of Faba bean (*Vicia faba* L.) in China. *Frontiers in Plant Science* 14. https://doi.org/10.3389/fpls.2023.1165658

Zhao Q., Wu Y.N., Fan Q., Han Q.Q., Paré P.W., …. Zhang J.L., 2016. Improved growth and metabolite accumulation in *Codonopsis pilosula* (franch.) Nannf. by inoculation of *Bacillus amyloliquefaciens* GB03. *Journal of Agricultural and Food Chemistry* 64(43): 8103–8108. https://doi.org/10.1021/acs.jafc.6b03390

Zubair M., Ramzani P.M.A., Rasool B., Khan M.A., Ur-Rahman M., … Iqbal, M., 2021. Efficacy of chitosan-coated textile waste biochar applied to cd-polluted soil for reducing cd mobility in soil and its distribution in Moringa (*Moringa oleifera* L.). *Journal of Environmental Management* 284: 112047. https://doi.org/10.1016/j.jenvman.2021.112047

Finito di stampare da
Logo s.r.l. – Borgoricco (PD) – Italia

Mediterranean Phytopathological Union

Founded by Antonio Ciccarone

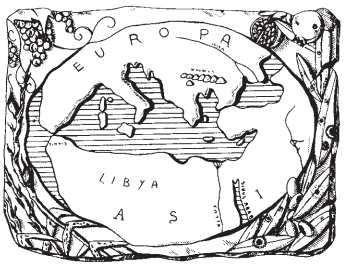

The Mediterranean Phytopathological Union (MPU) is a non-profit society open to organizations and individuals involved in plant pathology with a specific interest in the aspects related to the Mediterranean area considered as an ecological region. The MPU was created with the aim of stimulating contacts among plant pathologists and facilitating the spread of information, news and scientific material on plant diseases occurring in the area. MPU also intends to facilitate and promote studies and research on diseases of Mediterranean crops and their control.
The MPU is affiliated to the International Society for Plant Pathology.

MPU Governing Board

Affiliated Societies

Arab Society for Plant Protection (ASPP), http://www.asplantprotection.org/
French Society for Phytopathology (FSP), http://www.sfp-asso.org/
Hellenic Phytopathological Society (HPS), http://efe.aua.gr/
Israeli Phytopathological Society (IPS), http://www.phytopathology.org.il/
Italian Phytopathological Society (SIPAV), http://www.sipav.org/
Portuguese Phytopathological Society (PPS), http://www.spfitopatologia.org/
Spanish Society for Plant Pathology (SEF), http://www.sef.es/sef/

2024 MPU Membership Dues

Institutional MPU Membership: : € 200.00 (college and university departments, libraries and other facilities or organizations). Beside the open-access on-line version of *Phytopathologia Mediterranea*, the print version can be received with a € 50 contribution to mail charges (total € 250,00 to receive the print version). Researchers belonging to an Institution which is a member of the Union are entitled to publish with a reduced page contribution, as the Individual Regular members.
Individual Regular MPU Membership*: € 50.00 (free access to the open-access on-line version of Phytopathologia Mediterranea and can get the print version with a contribution to mail charges of € 50 (total € 100,00 to receive the print version).

*Students can join the MPU as a Student member on the recommendation of a Regular member. Student MPU members are entitled to a 50% reduction of the membership dues (proof of student status must be provided).

Payment information and online membership renewal and subscription at www.mpunion.com

For subscriptions and other information visit the MPU web site:
www.mpunion.com
or contact us at: Phone +39 39 055 2755861/862 – E-mail: phymed@unifi.it

Phytopathologia Mediterranea

Volume 63, April, 2024

Contents

Direttore responsabile: Giuseppe Surico • Autorizzazione del Tribunale di Firenze n. 4923 del 5-1-2000 • *Printed by* Logo S.r.l. - Padova, June 2024